

**Biochemistry and functional analysis of  
exopolysaccharide production in  
*Lactobacillus johnsonii***

**ENES DERTLI**

**A thesis submitted to the University of East Anglia for the degree of Doctor of  
Philosophy**

**Institute of Food Research**

**Norwich Research Park**

**Colney Lane**

**Norwich NR4 7UA**

**2013**

© This copy of the thesis has been supplied on the condition that anyone who consults it is understood to recognise that its copyright rests with the author and that use of any information derived there from must be in accordance with current UK Copyright Law. In addition, any quotation or extract must include full attribution.

**Biochemistry and functional analysis of exopolysaccharide production in  
*Lactobacillus johnsonii***

**Abstract**

Lactic Acid Bacteria (LAB) produce unique exopolysaccharides (EPS) that are important in food industry but they also play critical role in bacterial interactions during colonisation of the gastrointestinal tract. The role of this layer in the virulence of pathogenic bacteria has been well described but the biological importance of the EPS layer of probiotic bacteria have not been studied to the same extent. The aim of this thesis is to investigate the structure, biosynthesis mechanism and the biological role of the EPS produced by a probiotic strain of *Lactobacillus johnsonii* FI9785 that is able to competitively exclude *Clostridium perfringens* from gastrointestinal tract.

*L. johnsonii* harbours an *eps* gene cluster and a spontaneous mutation in the phosphoregulatory system of this cluster resulted in a colony switch from a rough morphology to a smooth one; similarly deletion of the *epsE* gene, that encodes the putative priming glycosyltransferase of the EPS biosynthesis, caused a huge increase in aggregation of *L. johnsonii*, which were shown to be related with EPS production levels. Structural analysis of the purified EPS showed that *L. johnsonii* could produce two types of EPS: EPS-1 and EPS-2. EPS-1 is a branched dextran with the unusual feature that every backbone residue is substituted with a 2-linked glucose unit and EPS-2 is composed of four glucose and two galactose units with a novel structure. Several mutants were generated with deletion of individual genes in *eps* cluster or the entire cluster to study the EPS biosynthesis mechanism. The  $\Delta epsE$  mutant produced only EPS-1 but not EPS-2 whilst the deletion of the putative transcriptional regulator, *epsA*, and the entire *eps* cluster resulted in an acapsular phenotypes. These alterations in the cell surface of EPS specific mutants were demonstrated by differences in binding of an anti-wild type *L. johnsonii* antibody. The loss of the EPS layer increased the adhesion and autoaggregation properties of *L. johnsonii* *in vitro* but EPS layer was found to be protective against several antimicrobials and environmental stress conditions. Additionally EPS layer was shown to be important on physicochemical properties and biofilm formation of *L. johnsonii*. Furthermore the *in vivo* persistence properties of acapsular mutant and wild type were assessed in a mouse model and no difference was detected in their persistence. Finally, several glycosyltransferases within the *eps* cluster were expressed, activity assays were performed and a potential glycosyltransferase was biochemically characterised.

## **Outputs from this project**

### **Publications**

- Horn N., Wegmann U., Dertli E., Mulholland F., Collins S. R. A., Waldron K. W., Bongaerts R. J., Mayer M. J., Narbad A. 2013. Spontaneous Mutation Reveals Influence of Exopolysaccharide on *Lactobacillus johnsonii* Surface Characteristics. PLoS One, 8 (3): p. e59957
- Dertli E., Colquhoun J. I., Gunning A. P., Bongaerts R. J., Le Gall G., Bonev B. B., Mayer M. J., Narbad A. 2013. Structure and biosynthesis of two novel exopolysaccharides produced by *Lactobacillus johnsonii* FI9785. Journal of Biological Chemistry.
- Dertli E., Mayer M. J., Colquhoun J. I., Narbad A. The putative transcriptional regulator is required for exopolysaccharide biosynthesis in *Lactobacillus johnsonii* FI9785. In preparation.
- Dertli E., Mayer M. J., Bongaerts R. J., Narbad A. Influence of the Exopolysaccharide Layer of *Lactobacillus johnsonii* FI9785 on Biofilm Formation, Cell Surface Characteristics and Autoaggregation Properties. In preparation.
- Dertli E., Mayer M. J., Narbad A. The Physiological role of the Exopolysaccharide Layer of *Lactobacillus johnsonii* FI9785. In preparation.

### **Posters**

- Dertli E., Bongaerts R. J., Gunning A. P., Mayer M. J., Narbad A. 2012. The role of Exopolysaccharides (EPS) of *Lactobacillus johnsonii* FI9785 on cell surface properties and bacterial adhesion. Turkey, Istanbul; XXIII International ICFMH Symposium, FoodMicro 2012; 3-7 September 2012.
- Dertli E., MacKenzie D. A., Mayer M., Juge N., Bongaerts R. J., Narbad A. 2012. Immunodetection of surface structures of probiotic bacteria by ELISA and Flow Cytometry. Cyto 2012, XXVII Congress of the International Society for the Advancement of Cytometry, June 23-27, Leipzig, Germany.

- Horn N., Wegmann U., Dertli E., Mulholland F., Bongaerts R. J., Gunning A. P., Mayer M. J., Narbad A. 2013. Exopolysaccharide production in *Lactobacillus johnsonii*. FEMS 2013; Federation of European Microbiology Society, 5<sup>th</sup> Congress of European Microbiologist July 21-15, Leipzig, Germany.
- Dertli E., Colquhoun J. I., Gunning A. P., Bongaerts R. J., Le Gall G., Mayer M. J., Narbad A. 2013. Two novel exopolysaccharides of *Lactobacillus johnsonii* FI9785 and their functional roles. BioMicroWorld2013; V International Conference on Environmental, Industrial and Applied Microbiology, October 2-4, Madrid, Spain.

### **Oral Presentations**

- Dertli E., Colquhoun J. I., Mayer M. J., Narbad A. 2013. The importance of the exopolysaccharide (EPS) layer for the survival of the probiotic *Lactobacillus johnsonii* FI9785. International Scientific Conference on Probiotics and Prebiotics, IPC 2013, Kosice, Slovakia.

## **Acknowledgements**

I sincerely thank ALLAH (c.c.), my God, the Most Gracious and the Most Merciful for enabling me to complete this thesis successfully, without his wish I would not have had the wisdom or physical ability to do so.

I owe my sincere thanks, deepest gratitude and appreciation to my supervisors Dr Arjan Narbad and Dr Melinda Mayer for their patience, sincere efforts, support, training and guidance throughout my project. Without their help this thesis would not be possible!

I am particularly grateful to Dr Ian Colquhoun for his excellent contribution to this project. I would like to give my special thanks to Dr Roy Bongaerts, A. Patrick Gunning and Dr Donald MacKenzie for their extensive training and friendship. I would also wish to acknowledge the contributions, advice and suggestions of Nikki Horn, Dr Udo Wegmann, Kathryn Cross, Dr Mary Parker, Carmen Nueno Palop, Dr Emmanuelle Crost, Dr Kevin Huges, Dr Lindsay Hall, Sam J. Collins, Mike Ridout, Dr Zara Merali, Dr Adrian Tett, Dr Chadia Toukoki, Dr Martin Rejzek, Prof Rob Field, Ellis O'Neill, Mark Philo, Dr Gwenaelle Le Gall, Gary Wortley, Maddy Houchen, David Fairbairn and Val Russell and all other people who made IFR a pleasant place.

My eternal thanks and gratitude goes to my beloved and wonderful family; my mother Nurhayat, my father Hakkı, my brothers Ibrahim, Ahmed and Furkan and my aunt Fethiye. No word can express my appreciation to them. Without their warm love, sincere prayers and support it would have been impossible for me to finish Ph.D.

Last but not least I would like to give my special thanks to Turkish Ministry of Education who funded my PhD education.

# **Biochemistry and functional analysis of exopolysaccharide production in *Lactobacillus johnsonii***

I certify that the worked contained in the thesis is entirely the result of my own work, except where reference is made to other authors. It has not been submitted in any form to the University of East Anglia or any other University.

## **Authors Declaration**

Dr Ian Colquhoun at IFR completed the NMR spectroscopy analysis of the exopolysaccharide samples. Patrick A. Gunning and Kathryn Cross at IFR completed Atomic Force Microscopy and Electron Microscopy analysis, respectively. Mark Philo at IFR performed the LC-MS analysis to monitor the glycosyl transfer reactions.

# Contents

# Page number

## Chapter 1

### General Introduction

1.1	Bacterial Polysaccharides	2
1.2	<i>Lactobacillus</i> in the Food Industry	5
1.3	<i>Lactobacillus</i> as a Member of Commensal Microbiota	5
1.4	Exopolysaccharides (EPS) of Lactic Acid Bacteria (LAB)	7
1.5	Cell Surface Structure of Lactobacilli	11
1.6	Biosynthesis of EPS in LAB	13
1.7	Genetics of EPS Production in LAB	18
1.8	Factors Affecting the EPS Biosynthesis Level of LAB	24
1.9	Physiological Role of EPS	26
1.10	Mechanism of cell adhesion in LAB	31
1.11	Description of <i>Lactobacillus johnsonii</i> FI9785	34
1.12	Genetics of EPS Production in <i>Lactobacillus johnsonii</i> FI9785	37
1.13	Background information about the thesis	41
1.14	Scope of the Thesis	43

## Chapter 2

### General material and methods

2.1	Microbiology Work	45
2.1.1	Culture Media	45
2.1.2	Bacterial Strains and Growth Conditions	45
2.1.3	Bacterial Growth Analysis	48
2.1.3.1	Bioscreen Experiments	48
2.1.3.2	Antibiotic Susceptibility	49
2.1.4	Isolation of Exopolysaccharides	49
2.1.5	Immunology	50
2.1.5.1	Production of Anti-Wild Type Antibodies	50
2.1.5.2	Enzyme Linked Immunosorbent Assay (ELISA)	50
2.1.6	Flow Cytometry (FCM) Applications	51
2.1.6.1	Bacterial Viability	51
2.1.6.2	The Detection of Antibody Responses	51
2.1.6.3	Assessment of Bacterial Cell Aggregation	51
2.1.6.4	Assessment of Cell Adhesion to Tissue Culture	52
2.1.7	Transmission Electron Microscopy (TEM)	53
2.2	Molecular Biology Work	53
2.2.1	Genomic DNA Extraction	53
2.2.2	Plasmid Preparation Kits	54
2.2.3	Gel Electrophoresis of Nucleic Acids	54
2.2.4	Restriction Digests	55
2.2.5	Dephosphorylation of Vector DNA	55

2.2.6	DNA Ligation	55
2.2.7	Polymerase Chain Reaction (PCR)	56
2.2.8	Ligation PCR	57
2.2.9	PCR with Whole Cells	58
2.2.10	Splice Overlap Extension PCR	58
2.2.11	DNA Purification	60
2.2.12	DNA Sequencing	60
2.2.13	Primer Design	61
2.2.14	Transformation of <i>E. coli</i>	61
2.2.15	Transformation of <i>L. johnsonii</i>	62
<b>2.3</b>	<b>Protein Biochemistry</b>	<b>62</b>
2.3.1	Protein Expression and Extraction from Bacterial Cells	62
2.3.2	Protein Assays	63
2.3.3	Sodium Dodecyl Sulphate Polyacrylamide Gel Electrophoresis	64
2.3.4	Western Blotting	65

## Chapter 3

### EPS of *L. johnsonii* FI9785

<b>3.1</b>	<b>INTRODUCTION</b>	<b>68</b>
<b>3.2</b>	<b>MATERIAL AND METHODS</b>	<b>70</b>
3.2.1	Quantification of EPS production	70
3.2.2	NMR spectroscopy analysis	71
3.2.3	Atomic Force Microscopy (AFM) Analysis	71
3.2.4	FTIR spectroscopy analysis	72
3.2.5	Analysis of cell surface alterations	72
<b>3.3</b>	<b>RESULTS</b>	<b>72</b>
3.3.1	Quantification of EPS production	73
3.3.2	Structural analysis of EPS	75
3.3.3	<i>In situ</i> localisation of galactose residues on cell surface	76
3.3.4	Alterations in EPS structure detected by FTIR	83
3.3.5	Detection of cell surface alterations	84
<b>3.4</b>	<b>Discussion</b>	<b>89</b>

## Chapter 4

### EPS and Cell Surface Interactions

<b>4.1</b>	<b>INTRODUCTION</b>	<b>97</b>
<b>4.2</b>	<b>MATERIAL AND METHODS</b>	<b>99</b>
4.2.1	Bacterial strains and growth conditions	99
4.2.2	Biofilm assays and Microscopy	99
4.2.3	Measurement of physicochemical cell surface characteristics	100
4.2.4	Autoaggregation and adhesion to tissue culture assays	101
<b>4.3</b>	<b>RESULTS</b>	<b>101</b>
4.3.1	<i>In vitro</i> biofilm formation of <i>L. johnsonii</i>	101
4.3.2	Comparison of biofilm formation of <i>L. johnsonii</i> and mutant strains	103
4.3.3	Influence of medium components on biofilm formation	105
4.3.4	Role of EPS on cell surface properties	106
4.3.5	Effect of EPS on autoaggregation and adhesion to tissue cell culture cells	108
<b>4.4</b>	<b>DISCUSSION</b>	<b>111</b>

## Chapter 5

### Genetics of EPS Biosynthesis in *L. johnsonii* FI9785

<b>5.1 INTRODUCTION</b>	117
<b>5.2 MATERIAL AND METHODS</b>	118
5.2.1 Deletion of the <i>epsA</i> gene in <i>L. johnsonii</i>	118
5.2.2 Deletion of the whole <i>eps</i> gene cluster of <i>L. johnsonii</i>	118
5.2.3 Complementation of the <i>epsA</i> gene	118
5.2.4 Isolation of EPS from new mutants and Structural analysis	119
5.2.5 Quantification of EPS production by phenol-sulphuric acid methodology	120
5.2.6 Assessment of Adhesion and Surface alterations by FCM and TEM	121
5.2.7 Analysis of <i>epsA</i> gene expression by qPCR	121
<b>5.3 RESULTS</b>	123
5.3.1 Deletion of <i>epsA</i> gene from the genome of <i>L. johnsonii</i>	123
5.3.2 Deletion of the <i>eps</i> gene cluster from the genome of <i>L. johnsonii</i>	127
5.3.3 Complementation of the <i>epsA</i> gene	131
5.3.4 Loss of EPS production after deletion of <i>epsA</i> gene and <i>eps</i> gene cluster	131
5.3.5 Structural analysis revealed the complementation of <i>epsA</i> gene	133
5.3.6 Adhesion and cell surface alterations after the loss of the EPS layer	135
5.3.7 Quantification of EPS production and qPCR analysis of <i>epsA</i> gene expression	138
<b>5.4 DISCUSSION</b>	139

## Chapter 6

### Physiological role of EPS Layer

<b>6.1 INTRODUCTION</b>	146
<b>6.2 MATERIAL AND METHODS</b>	148
6.2.1 Minimum Inhibitory Concentration (MIC) tests of nisin and antibiotics	148
6.2.2 Cell survival tests of wild type and mutant cells	148
6.2.3 Survival in bile salts and simulated <i>in vitro</i> digestion	148
6.2.4 <i>In vivo</i> colonisation studies	149
6.2.5 Analysis of microbiota composition by 454 pyrosequencing	151
<b>6.3 RESULTS</b>	152
6.3.1 EPS layer of <i>L. johnsonii</i> protects against antibiotics and nisin	152
6.3.2 Protective role of EPS layer in cell integrity under stress conditions	157
6.3.3 Survival in bile salts and simulated <i>in vitro</i> digestion	158
6.3.4 Colonisation analysis of wild type and mutants in mice model	160
6.3.5 Role of EPS layer on gut microbiota alterations	164
<b>6.4 DISCUSSION</b>	167

## Chapter 7

### Characterisation of Glycosyltransferases involved in EPS biosynthesis of *L. johnsonii*

<b>7.1 INTRODUCTION</b>	177
<b>7.2 MATERIAL AND METHODS</b>	180
7.2.1 Deletion of putative glycosyltransferase genes from <i>eps</i> gene cluster	180
7.2.2 Isolation of EPS from new mutants and analysis of EPS structure and production levels	183
7.2.3 Subcloning of two potential glycosyltransferases: <i>gtf1</i> and <i>gtf3</i>	183
7.2.4 Protein expression, analysis and purification	185
7.2.5 Glycosyl transfer activity assays	186
7.2.6 Glf mutase activity assay	188
<b>7.3 RESULTS</b>	189
7.3.1 Deletion of putative glycosyltransferases from the <i>eps</i> cluster	189
7.3.2 Quantification of EPS production and structural analysis	195
7.3.3 Glycosyltransferases and Glf mutase expression and GTF activity tests	197
7.3.4 Glf mutase activity tests	205
7.3.5 Biochemical characterisation of putative glycosyltransferases	208
<b>7.4 DISCUSSION</b>	217

## Chapter 8

### Final Discussion and Future Directions

<b>8.1 CONCLUSIONS AND FUTURE DIRECTIONS</b>	223
<b>APPENDIX</b>	
1- Antibiotics and their concentrations for plasmid selection	234
2- Primers used in this study	234
3- Buffers and their compositions used in this study	237
4- An example of GC Chromatogram	241
5- The calibration curve of sugar standards of GC analysis	242
6- Examples of calibration curves used for protein and sugar concentration analysis	243
7- Examples of calibration curves used for the qPCR analysis	244
8- Examples of FPLC chromatograms	245
<b>REFERENCES</b>	246

List of Figures		Page Number
<b>Chapter 1</b>		
Figure 1.1	Chemical structure of homopolysaccharide dextran	7
Figure 1.2	A typical heteropolymeric exopolysaccharide structure	8
Figure 1.3	Primary EPS structures from different LAB	9
Figure 1.4	EM pictures of EPS accumulation on cell surface of LAB	11
Figure 1.5	The architecture of the cell wall of Gram-positive bacteria	12
Figure 1.6	The detailed schematic illustration of EPS production of LAB	14
Figure 1.7	Model for Exopolysaccharide biosynthesis in <i>L. lactis</i> NIZO	16
Figure 1.8	Schematic representation of the general structure of GTFs	19
Figure 1.9	Organisation of the <i>eps</i> gene clusters of <i>L. lactis</i> subsp. <i>cremoris</i> NIZO B40 and <i>S. thermophilus</i> Sfi6	19
Figure 1.10	Putative health-promoting effects of LAB exopolysaccharides	29
Figure 1.11	Phylogenetic classification of <i>L. johnsonii</i> FI9785	34
Figure 1.12	Molecular organisation of the <i>eps</i> cluster of <i>L. johnsonii</i> FI9785	38
Figure 1.13	Morphology of the spontaneous mutant and wild type strains	41
Figure 1.14	Morphology of the spontaneous mutant and its complemented mutant	42
<b>Chapter 2</b>		
Figure 2.1	Hyperladder I fragment sizes and quantities	55
Figure 2.2	Illustration of ligation PCR procedure	57
Figure 2.3	Illustrations of splice overlap extension PCR procedure	58
Figure 2.4	The SeeBlue Plus ladder apparent molecular weights	64
Figure 2.5	Western Blot Methodology	65
<b>Chapter 3</b>		
Figure 3.1	The growth curve of wild type and mutant strains	73
Figure 3.2	Total sugar content of EPS samples of <i>L. johnsonii</i> strains	74
Figure 3.3	Line Drawing Structures of EPS-1 and EPS-2	75
Figure 3.4	Structures of EPS-1 and EPS-2	76
Figure 3.5	Imaging wild type and $\Delta epsE$ mutant cells by AFM	77
Figure 3.6	Force volume images obtained with a PA1 functionalised AFM tip	78
Figure 3.7	Adhesion data from force volume data in figure 3.9 depicted as histograms	80
Figure 3.8	<i>In-situ</i> characterisation of the physical properties of EPS-2 on <i>L. johnsonii</i>	82
Figure 3.9	FTIR spectra of capsular EPS isolated from the wild type and mutants	83
Figure 3.10	Viability of stationary phase <i>L. johnsonii</i> cells detected by PI staining	84
Figure 3.11	Anti-wild type antibody responses to the wild type and derivative strains measured by Flow cytometry	85
Figure 3.12	TEM analysis of <i>L. johnsonii</i> FI9785 and its mutants	87
Figure 3.13	TEM analysis of <i>L. johnsonii</i> FI9785	87
Figure 3.14	TEM analysis of <i>L. johnsonii epsC<sup>D88N</sup></i>	88
Figure 3.15	TEM analysis of <i>L. johnsonii ΔepsE</i>	88
Figure 3.16	TEM analysis of <i>L. johnsonii epsC<sup>D88N</sup>::pepsC</i>	88
Figure 3.17	TEM analysis of <i>L. johnsonii ΔepsE::pepsE</i>	89
Figure 3.18	TEM analysis of <i>L. johnsonii ΔepsE::pepsEA/S</i>	89
<b>Chapter 4</b>		
Figure 4.1	TEM picture of <i>L. johnsonii</i> wild type	102
Figure 4.2	Congo red binding phenotypes of colonies of wild type and mutants	102

Figure 4.3	Biofilm formation of <i>L. johnsonii</i> FI9785 on sterile microscope slides	103
Figure 4.4	Influence of EPS on biofilm formation by <i>L. johnsonii</i>	104
Figure 4.5	Effect of medium components on biofilm formation	105
Figure 4.6	Zeta potential of the <i>L. johnsonii</i> FI9785 and mutant strains	107
Figure 4.7	% Adhesion to hexadecane assays of <i>L. johnsonii</i> FI9785	107
Figure 4.8	OD measurements (OD <sub>600nm</sub> ) of <i>L. johnsonii</i> strains over 8 h period	108
Figure 4.9	Autoaggregation of wild type and its mutants	109
Figure 4.10	The aggregation percentage of <i>L. johnsonii</i> strains analysed by FCM	109
Figure 4.11	Adhesion of <i>L. johnsonii</i> strains to HT29 monolayers	110
Figure 4.12	Adhered bacteria and HT29 cell complex of $\Delta epsE$ and $epsC^{D88N}$ mutant detected by FCM	111
<b>Chapter 5</b>		
Figure 5.1	Agarose gel showing restricted <i>L. johnsonii</i> and vectors	123
Figure 5.2	Agarose gel showing preparation of pG+host9 construct for <i>epsA</i> deletion	124
Figure 5.3	Schematic representation of <i>epsA</i> gene deletion process	125
Figure 5.4	Agarose gel showing the double crossover for <i>epsA</i> construct resulted in <i>L. johnsonii</i> $\Delta epsA$	126
Figure 5.5	The growth curve of wild type and new mutants during the 11 h period	127
Figure 5.6	Schematic representation of <i>eps</i> gene cluster deletion process	128
Figure 5.7	Agarose gel showing amplification of <i>1170</i> and <i>CAT</i> gene from <i>L. johnsonii</i> and pUK200, respectively	129
Figure 5.8	Agarose gel showing the double crossover for <i>eps cluster</i> construct resulted in <i>L. johnsonii</i> $\Delta eps\_cluster$	130
Figure 5.9	Agarose gel showing the complementation of <i>epsA</i> gene	131
Figure 5.10	TEM analysis of <i>L. johnsonii</i> wild type and $\Delta eps\_cluster$ , $\Delta epsA$ and $\Delta epsA::pepsA$ mutants	132
Figure 5.11	600 MHz <sup>1</sup> H NMR spectra of EPS of $\Delta epsA::pepsA$ mutant	133
Figure 5.12	FTIR spectra of capsular EPS isolated from the wild type and $\Delta epsA::pepsA$ mutant	135
Figure 5.13	The aggregation percentage of wild type and mutant strains after overnight incubation analysed by FCM	136
Figure 5.14	Anti-wild type antibody responses to the wild type and derivative strains measured by FCM	137
Figure 5.15	Adhesion of <i>L. johnsonii</i> strains to HT29 monolayers	138
Figure 5.16	Total sugar content of <i>L. johnsonii</i> wild type and $\Delta epsA::pepsA$ mutant strain	139
<b>Chapter 6</b>		
Figure 6.1	Growth curve of wild type and mutants in MRS with 1 µg/ml ampicillin	153
Figure 6.2	Growth curve of wild type and mutants in MRS with 2 µg/ml ampicillin	154
Figure 6.3	Growth curve of wild type and mutants in MRS with 1 µg/ml tetracycline	154
Figure 6.4	Growth curve of wild type and mutants in MRS with 15 µg/ml furazolidone	155
Figure 6.5	Growth curve of wild type and mutants in MRS with 30 µg/ml furazolidone	156
Figure 6.6	Growth curve of wild type and mutants in MRS with 250 ng/ml nisin	156
Figure 6.7	Percentage of survival of <i>L. johnsonii</i> strains after heat shock	157
Figure 6.8	Percentage of survival of <i>L. johnsonii</i> strains after acid shock	158
Figure 6.9	Growth curve of wild type and mutants in MRS with 0.3% (w/v) bile	159
Figure 6.10	Survival of <i>L. johnsonii</i> strains after the <i>in vitro</i> digestion conditions	160

Figure 6.11	Persistence of wild type and mutants in C57BL/6 mice	162
Figure 6.12	Bacterial numbers (CFU) in caecum and colon samples	163
Figure 6.13	Agarose gel analysis of total DNA isolated from the faecal materials	164
Figure 6.14	Relative abundances of bacterial phylums determined by 454 analysis	165
Figure 6.15	Relative abundances of bacterial orders determined by 454 analysis	166
<b>Chapter 7</b>		
Figure 7.1	Molecular organisation of the <i>eps</i> cluster of <i>L. johnsonii</i> FI9785	180
Figure 7.2	An illustration of the gene replacement process for <i>gtf1</i>	182
Figure 7.3	The scheme of pET15b expression vector	184
Figure 7.4	ED-1 reaction mixture and expected final product after the GTF activity	187
Figure 7.5	Agarose gel showing the amplification of partial GTFs from <i>L. johnsonii</i> and <i>CAT</i> gene from pUK200	190
Figure 7.6	Agarose gel showing the splice PCR products and final constructs	190
Figure 7.7	Agarose gel showing the splice PCR products for construct <i>gtf5</i>	191
Figure 7.8	Agarose gel showing the integration of vector constructs to <i>L. johnsonii</i> genome and the confirmation of $\Delta$ <i>gtf1</i> mutant	192
Figure 7.9	Agarose gel showing $\Delta$ <i>gtf3</i> mutant	193
Figure 7.10	Agarose gel showing transformants of <i>gtf5</i>	194
Figure 7.11	Agarose gel showing integration of <i>gtf5</i> construct to <i>L. johnsonii</i>	194
Figure 7.12	Total sugar content of <i>L. johnsonii</i> wild type, $\Delta$ <i>gtf1</i> and $\Delta$ <i>gtf3</i> mutants	195
Figure 7.13	600 MHz $^1\text{H}$ NMR spectra of EPS of <i>L. johnsonii</i> strains	196
Figure 7.14	FTIR spectra of capsular EPS isolated from the wild type and mutants	197
Figure 7.15	Agarose gel showing amplification of <i>gtf1</i> and <i>gtf3</i>	198
Figure 7.16	Agarose gel showing positive colonies carrying pET15b <i>gtf1-gtf3</i>	199
Figure 7.17	Scheme of the pET15b <i>gtf1</i> and pET15b <i>gtf3</i> and the transformants	199
Figure 7.18	Expression of <i>gtf1</i> and <i>gtf3</i> in <i>E. coli</i> for different time points	200
Figure 7.19	Expression of <i>gtf1</i> and <i>gtf3</i> and extraction with different methods	202
Figure 7.20	Expression of <i>gtf2</i> , <i>gtf4</i> , <i>gtf5</i> and <i>glf</i> in <i>E. coli</i> for different time points	203
Figure 7.21	Purification of GTFs and Glf protein	204
Figure 7.22	Conversion of the UDP-Galp to UDP-Galf by Glf mutase	205
Figure 7.23	$^1\text{H}$ NMR-spectra of the reaction products of the crude mutase extract	206
Figure 7.24	$^1\text{H}$ NMR-spectra of the reaction products of the purified mutase	207
Figure 7.25	TLC analysis of ED-1 reactions with crude GTF extracts	208
Figure 7.26	Schematic representation of the activity assay in ED-1 reaction mixture with crude GTFs	209
Figure 7.27	Negative ion LC-MS chromatogram of control samples of ED-1	211
Figure 7.28	Negative ion LC-MS chromatogram of ED-1 incubated with crude <i>gtf5</i> and <i>gtf3</i> extracts	212
Figure 7.29	Negative ion LC-MS chromatogram of ED-1 reaction mixtures of crude and purified <i>gtf4</i>	213
Figure 7.30	TLC analysis and Negative ion LC-MS chromatogram of ED-2 reactions with putative GTFs	215
<b>Chapter 8</b>		
Figure 8.1	The schematic illustration of the gene functions in putative steps of EPS-2 biosynthesis	232

<b>List of Tables</b>		<b>Page Number</b>
<b>Chapter 1</b>		
Table 1.1	Examples of principal microbial EPS and producer organisms	3
Table 1.2	Strains of <i>L. johnsonii</i> with reported probiotic actions	36
Table 1.3	ORFs identified in the EPS gene cluster of <i>L. johnsonii</i> FI9785	40
Table 1.4	<i>L. johnsonii</i> mutant strains developed before this project	41
<b>Chapter 2</b>		
Table 2.1	List of organisms and growth conditions used in this thesis	47
Table 2.2	List of plasmid vectors used in this thesis	48
Table 2.3	Reaction composition for Go Taq polymerase	56
Table 2.4	Reaction composition for Phusion polymerase	57
Table 2.5	Sequencing reaction conditions	60
<b>Chapter 5</b>		
Table 5.1	Primers used for deletion of <i>epsA</i> and <i>eps</i> cluster and complementation process	119
Table 5.2	Primers designed for <i>epsA</i> , <i>16S</i> and <i>gyrB</i> genes for qPCR analysis	122
Table 5.3	<sup>1</sup> H and <sup>13</sup> C chemical shifts of $\Delta epsA::pepsA$ repeating unit	134
<b>Chapter 7</b>		
Table 7.1	The donor and acceptor molecules used for each reaction mixture	186
Table 7.2	Primer sets for the confirmation of the <i>gtf</i> gene deletions	189

## List of Abbreviations

Abbreviation	Expansion
2D	Two dimensional
AB	Antibody
Ac	Acetyl
AFM	Atomic Force Microscopy
Amp	Ampicillin
ATP	Adenosine triphosphate
BLAST	Basic local alignment search tool
bp	Base pairs
BSA	Bovine serum albumin
Caco-2	Human epithelial colorectal adenocarcinoma cells
CAT	Chloramphenicol
cDNA	Complementary DNA
CFU	Colony forming unit
COSY	Correlation spectroscopy
CPS	Capsular polysaccharides
CT	Threshold cycle
CWE	Cell wall extract
d	Days
Da	Dalton
DMEM	Dulbecco's modified eagle medium
DNA	Deoxyribonucleic acid
dNTP	Deoxyribonucleotide triphosphate
dTDP	Thymidine diphosphate
EDTA	Ethylenediaminetetraacetic acid
ELISA	Enzyme linked immunosorbent assay
EPS	Exopolysaccharides
Ery	Erythromycin
<i>f</i>	Furanose
FCM	Flow Cytometry
FPLC	Fast protein liquid chromatography
FTF	Fructosyltransferase
FT-IR	Fourier Transmission Infrared Spectroscopy
Gal	Galactose
GC	Gas Chromatography
Glc	Glucose
GlcNAc	N-acetyl-glucosamine
GIT	Gastrointestinal tract
GRAS	Generally recognized as safe
GTFs	Glycosyltransferase(s)
h	Hours
His	Histidine
HT29	Human colon adenocarcinoma cells
IBD	Inflammatory bowel disease
IFR	Institute of Food Research
IL-10	Interleukin-10

IPTG	Isopropyl- $\beta$ -D-1-thiogalactopyranoside
L	Luria
LAB	Lactic Acid Bacteria
LB	Luria-Bertani
LC-MS	Liquid chromatography-Mass spectroscopy
LDS	Lithium Dodecyl Sulfate
LPS	Lipopolysaccharide
LTA	Lipoteichoic acid
MEM	Minimum Essential Medium
MIC	Minimum Inhibitory Concentration
min	Minutes
MOPS	Morpholino propanesulfonic acid
mRNA	Messenger RNA
MRS	De Man-Rogosa-Sharpe
MUB	Mucus binding protein
MW	Molecular Weight
NMR	Nuclear magnetic resonance
nt	Nucleotide
OAc	Acetoxy group
ORFs	Open reading frame(s)
<i>p</i>	Pyranose
PBS	Phosphate buffered saline
PCR	Polymerase chain reaction
PDVF	Polyvinylidene difluoride membrane
PG	Peptidoglycan layer
PI	Propidium Iodide
PMT	Photomultiplier
ppm	Parts per million
Rha	Rhamnose
RNA	Ribonucleic acid
rRNA	Ribosomal RNA
rpm	Revolutions per minute
Rt	Retention time
RT	Room temperature
qPCR	Quantitative real-time PCR
s	Seconds
SCFAs	Short chain fatty acid(s)
SDS-PAGE	Sodium dodecyl sulfate polyacrylamide gel electrophoresis
SOC	Super optimal broth with catabolite repression
TCA	Tri-chloroacetic acid
TEM	Transmission electron microscopy
TLC	Thin-Layer Chromatography
Tm	Melting temperature
UDP	Uridine diphosphate
UP	Ultra-pure
UV	Ultraviolet
WHO	World Health Organization
WT	Wild type

# Chapter 1

---

**General Introduction**

## 1.1 Bacterial polysaccharides

Polysaccharides are one of the most important biological polymers in our planet. These biopolymers have several vital biological functions; they are used as energy storage material and are one of the main components of the cell wall material of living organisms, including bacteria [1]. For instance, bacterial cell wall components such as teichoic and teichuronic acids, lipopolysaccharides and peptidoglycan are composed of polysaccharides. Many eukaryotic and prokaryotic organisms such as algae [2], archaea [3], fungi [4] including yeast [5] and bacteria are also able to produce polysaccharides which are not included in the cell wall structure with a wide range of different structures, defined as extracellular polysaccharides. This term reflects the polymers which are produced by bacterial or microbial cells externally from the outer cell surface layer [6]. Bacteria are the main group of organisms for the production of extracellular polysaccharides for technological and industrial applications [7].

Extracellular polysaccharides can be either bound to the bacterial cell surface tightly, which are defined as capsular polysaccharides (CPS) or they can be excreted into the extracellular surrounding environment, described as exopolysaccharides (EPS) which can be loosely attached to the bacterial cells or completely detached from the bacteria. A large and growing body of literature has described these two types of extracellular polysaccharides with the term exopolysaccharides (EPS) [8]. Some of the main examples of the principal microbial exopolysaccharides are listed in Table 1.1.

Microbial EPS are classified into two groups according to their chemical composition, as either homopolysaccharides or heteropolysaccharides and show a wide diversity in their structures. **Homopolysaccharides** are composed of the same sugar subunit in their repeating unit structure with different linkages. Homopolysaccharides can be part of the outer capsule layer of Gram positive and Gram negative bacteria such as oral Streptococci and *Escherichia coli* and they can also be secreted to the environment as a slime material like the bacterial cellulose produced by *Acetobacter* spp. One of the most important examples of the microbial homopolysaccharides is dextran produced by *Leuconostoc mesenteroides* which has found a wide range of applications in medicine [9]. Several Lactic Acid Bacteria (LAB) also produce homopolymeric EPS which will be discussed in later in this section. **Heteropolysaccharides** are made of repeating units which are composed of two or more types of sugar subunits, substituted sugars and other organic and inorganic molecules [8, 10]. A general example of

microbial heteropolysaccharide is peptidoglycan which is the main component of bacterial cell walls and is composed of the repeating units of N-acetylglucosamine and N-acetylmuramic acid residues.

<b>Bacteria</b>	<b>EPS</b>	<b>Chemical structure</b>	<b>Reference</b>
<i>Pseudomonas aeruginosa</i> , <i>Pseudomonas putida</i>	Alginate	$\beta$ -1,4-linked mannuronic and $\alpha$ -1,4-linked guluronic acids	[11, 12]
<i>Acetobacter xylinum</i>	Bacterial cellulose	$\beta$ -1,4-linked glucose	[13]
<i>Sphingomonas paucimobilis</i>	Gellan	$\beta$ -d-glucuronic acid-1,4- $\beta$ -d- glucose-1,4- $\beta$ -l rhamnose	[14]
<i>Leuconostoc mesenteroides</i>	Dextran	$\alpha$ -1,6-linked glucose; some 1,2-, 1,3-, or 1,4-bonds are also present in some dextrans	[15]
<i>Alcaligenes faecalis</i>	Curdlan	$\beta$ -1,3-glucan	[16]
<i>Xanthomonas campestris</i>	Xanthan	Linear $\beta$ -1,4-glucan backbone with $\beta$ -mannose-1,4- $\beta$ - glucuronic acid-1,2- $\alpha$ - mannose trisaccharide side chain.	[17]
<i>Bacillus polymyxa</i>	Levan	$\beta$ -2,6-fructan	[18]

**Table 1.1.** Examples of principal microbial EPS, their structure and producer organisms.

These structural features as well as the demand for the natural components has led bacterial EPS to gain a special interest in recent years in chemistry, medicine, pharmaceuticals and especially in the food industry [19]. Several functions are attributed to the bacterial EPS such as protecting bacterial cells from desiccation and the environment, antibiotics, phagocytosis, phage attacks and they are also believed to play a role in biofilm formation [1, 20, 21]. Besides the role of EPS at the single cell level, they are widely used in the food industry as viscosifying, stabilizing and emulsifying agents because of their unique physicochemical properties related to their structures [19]. Dextrans, xanthan, gellan, pullulan, yeast glucans

and bacterial alginates are some examples of microbial EPS used in the food industry for decades to improve the physicochemical properties of food formulations [22]. There are many other examples of the technological applications of EPS in food or non-food industries, but this is beyond the scope of this thesis, so it will not be discussed in detail here. Recently, EPS also gained special interest after the recent reports showing that EPS may stimulate and modulate the immune system and they may play a role as antitumor, antiviral, anti-inflammatory and antioxidant agents [23, 24].

Lactic acid bacteria (LAB) are one of the most important groups among bacteria due to the “generally recognized as safe (GRAS)” status of this group and their products and members of this group mainly characterised for the formation of lactic acid as a final product of the carbohydrate metabolism [19, 25]. EPS from LAB are widely used in the food industry to improve the rheological, textural and sensory properties of fermented dairy and pastry products such as yoghurt, cheese and bread [26]. They also confer a mouth feel with an enhanced perception of taste in dairy products, allowing lower fat addition in dairy products formulations, and in addition use of EPS decreases the total cost of food formulations [27]. Moreover, several health claims have been reported for EPS of LAB such as lowering the blood cholesterol [28], immunostimulatory activity [29, 30] and antitumor effects [31].

In the last two decades, the main research interest for the EPS of LAB was related to the identification of new polymers, their structures and biosynthesis mechanism and investigation of their production by dairy starter cultures to improve the rheological and technological properties of dairy products such as yoghurt. Recent developments in the field of EPS have led to a renewed interest in the structure and biosynthesis mechanism of capsular EPS produced by gut commensal bacteria and their role in bacteria-bacteria and host-bacteria interactions.

*Lactobacillus johnsonii* FI9785 is a potential probiotic organism which has been previously shown to act as a competitive exclusion agent [32]. *L. johnsonii* FI9785 has been also previously shown to have an *eps* gene cluster potentially responsible for the production of EPS which may play a crucial role in the exclusion process and other functional properties of this bacterium [33]. The main aim of this thesis was to identify the structure, biosynthesis mechanism and functional role of EPS of *L. johnsonii* FI9785. To facilitate the understanding of the results presented in this thesis, an introduction about the biosynthesis mechanism and functional roles of EPS is included.

## **1.2 *Lactobacillus* in the Food Industry**

Lactobacilli are Gram positive, non-spore forming rods with a low GC content (below 50%) and they are strictly fermentative, aerotolerant or anaerobic showing complex nutritional requirements (carbohydrates, amino acids, peptides, fatty acids, vitamins) which is the main reason for their presence in nutrient rich environments such as fermented food products [25]. *Lactobacillus* is the largest genus of LAB with more than 100 recognised species. Traditionally, like many other LAB they are used in food fermentation with their contribution to the food preservation as well as development of texture and flavour properties in dairy products, fermented vegetables, fermented meats and sourdough bread [25]. *Lactobacillus* species can also be found in many niches including the oral cavities and especially gastrointestinal tracts (GIT) of humans and animals and they have received great attention due to their potential health-promoting properties [34, 35].

## **1.3 *Lactobacillus* as a member of commensal microbiota**

Gut microbiota is the term defining a vast number and collection of microorganisms, mostly bacteria that reside in the human or animal GIT playing a considerable role on host homeostasis, host biochemistry, physiology and immunology [35-37]. There are approximately  $10^{13}$  and  $10^{14}$  bacteria residing in the adult human intestine belonging to at least 500 different species and the number of bacterial cells in human microbiota is 10 times more than the number of cells constituting the human body [36, 38]. *Lactobacillus* strains are one of the first colonizers of human and animal GIT and they constitute approximately 1% of the adult human microbiota [39]. The differences in the physical and chemical properties of the GIT of different hosts (for example avian or mammalian) as well as the variations of these properties within different parts of their GIT results in the existence and development of specific bacterial communities in different hosts and different compartments of GIT such as stomach, small intestine and large intestine [40]. For instance in human GIT the microbial density and diversity increase from the proximal small intestine to the ileum and to the colon, in contrast, the proximal gut of some animals such as crops of chickens have relatively large number of bacteria especially lactobacilli which is likely to be related with the adhesion and ecological properties of special bacterial groups [25, 35].

In recent years due to developments in sequencing techniques genomics of *Lactobacillus* species has been boomed [35] and today 58 genome sequences of *Lactobacillus* species are publicly available (see <http://www.ebi.ac.uk/genomes/index.html>) and this number is likely to

increase. In fact this enabled researchers to take a closer view in order to understand lactobacilli in terms of its adaptation to different environmental niches, their metabolic capabilities and presence of specific gene or clusters that can be important in their colonisation to gut environment. For instance the genome sequences of *Lactobacillus johnsonii*, *L. acidophilus*, *L. gasseri* which are all GIT associated lactobacilli possess high number of proteins with predicted LPXTG motif, which are important for the adhesion to the intestinal mucus and epithelial cells [41]. These examples can be increased for the presence of other adaptation factors such as mucus-binding proteins, EPS and production of antimicrobial components for other lactobacilli strains persisting in GIT of humans and animals.

Several lactobacilli has been determined as autochthonous species which reflect a particular strain that has a particular long-term association with a particular host forming a stable population of characteristic size in a particular region of the gut, and has a demonstrable ecological function [25]. For instance several autochthonous *Lactobacillus* species have been identified in chickens as a host [42, 43] and lactobacilli colonised mainly the crop of poultry GIT and dominated the bacterial population in this particular region of digestive tract [42, 44]. This colonisation was shown to be related to their adhesion capacity and colonisation occurs within hours of hatching and persists throughout the life of the chicken [44, 45]. Several other factors were suggested to affect colonisation of lactobacilli to chicken crop such as the abundance of nutrients, low pH of the crop and relatively aerobic conditions in the crop. Furthermore, it was shown that the microflora of the other parts of the GIT conditioned by the crop microflora [44]. Recent studies demonstrated that members of *L. acidophilus* group and *L. reuteri* were early colonizers whereas *L. salivarius* was shown to be consistently detected in older chickens which can be related with the chicken physiology or dietary conditions establishing throughout the time [25, 42, 43]. Several *Lactobacillus* strains were also shown to be autochthonous species in oral cavities and GIT of human as well as in the GIT of mice, rats and pigs [25].

*Lactobacillus* species are important for animal and human health as they are one of the key members of the gut microbiota. Future research is required in order to identify how lactobacilli confer these characteristics within GIT and this study will explore the potential role of cell surface associated EPS as a surface molecule of lactobacilli cells which may contribute their adhesion and colonisation characteristics.

#### 1.4 Exopolysaccharides (EPS) of Lactic Acid Bacteria (LAB)

LAB are Gram positive bacteria which can occur in a wide variety of habitats, including human and animal gastrointestinal tracts and play a very important role in dairy and other food fermentations [46]. Furthermore, LAB have a GRAS status which strengthens their role in the food industry not only as a starter culture for food fermentations but also as food additives playing an important role in food formulations. Importantly, the vast majority of the commercial probiotics are members of LAB. Probiotics are living microorganisms which, when administered in adequate amounts, confer a health benefit to the host as defined by World Health Organization (WHO).

Several species of LAB including *Streptococcus thermophilus*, *Lactococcus lactis* and approximately 30 *Lactobacillus* strains are shown to produce EPS that are used in the food industry as thickeners, stabilisers, emulsifiers, fat replacers and for other important purposes [1, 8]. LAB are also able to synthesise both homopolymeric and heteropolymeric EPS. Homopolysaccharides of LAB are composed of either glucose units, which has been defined as glucans or dextrans (Figure 1.1), or fructose units described as fructans or levans [10]. The variety of glycosidic linkages and the branching positions of glucose and fructose residues results in unique homopolysaccharides.

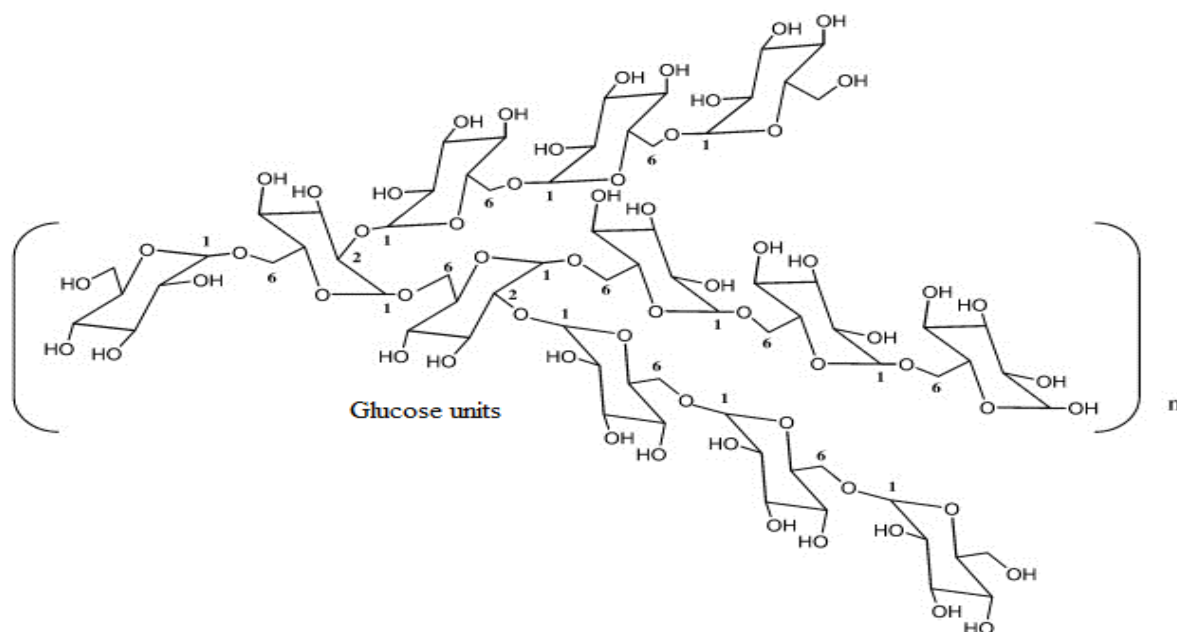


**Figure 1.1.** Chemical structure of homopolysaccharide dextran composed of glucose units produced by *Lactobacillus fermentum*, *L. sakei*, *L. parabuchneri* and *L. hilgardii* [1].

Heteropolysaccharides in LAB also differ in the sugar monomer composition among each species but generally they are composed of three main sugar monomers: galactose, glucose and rhamnose (Figure 1.2) [10]. But the variability of the number of monosaccharides, the linkages between these monomers and the presence of amino-sugars and non-carbohydrate components in the main repeating unit structure of heteropolysaccharides of LAB results in unique EPS produced by different species [1]. It is important to distinguish the capsular EPS of LAB which are tightly attached to the cell surface like an outer layer and extracellular EPS of LAB that are directly secreted to the environment.

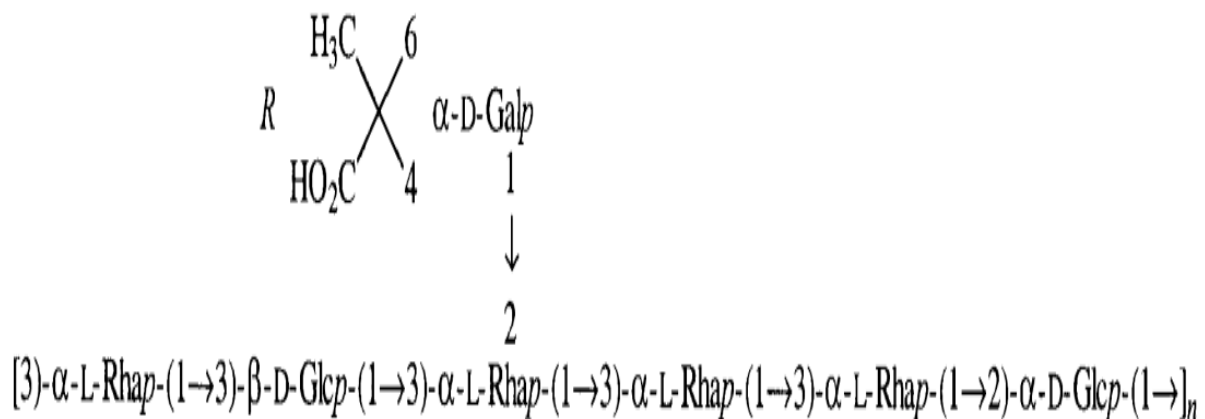


**Figure 1.2.** A typical heteropolymeric EPS structure composed of glucose, galactose and rhamnose units produced by *L. rhamnosus* RW-9595M and R (Glc, Glucose; Gal, Galactose; Rha, Rhamnose and *p*, pyranose) [47].

Until recently, the main focus of interest in EPS of LAB was related to the extracellular EPS as several of them are commercial products such as dextrans that found a wide range of application in chemistry such as gel filtration and chromatography processes (Sephadex columns) and in medicine as blood plasma substitutes (Dextran 70) [1, 48]. EPS of LAB which are viscosifying, stabilizing and emulsifying agents are also in this group associated with food science and the food industry and they have received a lot of attention due to their role on structural and textural properties of fermented and non-fermented food products [46]. Some examples of the primary homopolymeric and heteropolymeric EPS structures of produced by LAB are shown in Figure 1.3.



subsp. *cremoris* B891 [53]; f, *Lactobacillus delbrueckii* subsp. *bulgaricus* 291 [54]; g, *Lactobacillus rhamnosus* GG [55]; *Lactobacillus johnsonii* 151 [56]; *Lactobacillus rhamnosus* KL37B [57] (heteropolysaccharides). Glc, glucose; Gal, galactose; GlcNAc, N-acetyl-glucosamine; Rha, rhamnose; Ac, A, acetyl; *p*, pyranose form; *f*, furanose form; The D- and L- indicate the configuration.

In contrast, the role of cell surface associated (capsular) EPS of LAB has remained unclear; they may play a very important role in bacteria-bacteria and bacteria-host interactions. In fact, the role of capsular polysaccharide formation in pathogenic bacteria has been extensively studied and the pathogenicity of these bacteria was related to the capsule formation which is a natural barrier to phagocytosis [58]. However, the conclusive role of cell surface associated EPS in LAB has yet to be determined. Recently, several reports suggest the potential biological roles of cell surface associated EPS of LAB. The structure of EPS from *L. johnsonii* 142 (Figure 1.4C), a strain isolated from the intestine of mice with inflammatory bowel disease (IBD) was recently identified. The antibodies against *L. johnsonii* 142 whole cells cross-reacted with EPS of *L. animalis*, which was also isolated from a mice with IBD while there was no reaction against the EPS from *L. johnsonii* 151 cells which were isolated from a healthy mouse [59]. This may suggest that the structure of the EPS may have an effect on host responses related to the inflammatory processes in IBD. Additionally, EPS from *L. casei* shirota suppressed the pro-inflammatory responses in macrophages showing an important role of EPS on the host signalling mechanism [60]. In *L. rhamnosus* GG, another well-known probiotic organism, the loss of galactose rich EPS (Figure 1.4B) on the cell surface resulted in increased binding to intestinal epithelial cells possibly due to uncovering of adhesion sites on the bacterial cell surface and this EPS was also shown to play a role in biofilm formation [61].

Similarly the loss of the capsular EPS layer in *L. johnsonii* NCC 533 (Figure 1.4A), which was derived from the human gut, resulted in a slightly increased persistence in the murine gut [62]. Additionally, it was reported that cell surface associated EPS of LAB may contribute to *in vitro* aggregation and *in vivo* colonisation properties [63]. There is a big gap between the knowledge of the role of capsular polysaccharides of pathogenic bacteria in immune modulation [64] in comparison to the role of capsular polysaccharides of commensal bacteria such as LAB. However, recent observations revealed that cell surface associated EPS of LAB and bifidobacteria are also involved in immune modulation activities [65, 66]. The capsular polysaccharides of *L. plantarum* was shown to decrease immune responses of host immune cells [46].

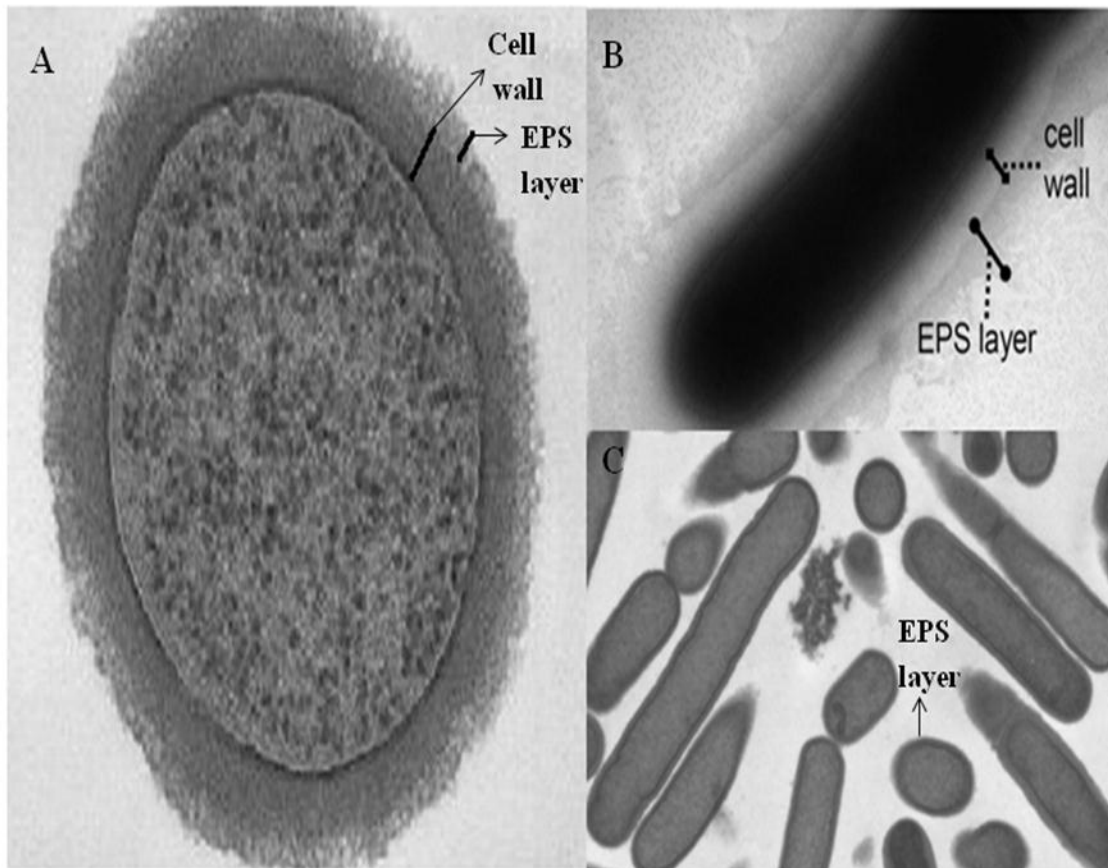


**Figure 1.4.** Electron Microscopy (EM) pictures of EPS accumulation around (A) *L. johnsonii* NCC 533, adapted from Denou et al., [62], (B) *L. rhamnosus* GG, adapted from Lebeer et al., [61] and (C) *L. johnsonii* 142, adapted from Gorska et al., [59], respectively.

Also, it was shown that cell surface associated EPS of *L. rhamnosus* GG may protect bacteria from the innate immune responses such as a host defence peptide LL-37 [67]. Consequently, characterisation of the structures and biological roles of more EPS of LAB will help to understand the role of these biopolymers in the gastrointestinal tract as well as in their probiotic properties.

### 1.5 Cell surface structures of Lactobacilli

The cell envelope of Gram positive bacteria is composed of a thick multilayered peptidoglycan decorated with teichoic acids, polyphosphates, proteins and polysaccharides which has a contribution to the general interactions and characteristics of LAB (Figure 1.5) [20, 68]. Each of these surface macromolecules of LAB have an effect on probiotic action related to host-bacteria interactions [69]. The peptidoglycan layer (PG) is the essential component of the cell wall with the function of preserving the cell integrity and protecting the cell against lysis [20, 70]. Additionally, other cell wall components such as teichoic acids,

lipoteichoic acids, proteins and polysaccharides are covalently or non-covalently attached to the peptidoglycan layer which is the scaffold for these components [70]. The chemical structure of the PG is a polymer of N-acetylglucosamine where the glycan residues are cross-linked by short peptides [71].

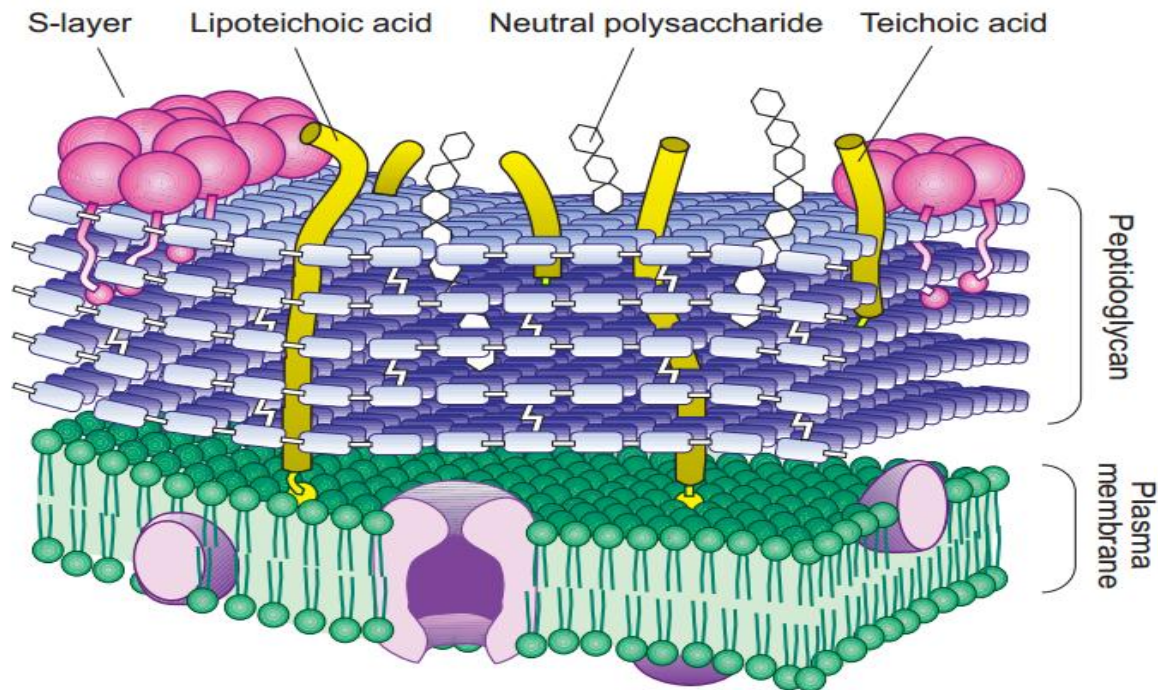


**Figure 1.5.** The architecture of the cell wall of Gram positive bacteria. Reproduced from Delcour et al [71].

The Gram positive cell wall also includes teichoic acids which are anionic polymers that can be either covalently linked to the PG, defined as teichoic acid, or directly attached to the cytoplasmic membrane which also has a lipid anchor, defined as lipoteichoic acid [71]. The basic structure of teichoic acids is composed of polyglycerol phosphate or polyribitol phosphate repeating units but depending on various conditions such as species or strain, stage or rate of growth, pH of the medium, carbon source, availability of phosphate, etc., the structure and abundance of this polymer can be quite different [71, 72]. This variability in structural and abundance properties of teichoic acids results in variability in the physicochemical properties of LAB even at strain level related to probiotic action [20]. Another key component of the bacterial envelope of Gram positive bacteria are cell surface associated proteins which can be large or small and composed of repeating modules or particular domains [20]. One of the important examples of surface proteins is S-layer proteins that form a superimposed surface layer anchored strongly to the PG layer in some LAB [71]. These proteins are usually small proteins that can be glycosylated or non-glycosylated with a

highly basic chemical structure [20, 71]. It was suggested that S-layer proteins could be important in adhesion properties of LAB to the intestinal epithelium and other extracellular matrix components [73, 74]. Some other cell surface proteins were also shown to be involved in adhesion to human intestinal cells and mucins, stimulation of cytokine secretion and mediation of co-aggregation of probiotic bacteria with pathogenic bacteria [75, 76]. Finally, the cell envelope of LAB consists also cell surface associated polysaccharides [20]. As mentioned in the previous section, surface polysaccharides can be either covalently attached to the PG (capsular polysaccharides) or directly secreted to the environment (exopolysaccharides). For LAB generally, the term EPS cover both types of polysaccharides and this term will be used in these thesis for cell surface associated polysaccharides [20]. Structure, level of accumulation and interactions with other surface molecules are such factors that affect the role of cell surface associated EPS in LAB.

### **1.6 Biosynthesis of EPS in LAB**

Many LAB strains produce a wide variety of different homopolymeric or heteropolymeric EPS with different unique structures depending on the nature of the specific glycosyltransferase enzymes responsible for the production of the EPS repeating units. However the basic biosynthesis mechanism of EPS production is highly conserved among LAB [77]. Heteropolymeric EPS biosynthesis in LAB is a complex process that contains specific roles for several gene products that are encoded by *eps* gene clusters, additionally this process also requires the function of several housekeeping gene products [78]. Similarly, the products of housekeeping genes in the cytoplasm is the starting point for homopolymeric EPS production but only a single specific gene product is responsible for their production compared to the heteropolymeric EPS. The specific gene clusters for EPS production are generally located on plasmids for mesophilic LAB genera such as *Lactococcus* and chromosomally located for thermophilic genera like *Streptococcus* and *Lactobacillus* [78]. Additionally the EPS production of *Lactobacillus casei* CG11 was shown to be linked to a plasmid but in another *L. casei* strain the EPS production was suggested to be chromosomally related [79, 80]. The first key element for EPS biosynthesis is glucose-6-phosphate which is the final product of the catabolic sugar degradation in cell metabolism [81] (Figure 1.6).

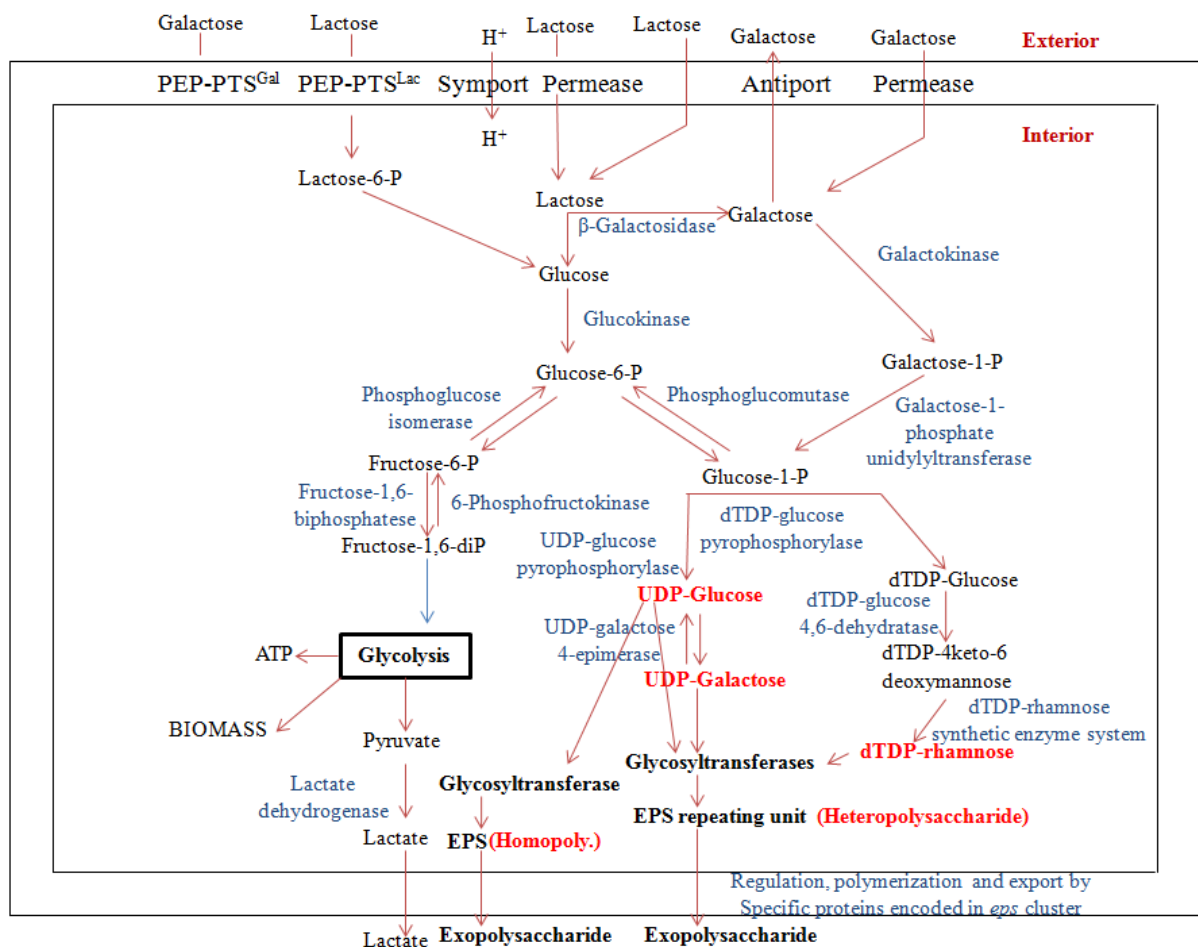


**Figure 1.6.** The detailed schematic illustration of EPS production of LAB via the conversion of lactose, galactose and glucose in cytoplasm. Adapted from [81] with some modifications (PEP-PTS: The phosphoenolpyruvate:carbohydrate phospho-transferase system).

A housekeeping gene product, the enzyme phosphoglucomutase (pgm), then converts glucose-6-phosphate to glucose-1-phosphate [78]. Besides glucose-1-phosphate production, the biosynthesis of the lipid carrier on the inner side of the cell membrane, which is essential for heteropolysaccharide biosynthesis, is another example for the role of housekeeping enzymes in EPS production. This lipid carrier is also involved in assembly of the cell envelope structure such as PG, teichoic acids and lipoteichoic acids [8, 71]. Lastly, the formation of sugar nucleotides from glucose-1-phosphate is an essential process for heteropolysaccharide production in which the housekeeping enzymes are also involved [78] (Figure 1.6), for instance UDP-glucose pyrophosphorylase and dTDP-glucose pyrophosphorylase that converts glucose-1-phosphate to sugar nucleotides UDP-glucose and dTDP-glucose, respectively [81]. Several other genes encoding enzymes for the production of sugar nucleotides have also been identified for other LAB strains [10, 82-85]. For instance,

the *eps* clusters of five *L. rhamnosus* strains were shown to harbour genes responsible for the biosynthesis of a dTDP-rhamnose precursor [61, 85]. These sugar nucleotides are required for the polymerization of monosaccharides and also sugar interconversions (epimerization, decarboxylation and dehydrogenation) to produce other types of monosaccharides for heteropolymeric EPS biosynthesis [10].

After the production of the sugar nucleotides by housekeeping genes or specific genes located in *eps* clusters, assembly of the monosaccharide repeating unit from activated sugar nucleotides and subsequent steps of EPS production occur by the activity of the specific glycosyltransferases and specific enzymes, respectively [10]. These specific enzymes, which are encoded by *eps* gene clusters in LAB, have been identified for several LAB species [86-89]. In addition to the glycosyltransferases, these *eps* clusters also harbour several important genes encoding enzymes related to the regulation of sugar biosynthesis, chain length determination that are responsible for the biosynthesis of repeating unit, polymerization and export [1].

Glycosyltransferases are prokaryotic and eukaryotic enzymes which are involved in the biosynthesis of disaccharides, oligosaccharides and polysaccharides including EPS. These enzymes transfer a sugar residue from donor molecules, which are generally an activated nucleotide sugar but the donor molecules can also be a sugar phosphate or a disaccharide, to the specific acceptor molecules which can be a growing carbohydrate chain or a lipid carrier molecule or a sugar monomer with the formation of a new glycosidic bond depending on the structure of the glycosyltransferase enzyme [90].

If the glycosyltransferase is an  $\alpha$ -glycosyltransferase, the anomeric configuration of the donor sugar residue will be retained with  $\alpha$  linkages or if it is a  $\beta$ -glycosyltransferase, the anomeric configuration of the donor sugar residue will be inverted which will be the result of the  $\beta$ -glycosidic bonds in the final structure [91, 92]. Glycosyltransferases can also be divided into two groups depending on their mechanism of action: processive enzymes which can transfer sugar residues to the acceptor or non-processive enzymes which can only catalyze the transfer of a single sugar residue to the acceptor molecule [90]. These processive and non-processive glycosyltransferases are also responsible for the biosynthesis of the novel repeating unit structures for homopolymeric and heteropolymeric EPS of LAB, respectively.

The first step in the heteropolymeric EPS production is the attachment of the first sugar nucleotide to the isoprenoid lipid carrier, undecaprenyl phosphate, which is attached to the

cytoplasmic membrane of the cell, by the priming glycosyltransferase. This is followed by the sequential addition of the sugar nucleotides by the related glycosyltransferases which are encoded in the *eps* gene clusters to form the repeating unit of the EPS in LAB (Figure 1.7) [10].

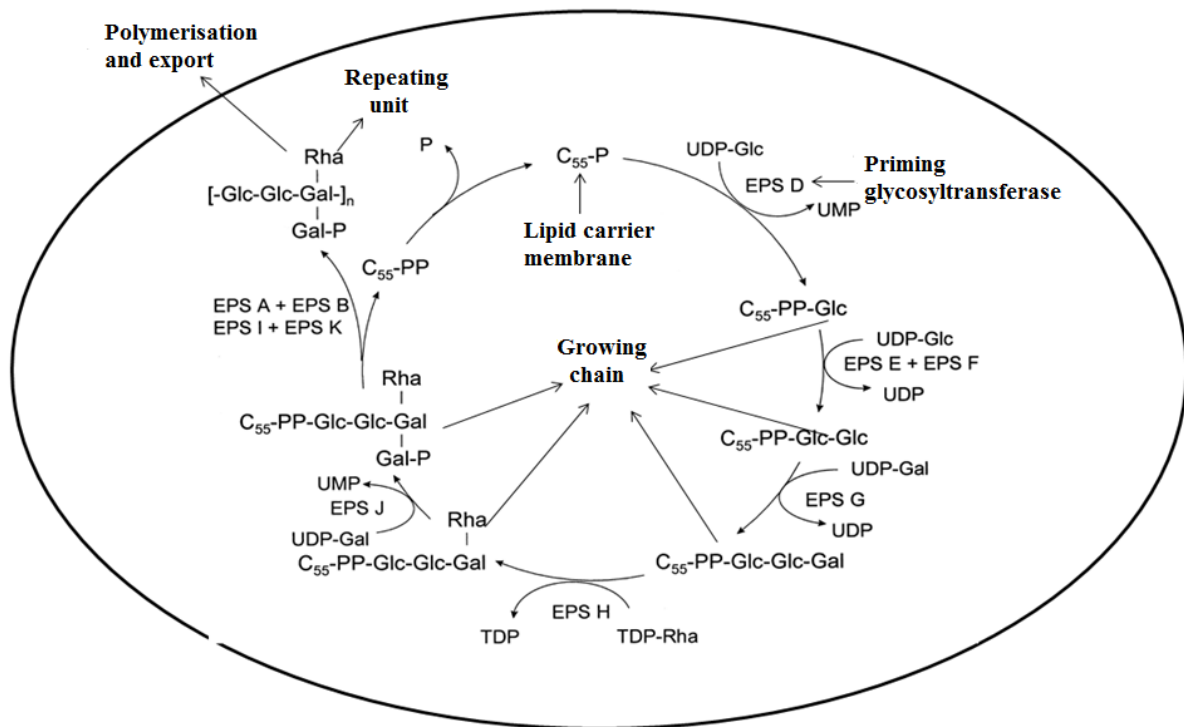


**Figure 1.7.** Model for EPS biosynthesis in *L. lactis* NIZO [87]. Adapted from De Vuyst and Degeest et al., [10].

Specific sugar nucleotides for the repeating unit structure of EPS are assembled by enzymes that can be encoded in specific *eps* clusters or the housekeeping genes of LAB responsible for the interconversion of the sugar nucleotides present in the sugar pool of the cytoplasm [8]. GalE is one of the examples of these enzymes which is a UDP-glucose 4-epimerase that catalyses the interconversion of UDP-glucose and UDP-galactose that are both required for the repeating unit structure of the EPS in *Streptococcus thermophilus* [71, 93].

The next step is the polymerization and export of the repeating unit from the inner part of the cell membrane to the outer part of the membrane. Basically, three different proteins which are also encoded in the *eps* gene clusters carry out the polymerization and export process: firstly, a flippase or a translocase moves the lipid carrier-repeating unit complex from the cytoplasmic face of the membrane to the periplasmic face of the membrane; secondly, a polymerase catalyses the coupling of these repeating units and lastly, a chain length determination protein detaches the lipid carrier-repeating unit complex to stop the

polymerization and export process that also determines the chain length of the final EPS [78]. Several other gene products such as tyrosine kinases also play important roles in the determination of the chain length of the final EPS [94-96]. Then these EPS polymers are directly secreted to the environment as extracellular EPS or remain attached to the cell surface as capsular EPS [10]. In Gram positive bacteria the majority of the capsular EPS remains attached to the peptidoglycan or the membrane components via covalent linkages though some polymers may be released from cell surface [97]. Although the mechanism determining the attachment of EPS to the cell surface or its direct secretion to the environment is not known yet, an outer membrane protein Wzi in Gram negative *E. coli* was shown to be involved in the surface assembly of capsular EPS and absence of this protein resulted in an increase in the amounts of released polymers to the outer environment [98]. The mechanism of the determination of the location of the final EPS in LAB requires further characterisation.

Homopolymeric EPS production is a less complex process. LAB are capable of producing different types of homopolymeric EPS such as dextran, levan, pullulan and reuteran [1, 99, 100]. Dextran was first discovered by Pasteur in the jellification process of cane sugar syrups related to microbial activity, and as a result of the positive rotatory power of the product causing the jellification process, the product was defined with the term “dextran” [101]. The structures of homopolysaccharides in LAB are composed of either glucose or fructose units with different glycosidic linkages and are either linear or with different degrees and types of branching points, with different lengths of monosaccharide chains, molecular mass and conformation depending on the role of glycosyltransferases [101]. The biosynthesis of homopolysaccharides occurs either in the cytoplasm or outside the cell [100]. Internally, the related glycosyltransferases transfer the activated monosaccharide molecules to an acceptor molecule forming a glycosidic bond [1, 8]. The extracellular glycosyltransferases catalyse the degradation of sucrose in the culture medium and they use the energy liberated in the degradation process to transfer the glycosyl residues to the acceptor molecules to form polysaccharides [1]. The intracellular cell wall bound glycosyltransferases may combine two activities: glycosyltransferase activity and the transport activity [102]. Intracellular biosynthesis of homopolysaccharides also requires the function of some housekeeping enzymes which may limit their production [8]. Strains of the genus *Lactobacillus* generally produce dextrans such as glucans or fructans such as levan or inulin type homopolysaccharides and single glycosyltransferases or fructosyltransferases encoded by *gtf*

and *ftf* genes are responsible for glucan and fructan production, respectively, with different linkages depending on the conformation of the each enzyme [1, 63, 99, 103-105]. Microbial glucans can be divided into two groups depending on the glycosidic bonds among glucose units;  $\alpha$ -glucans and  $\beta$ -glucans and several different glucans have been described for LAB. In contrast, only two different fructans, an inulin type with  $\beta$ -(2 $\rightarrow$ 1) and levan with  $\beta$ -(2 $\rightarrow$ 6) linkages, have been characterized for LAB [106]. These GTF and FTF enzymes transfer the monosaccharides and polymerise them with different linkages resulting in the unique homopolysaccharides produced by LAB that play enormously important roles in the food industry.

### **1.7 Genetics of EPS production in LAB**

A single gene is responsible for the homopolymeric EPS production while for the heteropolymeric EPS a specific *eps* gene cluster is required as mentioned in the previous section. Several LAB have been shown to encode the *gtf* or *ftf* genes for the production of homopolymeric glucans and fructans [63, 99, 105, 107-109]. Some LAB can also harbour more than one *gtf* genes in their genome [106]. Based on the cluster analysis of the amino acid sequences of GTFs and FTFs, the latter show high similarity while the similarity among GTFs is lower [106]. This can explain the great variability of the glucan structures among LAB while the fructan structures are quite consistent. The *gtf* genes and enzymes were investigated in six different *Lactobacillus* strains and the location of the *gtf* genes within the chromosome was found to be quite variable for these six strains but the flanking transposase homologues of these *gtf* genes were highly frequent [99]. The same researchers found that all six different GTF amino acid sequences have a common structure consisting of: a) a typical Gram positive signal peptide; b) a very large and highly variable region, deletion of which was shown to not affect the linkage or the molecular mass of the final product [110, 111]; c) a highly conserved catalytic domain which comprises three conserved essential amino acids for enzymatic activity and d) a putative glucan-binding domain [111] (Figure 1.8). This common structure of the GTF enzymes in LAB was also reported previously in which more than thirty GTF enzymes from different LAB were analysed and shown to have the architecture illustrated in Figure 1.8.

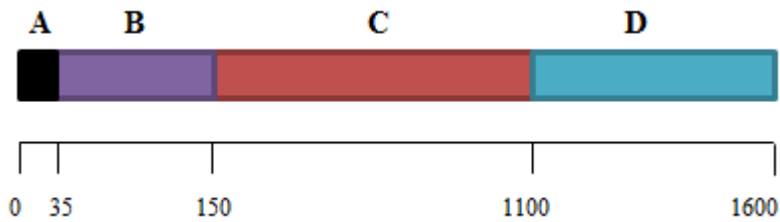


**Figure 1.8.** Schematic representation of the general structure of GTFs; A) N-terminal signal sequence, B) variable region, C) catalytic domain, D) glucan binding domain. Adapted from Monsan et al., [48].

In contrast to the homopolymeric EPS production, the heteropolymeric EPS production requires cooperation of several genes which are encoded in the *eps* gene clusters and is a complicated genetic mechanism, as mentioned in the previous section. To date, several *eps* clusters have been identified for LAB [61, 86-89]. These *eps* clusters harbour conserved genes among LAB which are organised in four functional regions: firstly, a central region composed of specific glycosyltransferases responsible for the biosynthesis of EPS repeating unit; secondly, the region that has the genes for proteins thought to be involved in the chain length determination of the final EPS which is generally located upstream of the central region; a third region which is formed by the polymerization and export genes located downstream of the central region and lastly, the fourth region responsible for the transcriptional regulation of EPS biosynthesis located at the beginning of *eps* clusters (Figure 1.9) [10].

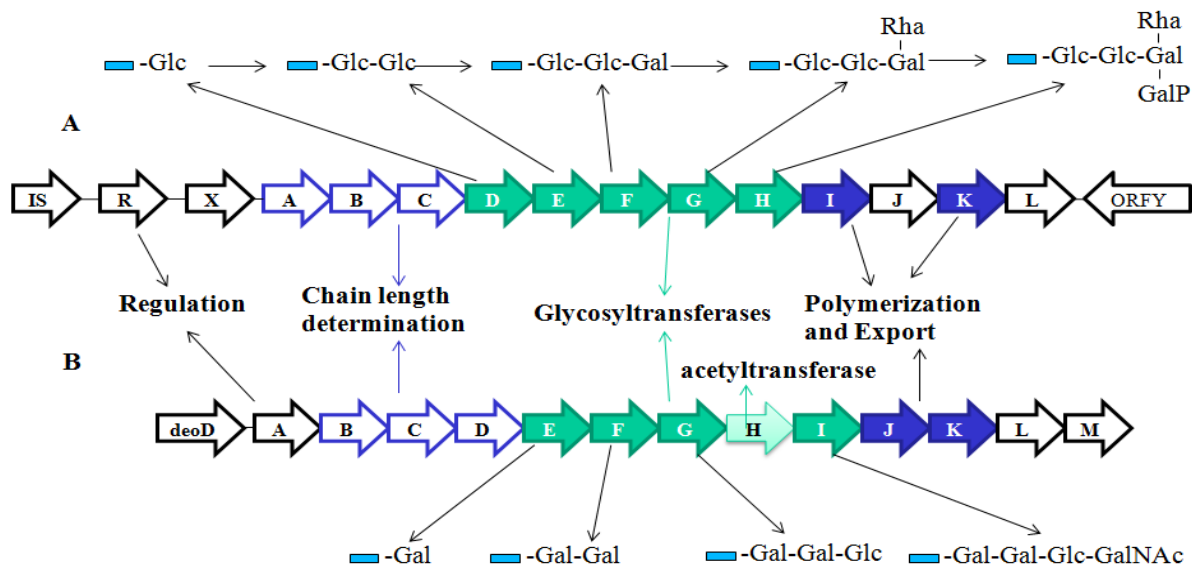


**Figure 1.9.** Organisation of the *eps* gene clusters of (A) *L. lactis* subsp. *cremoris* NIZO B40 [87] and (B) *S. thermophilus* Sfi6 [86] and their putative functional mechanisms.

As mentioned previously these *eps* clusters are generally plasmid-located for *Lactococcus* strains while they are chromosomally located in *Streptococcus* and *Lactobacillus* strains [78]. These clusters are named as *eps* or *cps* clusters reflecting exopolysaccharides or capsular exopolysaccharides and also the names for individual genes in these clusters are defined differently for different strains which make the nomenclature somewhat confusing. The putative functions of the genes are the same and based on their homology but depending on the nomenclature used by the researchers they were named differently. The first *eps* cluster for LAB was described for *S. thermophilus* Sfi6 in 1996, and was a 14.5 kb region with 13 genes (*epsA* to *epsM*) that showed high levels of homology with genes from different organisms related to capsular polysaccharide formation (Figure 1.9) [86]. Later on a 12 kb gene cluster was identified in *L. lactis* NIZO B40 located on a 40 kb plasmid (Figure 1.9) [87]. The orientation of the genes in these *eps* clusters were in same direction and it was shown for the *L. lactis* NIZO B40 strain that the transcription of the *eps* gene cluster occurred as a polycistronic single mRNA [87]. But in a previous study, Stingle et al., showed the formation of different gene groups in the *eps* gene cluster depending on their GC content and each group of genes were preceded by a region containing extremely low GC content and they suggested that the presence of the low GC content regions in different gene groups could be related to different transcriptional units [86]. More recently the *eps* locus of the *Bifidobacterium breve* UCC2003 was identified and two different transcriptional sites designated as *eps1* and *eps2* were demonstrated and more importantly it was shown that the putative priming glycosyltransferase gene and the putative EPS chain-length regulation gene were transcribed as monocistronic mRNAs [66]. In another study comparing the *eps* clusters of four *L. rhamnosus* strains that contain 18 *eps* genes were in the same orientation except for two genes that encodes the putative transcriptional regulator and a putative transposase, respectively and fifteen of these genes were transcribed polycistronically which was in agreement with the previous reports [85]. But the researchers identified five different promoters in the *eps* clusters of *L. rhamnosus* strains, showing the complexity of the regulation of the expression of the *eps* genes [85]. Similar to the transcription of the putative priming glycosyltransferase gene of *B. breve* UCC2003 from its own promoter, it was determined that the putative priming glycosyltransferase genes of *L. rhamnosus* strains were transcribed from their own promoters, suggesting that the independent expression of the priming glycosyltransferase gene may accelerate the initiation of the EPS biosynthesis [85]. These results suggest that in general the orientation of the genes in the *eps* clusters are in the same direction, particularly in lactobacilli, and the transcription of the *eps* gene clusters can

be either as a polycistronic single mRNA or as separate monocistronic mRNAs depending on the genetic structure of the genes in *eps* clusters. Due to the importance of the EPS, researchers focused on the EPS biosynthesis mechanism in different LAB and several gene clusters with the same genetic organization in different LAB have been identified: starting with the regulatory genes for EPS biosynthesis, followed by the genes responsible for the chain length determination and a central region with full of glycosyltransferases for the repeating unit biosynthesis and finishing with the genes related to the polymerization and export [89, 112-114]. Recently, a gene cluster related to cell surface associated EPS was identified in a well-known probiotic strain *L. rhamnosus* GG which shows considerable differences from the gene clusters of LAB and lactobacilli, as this gene cluster harbours specific genes related to the dTDP-rhamnose precursor biosynthesis [61]. In fact previously it was reported that the organisation of the *eps* gene clusters of *L. rhamnosus* strains varies remarkably from lactobacilli but among the *L. rhamnosus* strains, which is also in agreement with the *eps* cluster of *L. rhamnosus* GG, the *eps* clusters are highly similar [85]. Although some differences in the organisational structure of *eps* clusters of LAB were detected, the *eps* cluster of lactobacilli strains show highly similar genetic organisation [77].

Generally, the *eps* clusters of LAB start with a single gene that was identified as the transcriptional regulator “*epsA*”. The role of the transcriptional regulator in EPS biosynthesis was demonstrated for *Streptococcus* strains where deletion of this gene resulted in reduced capsule formation [94, 96, 115]. Also it was shown, in a *Lactococcus* strain, that deletion of the transcriptional regulator from the *eps* cluster, which was located on a plasmid, resulted in complete loss of EPS biosynthesis in this strain [88]. A considerable number of studies have been reported on EPS of *Lactobacillus* species but the data on the role of the transcriptional regulation of the *eps* cluster is lacking. The homology between transcriptional regulator genes in LAB is high, but the actual mechanism of the regulation of the transcription is not yet determined.

In the *eps* clusters of LAB, the *epsA* gene is followed by three genes that act as a complex and are generally defined as *epsB*, *epsC* and *epsD*, responsible for the chain length determination of the final EPS [8]. There is also a lack of information on how this complex *epsB-C-D* works together to determine the chain length of the final product in *Lactobacillus*. However, these three genes show high similarity among different species and *epsB*, *epsC* and *epsD* genes encode for the putative polymerisation and chain length determination protein, putative protein tyrosine kinase and phosphotyrosine-protein phosphatase, respectively [77].

It should be noted that although these genes act as a phosphoregulatory complex but the order of these three genes in the *eps* or *cps* clusters can be different among different species. A number of different organisms (eukaryotes, prokaryotes) have been shown to have protein-tyrosine kinases and phosphotyrosine-protein phosphatases playing important roles in cellular metabolism including EPS biosynthesis [116]. Previously, two proteins of Gram negative *E. coli* were characterized as a protein-tyrosine kinase (Wzc) and as a phosphotyrosine-protein phosphatase (Wzb), respectively. These two proteins exhibited opposing activities: the Wzc protein autophosphorylated on tyrosine residues whereas the Wzb protein dephosphorylated the Wzc and this observation supported the regulatory role of the reversible protein phosphorylation on tyrosine residues on bacterial metabolic processes. The authors proposed that due to the presence of this gene complex in several bacterial species related to their EPS production mechanism, it would be possible that these proteins function in a reversible phosphorylation process which could be a critical action for the EPS production [116]. Similar observations were also detected for the Gram positive bacterial species. The role of *cpsD*, autophosphorylating protein-tyrosine kinase, located in the capsular polysaccharide cluster of *Streptococcus pneumoniae* was shown to be crucial for EPS biosynthesis as deletion of this gene or a mutation in the ATP binding domain in this gene (Walker A motif) resulted in non-capsule formation [96]. It was proposed that Streptococcal *cpsC* and *cpsD* (*epsB* and *epsC*, respectively for *Lactobacillus eps* clusters) interact with each other and ATP binds to this complex and phosphorylates *cpsD* (*epsC*) which results in tyrosine-phosphorylation and *cpsB* (*epsD*) then dephosphorylates this complex which regulates the EPS production and determines the chain length of the final product [96, 117]. The cooperation of these genes to form a complex to determine the chain length of EPS was also proposed for other Streptococcal strains [94, 118]. Although it was shown that the dephosphorylation of *cpsD* is required for capsule formation in Streptococcal strains, another study on capsule formation of *S. pneumoniae* showed that the phosphorylated form of *cpsD* resulted in higher capsule formation [115]. Besides the phosphorylated or dephosphorylated form of *cpsD*, it was shown that inactivation of *cpsC* and *cpsD* in *Streptococcus agalactiae* resulted in reduction of the EPS chain length [94]. In another comprehensive study to show the mechanism of the chain length determination of capsule formation in *S. pneumoniae*, the researchers showed that *cpsB*, *cpsC*, *cpsD* and ATP form a stable complex to regulate the capsule formation [119]. Additionally, mutants that lack the *epsC* and *epsD* encoding the putative polymerisation and chain length determination protein and the protein-tyrosine kinase, respectively, showed no EPS biosynthesis in *S. thermophilus* but the deletion of the

phosphotyrosine-protein phosphatase, *epsB* (*epsD*, for *Lactobacillus eps* clusters) did not terminate the EPS production [120]. The phosphorylation of *epsD* required the *epsC* gene activity and the activity of the priming phosphogalactosyltransferase gene *epsE* was not present in either *epsC* or *epsD* deletion mutants, suggesting that the *epsE* gene may be the target for the phosphorylation complex in this strain [120]. These observations clearly show the role of the regulatory region in *eps* clusters composed of *epsB*, *epsC* and *epsD* genes but nevertheless it is clear that the information on the regulation mechanism of EPS production in the genus *Lactobacillus* requires further investigation.

The central region in *eps* clusters is composed of specific glycosyltransferases responsible for the biosynthesis of EPS repeating units [10]. This region generally starts with the *epsE* gene, which is commonly located just upstream of all glycosyltransferases, that encodes the priming glycosyltransferase in LAB responsible for the addition of the first sugar monomer from an activated sugar nucleotide to the phosphorylated lipid carrier as described above [8, 10, 61, 77, 87, 89, 113, 114]. Additionally the putative priming glycosyltransferase gene in *L. rhamnosus* strains was also reported to be located after the other glycosyltransferase genes [61, 85]. It was shown that deletion of the *epsE* gene, the priming glycosyltransferase gene, resulted in loss of EPS production in several bacterial species [87, 94, 120-122]. In addition, it was shown that deletion of *epsE* gene in *L. rhamnosus* GG resulted in the loss of the galactose rich EPS but a glucose rich EPS was still present on cell surface, suggesting that *L. rhamnosus* GG may produce two types of EPS and the *epsE* gene can be the priming glycosyltransferase for the galactose rich EPS but not for the glucose rich one [61]. Functional analysis of *epsE* genes in several LAB also confirmed the biochemical role of *epsE* as a priming glycosyltransferase that initiates the EPS production by adding a galactosyl-1-phosphate or a glucosyl-1-phosphate to the phosphorylated lipid carrier on the inner face of the cytoplasmic membrane [86, 89, 93, 113]. After the addition of the first sugar to the lipid carrier membrane each glycosyltransferase of the *eps* cluster adds its sugar monomer to the lipid carrier-sugar complex sequentially to form the EPS repeating unit [8].

Downstream of the central region, genes encoding proteins predicted to be responsible for the polymerization and export, mutases and some enzymes with unknown functions are located [8, 61, 71, 93]. A flippase, which is encoded in the polymerization and export region of *eps* clusters of LAB, translocates the lipid carrier linked repeating unit from the inner face of the membrane to the periplasmic face of the membrane [77, 78]. This region harbours another important gene responsible for the polymerization of the repeating units of EPS across the

membrane: the polymerase which attaches the repeating units to form the polysaccharide chains [77]. Although these genes show high homology within the *eps* clusters of LAB, the function of these proteins has not been identified yet for LAB. The last putatively identified gene in the *eps* clusters of LAB is *glf* which is predicted to encode a mutase that catalyzes the interconversion of the sugar nucleotides related to the repeating unit structure of the EPS from the sugar pool of bacteria [46, 61]. Similarly *eps* clusters of *L. rhamnosus* strains were shown to contain genes related to the dTDP-rhamnose precursor biosynthesis related final EPS structure [61, 85]. Finally, the *eps* clusters of LAB harbours several genes with unknown functions [8].

### **1.8 Factors affecting the EPS biosynthesis level of LAB**

EPS from LAB is a very important source of the natural biothickeners and stabilizers of the food industry; however the production levels of these biopolymers are relatively low and very variable and several conditions including medium composition, physicochemical and kinetic parameters may affect the EPS production by LAB [80, 123]. For instance, it was shown that the final yields of the EPS production in four *L. rhamnosus* strains were significantly different changing between 61-1611 mg/l, although they have a similar genetic organization for EPS biosynthesis [85]. It should be noted that there was no alteration in the primary EPS structure of two *L. rhamnosus* strains, which showed different EPS production levels, depending on the carbon source, temperature and fermentation time as previously reported [47]. In contrast it was reported that not only the yield but also the composition of the EPS produced by *L. casei* CG11 altered depending on the carbon source present in the culture medium [124]. Several intracellular and extracellular factors can affect the production levels including media and growth conditions (temperature, incubation time, carbon: nitrogen ratio, pH, other nutrients like vitamins and mineral salts) [8, 10], the availability of sugar nucleotides in basal cell metabolism [125-127], the expression level of genes in sugar catabolism pathways [126, 128], and the carbon source utilised by the bacteria as well as the transcriptional level of the genes responsible for the EPS production [129]. Understanding the factors that can affect the EPS production is highly valuable to engineer the EPS metabolism, to increase the EPS production levels and to modify the EPS structures of LAB. Previously the EPS production of three *Lactobacillus* strains was tested under different conditions and it was found that there was no significant difference in the quantity of EPS production levels depending on having glucose or lactose as a carbon source or fermentation temperature (32 or 37°C) but the EPS production varied among these lactobacilli strains [80]. In another study it

was reported that the EPS production of yoghurt starter cultures altered depending on the pH, temperature and incubation time [130]. Furthermore, degradation of EPS during the incubation period was also reported for several bacterial EPS [131, 132] and Pham et al., reported that the degradation of the EPS produced by *L. rhamnosus* during the prolonged fermentation was due to the function of several glycohydrolases produced by this bacterium [133]. It should be noted that not only understanding the extrinsic factors affecting the EPS production levels but also understanding the role of the genes in the *eps* clusters in EPS biosynthesis, including the repeating unit biosynthesis and determination of the final chain length of these repeating unit blocks, is required to increase the EPS production levels.

Previously, several researchers have studied the EPS production at a genetic engineering level. It was reported that over-expression of the plasmid encoded *eps* gene cluster in *L. lactis* NIZO B40 resulted in a three-fold increase in the expression level of this cluster and a four-fold increase in the final EPS production level, but the growth rate of the over-expression strain was lower than the wild type strain [123]. In fact the lower growth rate in the engineered mutant was in agreement with the fact that the starting elements of the EPS production are the sugar nucleotides, present in the sugar pool of bacteria which are also the source for the bacterial metabolic activities including cell wall biosynthesis, and over-expression of the *eps* cluster might have resulted in over-consumption of these sugar nucleotides by the EPS biosynthesis pathway [123, 127, 134]. Additionally, it was also reported that the EPS production increased without any change in the growth of *L. casei* CG11 and the authors suggested that this might be due to the availability of the isoprenoid phosphate lipid carrier for EPS biosynthesis [124]. Furthermore, the role and the importance of the central sugar metabolism in final EPS yield was reported in *S. thermophilus* LY03 in which the over-expression of the *galU* gene, which encodes the UDP-pyrophosphorylase (GalU), together with *pgmA* gene which encodes the phosphoglucomutase resulted in a nearly two fold increase in the final EPS yield [126]. In a previous study, over-expression of the priming glycosyltransferase in the same strain resulted in a 15% increase in the EPS production level [135]. Similarly, a higher transcription level of the priming glycosyltransferase resulted in increased EPS production in *Bifidobacterium longum* subsp. *longum* strain CRC 002 [129]. Researchers also used genetic engineering to modify the final EPS structure to obtain new rheological properties [1]. It was reported that reducing the transcriptional level of the priming glycosyltransferase gene (*welE*) in *L. rhamnosus* and therefore the level of the priming glycosyltransferase resulted in a lower molecular mass of

the final EPS, which is probably due to the alterations in the determination of the EPS chain length process [136].

Natural mutations can also affect the EPS production depending on which pathway has been affected after the mutation. It was shown that after treatment of *L. sakei* strain 0-1 with the mutagen ethylmethane sulfonic acid, ten mutants that lacked the ropy phenotype were observed, of which eight had lost the normal EPS production; Detailed enzyme analyses revealed that six of these eight mutants could not produce any EPS due to the changes in sugar nucleotide pathways while the reason for non-EPS production for the remaining two was the alterations in the *eps* gene cluster. Additionally, one of these ten mutants started to produce EPS with a different structure. Furthermore, two mutants were still producing the same EPS but the cell morphology of these two mutants were changed; this was proposed to be due to the modification of the cell wall after the mutation [137]. As discussed above one of the important factors that can affect the final EPS yield of LAB is the carbon source. In addition some LAB can produce different EPS structures depending on the utilized carbon source [124] but some of them cannot [138], probably due to the specific role of the glycosyltransferases encoded in *eps* clusters of LAB.

### **1.9 Physiological role of EPS**

Besides the identification of the mechanism of EPS production and novel EPS structures produced by LAB, the physiological role of these biopolymers is an important consideration as EPS is one of the most important structural components of LAB cell envelope. Secondly, they are of interest as an industrial product due to the GRAS status of LAB. One of the main reasons for the usage of EPS of LAB is mainly as a biothickeners to improve the textural properties of food products, to prevent the syneresis of yogurt and other dairy products, to replace high fat containing additives without changing the rheological properties of final product as well as the use of EPS to lower the input costs [10]. Due to these broad applications of EPS, to date several physiological roles of EPS have been determined (Figure 1.10). It was proposed that EPS around cells are thought to play a role in protection of cells against desiccation, antibiotics, bacteriophages, metal ions, antimicrobials such as nisin and lysozyme, osmotic stress, phagocytosis, macrophages and they are also thought to increase the adhesion capability of cells to solid surfaces [10, 139, 140] and importantly, they are shown to play a role in biofilm formation [63, 141, 142]. In addition to the essential protective role of EPS for the producing LAB themselves, several reports attribute to the

positive role of EPS on the human health. It was suggested that the positive effect of the fermented milk products on human health could originate from the EPS produced by LAB [31]. For instance EPS can function as prebiotics, which are non-digestible food ingredients that can stimulate the growth and/or activity of the gut microbiota in ways claimed to be beneficial to host health maintenance [143]. Several carbohydrates are now being used as prebiotics but they are generally oligosaccharides that are composed of 2-20 monomers depending on their source. The health promoting bacteria can digest them and use them as a carbon source which increases their potential to compete against pathogenic organisms [1]. Korakli and coworkers have successfully showed the potential prebiotic effect of a fructan type EPS produced by *L. sanfranciscensis* [144]. Although EPS of LAB can stimulate the growth of other bacteria in the GIT, they are not able to catabolize the EPS polymers that they produce as an energy source for their cell metabolism [145]. But it was shown that glycohydrolases presented in the bacterial cell extracts of *L. rhamnosus* R were responsible for the degradation of the EPS produced by this bacterium in the prolonged fermentation process although the catabolisation of the liberated products was not shown [133]. Moreover, it was reported that EPS of LAB contribute to human health with their antitumor, antiulcer, immunomodulatory or cholesterol-lowering functions [10, 140]. The proposed mechanism of the antitumor or the anticarcinogenic activity of EPS is the mediation of the immune system which results in the prevention of tumor proliferation in host cells [140]. In fact, most of the potential health promoting effects of EPS are related to the host-bacteria interactions and one of the important role of EPS in this interaction is the modulation of the immune system of the host, which is dependent on the structure and characteristics of EPS produced by LAB or other commensal bacteria such as bifidobacteria [65].

The role of the cell surface components including LPS (lipopolysaccharide) and EPS from pathogenic bacteria on host immune responses have been shown in numerous reports. But the role of the cell surface associated EPS from commensal bacteria on immune functions have only gained special interest in the last decade after the identification of *eps* gene clusters and the availability of the mutants that show different EPS characteristics compared to their parental strains and several reports have been published on this issue. One of these reports shows the role of EPS from probiotic *L. casei* shirota on immune modulation [60]. The researchers compared the WT cells, where a high molecular weight surface polysaccharide covers the cell surface, with the *eps* genes knock-out mutants, in which less EPS covers the cell surface, for their effect on the induction of cytokines in mouse macrophage cell line.

They found that the mutants with reduced EPS were able to induce higher amounts of cytokines than WT cells which suggested the immune-silencing effect of EPS [60]. Similarly, this effect of EPS was also shown in wild type *L. plantarum* cells compared to the non-EPS producing cells [46] and for *L. rhamnosus* RW-9595M where the authors concluded that EPS induced immune suppression by the production of macrophagic anti-inflammatory interleukin (IL)-10 [146]. In another study, an EPS<sup>+</sup> *L. paraplantarum* strain showed less immune responses compared to EPS<sup>-</sup> mutants [147]. Recently, a similar pattern was observed for *B. breve* UCC2003 cell surface associated EPS [66]. In this study, the EPS<sup>+</sup> wild type strain showed significantly lower levels of pro-inflammatory cytokines compared to the isogenic *B. breve* EPS<sup>-</sup> mutant which supports the role of the EPS of commensal bacteria on suppression of host immune responses [66].

Besides the immune silencing effect of EPS, several other reports also showed the immunomodulatory effects of EPS where EPS can stimulate the immune responses depending on its structure [148-151]. For instance it was reported that the phosphorylation of EPS which results in a negatively charged polymer from *Lactobacillus delbrueckii* subsp *bulgaricus* have been shown to be required for lymphocyte activation [31]; similarly it was shown that artificial phosphorylation of a dextran from *Leuconostoc mesenteroides* increased its immunostimulatory potential [152]. Furthermore it was reported that the de-phosphorylation of EPS from *L. delbrueckii* subsp *bulgaricus* reduced the mitogenic activity of the EPS in lymphocytes [31]. Based on these observations it was proposed that EPS which are negatively charged or small in size could mildly stimulate the immune cells, whereas the non-charged EPS and large in size could suppress the reaction of immune cells [65].

Another physiological role of cell surface associated EPS is their protective role against antimicrobials and antibiotics and also their role under harsh conditions such as acid and bile conditions. It was shown that EPS produced by *Lactococcus lactis* was required for the protection of cells against bacteriophages, lysozyme and antimicrobial nisin whereas EPS did not show any protective effect against the increased temperatures, freezing, freeze-drying or antibiotics penicillin and vancomycin [139]. Similarly, the EPS layer of *B. breve* UCC2003 was shown to have a protective role against low pH and bile salts [66]. Although there are numerous reports about the identification of new EPS and the technological functions of LAB, the potential protective role of EPS against harsh conditions has not been determined in detail. Additionally, EPS from different commensal bacteria have also reported for their potential antioxidant properties [19, 151, 153].

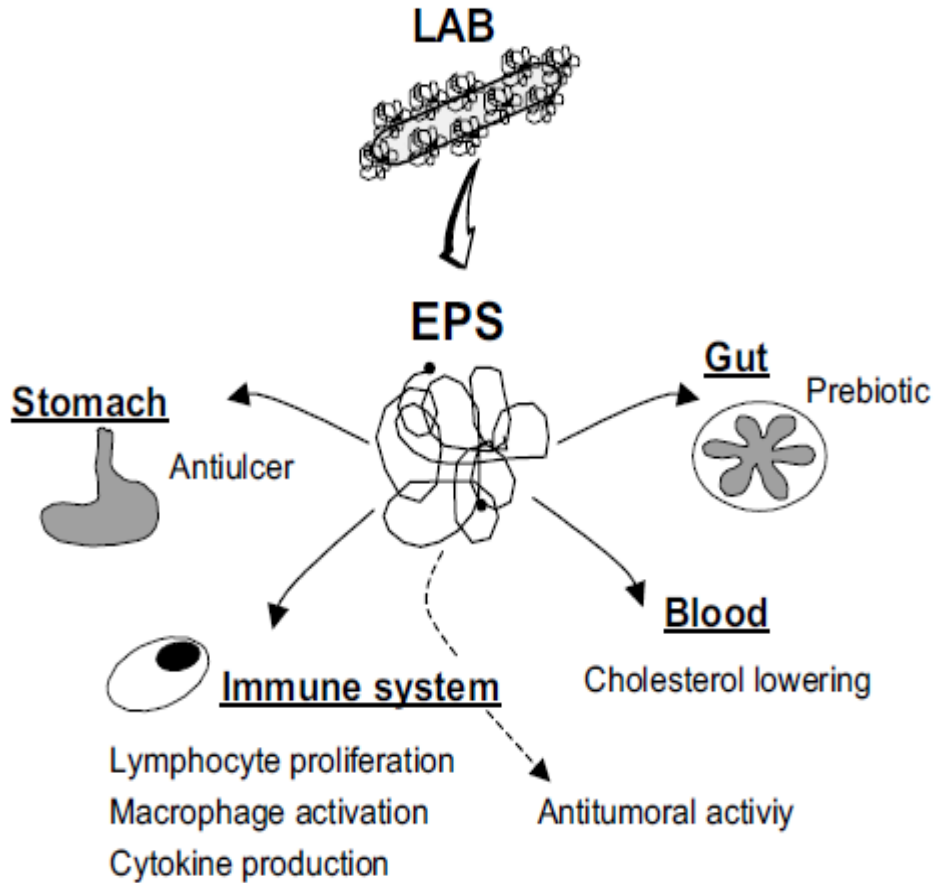


**Figure 1.10.** Putative health-promoting effects of LAB exopolysaccharides. Adapted from Ruas-Madiedo et al., [140].

Biofilm formation has also gained special interest for probiotic bacteria, although the main research on bacterial biofilm formation is still to understand how pathogenic bacteria form biofilms in order to eliminate them. Bacterial biofilm formation is a step by step process which occurs by aggregation of bacteria to form a multicellular matrix consisting of a mixture of polymeric compounds including extracellular DNA, proteins and polysaccharides [154]. EPS are the main components of bacterial biofilms and constitute 50-90% of the molecules in biofilms depending on the type of microorganisms, age of the biofilms and the environmental conditions [155]. EPS also determine the architecture of the bacterial biofilms [156]. These biofilms are far more protective for bacteria than at the single cell level to the harsh environmental conditions such as bacteriophages, host immune responses and antibiotics [154].

Biofilm formation of LAB can be directly related to the colonisation and survival properties which are important features that any probiotic bacteria should possess. It was reported that probiotic *L. reuteri* was able to produce biofilms which showed immunomodulation effects

and also showed different levels of the antimicrobial reuterin production and the authors proposed that biofilm formation also has to be considered as a criterion for being probiotic [157]. Bacterial aggregation ability is very important for the biofilm formation process [158]. It was shown that EPS produced by *L. reuteri* TMW1.106 determined the autoaggregation and *in vitro* biofilm formation properties of this bacterium, which were shown to be directly related [63]. In this study, the disruption of the glycosyltransferase gene (*gtf*) altered the *in vivo* colonisation ability of the mutant strain compared to the wild type strain while disruption of the fructosyltransferase (*ftf*) gene did not change the colonisation ability of the mutant strain. Similarly, in *L. reuteri* 100-21 the *ftf* mutant was able to form biofilms as wild type strain on the forestomach epithelial surface [142] which may show that biofilm formation in *L. reuteri* strains may be independent from the fructan-like EPS.

Biofilm formation analysis in *L. rhamnosus* GG demonstrated that EPS can be involved in this process but the effect of EPS in biofilm formation was more likely to be medium dependant [141]. The authors proposed that not only the level of EPS production but also the compositional and conformational properties of cell surface associated EPS including the polymer size might also affect the biofilm formation.

More studies are required to understand the biofilm formation of LAB and the role of EPS in this process to determine the interaction of biofilm formation with host health maintenance. It has to be mentioned that not only the EPS from Gram positive bacteria like LAB but also EPS from Gram negative symbiotic commensal bacteria was shown to play a role in maintenance of the human health via different mechanisms. One of the important examples of EPS producing Gram negative commensal bacteria is *Bacteroides fragilis* and several reports showed the role of cell surface associated EPS of this bacterium on host health. Interestingly, it was shown that the capsular polysaccharide A (PSA) of *Bacteroides fragilis* was protective against central nervous system demyelinating disease which can cause deficiency in sensation, movement, cognition, or other functions depending on which nerves are involved [159]. Similarly, the same EPS was also shown to be protective against intestinal inflammation by regulating IL-10-production [160]. More recently, it was reported that capsular polysaccharide A (PSA) can function as an activator of the intestinal sensory neurons and it was found that PSA was necessary and sufficient for the neuronal effects [161].

## 1.10 Mechanism of cell adhesion in LAB

Bacterial adhesion to the gastrointestinal tract is a complex process which is a contributing factor for probiotic properties. Additionally, it is also the initial step for the biofilm formation and colonisation of the pathogenic bacteria. In general, factors related to the cell surface envelope that determine the adherence mechanism of LAB can be divided into two main groups as specific and nonspecific factors. The specific factors affecting the adhesion of LAB are mainly surface proteins which are specific adhesins such as mucus binding proteins (MUB), sortase-dependent proteins, S-layer proteins, proteins interacting with the extracellular matrix components of the intestinal cells [162]. The mucus layer which covers the intestinal epithelial cells protects the host from the attachment of pathogenic and harmful bacteria but it also forms a habitat for commensal bacteria for a short residence time [162]. It was reported that mucus binding proteins of *L. reuteri* strains contribute to the *in vitro* adhesion and aggregation properties [163, 164]. Besides mucus binding proteins, the involvement of S-layer proteins in the adhesion process of lactobacilli, where they comprise 10-15% of the total protein of bacterial cells [165], were demonstrated for several species [166, 167]. Also the surface characteristics of lactobacilli can be related to the structure of the S-layer proteins [168]. Buck and co-workers suggested that the involvement of the surface proteins in the adhesion can be either their direct adherence to the epithelium or their attachment to surface components of the epithelial environment like fibronectin and they reported that the fibronectin-binding protein, mucus binding protein (MUB) and S-layer protein, each contribute to the adhesion of *L. acidophilus* NCFM, individually [73]. A recent study demonstrated that deletion of the housekeeping sortase gene that is involved in the covalent attachment of sortase-dependent proteins to the peptidoglycan layer significantly decreased the adhesion of *L. plantarum* strain to the human vaginal epithelial cells [169]. Similarly, a novel surface protein elongation factor Tu was shown to be important for the attachment of *L. johnsonii* NCC 553 to intestinal epithelial cells and mucoproteins [170]. Another surface protein of *L. johnsonii* NCC 553, GroEL, was also reported for its contribution in adhesion to mucus and epithelial cells [76]. Introduction of a MUB protein to the cell surface of *Lactobacillus casei* increased its adhesion ability to Caco-2 cells compared to its parental strain that lacks this protein [171]. All these examples suggest the role of surface proteins as a specific factor for the adhesion of LAB to epithelial cells. Similarly cell surfaces of lactobacilli cells including *L. johnsonii* La1 were shown to contain lectins or specific adhesins that recognise specific glycoconjugates on intestinal epithelial cells, which

are also proteinaceous components affecting the adhesion properties as a specific factor [172-174].

Another specific factor for the determination of the adhesion of bacteria is the electrostatic interactions between the cell surface and the epithelial cells, in which physicochemical properties of *Lactobacillus* cells play an important role. The physicochemical characteristics of cell surfaces of lactobacilli are generally determined with Zeta potential and cell surface hydrophobicity measurements [175]. The overall net charge and physicochemical properties of bacteria are determined by the composition and the structure of cell surface components and these components may affect these properties individually [176]. Zeta potential can be described as the net cell surface charge of bacteria which is the electrical potential between the bacteria and the aqueous environment interfacial region [177]. Similarly, bacterial hydrophobicity which is determined by the cell surface components and their degree of freedom on cell surface affects the adhesion properties of probiotic bacteria [175]. The evaluation of the zeta potential and the cell surface hydrophobicity reflects the composition of the cell surface of lactobacilli. For instance, high zeta potential values and high hydrophobicity demonstrates the dominant effect of cell surface proteins in the determination of cell surface characteristics while weak electrical charge or low hydrophobicity indicates the covering of cell surface by polysaccharides [175]. Also extracellular environmental conditions such as pH contribute to the physicochemical properties and adhesion of *Lactobacillus* cells [176].

In general the nonspecific factors determining the adherence capacity of bacteria to the gastrointestinal tract include nonspecific adhesins that are located on the bacterial cell surface such as LTA, LPS, EPS and pili (also called fimbriae). In fact it was shown that pili, that are lengthened filamentous protein structures, determine the adhesion and biofilm formation properties of *L. rhamnosus* GG cells specifically to the mucus and intestinal epithelium cells which can also be assigned as a specific factor for the adhesion of lactobacilli cells [178, 179]. Nevertheless future reports would identify the interaction between surface components of probiotic lactobacilli and epithelial cells and mucus which will help to distinguish these factors as specific or nonspecific. It was reported that LTA present at the cell surface of *L. johnsonii* La1 is involved in the adhesion to Caco-2 intestinal cells and the authors suggested that the role of LTA was probably due to the electrostatic role of this molecule on the net charge of *L. johnsonii* La1 [180]. LPS was also shown to be important in Gram negative bacterial adhesion which will not be discussed further. EPS accumulation on the cell surface

of bacteria was also proposed as an important factor for bacterial adhesion [181]. It was shown that EPS from probiotic bacteria could increase their adhesion properties, although the role of EPS was dose and structure dependant [181]. Although EPS on cell surface is an important attachment site for bacteria and affects the adhesion, there is no clear fundamental principle of how EPS play a role in this process. For instance, Denou et al., [62] showed that the loss of capsular EPS layer of *L. johnsonii* NCC 533 increased the gut persistence time of this strain. The authors pointed out that the alteration of cell surface charge after the loss of EPS layer might have led to the increased persistence time. In another study, it was shown that lower EPS accumulation on the cell surface of *L. rhamnosus* GG resulted in increased adhesion to pig mucus and Caco-2 cells compared to the parental strain and the authors suggested that in wild type *L. rhamnosus* GG, EPS covers the proteinaceous surface adhesins and reduction in this coverage resulted in an increased adhesion [61]. The reduction in the adhesion due to the coverage of surface adhesins by CPS was also reported in other bacteria [182, 183]. In contrast, Walters et al., [63] observed that loss of the homopolymeric EPS production after the disruption of *gtf* and *ftf* genes of *L. reuteri* negatively affected colonisation, autoaggregation and biofilm formation. In another study, the researchers showed that the non-EPS producing mutant of *L. reuteri* 100-23 was still able to colonise mice in the absence of the competition with wild type while in the competition with wild type its colonisation was significantly decreased [142]. Similarly, it was shown that EPS production in Bifidobacteria resulted in long persistence time and facilitated colonisation compared to the non-EPS producing strains [66]. It is clear that EPS affects the adhesion properties of probiotic bacteria depending on several factors such as its structure and its production level but the main factor of the EPS on this effect can be its contribution on the overall physicochemical properties and its coverage of the proteinaceous cell surface adhesins.

Apart from the specific or nonspecific factors related to the surface components and surface characteristics, biofilm formation and autoaggregation properties, which themselves determined by the surface components, play a role in bacterial adhesion properties of lactobacilli. Bacterial biofilm formation requires the attachment, adhesion and aggregation of single cells to form a multi-cellular environment which is related to cell surface characteristics. There are several reports showing the *in vitro* biofilm formation process of *Lactobacillus* cells [141, 184-186]. Although the *in vitro* processes have been characterized the *in vivo* mechanism of biofilm formation is less well understood [187]. It should be noted

that a high number of lactobacilli cells in the gut environment also produce EPS [188] and EPS are involved in the biofilm formation process [154, 156] which may improve colonisation and aid survival [62, 63, 157]. A recent *in vivo* study showed that a homopolymeric EPS production did not alter the biofilm formation of *L. reuteri* 100-23 compared to its wild type parental strain on the forestomach epithelial surface in a *Lactobacillus*-free mouse model [142]. The structure of the EPS and their role in determining the surface characteristics can be very unique for different species, so to understand the exact mechanism of EPS on *in vivo* biofilm formation properties more studies are required. In addition to biofilm formation autoaggregation, which is the ability to form multicellular aggregates, could also be important in the adhesion and colonisation of probiotic strains [189, 190] and it has been suggested that EPS may contribute to the aggregation properties of LAB [63]. In addition to affecting colonisation, aggregation of probiotic strains is important for their ability to inhibit the adherence of pathogenic bacteria to the gastrointestinal tract [191]. There is some evidence for the role of EPS in aggregation of probiotic bacteria but the fundamental surface component affecting the aggregation properties is cell surface proteins, particularly aggregation promoting proteins [191-193].

### 1.11 Description of *Lactobacillus johnsonii* FI9785

*L. johnsonii* is a member of LAB and belongs to the Bacilli class which is a major group in the *Firmicutes* phylum that dominates the gut microbiota together with the Gram negative Bacteroidetes [194] (Figure 1.11).

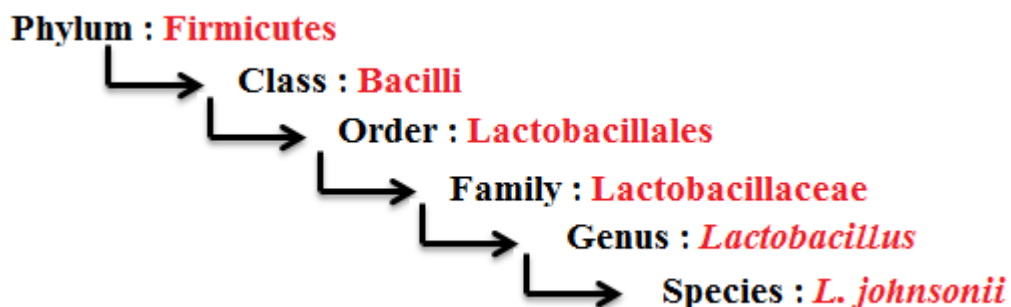


**Figure 1.11.** Phylogenetic classification of *L. johnsonii* FI9785.

*L. johnsonii* FI9785 is a mesophilic Gram positive microorganism which belongs to the lactic acid bacteria group (LAB). This strain, a poultry isolate, has been extensively studied at Institute of Food Research (IFR) for its probiotic-associated activities. Furthermore, *L.*

*johnsonii* FI9785 was defined as a competitive exclusion agent against *Clostridium perfringens* in poultry *in vivo* and also showed limited activity against *Escherichia coli* O78:K80 although it did not exclude *Salmonella enterica* serotype enteritidis [32]. In this study the activity of culture supernatant of *L. johnsonii* was tested against these pathogens but no difference were recorded in their numbers compared to the control group suggesting the potential role of *L. johnsonii* was not related with production of antimicrobial components against pathogens. Pre-dosing pathogen free chicks with *L. johnsonii* and their challenge tests with *S. Enteritidis* showed that there was no alteration in the recovery of this pathogen for all of the GIT tissues whether chicks dosed with *L. johnsonii* or not. This was also the case for *E. coli* O78:K80 in which no difference was detected between the number of *E. coli* O78:K80 in control group and *L. johnsonii* pre-dosed group although there was a trend towards the decrease of this pathogen in *L. johnsonii* group which was found to be statistically insignificant. However shedding *E. coli* O78:K80 with cloacal swabbing showed that the number of *E. coli* O78:K80 was reduced significantly compared to the control group after 1 day of challenge but for the rest of shedding time points the decrease in the recovery rates of this pathogen was insignificant. The pathogen challenge study for *C. perfringens* showed a clear decrease in the recovery of this pathogen from different parts of GIT of *L. johnsonii* pre-dosed chicks compared to the control group and most importantly after 5-6 days of pre-dosing there was significantly lower shedding from birds pre-dosed with *L. johnsonii* through the 36 days of post inoculation period [32]. These results showed that a single oral dose of  $1 \times 10^9$  CFU of *L. johnsonii* FI9785 reduced the colonisation and persistence of *C. perfringens*. The authors suggested that the effect was a result of competitive exclusion and competition for the bacterial receptor sites of epithelial cells related with the adhesion properties of *L. johnsonii* might be the reason for this exclusion [32]. However the information on the surface properties related to attachment to epithelial cells and the mechanism of the adhesion is not fully understood. Preliminary information derived from naturally occurring mutants lacking the surface polysaccharide indicates that EPS production may play a role in the colonisation capability of this strain. The complete genome of FI9785 has recently been sequenced and a gene cluster (14.9 kb) with 14 putative *eps* genes which may be responsible for the bacterial EPS biosynthesis has been identified [195]. Bioinformatic analysis of this cluster indicates the presence of genes which may encode novel glycosyltransferases suggesting that EPS production in this bacterium may have unique structural and functional characteristics.

Besides *L. johnsonii* FI9785, several other *L. johnsonii* strains have had their genomes sequenced and complete annotated genome sequence is available for NCC 533 which is a human isolate (Genbank accession number [AE017198.1](#)), and DPC 6062 which is a porcine isolate (Genbank accession number [CP002464.1](#)). Additionally, the draft genomes of four other *L. johnsonii* strains are also available including ATCC 33200 (human isolate), pf01 (piglet isolate), 135-1-CHN (human isolate) (see <http://goo.gl/I0wg5r>). *L. johnsonii* is a member of the acidophilus complex which comprises a number of *Lactobacillus* strains which are thought to be involved in probiotic action and the numbers of the genome identification studies show the importance of *L. johnsonii* strains for their potential probiotic applications. Member of this complex have been extensively studied for their attachment to epithelial cells, immunomodulation potential and their role in competitive exclusion of pathogens which represent their probiotic activities [196] and all these potential roles are directly related to the surface components including EPS. Table 1.2 shows some of the probiotic related actions of *L. johnsonii* strains.

<b>Strain of <i>L. johnsonii</i></b>	<b>Probiotic action</b>	<b>Reference(s)</b>
FI9785	Competitive exclusion agent	[32]
La1	Immune modulation	[197, 198]
NCC 533	Immune modulation and colonisation	[199]
La1	Inhibition of pathogens	[200]
N6.2	Reduction of the incidence of diabetes development	[201]
MH-68, La1	Reducing the risk of <i>Helicobacter pylori</i> infection	[202, 203]
F0421	Inhibition of <i>Shigella sonnei</i>	[204]
VPI 11088	Inhibition of <i>Enterococcus faecalis</i>	[205]
CRL 1647	Beneficial role for honeybee colonies	[206]
N6.2	Immune modulation	[207]
La1, NCC 533	Antimicrobial activity against pathogens	[208, 209]

**Table 1. 2.** Strains of *L. johnsonii* with reported probiotic actions.

One of the main aims of researchers in the field of probiotic bacteria is to identify novel strains that may have some beneficial effects on their hosts including human. Some of the current *in vitro* tests to evaluate and select probiotic organisms are: resistance to gastric acidity, bile acid resistance, adherence to mucus and/or human epithelial cells and cell lines, antimicrobial activity against potentially pathogenic bacteria, ability to reduce pathogen adhesion to surfaces [210]. All these tests can be directly related to the production of EPS and their accumulation on cell surface of probiotic bacteria. EPS have been shown to play a role in protecting bacterial cells against antibiotics and bile salts as an outer layer [21, 211, 212]. Similarly, it was shown that EPS production increased the survival of LAB under harsh conditions evaluated in an *in vitro* gastric model [213]. EPS production can increase the tolerance of LAB to antimicrobial substances such as nisin [139]. Several reports also showed the importance of EPS production in adherence of bacteria to human epithelial cells and cell lines [61]. EPS were also shown to play an important role in biofilm formation which can be related to the ability to reduce pathogen adhesion to surfaces [154].

### **1.12 Genetics of EPS production in *Lactobacillus johnsonii* FI9785**

The genome sequence of *L. johnsonii* FI9785 has been sequenced previously [195] and a gene cluster (14.9 kb) containing 14 genes (ORFs) that putatively encode proteins involved in the biosynthesis of EPS has been characterized as “*eps*” gene cluster (Figure 1.12). All the genes in this cluster are located in the same orientation. This gene cluster of *L. johnsonii* FI9785 is a typical gene cluster for heteropolymeric EPS production [33]. According to the protein BLAST analysis, the first gene in the *eps* cluster of *L. johnsonii* FI9785 is predicted to encode a protein which putatively functions as a transcriptional regulator which corresponds to the fact that the region responsible for the regulation of EPS biosynthesis is commonly located in the beginning of *eps* clusters of LAB [10]. The *epsA* gene encodes a protein which has a predicted amino acid sequence with homology to the putative transcriptional regulator of *L. johnsonii* NCC 533 (Table 1.3). In addition *epsA* protein consists a conserved domain, *lytR\_cpsA\_psr*, which is a cell envelope-related function transcriptional attenuator common domain, supporting its role as a putative transcriptional regulator. The second ORF in the *eps* gene cluster designated as “*epsB*” shows 91% amino acid identity with the polymerization and chain length determination protein of *L. johnsonii* ATCC 33200 and also shows 90% amino acid identity to the tyrosine-protein kinase trans-membrane modulator of *L. johnsonii* pf01 and is described as the polymerization and chain length determination protein [33]. After *epsB* the *eps* cluster of *L. johnsonii* FI9785 continues with two genes, *epsC* and *epsD*

which are predicted to encode a tyrosine protein kinase and a protein-tyrosine-phosphate phosphohydrolase respectively, homologues of which were shown to be involved in the determination of the chain length of the final EPS via forming a complex with *epsB* in streptococci as described earlier [33].

Similar to the regulation region at the beginning of the *eps* cluster, downstream of this region contains the three genes, *epsB*, *epsC* and *epsD*, encodes the proteins for the chain length determination of final EPS in accordance with the typical *eps* clusters of LAB [10]. In addition to the first two regions, the central region of the *eps* cluster of *L. johnsonii* FI9785 contains six genes that encode putative glycosyltransferases responsible for the actual biosynthesis of EPS repeating unit [33]. This central region starts with the *epsE* which displays 96% identity to the phospho-glycosyltransferase of *L. johnsonii* ATCC11506 and described as an undecaprenyl-phosphate galactosephosphotransferase which putatively encodes the priming glycosyltransferase that transfers the first sugar monomer from an activated sugar nucleotide to the lipid membrane carrier [33].

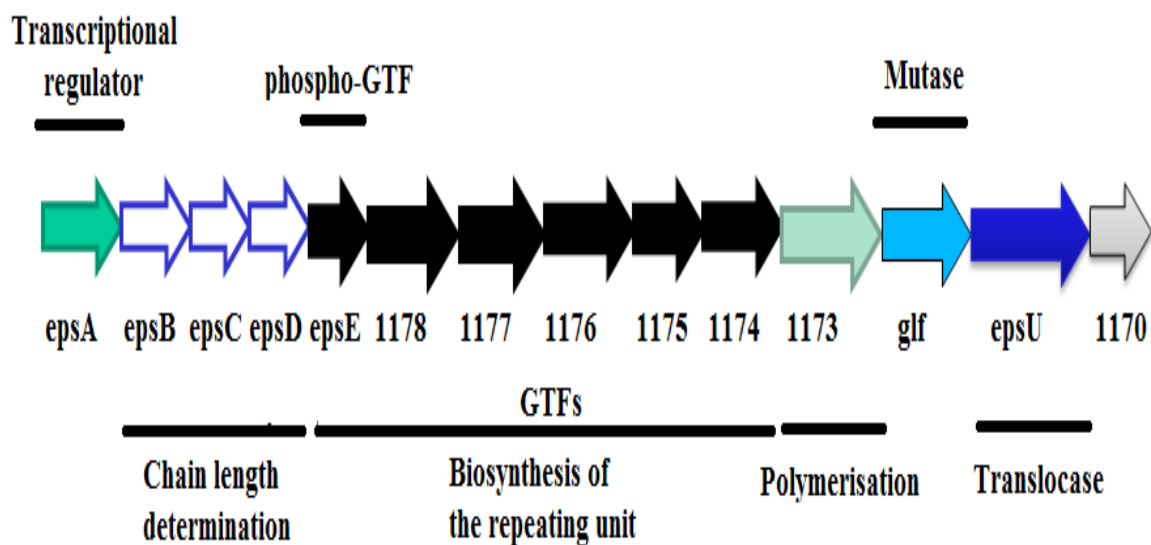


**Figure 1.12.** Molecular organisation of the *eps* cluster of *L. johnsonii* FI9785; The cluster has 14 genes that are predicted to encode; a transcriptional regulator (*epsA*), a polymerization and chain length determination protein (*epsB*), a tyrosine-protein kinase (*epsC*), a protein-tyrosine-phosphate phosphohydrolase (*epsD*), the priming glycosyltransferase UDP-phosphate galactose phosphotransferase (*epsE*) and five glycosyltransferases (1178-1174), an oligosaccharide repeat unit polymerase (1173), mutase (*glf*), oligosaccharide translocase (*epsU*) and lastly an EPS biosynthesis protein with unknown function (1170).

The central region of the *eps* cluster contains five more putative glycosyltransferase genes, *FI9785\_1178* to *FI9785\_1174*, which show homology with the other annotated glycosyltransferase genes and are probably responsible for the addition of the related monosaccharide units to the growing EPS repeating unit in an ordered fashion with specific glycosidic linkages determined by their function to form the final EPS repeating unit [61]. The fourth region of the *eps* clusters of LAB is formed by the polymerization and export genes located in downstream of the central region which is also the case for *L. johnsonii* FI9785. This region contains two genes designated as *FI9785\_1173* and *epsU* with the predicted protein sequence of *FI9785\_1173* gene showing homology with EPS polymerases that are responsible for the polymerisation of the oligosaccharide repeating unit at the outer side of the cytoplasmic membrane and designated as the oligosaccharide repeat unit polymerase. Similarly, the BLASTp analysis of *epsU* gene showed 92% similarity with a putative membrane protein involved in the export of the cell wall components from *L. johnsonii* pf01 and also showed similarity with the oligosaccharide translocases responsible for the flipping of the EPS oligosaccharide repeating unit across the cytoplasmic membrane and described as the oligosaccharide translocase (flippase) [33, 61].

In the middle of these two genes, another important gene was located at the *eps* cluster of *L. johnsonii* FI9785: *glf*. The BLASTp analysis of the *glf* protein of *L. johnsonii* FI9785 showed that this protein showed higher similarity with the UDP-galactopyranose mutases [33]. The *glf* gene putatively encodes the UDP-galactopyranose mutase which is responsible for the synthesis/conversion of the specific nucleotide sugars related to the EPS repeating unit structure which cannot be produced by the central sugar metabolism of *L. johnsonii* FI9785 [61]. Previously, it was shown that the EPS structure of *L. rhamnosus* GG contains galactofuranose residues which supports the role of the *glf* gene converting the galactopyranose to galactofuranose found in the EPS repeating structure [55]. The last gene in the *eps* cluster is *FI9785\_1170* which is predicted as a EPS biosynthesis protein with unknown function and is followed by a transposase pseudo gene [33].

ORF	Predicted product	Top conserved domain (E value) / superfamily	Top BLASTp match (E value)
<i>epsA</i>	transcriptional regulator	PRK09379 LytR (5.3e-79) / LytR_cpsA-psr	Hypothetical protein, <i>L. johnsonii</i> NCC 533 (e0)
<i>epsB</i>	polymerisation and chain length determination protein	TIGR01006 Polys_exp_MPA1 (4.3e-27) / Wzz	Capsular polysaccharide biosynthesis protein, <i>L. johnsonii</i> DPC6026 (e0)
<i>epsC</i>	tyrosine protein kinase	TIGR01007 eps_fam (1.9e-55) / P-loop NTPase	Tyrosine-protein kinase, <i>L. gasseri</i> (1e-164)
<i>epsD</i>	protein-tyrosine-phosphate phosphohydrolase	COG4464 CapC (2.9e-68) / -	Manganese-dependent protein-tyrosine-phosphatase <i>L. johnsonii</i> pf01 (e0)
<i>epsE</i>	undecaprenyl-phosphate galactosephosphotransferase	Pfam02397 Bac_transf (3.1e-93) / Bac_transf	Phosphor-glycosyltransferase <i>L. johnsonii</i> ATCC11506 (1e-152)
<i>1178</i>	glycosyltransferase	cd03808 GT1_cap1E_like (1.4e-87) / Glycosyltransferase GTB_type	Glycosyltransferase <i>L. johnsonii</i> pf01 (e0)
<i>1177</i>	glycosyltransferase	cd00761 Glyco_tranf_GTA_type (1.7e-28) / Glyco_tranf_GTA_type	Beta-1,3-glucosyltransferase <i>L. johnsonii</i> pf01 (e0)
<i>1176</i>	glycosyltransferase	Pfam00535 Glycos_transf_2 (7.3e-39) / Glyco_tranf_GTA_type	Glycosyltransferase <i>L. johnsonii</i> pf01 (e0)
<i>1175</i>	glycosyltransferase	Pfam04488 Gly_transf_sug (1.9e-16) / Gly_transf_sug	Polysaccharide biosynthesis protein CpsM <i>L. johnsonii</i> pf01 (e0)
<i>1174</i>	glycosyltransferase	PRK09814 beta-1,6-galactofuranosyltransferase (7.8e-120) / Glycosyltransferase GTB_type	Putative Galf transferase <i>L. johnsonii</i> pf01 (1e-141)
<i>1173</i>	oligosaccharide repeat unit polymerase	- / -	Putative Galf transferase <i>L. johnsonii</i> pf01 (e0)
<i>glf</i>	UDP-galactopyranose mutase	COG0562 Glf (4.6e-166) / GLF	UDP-galactopyranase mutase, <i>L. johnsonii</i> NCC 533
<i>epsU</i>	oligosaccharide translocase	Pfam01943 Polysacch_synt (1.2e-34) / MatE	Membrane protein <i>L. johnsonii</i> pf01 (e0)
<i>1170</i>	exopolysaccharide biosynthesis protein	- / DUF1919	Exopolysaccharide biosynthesis protein <i>L. johnsonii</i> pf01 (2e-138)

**Table 1.3.** ORFs identified in the EPS gene cluster of *L. johnsonii* FI9785 [33].

### 1.13 Background information about the thesis

As described in section 1.10, a typical *eps* gene cluster has been identified after the genome sequencing and bioinformatics project of *L. johnsonii* FI9785 [33, 195]. Before the start of this thesis project a number of *eps* mutants of *L. johnsonii* FI9785 have been already identified/constructed by Dr Arjan Narbad's group at IFR [33] to understand role of the putative genes in EPS biosynthesis mechanism. These mutants are listed in Table 1.4.

Strain	Description	Plasmid	Nomenclature
FI9785	Wild type, rough	-	Wild type
FI10386	1 bp change in <i>epsC</i> gene, smooth	-	<i>epsC</i> <sup>D88N</sup>
FI10844	<i>epsE</i> gene deleted	-	$\Delta$ <i>epsE</i>
FI10773	FI10386 complemented with wild type <i>epsC</i> gene	pFI2660, <i>epsC</i>	<i>epsC</i> <sup>D88N</sup> :: <i>pepsC</i>
FI10878	FI10844 complemented with wild type <i>epsE</i> gene in sense orientation	pFI2721, <i>epsE</i>	$\Delta$ <i>epsE</i> :: <i>pepsE</i>
FI10879	FI10844 complemented with wild type <i>epsE</i> gene in antisense orientation	pFI2722, <i>epsEA/S</i>	$\Delta$ <i>epsE</i> :: <i>pepsEA/S</i>

**Table 1.4.** *L. johnsonii* mutant strains which were developed before the start of this project [33].

The development of these mutants was carried out by Nikki Horn (IFR). In this process a significantly altered phenotype with a smooth colony morphology (Figure 1.13c, d [33]) in contrast to the rough colony morphology of the wild type (Figure 1.13a, b [33]) was discovered. The production of the smooth variants was a rare but consistent occurrence [33].

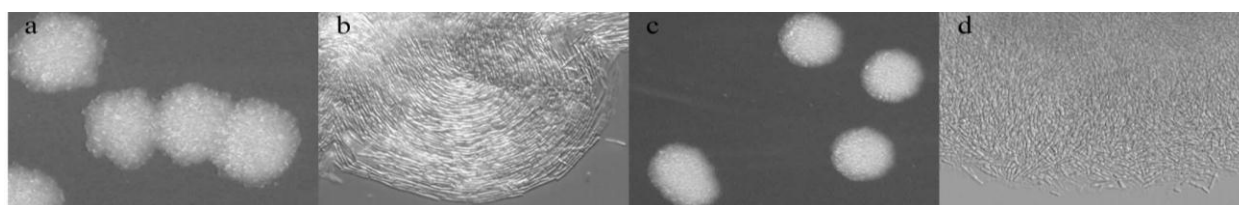


**Figure 1.13.** Morphology of (a, b) the wild type and (c, d) spontaneous mutant strains; (b, d, magnification  $\times 40$ ) [33]. Images provided by Nikki Horn and Dr Mary Parker (IFR).

The smooth colony mutant was isolated, its proteins extracted and subjected to two-dimensional proteomic analysis with the wild type strain and this analysis showed that there was a protein spot in this mutant with different migration properties in comparison to the wild type strain. These two spots from mutant and wild type strain were isolated and analysed for their peptide configuration using peptide mass fingerprinting and then the identified sequence was searched against the *L. johnsonii* sequence and found to be a putative tyrosine kinase, *epsC*, which was encoded by a gene *epsC*, located in the identified *eps* gene cluster of *L. johnsonii* FI9785. The first four ORFs including *epsC* gene were further sequenced and it was found that there was a change of a Guanine (G) to an Adenine (A) in the position 262 of the *epsC* coding strand which resulted in the substitution of an aspartic acid (D) residue at position 88 (D88) to an asparagine (N) residue (N88). The change in the molecular mass of the *epsC* in this smooth mutant also confirmed the alteration of aspartic acid to an asparagine. Overall, the smooth mutant was characterized as a spontaneous mutant in the *epsC* gene, the putative tyrosine kinase, of the identified *eps* cluster (*epsC*<sup>D88N</sup>) [33].

To confirm the role of the *epsC* gene on the smooth phenotype, the spontaneous mutant was complemented with the wild type *epsC* gene with an engineered flexible expression plasmid, which allows the constitutive expression of the target gene [33], which was originally isolated from wild type *L. johnsonii* FI9785 [214]. Expressing the wild type *epsC* gene resulted in a reversion of the smooth colony morphology to the original rough phenotype of the wild type in the *epsC*<sup>D88N</sup>::*pepsC* mutant (Figure 1.14) [33].

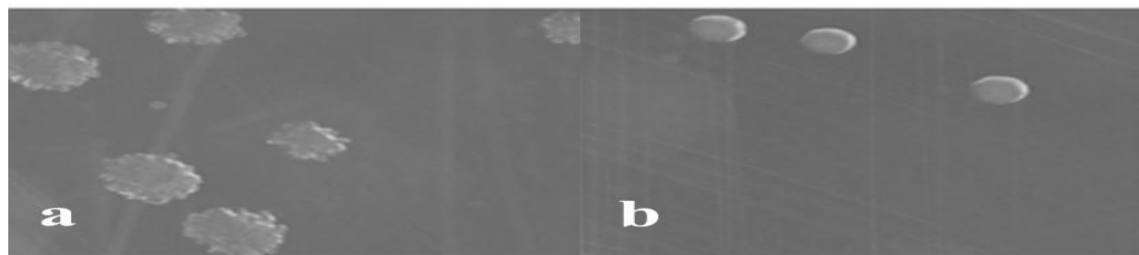


**Figure 1.14.** The morphology of (a) the smooth mutant expressing the *epsC* gene (*epsC*<sup>D88N</sup>::*pepsC*) and (b) the smooth mutant (*epsC*<sup>D88N</sup>) [33]. Pictures provided by Nikki Horn (IFR).

Another mutant that was generated in this process was the  $\Delta$ *epsE* mutant, in which the *epsE* gene from the *eps* cluster encoding a putative undecaprenyl-phosphate galactosephosphotransferase which is the putative priming glycosyltransferase gene, has been deleted [33]. Compared to the wild type there was no morphological difference on plate culture in the  $\Delta$ *epsE* mutant which showed a rough colony morphology. The only visual

difference between the  $\Delta epsE$  mutant and wild type was observed in liquid culture, where the new mutant showed much higher aggregation levels compared to the wild type [33]. Similarly, the complementation of the  $\Delta epsE$  mutant with the wild type *epsE* gene was applied using the same constitutive expression plasmid not only in sense orientation which resulted in mutant  $\Delta epsE::pepsE$ , but also in the antisense orientation giving the  $\Delta epsE::pepsEA/S$  mutant. These two mutants also showed a rough phenotype similar to the wild type and their original mutant strain [33].

#### **1.14 Scope of the thesis**

Cell surface components of lactobacilli play enormous roles in probiotic related activities such as adhesion, aggregation, colonisation and persistence, immunomodulation and they interact with host receptors and inducing signalling pathways resulting in probiotic effects [69]. One of these cell surface molecules is exopolysaccharides and they can be crucial for probiotic action and identification of their structure and biosynthesis mechanism is required in order to understand their contribution. The hypothesis of this project is *L. johnsonii* FI9785 has an *eps* gene cluster and this potential probiotic strain may produce EPS depending on the activity of this cluster or not which can be related with its pathogen exclusion activity as EPS may play a role in bacterial adhesion. Overall, the aim of this thesis is to identify the structure and the biosynthesis mechanism of the EPS produced by *L. johnsonii* FI9785, to show the role of the EPS on cell surface characteristics, adhesion and host-bacteria interactions, to find out the role of the EPS in colonisation and survival of this strain and finally to demonstrate the role of the glycosyltransferases in the production of the EPS repeating unit located in the putative *eps* gene cluster of *L. johnsonii* FI9785. The results of this research should help in the understanding of EPS production by a probiotic organism and the role of EPS in probiotic related properties and functions.

# Chapter 2

---

**General material and methods**

## 2.1 MICROBIOLOGY WORK

All chemicals were purchased from Sigma Aldrich (Dorset, UK) unless stated otherwise.

### 2.1.1 Culture media

All media were prepared as follows:

MRS medium (modified with glucose or sucrose addition): 8 g l<sup>-1</sup> lab lemco (Oxoid), 10 g l<sup>-1</sup> peptone (Oxoid), 5 g l<sup>-1</sup> yeast extract (Difco), 5 g l<sup>-1</sup> sodium acetate.3H<sub>2</sub>O, 2 g l<sup>-1</sup> K<sub>2</sub>HPO<sub>4</sub>, 2 g l<sup>-1</sup> triammonium citrate, 5.75 mg l<sup>-1</sup> MgSO<sub>4</sub>.7H<sub>2</sub>O, 1.4 mg l<sup>-1</sup> MgSO<sub>4</sub>.4H<sub>2</sub>O, 1 ml Tween 80 and 20 g l<sup>-1</sup> glucose or 20 g l<sup>-1</sup> sucrose.

LB medium: 10 g l<sup>-1</sup> bacto tryptone, 5 g l<sup>-1</sup> bacto yeast extract, 10 g l<sup>-1</sup> NaCl.

L medium: 10 g l<sup>-1</sup> bacto tryptone, 5 g l<sup>-1</sup> bacto yeast extract, 5 g l<sup>-1</sup> NaCl, 1 g l<sup>-1</sup> glucose.

SOC medium (super optimal broth with catabolite repression) was prepared as previously described [215]: 2% Tryptone, 0.5% Yeast Extract, 0.4% glucose, 10 mM NaCl, 2.5 mM KCl, 10 mM MgCl<sub>2</sub> & 10 mM MgSO<sub>4</sub>.

Solid media were prepared by adding 1.5% (w/v) agar to the appropriate medium before autoclaving.

The other mediums used in this work were mentioned in related sections.

### 2.1.2 Bacterial strains and growth conditions

Lists of the bacterial strains and plasmids used in this thesis are given in Tables 2.1 and 2.2, respectively. *Lactobacillus johnsonii* strains, listed in Table 2.1 were obtained from in-house culture collections (IFR, Norwich, UK) and some of them were generated in this study. All *L. johnsonii* strains were stored at -80°C in single use 200 µl aliquots in 20% glycerol and grown in MRS with 2% glucose at 37°C. All bacterial strains were grown in aerobic conditions but if stated the anaerobic conditions were carried out in an anaerobic chamber (Don Whitley, UK) with materials pre-reduced in the chamber overnight in an atmosphere of 5% CO<sub>2</sub>, 10% H<sub>2</sub> in N<sub>2</sub>.

Cell density was measured with a CECIL CE2041 S/W version R0044 spectrophotometer using bandwidth 4 nm wavelength 600 nm.

Strain name	Description, details about the transformed plasmid	Growth condition	Media	Antibiotic resistance
<i>Lactobacillus johnsonii</i> FI9785	Wild type	37°C, static	MRS	-
<i>L. johnsonii</i> FI10386	1 bp change in <i>epsC</i> gene	37°C, static	MRS	-
<i>L. johnsonii</i> FI10844	<i>epsE</i> gene deleted	37°C, static	MRS	-
<i>L. johnsonii</i> FI10773	FI10386 complemented with wild type <i>epsC</i> gene	37°C, static	MRS	Cat
<i>L. johnsonii</i> FI10878	FI10844 complemented with wild type <i>epsE</i> gene in sense orientation	37°C, static	MRS	Cat
<i>L. johnsonii</i> FI10879	FI10844 complemented with wild type <i>epsE</i> gene in antisense orientation	37°C, static	MRS	Cat
* <i>L. johnsonii</i> FI10910	<i>eps</i> cluster deleted	37°C, static	MRS	Cat
* <i>L. johnsonii</i> FI10917	<i>epsA</i> gene deleted	37°C, static	MRS	-
* <i>L. johnsonii</i> FI10920	FI10917 complemented with wild type <i>epsA</i> gene	37°C, static	MRS	Cat
* <i>L. johnsonii</i> FI10978	<i>1178</i> gene deleted	37°C, static	MRS	Cat
* <i>L. johnsonii</i> FI10976	<i>1176</i> gene deleted	37°C, static	MRS	Cat
<i>Escherichia coli</i> MC1022	Suitable for handling most of the shuttle vectors.	37°C, 250 rpm	LB	-
<i>E. coli</i> TOP10	Cloning host (Invitrogen)	37°C, 250 rpm	LB	-
<i>E. coli</i> BL21 (DE3)	Expression host (Invitrogen)	37°C, 250 rpm	LB	-
* <i>E. coli</i> FI9701	pG <sup>+</sup> host9 carrying 370 bp from 5 upstream of <i>epsA</i> (pG <sup>+</sup> host9epsAp)	37°C, 250 rpm	LB	Ery
* <i>E. coli</i> FI9702	pG <sup>+</sup> host9epsAp carrying 539 bp from 5 upstream of <i>epsB</i> (pG <sup>+</sup> host9epsABp)	37°C, 250 rpm	LB	Ery
* <i>E. coli</i> FI9703	pG <sup>+</sup> host9epsAp carrying <i>Cat</i> gene and partial <i>1170</i> gene with 280bp of non-coding region of <i>eps</i> cluster (pG <sup>+</sup> host9epsACat1170p)	37°C, 250 rpm	LB	Ery, Cat
* <i>L. johnsonii</i> FI8501	pG <sup>+</sup> host9epsABp transformed for the deletion of the <i>epsA</i> gene	37°C, static	MRS	Ery
* <i>L. johnsonii</i> FI8502	pG <sup>+</sup> host9epsACat1170p transformed for the deletion of the <i>eps</i> gene cluster	37°C, static	MRS	Ery, Cat
* <i>L. johnsonii</i> FI10917	pFI2585 transformed for the complementation of <i>epsA</i> gene	37°C, static	MRS	Cat
* <i>E. coli</i> FI9704	pG <sup>+</sup> host9 carrying partial <i>epsE</i> + <i>Cat</i> gene + partial <i>1177</i> gene (pG <sup>+</sup> host9epsEpCat1177p)	37°C, 250 rpm	LB	Ery, Cat

* <i>E. coli</i> FI9705	pG <sup>+</sup> host9 carrying partial 1178 + Cat gene + partial 1176 gene (pG <sup>+</sup> host91178pCat1176p)	37°C, 250 rpm	LB	Ery, Cat
* <i>E. coli</i> FI9706	pG <sup>+</sup> host9 carrying partial 1177 + Cat gene + partial 1175 gene (pG <sup>+</sup> host91177pCat1175p)	37°C, 250 rpm	LB	Ery, Cat
* <i>E. coli</i> FI9707	pG <sup>+</sup> host9 carrying partial 1176 + Cat gene + partial 1174 gene (pG <sup>+</sup> host91176pCat1174p)	37°C, 250 rpm	LB	Ery, Cat
* <i>E. coli</i> FI9708	pG <sup>+</sup> host9 carrying partial 1175 + Cat gene + partial 1173 gene (pG <sup>+</sup> host91175pCat1173p)	37°C, 250 rpm	LB	Ery, Cat
* <i>L. johnsonii</i> FI8503	pG <sup>+</sup> host9epsEpCat1177p transformed for the deletion of 1178 gene	37°C, static	MRS	Ery, Cat
* <i>L. johnsonii</i> FI8504	pG <sup>+</sup> host91178pCat1176p transformed for the deletion of 1177 gene to wild type	37°C, static	MRS	Ery, Cat
* <i>L. johnsonii</i> FI8505	pG <sup>+</sup> host91177pCat1175p transformed for the deletion of 1176 gene to wild type	37°C, static	MRS	Ery, Cat
* <i>L. johnsonii</i> FI8506	pG <sup>+</sup> host91176pCat1174p transformed for the deletion of 1175 gene to wild type	37°C, static	MRS	Ery, Cat
* <i>L. johnsonii</i> FI8507	pG <sup>+</sup> host91175pCat1173p transformed for the deletion of 1174 gene to wild type	37°C, static	MRS	Ery, Cat

**Table 2.1** List of organisms and growth conditions used in this thesis. \* Generated in this study. The putative glycosyltransferase genes; 1178, 1177, 1176, 1175 and 1174 are re-labelled as gtf1, gtf2, gtf3, gtf4 and gtf5, respectively in Chapter 7.

The transformants and the plasmids that these transformants are carrying, that are generated and used in this thesis for genetic modification studies are listed in Table 2.1.

The antibiotics used for general genetic modification and selection studies are listed in Appendix 1.

Plasmid	Details	Purpose	Antibiotic selection
pG <sup>+</sup> host9	Thermo-sensitive vector [216]	Genetic modification	Ery
pUK200	Expression plasmid [217]	Source of <i>Cat</i> gene	Cat
pFI2560	Horn <i>et al.</i> , [33]	Engineered plasmid originated from <i>L. johnsonii</i>	Cat
pET15b	Novagen (UK)	Expression vector	Amp
*pFI2585	pFI2560 carrying the <i>epsA</i> gene	<i>epsA</i> complementation	Cat
*pFI8578	pET15b with 1178 subcloned into <i>NdeI XhoI</i> sites	Expression vector	Amp
*pFI8576	pET15b with 1176 subcloned into <i>NdeI XhoI</i> sites	Expression vector	Amp
pFI2431	Original plasmid of <i>L. johnsonii</i> [214]	Selection of <i>L. johnsonii</i>	Cat

**Table 2.2** List of plasmid vectors used in this thesis. \*Generated in this study.

### 2.1.3 Bacterial growth analysis

#### 2.1.3.1 Bioscreen experiments

Bioscreen experiments were performed on a Labsystems Bioscreen C machine (Labsystems Oy, Helsinki, Finland). Each strain was grown overnight from -80°C stocks and induced appropriately before performing the assays. The appropriate media were then inoculated with 1% (v/v) concentration with the overnight culture of each strain. Bioscreen plates (honeycomb, Thermo Fisher Scientific) were prepared with 300 µl of the inoculated media per well. Plates were transferred immediately to the bioscreen pre-warmed to the incubation temperature of the test organism and the measurements were started with 5 min between OD measurements at 600 nm which were preceded by plates shaking for 10 seconds.

### **2.1.3.2 Antibiotic susceptibility**

Antibiogram for *L. johnsonii* strains was determined using the antibiotic diffusion discs (Oxoid). Each strain was inoculated in MRS broth and incubated at 37°C overnight. 100 µl of the diluted culture (approximate  $10^7$  viable cells) was spread onto MRS agar and antibiotic discs were applied onto the surface using an antibiotic disc dispenser (Oxoid). The antibiotics tested were used at the following concentrations: Furazolidone 15 µg, Tetracycline 10 µg, Chloramphenicol 10 µg, Kanamycin 30 µg, Erythromycin 15 µg, Rifampicin 30 µg and Vancomycin 30 µg. Plates were incubated at 37°C under aerobic conditions and evaluated after 24 h inoculation. The antibiotics that showed a relative zone of inhibition were then used in Minimum Inhibitory Concentration assays which will be further explained in a related section.

### **2.1.4 Isolation of Exopolysaccharides (EPS)**

*L. johnsonii* strains were grown as described above and 1% (v/v) of overnight cultures were inoculated into 500 ml of MRS broth and incubated at 37°C for 2 d. Cells were harvested at 6000 x g (4°C, 30 min) and washed twice with PBS (Phosphate Buffered Saline). The bacterial pellets were resuspended in 50 ml of UP H<sub>2</sub>O to extract the capsular (cell-surface associated) EPS by sonication and the culture supernatants were also collected to isolate loosely attached EPS that can pass to the culture supernatants during the long centrifugation process. Bacterial pellet samples were sonicated in a Soniprep 150 (Sanyo, UK) for 5-6 times for 10 s at 7-10 amplitude microns using the small probe (9.6 mm of tip diameter). Between each sonication step, samples were cooled on ice for 30 s to prevent degradation. The cell debris was removed by centrifugation at 6000 x g for 30 min at 4°C and an equal volume of chilled ethanol was added to the supernatants followed by the overnight incubation at 4°C to precipitate the EPS from bacterial cell pellets. Similarly, for the isolation of the loosely attached EPS from culture supernatants an equal volume of chilled ethanol was added to the culture supernatants followed by overnight precipitation at 4°C. After this step the same procedures were followed for EPS isolation from either bacterial pellets or the culture supernatants. Samples were centrifuged at 10000 x g for 30 min at 4°C and the pellet of the precipitates was retained. Samples were resuspended in water with gentle heating (50°C) and EPS were recovered by precipitation upon the addition of 2 x volumes of chilled ethanol. After centrifugation at 10000 x g for 30 min at 4°C the resulting EPS were resuspended in distilled water with gentle heating (less than 50°C) followed by dialysis (12000–14000-Da

visking dialysis membrane, Medicell International, UK) for 72 h with two changes of H<sub>2</sub>O per day at 4°C. The contents of the dialysis tubing were freeze-dried to provide EPS which were further purified by dissolving them in 10% TCA and stirring overnight. The precipitated proteins were removed by centrifugation at 10000 x g for 15 min at 4°C. The pHs of the resulted supernatants were adjusted to pH 7 and EPS were precipitated again with 2 x volumes of chilled ethanol. The pellets were dissolved in distilled water and then lyophilized. The EPS samples were stored at 4°C for further analysis.

## **2.1.5 Immunology**

### **2.1.5.1 Production of anti-wild type antibodies**

*L. johnsonii* FI9785 was grown in MRS and the cells were inactivated with 1% formalin and incubated for 30 min at room temperature. Inactivated cells were dialyzed against PBS. Polyclonal anti-wild type antibodies were raised in rabbits by BioGenes (Germany) to a titre of >1: 200000. The specificity of the antibody was tested by ELISA.

### **2.1.5.2 Enzyme linked immunosorbent assay (ELISA)**

Wild type and mutants were grown to stationary phase at 37°C, washed twice in PBS and resuspended in PBS to OD<sub>600nm</sub> of 1.0. Cells were transferred (100 µl per well) onto high protein binding Microlon plates (Greiner, 96-well flat-bottomed polystyrene); BSA (1 mg ml<sup>-1</sup> in PBS) was included as a negative control and plates were left overnight (16-18 h) at 4°C. The plates were washed with PBST (PBS, pH 7.4, + 0.05%, v/v, Tween-20) in the plate washer (Applied Quality Systems, Tonbridge, UK) and tapped several times on paper towel to dry. A 250 µl of blocking reagent (PBS buffer with 1%, w/v, BSA) was then added to each well and incubated at RT for 2 h followed by a wash in the plate washer. 100 µl of the primary antibody solution was then added in dilution series ranging from 1/100, 1/300, 1/900, 1/2700, 1/8100, 1/24300, 1/72900 to 1/218700 in PBS (a stock solution of 1/100 dilution of primary antibody was prepared in PBS and diluted by a factor of 1/3) and incubated at RT for 1 h followed by a wash step. Then 100 µl of secondary, conjugated antibody (Sigma goat anti-rabbit IgG-alkaline-phosphatase conjugate, diluted 1:30,000) was added and incubated at RT for 1 h. After washing the plate, a 100 µl of 1 mg/ml pNP-phosphate solution in 0.2 M Tris buffer, pH 9.6-10.5 (SIGMAFAST pNPP; Tris buffer tablets and pNP-phosphate tablets [Sigma N1891-5SET] was made up in 37°C pre-warmed UP H<sub>2</sub>O about 5-10 mins before use) was added to each well and incubated at RT in the dark for 1 h (covered with foil or

placed in a dark cupboard/drawer). After the incubation the absorbance at 410 nm was read in a FLUOstar (BMG Labtech, UK) microplate reader and the antibody response to each strain was calculated.

## **2.1.6 Flow cytometry (FCM) applications**

### **2.1.6.1 Bacterial viability**

All Flow cytometry (FCM) experiments in this thesis were performed on a Cytomics FC500 MPL (Beckman Coulter). Bacterial viability of each strain was assessed using propidium iodide (PI, Invitrogen Molecular Probes) and analyzed on an FC500 machine and expressed as a percentage of the initial added bacteria for each strain.

### **2.1.6.2 The detection of antibody responses**

Wild type and mutants of FI9785 were grown to stationary phase at 37°C, washed twice in PBS and resuspended in PBS to OD<sub>600nm</sub> of 1.0. Cells were transferred (100 µl per well) onto a normal-binding microtitre plate (Greiner BioOne); BSA (1 mg ml<sup>-1</sup> in PBS) was included as negative control. 25 µl of diluted anti-wild type antibody (1: 200 in PBS) was added per well and incubated at room temperature for 30 min. 175 µl of PBS was added to each well and the plates were centrifuged at 4000 x g for 15 min and the pellet was resuspended in 100 µl of fluorescein-conjugated goat anti-rabbit IgG (Sigma-Aldrich, USA) (1: 750 in PBS) solution. The antibody-bacteria complexes were then incubated at room temperature for 15 min. PBS (200 µl) was added to each well and the antibody response to the wild type and its mutants were analysed in a Cytomics FC500 MPL (Beckman Coulter). A total of 20000 events per sample were acquired at low flow rate. The bacteria numbers were determined in each run. The fluorescence from the green fluorescein was detected via PMT sensors in channel FL1 (530/30). FCM data were analysed using FlowJo version 7.6.5 (TreeStar).

### **2.1.6.3 Assessment of bacterial cell aggregation**

Autoaggregation analysis was also performed by FCM for the accurate quantification. Strains of *L. johnsonii* were grown in MRS (supplemented with 7.5 µg/ml chloramphenicol for plasmid containing strains) for 16 h at 37°C. To investigate the aggregation level of each strain, 20 µl aliquots of bacterial suspension were taken from the top of the overnight grown culture medium before and after vortexing for 3 min and resuspended in 180 µl of PBS to enumerate the number of bacteria at two time points in aliquots of each strain by using FCM.

The number of bacteria in the cell suspension before and after vortexing was quantified and light scatter information was obtained by measuring at 488 nm forward scatter (FSC) and side scatter (SSC) signals. FCM data were analysed using Flowjo and the data expressed as % aggregation level for each strain.

#### **2.1.6.4 Assessment of cell adhesion to tissue culture**

The HT29 cell line (human colon adenocarcinoma, ATCC HTB-38<sup>TM</sup>, LGC) was maintained in tissue culture medium (Dulbecco's modified eagle medium (DMEM, Sigma) supplemented with 10% heat inactivated fetal calf serum (Invitrogen) and 1% MEM non-essential amino acids (Sigma)) with 1% Penicillin/Streptomycin (Sigma) in T75 flasks at 37°C in 5% CO<sub>2</sub>. After 3-4 d when cells were at 80% confluence, they were released with 0.25% trypsin-EDTA (Sigma) and subcultured as recommended (LGC, UK). For adhesion assays cells were grown in 24-well plates (TPP, USA) at a seeding density of c.  $6 \times 10^4$  cells/cm<sup>2</sup> and cultured for 2 d until confluent.

Adhesion assays were performed with *L. johnsonii* strains utilising FCM for the accurate quantification of bacterial numbers. Strains were grown overnight in MRS, with chloramphenicol selection for strains containing expression vectors, then harvested by centrifugation. After two washes with 20 ml PBS, cells were resuspended in PBS to an OD<sub>600nm</sub> of 1.0. Cells were then diluted in DMEM to a concentration of  $1 \times 10^7$  cells/ml and 1 ml aliquots were added to monolayers that had been pre-washed 4 times with tissue culture medium without antibiotics, with each strain being tested in triplicate. To confirm initial cell numbers, 20 µl of the bacterial suspension was diluted with 180 µl PBS and analysed by FCM. After incubation for 2 h at 37°C in 5% CO<sub>2</sub>, non-adhered bacteria were removed by aspiration and monolayers were gently washed 3 times each with 1 ml tissue culture medium without antibiotics, and then dislodged with 1 ml trypsin/EDTA. After serial dilution in PBS, the number of adhered bacteria was analysed by FCM and expressed as a percentage of the initial added bacteria for each strain.

After adhesion experiments, the bacteria-HT29 cell complexes were quantified and morphological scatter information was obtained by measuring 488 nm forward scatter (FSC) and side scatter (SSC) signals. FCM data were analysed using Flowjo.

### **2.1.7 Transmission electron microscopy (TEM)**

*L. johnsonii* strains were grown overnight from -80°C stocks. 1 ml of cell suspension from 16 h cultures were pelleted by centrifugation (1 min, 10000 g, RT), and washed twice in PBS and resuspended in 1 ml PBS. 100 µL of 25% glutaraldehyde was added to 1 ml bacterial suspension in an eppendorf tube and left to fix for 1.5 h. The suspensions were centrifuged and washed three times in 0.05 M sodium cacodylate buffer. After the final wash, the cell pellets were mixed 1:1 with molten 2% low-melting-point agarose (Type VII, Sigma), which was solidified by chilling and chopped into small pieces (approximately 1 mm<sup>3</sup>). The sample pieces were left overnight in 2.5% glutaraldehyde/0.05 M sodium cacodylate buffer (pH 7.2). The samples were transferred to a Leica EM TP tissue processor (Leica Microsystems UK Ltd., Milton Keynes) where they were washed, post-fixed in 1% osmium tetroxide/0.05M sodium cacodylate for 2 h, washed and dehydrated through an ethanol series (30%, 50%, 70%, 90%, 100% x 2) with 1 h between each change. The samples were infiltrated with a 1:1 mix of LR White medium grade resin (London Resin Company Ltd) to 100% ethanol, followed by a 2:1 and a 3:1 mix and finally 100% resin, with 1 h between each change. This was followed by two more changes into fresh 100% resin, with periods of 8 h between. Six tissue blocks from each sample were placed into gelatine capsules with fresh resin and polymerised overnight at 60°C. Sections approximately 90 nm thick were cut using an ultramicrotome (Ultracut E, Reichert-Jung) collected on film/carbon coated copper grids, and stained sequentially with uranyl acetate (saturated in 50% ethanol) and Reynold's lead citrate. Sections were examined and imaged in a FEI Tecnai G2 20 Twin transmission electron microscope at 200kV.

## **2.2 MOLECULAR BIOLOGY WORK**

Molecular biology protocols were performed by conventional methods [215] or using kits according to manufacturer's instructions.

### **2.2.1 Genomic DNA extraction**

Genomic DNA was extracted from mid exponential phase cells of *L. johnsonii* using the Genomic DNA extraction kit with Genomic Tip 20/G columns (Qiagen) as described by the manufacturer, with the addition of 50 U mutanolysin (Sigma) to favor cell lysis. Concentrations of DNA were measured using an Eppendorf Biophotometer at an optical density of 260 nm.

### **2.2.2 Plasmid preparation kits**

The following kits were used following manufacturers' protocols: E.Z.N.A Plasmid Mini Kit I (Omega Bio-Tec), QIAprep spin miniprep kit (Qiagen) and QIAGEN plasmid mini kit.

10 ml centrifuged culture of *L. johnsonii* or other Gram positive organisms were used for plasmid preparations (10 min, 4000 g, 4°C). The pellets were resuspended in 300 µl P1 (Qiagen plasmid kit) containing 5 mg/ml lysozyme powder and removed to 1.5 ml eppendorf tubes. An additional 3 µl mutanolysin (10000 U/ml) was added, and the cells were incubated for 15 min at 37°C before continuing with the manufacturers' instructions including addition of 1 µl glycogen (10 mg/ml, Roche) to aid DNA precipitation when using the QIAGEN plasmid mini kit.

Plasmid preparations of *E. coli* cells were performed according to the manufacturers' protocols.

### **2.2.3 Gel electrophoresis of nucleic acids**

Agarose gels were made at a concentration of 0.8-1.5% (Melford Laboratories) and for shorter bands the agarose concentration was increased up to 1.5% concentration. 5-10 µl of DNA samples were loaded to the wells in agarose gels and electrophoresed in 0.5 x Tris borate EDTA (TBE, Fisher). If samples required a loading dye, 1 µl spots of loading buffer (0.015% bromethyl blue (Sigma), 10% glycerol (Sigma) in 0.5 x TBE buffer) were dispensed onto parafilm (M Laboratory) and mixed with samples prior to loading into the gel. The gels were stained in 1 mg/l ethidium bromide for 30 min, briefly rinsed in deionised H<sub>2</sub>O and visualised with UV light using the AlphaImager (Alpha Innotech). Specific DNA fragments were extracted from the agarose gels using QIAEXII Gel extraction kit (Qiagen).

Hyperladder I (Bioline, UK) was used as a DNA ladder in every electrophoretic gel. The sizes of fragments and their related quantities in 5 µl loaded ladder are shown in Figure 2.1.

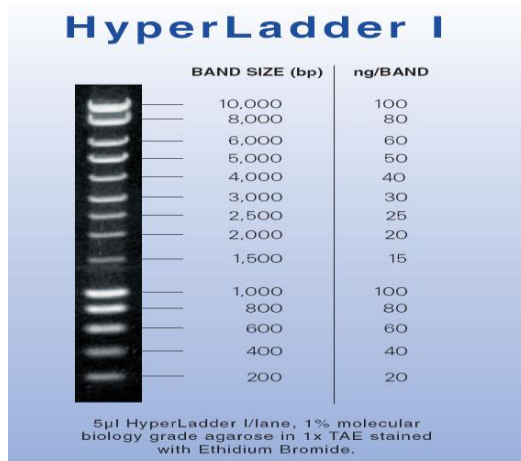


**Figure 2.1.** Hyperladder I (Bioline, UK) fragment sizes and quantities based on 5 µl loaded onto a 0.8-1.5% agarose gel stained with ethidium bromide.

### 2.2.4 Restriction digests

Restriction digests were performed in 10-40 µl of reaction volumes following the conditions described by the manufacturer (NEB, Herts, UK). Restriction enzymes were heat-inactivated after the digestions and products were purified with Sure-Clean (Bioline) to remove the enzymes.

### 2.2.5 Dephosphorylation of vector DNA

Antarctic Phosphatase (NEB) was used to remove 5' phosphate groups from vectors after restriction digestion to prevent the self-ligation following manufacturer's materials and protocol. The dephosphorylation processes were carried out for 15 min for 5' extensions, 1 h for 3' extensions and blunt ends at 37°C in 25 µl reactions containing 20 µl vector DNA, 2.5 µl 10 × AP Buffer, 1.5 µl Antarctic Phosphatase and 1 µl sterile H<sub>2</sub>O. Reactions were then inactivated at 65°C for 20 min. Products were purified using Sure-Clean (Bioline) to remove the enzyme.

### 2.2.6 DNA Ligation

Ligations were performed by using Fast-Link™ DNA Ligation Kit (Epicentre Biotechnologies). Briefly, ligation reactions were conducted with restricted and dephosphorylated plasmid vector and restricted insert following the manufacturer's materials and protocol. A 1:3 molar ratio of vector: insert was used and the following was used to calculate the molar ratios to mass ratios of y amount of vector and insert:

$(\text{ng of vector (y)} \times \text{kb size of insert/kb size of vector}) \times \text{molar ratio of insert/vector} = \text{x}$   
amount of insert

The ligation reactions were performed overnight at RT using the insert to vector ratio in 15  $\mu\text{l}$  reactions containing 1.5  $\mu\text{l}$  10  $\times$  Fast-Link Ligation Buffer, 1.5  $\mu\text{l}$  10 mM ATP, y amount of vector ( $\mu\text{l}$ ) DNA, x amount of insert ( $\mu\text{l}$ ) DNA, sterile  $\text{H}_2\text{O}$  and 1  $\mu\text{l}$  Fast-Link DNA Ligase.

### 2.2.7 Polymerase chain reaction (PCR)

Primers were obtained from Sigma Genosys (UK) and annealing temperatures were calculated for GoTaq reactions using the website <http://www.oligoevaluator.com/OligoCalcServlet>, for Phusion polymerase reactions using the website <http://www.thermoscientificbio.com/webtools/tmc/>, respectively and the primers were swapped using the website <http://www.basic.northwestern.edu/biotools/oligocalc.html> (except the splice PCR primers). Amplification of DNA using GoTaq polymerase was performed with the reaction mix shown in Table 2.3. Amplification of the target DNA with GoTaq polymerase was carried out using the cycling conditions as follows: 2 min at 95°C for one cycle; then 30 s 95°C, 30 s 55°C (depending on the primer melting temperature ( $T_m$ )) and 1 min per kb at 72°C for 25-30 cycles; a final step of 5 min at 72°C for one cycle.

Component	Quantity
DNA template	1 $\mu\text{l}$ (~500ng)
5 x GoTaq Reaction Buffer (Promega)	10 $\mu\text{l}$
0.2 mM each dNTP (Bioline)	0.4 $\mu\text{l}$
Forward primer 20 $\mu\text{M}$ (Sigma Genosys)	1 $\mu\text{l}$
Reverse primer 20 $\mu\text{M}$ (Sigma Genosys)	1 $\mu\text{l}$
Deionised $\text{H}_2\text{O}$	36.35 $\mu\text{l}$
1.25 U/ $\mu\text{l}$ GoTaq DNA Polymerase (Promega)	0.25 $\mu\text{l}$

**Table 2.3.** Reaction composition for GoTaq polymerase.

PCR was performed using PCR Sprint (Thermo Scientific) and the T professional Thermocycler (Biometra), with the polymerases Phusion polymerase (Finnzymes, New

England Biolabs) for high fidelity application such as amplification of a gene for cloning and GoTaq polymerase (Promega) for colony or ligation PCR.

Similarly, reactions with the high fidelity polymerase Phusion are carried out with the composition listed in Table 2.4. Amplification of the target DNA with Phusion polymerase was carried out using the cycling conditions as follows: 30 s at 98°C for one cycle; then 10 s 98°C, 30 s at T<sub>m</sub> or T<sub>m</sub>+3°C for >20bp primers and 15-30 s per kb at 72°C for 25-30 cycles; a final step of 5 min at 72°C for one cycle.

Component	Quantity
DNA template	1 µl (~5 or 50ng)
5 x Phusion Reaction Buffer (NEB)	10 µl
0.2 mM each dNTP (Bioline)	0.4 µl
Forward primer 20 µM (Sigma Genosys)	1.25 µl
Reverse primer 20 µM (Sigma Genosys)	1.25 µl
Deionised H <sub>2</sub> O	35.7 µl
1 U/µl Phusion Polymerase (NEB)	0.4 µl

**Table 2.4.** Reaction composition for Phusion polymerase.

### 2.2.8 Ligation PCR

Ligation PCR to confirm the successful ligation was performed using 1 µl of a 10 x dilution of ligated DNA in a PCR reaction with primers which flank the plasmid insert located in plasmid and therefore amplify the inserted DNA as illustrated in Figure 2.2.

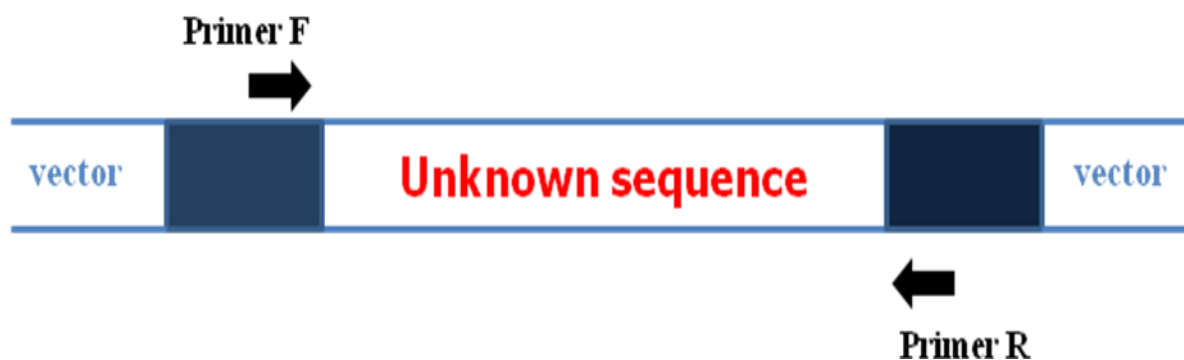


**Figure 2.2.** Illustration of ligation PCR procedure with primers Forward (F) and Reverse (R).

### 2.2.9 PCR with whole cells

Cells from a colony were picked with sterile toothpicks and resuspended in 10  $\mu$ l sterile H<sub>2</sub>O. One  $\mu$ l of cell suspension was used as template in PCR with the GoTaq as described in section 2.2.7. Also PCR was carried out with the bacterial cells grown in liquid media. 1  $\mu$ l of DNA template was obtained from 150  $\mu$ l of overnight liquid culture centrifuged (1 min, 10000 g, RT), washed with STE buffer (appendix 3) and boiled at 95°C for 5 min and resuspended in 10  $\mu$ l of ultrapure H<sub>2</sub>O before PCR reaction. One  $\mu$ l of cell suspension was used as the template in PCR with the GoTaq as described in section 2.2.7.

Colonies from the transformants were also screened by PCR using 96-well format by pipetting 50  $\mu$ l UP H<sub>2</sub>O in 7 rows of the plate, picking colonies into each well and pooling 10  $\mu$ l each solution from each row in the 8<sup>th</sup> row. Colony PCR was performed using 10  $\mu$ l of the mixed solution from 8<sup>th</sup> as a DNA template as described in section 2.2.7.

### 2.2.10 Splice overlap extension PCR

To insert specific mutations in *eps* gene cluster, splice overlap extension PCR was performed as illustrated in Figure 2.3 as described previously [218] (Figure 2.3).

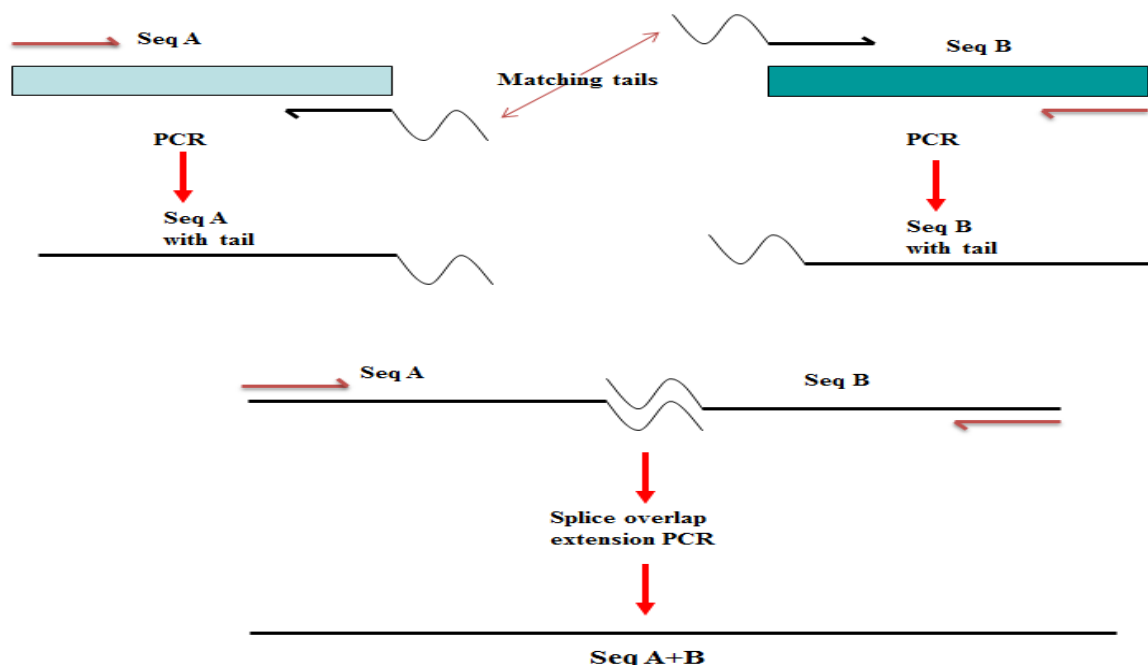


**Figure 2.3.** Illustrations of splice overlap extension PCR procedure.

This approach allows the fusion of two different sequences of DNA without the use of restriction enzymes. Briefly, splice overlap extension PCR joins two DNA fragments having

regions of short sequence complementary between the 3' end of the first sequence and the 5' end of the other. The sequences are fused during PCR, as the overlapping sequences will hybridize and extend to produce a full-length chimeric sequence. Sequence complementarity at the fusion site can be introduced into two unrelated fragments by incorporating common sequence tags into primers in a first-round PCR.

Two splice overlap primers were designed with 100% match to the right hand end of seqA with a tail to give a 100% match to the beginning of seqB and primer with 100% match to the left hand end of seqB with a tail to give a 100% match to the right hand end of seqA. Also two primers for the other ends of the genes were designed (Figure 2.3) and each primer pair was used to make copies of seqA and seqB with tails. Primers have to be designed taking the following points into account: a) for splice primers, the 100% matching sequence should be about 15 bp with a similar length of tail; b) the nearest neighbour (NN) values should be >37°C, which can be calculated from the oligonucleotide properties calculator (<http://www.basic.northwestern.edu/biotools/oligocalc.html>); c) for end primers with a maximum of 20 bp length, the lower T<sub>m</sub> is suitable for annealing which can be checked from the T<sub>m</sub> determination website: <http://www.thermoscientificbio.com/webtools/tmc/>; d) for end primers longer than 20 bp, the annealing temperature should be 3°C higher than the lower T<sub>m</sub> given by the T<sub>m</sub> determination website. The first PCR reactions are run using 5 cycles of the NN of the splice primer 100% matching sequence and 20 cycles of the NN of the whole splice primer (or the annealing temperature calculated for the end primer, whichever is lower) using the protocol below:

DNA (genomic)	1-5 ng and 4-10 ng template	98°C	30 s	
5 x Phusion buffer	10 µl	98°C	10 s	}
dNTP (100 mM stock)	0.4 µl	Ta1	30 s	}x5
primer 1 (20 uM stock)	1.25 µl	72°C	15-30 s/kbs	}
primer 2 (20 uM stock)	1.25 µl	98°C	10 s	}
Phusion (Finnzymes)	0.4 µl	Ta2	30 s	} x 20
H <sub>2</sub> O	to 50 µl	72°C	15-30 s/kb	}
		72°C	5'	

After finishing and purifying the first PCR reactions, the splice overlap PCR reaction using the two DNA products with a matching tail was performed using 1 ng or 4 ng of each product and the end primers, using the NN of the whole region of overlap between the two sequences as the annealing temperature (or the lowest annealing temperature calculated for the end primers if this is lower).

### 2.2.11 DNA purification

PCR products were purified with Sure-Clean (Bioline), a rapid DNA cleaning tool to remove buffers, dNTP, short DNA fragments and enzymes. The DNA was incubated for 30 min at RT with the same volume of Sure-Clean buffer and centrifuged (30 min, 14000 x g, RT). Then 150 µl of 70% ethanol was added and centrifuged again (30 min, 14000 x g, RT). After this step ethanol was removed, the pellet air dried and resuspended in 20 µl of TE buffer (Appendix 3). DNA concentration was measured using the Nanodrop (Thermo scientific) and finally sequenced.

### 2.2.12 DNA sequencing

Purified DNA was sequenced with the BigDye® Terminator v3.1 Cycle Sequencing Kit (ABI Applied Biosystems, UK). Reagents were added to the reaction in the following order: template DNA (100-200 bp, 1-3 ng; 200-500 bp, 3-10 ng; 500-1000 bp, 5-20 ng, 1000-2000 bp, 10-40 ng; > 2000bp, 20-50 ng), 2 µl 1.6 µmol/µl primer, 3.5 µl 5 x buffer, 1µl of the BigDye Terminator v3.1 Cycle Sequencing Kit (ABI Applied Biosystems, UK). Sequencing was performed in a Biometra T professional Thermocycler using the following program described in Table 2.5. The products were sequenced at TGAC (Norwich).

Denaturation:	96°C 2 min 1 cycle
Denaturation:	96°C 30 sec }
Annealing:	50°C 15 sec } 25 cycles
Extension:	60°C 4 min }
Hold:	4°C

**Table 2.5.** Sequencing reaction conditions.

### 2.2.13 Primer design

DNA primers were ordered from Sigma Genosys. They were resuspended in sterile UP H<sub>2</sub>O and stored at -20°C. The list of primers used in this thesis is listed in Appendix 2. Usually the primers are designed with 100% match to the sequence, one on the top strand (forward) and one on the bottom one (reverse). They should be between 18-24 nt, should not contain runs of more than 3 bases, often work best if the last nucleotide are G or C and their last 3 nt are not complementary to each other. To insert a restriction enzyme site to the primers for the target gene, the numbers of nucleotides from the end required for the specific restriction enzymes were checked from the New England Biolabs website: "<http://www.neb.com/tools-and-resources/usage-guidelines/cleavage-close-to-the-end-of-dna-fragments>". Usually when a change in the nucleotide occurs to insert or remove a particular site, the 100% match sequence must be more than 15 nt long. The melting temperature T<sub>m</sub> of the 100% match sequence was calculated by using "<http://www.thermoscientificbio.com/webtools/tmc/>" then the T<sub>m</sub> of the entire primer was calculated in the same way. Also the "nearest neighbor (NN)" usually required in Splice overlap PCR was calculated using the "<http://www.basic.northwestern.edu/biotools/oligocalc.html>" website as described above.

### 2.2.14 Transformation of *E. coli*

*E. coli* MC1022 cells were prepared to make them electro-competent for transformation purposes. Fresh 40 ml L-broth containing the appropriate antibiotic selection was inoculated with 800 µl of an overnight culture of *E. coli* and shaken (250 rpm) at 37°C until the OD<sub>600nm</sub> reached 0.5-0.6. The cultures were chilled on ice and processed immediately. Cells were harvested by centrifugation (3000 g, 10 min, 4°C) in a pre-chilled rotor (4°C), washed twice in ice-cold 10% glycerol with resuspension by gentle agitation then centrifuged (10 min, 3000 g, 4°C) and the final cell pellet was resuspend in 400 µl of ice-cold 10% glycerol. If not continuing immediately with a transformation, cells were aliquoted as 40 µl volumes into pre-chilled 0.5 ml sterile microfuge tubes, snap frozen using liquid nitrogen or dry ice and stored at -80°C.

The second step of the transformation is the electroporation of the target DNA to the electro-competent *E. coli* cells. All materials and solutions were pre-chilled for at least 2 h on ice. A maximum of 5 µl DNA or ligation mix was added to 40 µl aliquots of electro-competent cells, mixed and incubated for 1 min on ice. A positive control using 5 ng of vector and a negative control using H<sub>2</sub>O were prepared in parallel. The cell mixture was pipetted into pre-

chilled electroporation cuvettes (Cellprojects, UK) which were closed, placed into the pre-chilled holder and introduced into an electroporation chamber. The electroporation apparatus, Gene Pulse Xcell (BioRad, UK), was set to deliver a 25  $\mu$ F capacitance, 2.5 kV and 200  $\Omega$  resistance pulses. After a pulse, a time constant ranging from 4.7 to 5.0 millisecon with field strength of 12.5 kV/cm was registered. 460  $\mu$ l of SOC broth at RT was then added to the cuvettes and the bacteria were transferred into 2 ml screw cap tubes and incubated with shaking for 1-2 h at 30-37°C depending on the plasmid. Then 100  $\mu$ l of electroporated cells were plated onto selective L agar and incubated 1-2 d at 30-37°C depending on the plasmid.

### **2.2.15 Transformation of *L. johnsonii***

To prepare electro-competent *L. johnsonii* cells, pre-warmed 95 ml MRS with 2% glucose was inoculated with 1 ml of an overnight culture. The culture was then grown to an OD<sub>600nm</sub> of about 0.6. Then the culture was divided into two Oakridge tubes and centrifuged for 10 min at 3000 x g at 4°C using the pre-chilled rotor JA17. The pellet was gently resuspended with 500  $\mu$ l ice-cold 10 mM MgCl<sub>2</sub> then a further 9.5 ml was added to wash the cells. The centrifugation and wash step was repeated twice, with 0.5 M sucrose in 10% glycerol being used for the final wash. Cells were finally centrifuged as previously and resuspended in 250  $\mu$ l of 0.5 M sucrose in 10% glycerol. Cells were then aliquoted in 50  $\mu$ l amounts and transformed or stored at -80°C until use.

A maximum of 5  $\mu$ l of the ligation reaction were added to 50  $\mu$ l of electro-competent cells, mixed and incubated for 1 min on ice. The cell/DNA mixture was then transferred to a pre-chilled electroporation cuvette which was transferred into an electroporation chamber. The electroporation apparatus was set to deliver a pulse of 25  $\mu$ F capacitance, 1.5 kV and 800  $\Omega$  resistances. After the successful electroporation 450  $\mu$ l of MRS with 2% glucose, 20 mM MgCl<sub>2</sub>, 2 mM CaCl<sub>2</sub> was then added and the cells were transferred into a 2 ml screw cap tube and incubated for 2 h at 30-37°C depending on the plasmid. 100  $\mu$ l of electroporated cells were plated onto MRS agar with 2% glucose and selective antibiotics and incubated 1-2 d at 30-37°C depending on the plasmid. A positive control of 100-500 ng plasmid was used.

## **2.3 PROTEIN BIOCHEMISTRY**

### **2.3.1 Protein expression and extraction from bacterial cells**

The specific glycosyltransferase genes were cloned to the IPTG (Isopropyl-Isopropyl- $\beta$ -D-1-thiogalactopyranoside) inducible vector pet15b (Novagen) (The details about cloning

procedure will be explained in Chapter 7) and expressed in the host *E. coli* BL21 (DE3) (Invitrogen). Briefly, the transformed *E. coli* cells were induced with IPTG (0.1 M) when they reached to mid logarithmic phase ( $OD_{600nm}$  0.4-0.6) for a period of time depending on the protocol followed (Chapter 7) and then centrifuged (3000 x g, 10 min, 4°C) and kept at -20°C for overnight before protein extraction. Three different extraction buffers were used to optimise the extraction conditions; Buffer 1: 100 mM Tris pH 7.5, 300 mM NaCl, 200 mM imidazole; Buffer 2: 20 mM Tris-HCl, 50 mM NaCl pH 7.5; Buffer 3: 20 mM phosphate buffer pH 7.5. The cell pellets were resuspended in 250-500  $\mu$ l of one of the extraction buffers and subjected to sonication or bead-beating process.

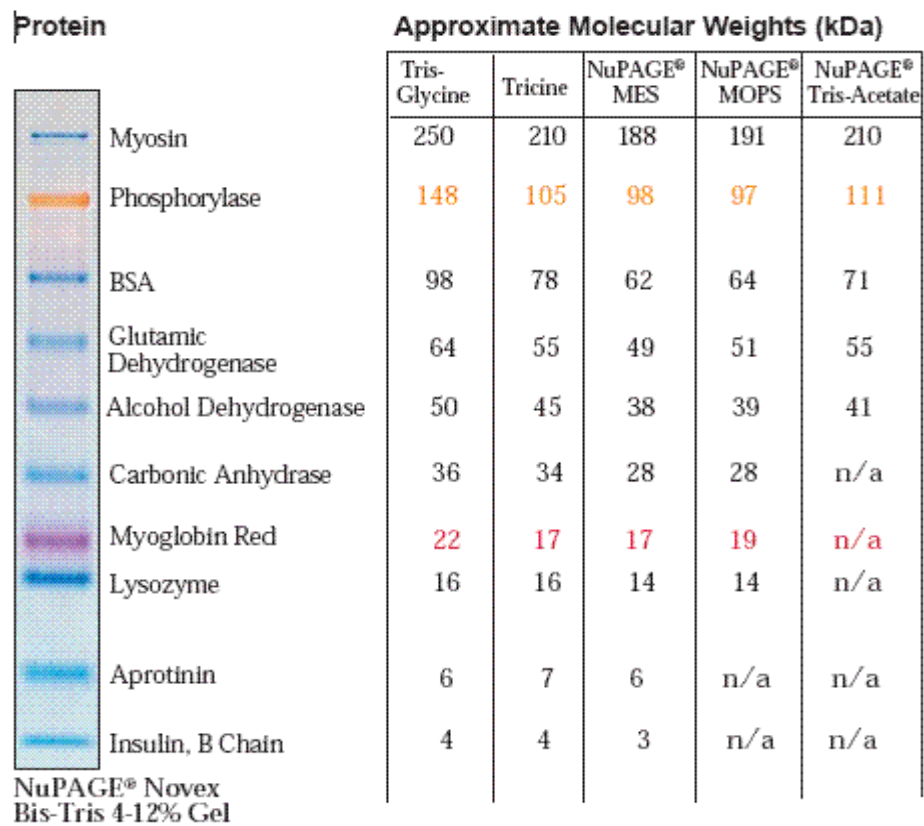
Cells were mixed with 100  $\mu$ l acid washed glass beads (0.1 mm, Sigma) and then bead-beaten using a FastPrep FR120 (Qbiogene, USA) cell disrupter 4 times for 30 seconds at speed 6 with 5 to 10 min interval on ice between each beating steps. Sonication was found to be the most promising technique in our experience for protein extraction from Gram negative *E. coli* cells. Basically, the cell suspension in extraction buffer was subjected to sonication in Soniprep 150 sonicator (Sanyo, UK) for 3-5 times for 10 seconds at 10-15 amplitude microns using the small probe (9.6 mm of tip diameter). In each sonication step samples were cooled on ice for 30 seconds to prevent protein degradation. Samples were then centrifuged (13,000 g, 30 min, 4°C) and the supernatants containing cell extracts transferred into new tubes and stored at 4°C.

### **2.3.2 Protein assays**

Protein concentrations were determined using the Bradford method [219] with the Biorad (UK) protein assay kit, using bovine serum albumin (BSA) as a standard. It is a colorimetric protein assay, based on an absorbance shift of the dye Coomassie Brilliant Blue G-250, whose red form under acidic conditions is converted into its bluer form after binding to the protein being assayed. Proteins were quantified using Bradford's reagent (Biorad) and standard dilutions of 200 to 0  $\mu$ g/ml of BSA were prepared for calibration purposes (Appendix 6). The bacterial protein extracts were diluted x10, x20, x40 and 10  $\mu$ l of each dilution series were placed onto Grenier 96-well plates in duplicate and 190  $\mu$ l 4 x diluted reagent (Biorad) were added per each well. The samples were mixed in the plate reader, incubated for 5 min then read at  $OD_{600nm}$ .

### 2.3.3 Sodium dodecyl sulfate polyacrylamide gel electrophoresis (SDS-PAGE)

All SDS-PAGE materials were purchased from Invitrogen (Paisley, UK). Protein samples with Lithium Dodecyl Sulfate (LDS) buffer and reducing agent (6.5:1:2.5 v:v:v) were heated at 70°C for 10 min and immediately chilled on ice for 2 min before loading; once the protein sample has been heated at 70°C for 10 min, the NuPAGE LDS sample buffer maintains polypeptides in a denatured state. Samples commonly contained 10 µg proteins in a final volume of 10-20 µl. The SeeBlue Plus ladder (Invitrogen) was used as a size marker (Figure 2.4).



©1999-2002 Invitrogen Corporation. All rights reserved.

IM-1008F 072602

**Figure 2.4.** The SeeBlue Plus ladder apparent molecular weights in several buffer systems.

Protein samples were electrophoresed on 10% NuPage Novex Bis-Tris gels in 3-N-morpholino propanesulfonic acid (MOPS) buffer with antioxidant. The samples were run for 50 min at 200 V. The gel was then washed 3 times for 5 min in dH<sub>2</sub>O, stained for 1 h in 20 ml Simply Blue Safestain (Invitrogen) and finally destained for 1 h or overnight in H<sub>2</sub>O and the destained gels were scanned.

### 2.3.4 Western blotting

Western Blotting (or immunoblotting) procedure is used to verify the expression of a protein and determine the relative amount of the protein present in different samples. Protein separation according to molecular weight is achieved using denaturing SDS-PAGE. After transfer onto a polyvinylidene difluoride membrane (PDVF) by using NuPage buffer (Invitrogen) the 6xHis-tagged target protein was detected by using an anti-His tag monoclonal antibody (Novagen) with alkaline phosphatase linked anti-mouse immunoglobulin G (Sigma) as the secondary antibody and detected by colorimetric detection with Sigma Fast BCIP (5-bromo-4-chloro-3-indolylphosphate) nitroblue tetrazolium as the substrate (Figure 2.5).

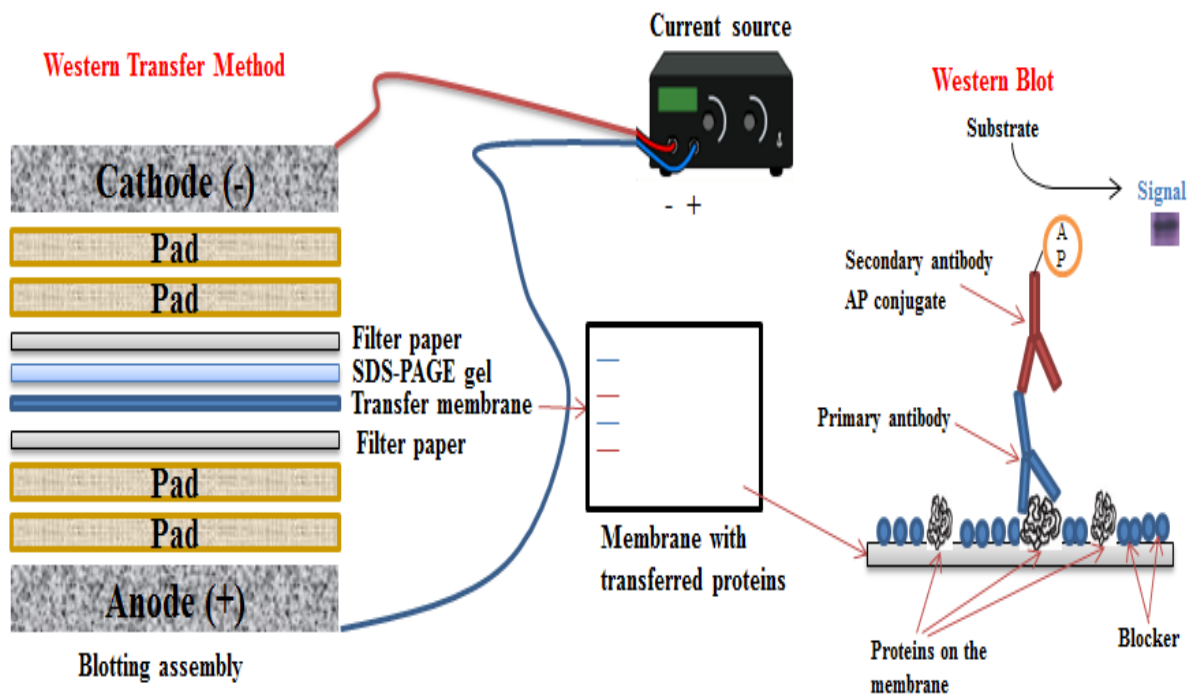


**Figure 2.5.** Western Blot Methodology.

Transfer of proteins from SDS-PAGE onto PVDF membrane was performed in an XCell II blot module (Novagen). Blotting pads were soaked in 350 ml 1x NuPAGE transfer buffer at least for 30 min before use. PDVF membrane (LC2002, 0.2 $\mu$ m pore size with filters) was pre-wetted for 30 sec in methanol, then rinsed in deionised water and placed in a shallow dish with 50 ml of 1x NuPAGE transfer buffer for several minutes. The gel/membrane module was constructed with two blotting pads, 3 mm filter paper, gel, membrane, filter paper and a further two blotting pads. The blot module was inserted into the lower buffer chamber of the electrophoresis tank (Invitrogen), and filled with 1 x transfer buffer until the membrane was

covered. The outer buffer chamber was filled with 650 ml deionized water and the system connected to the electrical leads. The transfer was performed using 30 V for about 1 h. The membrane was washed twice with TBS buffer (Appendix 3) for 10 min and then incubated in blocking buffer overnight at 4°C, to avoid non-specific interactions of the antibody with the membrane (the excess space on the membrane is covered with a dilute solution of a generic protein).

The membrane was washed twice with 50 ml TBS-Tween/Triton buffer (Appendix 3) for 10 min and once with TBS buffer. It was then incubated with the primary antibody (anti-His tag monoclonal antibody, 2.5 µl in 5 ml 3% BSA) for 1 h. The unbound primary antibody was washed away twice with TBS-Tween/Triton buffer for 10 min and once with TBS buffer, the membrane was then exposed to the secondary antibody alkaline phosphatase linked anti-mouse immunoglobulin G (2.5 µl in 5 ml 3% BSA) for 1 h at RT. Then the membrane was washed 4 times for 10 min with TBS-Tween/Triton buffer for 10 min. Detection was performed using a SIGMA FAST:BCIP/NBT tablet resuspended in 10 ml, added to the protein side of membrane and left without moving for 1-15 min until colour development was seen. The reaction was stopped by washing the membrane twice with H<sub>2</sub>O.

# Chapter 3

---

**Exopolysaccharides of *L. johnsonii***

### 3.1 INTRODUCTION

Research on exopolysaccharides (EPS) of the genus *Lactobacillus* was originally aimed at identifying novel EPS structures produced by different species and to understand the molecular mechanism of EPS production. Similarly, the role of specific genes located within the *eps* clusters for heteropolymeric EPS production or the role of single *gtf* or *ftf* genes for homopolymeric EPS production was also investigated. Although the EPS biosynthesis mechanism is quite similar amongst *Lactobacillus* species, each repeating unit of the final EPS is also quite novel depending on the structure and the number of the glycosyltransferases encoded in the genome. So far novel EPS structures of around 30 *Lactobacillus* species have been identified [1, 10]. Given the importance of EPS structures of *Lactobacillus* species and the role of putative genes in EPS production, the quantification of EPS production has also been the focus of numerous studies in the last three decades [10, 79, 124, 138, 145].

Several different methods have been determined for isolation of capsular EPS or extracellular EPS from bacterial cells or bacterial supernatants which have included the precipitation of polysaccharides with ethanol and removal of the proteins with a related chemical compound generally TCA and some purification steps of final EPS [220, 221]. After isolation of EPS, samples are then analysed by total sugar analysis to quantify the total sugar levels of extracted EPS samples. As EPS are carbohydrate structures, simple carbohydrate analyses based on colorimetric reactions can be performed to quantify the total EPS levels produced by LAB. The most common and simple colorimetric method for quantification of total EPS production is the phenol-sulphuric acid test which is based on the breakdown of EPS into simple sugar monomers by concentrated sulphuric acid and the reaction of derivatives of these monomers with phenol in order to produce a yellow-gold color [222]. Although this method is quite simple and reliable, for the most accurate determination of total sugar and monosaccharide content of EPS samples, chromatographic methods, such as Gas Chromatography (GC), are methods of choice. Characterization of the monosaccharide content of EPS samples by GC is based on the initial hydrolysis of polysaccharide with strong acids to its monomers and then the acetylation of the hydrolysates for derivatization to their alditol acetates which will be eluted from a specific column at a particular retention time (Rt). Monosaccharides or total sugar content will then be identified with the comparison of these retention times with those of a set of standards [223]. The absolute configuration and linkages analysis between each monosaccharide unit can be carried out by Nuclear Magnetic Resonance (NMR) spectroscopy or methylation analysis, where NMR is the most definitive

technique to determine the anomeric conformation of each monosaccharide units, linkage type and their substituents within the structure [1, 47, 224]. In most recent studies, Fourier Transmission Infrared Spectroscopy (FTIR) also became an important tool to identify the functional groups that EPS samples are composed of [19]. More detailed information about all these and other techniques for carbohydrate analysis can be found at the University of Georgia Complex Carbohydrate Research Centre database, at [www.cccr.uga.edu](http://www.cccr.uga.edu).

The accumulation of EPS on the cell surface of *Lactobacillus* strains gained special interest after recent reports which showed the role of EPS on adhesion to human cells, immunomodulation, aggregation and other important phenotypic features related to probiotic function [33, 57, 60, 61, 65]. These observations revealed that EPS determines the cell surface characteristics of *Lactobacillus* cells depending on its structure and physicochemical properties. The cell surface structure and architecture of *Lactobacillus* cells has been studied extensively with different techniques including Atomic Force Microscopy (AFM). As EPS are one of the most important components of the cell surface of lactobacilli cells determining the cell surface characteristics, the experience of using AFM on biological surfaces has led the investigation of the localisation and conformational of EPS *in situ*, on the cell surface of lactobacilli cells [225]. Additionally, several other studies investigated morphology and structure characteristics of EPS isolated from bacterial cells by AFM [226-229]. Similarly, Flow Cytometry (FCM) is an important tool that can detect the cell surface components and their alterations in living cells with antibody based techniques or via specific colorimetric components that can react with the surface components.

This chapter describes the isolation and quantification of EPS production levels and identification of EPS structure produced by *L. johnsonii* FI9785 and mutant strains. The role of the putative genes in EPS production mechanism encoded in the *eps* gene cluster of *L. johnsonii* FI9785 was also investigated. Quantification of EPS production revealed either increase or decrease of EPS production among mutants compared to the wild type. The structure of the two different capsular EPS produced by *L. johnsonii* FI9785 and the role of the putative priming glycosyltransferase in EPS biosynthesis were identified. Additionally, we confirmed the localization of specific sugar residues *in situ* by AFM and detected cell surface alterations after changes in EPS production levels and structures among wild type and mutant strains by FCM.

## 3.2 MATERIAL AND METHODS

*L. johnsonii* strains; wild type, *epsC*<sup>D88N</sup>,  $\Delta$ *epsE*, *epsC*<sup>D88N</sup>::*pepsC*,  $\Delta$ *epsE*::*pepsE* and  $\Delta$ *epsE*::*pepsEA/S* mutant strains (Table 1.4) were grown under the conditions described in section 2.1.2. The growth curve analysis of these strains was conducted for 11 h by measuring the cell density after vortexing each culture at each time point as described in section 2.1.2. The EPS were isolated from wild type and mutant strains as described in section 2.1.4.

### 3.2.1 Quantification of EPS production

Total sugar analysis was carried out by Gas Chromatography (GC). GC allows the identification and separation of chemically treated, volatilized monosaccharides which are then passed through a specific column. After the chemical treatment which is described below, a different volatile compound is formed (alditol acetates) from each monosaccharide. Then each volatile compound is eluted in a column (RTX-225; Restek, US) with a particular retention time (Rt) which will be compared with a set of standards consisting the main monosaccharide groups that reported EPS samples of LAB were composed of. This direct comparison results in a chromatogram for each sample showing the monosaccharide content an example of which is reported in Appendix 4. Then the concentration of each monosaccharide is calculated from the peak area of each monosaccharide in the chromatogram using the template reported in Appendix 5.

EPS were isolated from the pellet and supernatant of wild type and mutant cells as well as MRS media control (MRS), as yeast extract within MRS contains cell wall polysaccharides. All samples of EPS were hydrolysed to monosaccharides using a modified Saeman hydrolysis (dispersion in 72% H<sub>2</sub>SO<sub>4</sub> with periodic agitation for 3 h at RT followed by dilution to an acid concentration of 1 M H<sub>2</sub>SO<sub>4</sub> and then further hydrolysis for a total of 2.5 h at 100°C in a hot block). Hydrolysates were made alkaline, reduced, acidified using acetic acid and then derivatized as their alditol acetates as described previously [223] and analysed by capillary GC using a Perkin-Elmer Autosystem XL with an RTX-225 column (Restek, US) with flame ionization detection. Samples were assayed for their levels of rhamnose, fucose, arabinose, xylose, mannose, galactose and glucose using an internal standard of 2-deoxy glucose for calibration purposes. The total amount of EPS from both the bacterial cell pellet and the culture supernatant was combined and expressed as  $\mu\text{g}$  EPS per  $10^9$  cells ( $10^9$  represent the bacteria count of each strain present in 500 ml cultures). Finally, the data were

analysed in Excel (Microsoft, Washington, USA), statistical analysis using an independent t-test with unequal variance, comparing the level of EPS production of each strain to the wild type's EPS levels.

### 3.2.2 NMR spectroscopy analysis

NMR spectroscopy analysis of EPS produced by FI9785 and its derivatives was performed by Dr Ian J. Colquhoun (IFR) which was explained in detail elsewhere [230].

### 3.2.3 Atomic Force Microscopy (AFM) Analysis

AFM analysis of the sugar residues accumulated on cell surface of wild type and  $\Delta epsE$  mutant strain were performed in collaboration with A. Patrick Gunning (IFR). Firstly, the AFM tips were functionalized with a galactose specific lectin (PA1 from *Pseudomonas aeruginosa*, Sigma Chemicals Ltd., Poole, Dorset, UK) to detect the galactose residues on cell surface of wild type and to confirm the lack of galactose residues on cell surface of  $\Delta epsE$  mutant *in situ*. A four step procedure were carried out at 21°C to immobilise the lectins on Silicon nitride AFM tips (PNP-TR, Nanoworld AG, Switzerland): the first step involved incubation of the tips in a 2% solution of 3-mercaptopropyltrimethoxy silane (MTS, Sigma) in toluene (dried over a 4Å molecular sieve) for 1 h, followed by washing with toluene and then chloroform. In the second step, the silanised tips were incubated for 1 h in a 0.1% solution of a heterobifunctional linker, MAL-PEG-SCM, 2 kD (Creative PEGWorks, Winston-Salem, NC, USA) in chloroform. Unbound linker was washed off with chloroform and the tips dried with argon. The third step involved covalent attachment of the lectin (PA1, Sigma) by incubation of the tips in 1 mg ml<sup>-1</sup> solutions of the lectin in PBS at pH 7.4 for 1 h at 21°C, followed by a PBS washing step. The fourth step involved incubation of the lectin-functionalised cantilevers in a 10 mg ml<sup>-1</sup> solution of glycine in PBS to 'amine'-cap any unreacted succinimide groups, followed by washing in PBS. Lectin-functionalised tips were stored under PBS at 4°C overnight before use.

All binding measurements on cell surfaces were carried out under PBS using a MFP-3D BIO AFM (Asylum Research Inc. Santa Barbara, CA USA). The experimental data were captured in 'force-volume' (FV) mode (at a rate of 2 µm s<sup>-1</sup> in the Z direction and at a scan rate of 1 Hz and a pixel density of 32 x 32). In this mode the instrument ramps the Z piezo element of the scanner by a predetermined amount at each sample point over a selected scan area and records the subsequent deflection of the cantilever as it is pushed into (maximum load force

300 pN), then retracted away from the sample surface. This produces a matrix of 1024 force versus distance curves relating to the image coordinates. The spring constant,  $k$ , of the cantilevers was determined by fitting the thermal noise spectra [231], yielding typical values in the range 0.01-0.04 N/m. Adhesion in force spectra was quantified using a bespoke Excel macro [232] which fits a straight line to the baseline of the retract portion of the force-distance data and worm-like chain fitting of the adhesion peaks was performed using a routine in the instrument's software.

### **3.2.4 FTIR Spectroscopy analysis**

Fourier transform infrared (FTIR) spectra of the pure capsular EPS isolated from wild type and mutants cell pellets were measured with a FTS 175C Digilab FT-IR spectrometer (Bio-Rad, US) equipped with a MCT detector and a single-reflection diamond ATR sampling accessory (GoldenGate, Specac). The spectra were recorded in the region of 4000-800  $\text{cm}^{-1}$  with 128 scans at 4  $\text{cm}^{-1}$  resolution and processed by the spectrometer software. The fingerprint region of 800-1800  $\text{cm}^{-1}$  spectra of EPS samples were analysed in detail.

### **3.2.5 Analysis of cell surface alterations**

The alterations in the cell surface after mutations in the *eps* gene cluster was analysed by FCM using an anti-*L. johnsonii* polyclonal antibody as described in section 2.1.5 and 2.1.6. Additionally, the TEM analysis of wild type and mutant cells was performed by Kathryn Cross (IFR) as described in section 2.1.7.

## **3.3 RESULTS**

In order to understand the physiological role of mutations in the *eps* gene cluster on the growth of *L. johnsonii* wild type as well as mutant strains growth curves were prepared at 37°C using a spectrophotometer. This analysis showed that there was no large difference in the growth of wild type and mutant strains during the 11 h time period as can be seen in Figure 3.1.

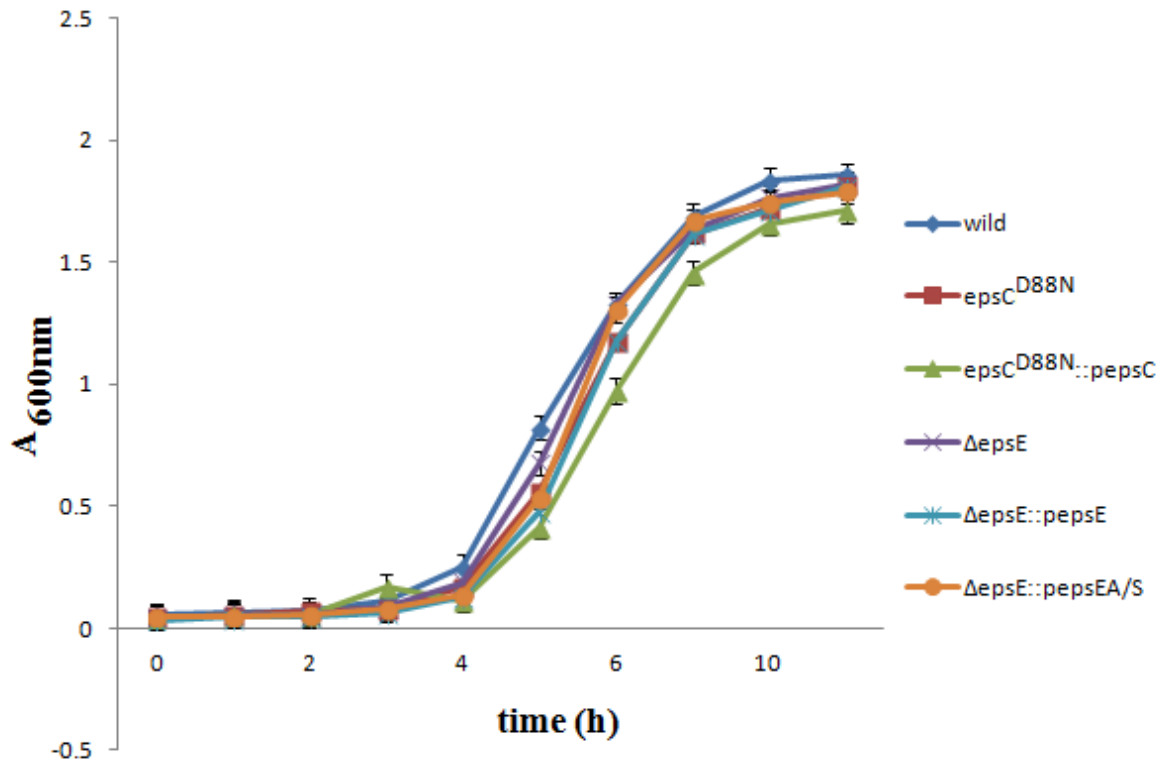


**Figure 3.1.** The growth curve of wild type and mutant strains during the 11 h period.

### 3.3.1 Quantification of EPS production

As described in the introduction (section 1.11), a spontaneous mutation in *epsC* gene resulted in a smooth variant compared to the rough colony morphology of the wild type strain. Similarly, deletion of the putative priming glycosyltransferase gene, *epsE* caused an increased aggregating phenotype compared to the wild type strain. In order to understand the role of these genes in EPS production of *L. johnsonii* FI9785 and also the role of EPS production in the phenotypic alterations, total EPS production of wild type and mutant cells were analysed by GC as a quantity  $\mu\text{g}$  of EPS production per  $10^9$  cells. The polysaccharide content of the MRS medium as a control was also quantified by GC and found to be  $201.0695 \pm 9.55 \mu\text{g}$  for 500 ml culture. This value was therefore subtracted from each sample. Total EPS production was significantly different in *L. johnsonii* and its mutants (Figure 3.2).

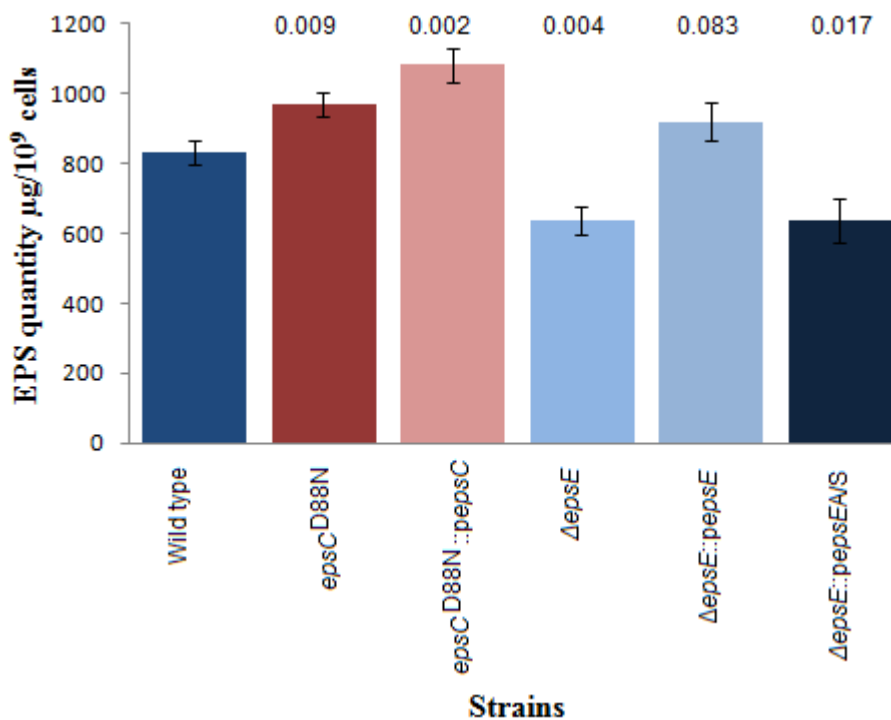


**Figure 3.2.** Total sugar content of EPS samples of *L. johnsonii* wild type and mutant strains. Results are the mean of the triplicate measurements +/- standard deviation. Numbers above bars represent the p values to assess the statistical difference of each strain compared with the wild type.

The smooth variant *epsC*<sup>D88N</sup> mutant produced nearly 15% higher EPS levels than the wild type which was found to be statistically significant. Similarly, the EPS production of *epsC*<sup>D88N</sup>::*pepsC* mutant, which co-expresses the wild type *epsC* gene in this smooth variant, was 30% higher than wild type and doubled the increase of the EPS production of the smooth variant although it has a rough colony morphology like the wild type. This result demonstrates that an increase in the EPS production is not the only reason for the colony morphology alteration in the smooth variant. Δ*epsE* and Δ*epsE*::*pepsEA/S* mutants were still able to produce EPS but with a considerable decrease in EPS production levels compared to the wild type which was found to be statistically different (Figure 3.2). As a result of co-expression of wild type *epsE* gene in Δ*epsE* background, the Δ*epsE*::*pepsE* mutant was fully restored the EPS production with a slight increase in production levels but there were no statistically significant differences in terms of EPS production with wild type strain (Figure 3.2). Overall, these results show the potential involvement of *epsE* gene as a putative priming glycosyltransferase gene in EPS biosynthesis but its deletion did not completely abolish the EPS production.

### 3.3.2 Structural analysis of EPS

In order to investigate the structure of EPS produced by *L. johnsonii* FI9785 and mutant strains, the EPS isolated from cell pellets and culture supernatants were subjected to NMR spectroscopy analysis which was conducted by Dr Ian J. Colquhoun (IFR) and his analysis has been explained in detail elsewhere [230]. Based on structural analysis we found that *L. johnsonii* FI9785 was able to produce two novel EPS: homopolymer EPS-1 which is a branched dextran ( $\alpha$ -glucan) with the unusual feature that every backbone residue is substituted with a 2-linked glucose unit and heteropolymer EPS-2 which was shown to have a hexasaccharide repeating unit composed of two galactose and four glucose residues with different types of linkages between each sugar residue (Figure 3.3). Furthermore EPS-1 and EPS-2 were shown to be partially acetylated [230].

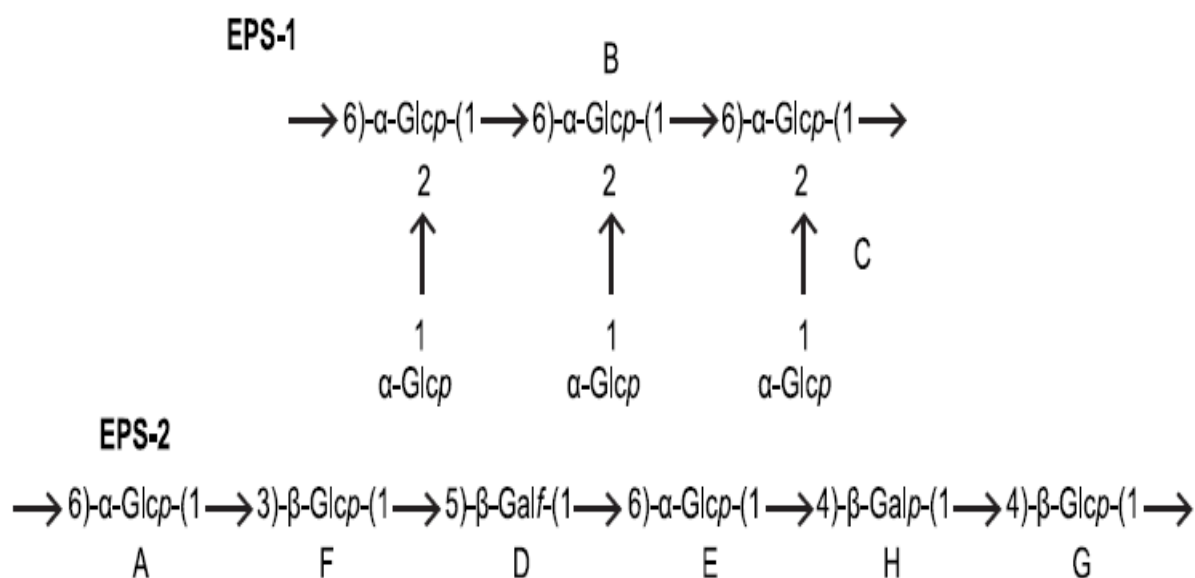


**Figure 3.3.** Line Drawing Structure of exopolysaccharides EPS-1 and EPS-2. The letters show the sugar rings for EPS-1 and EPS-2 (A to H) [230].

The composition of the EPS mixtures produced by the wild type, the *epsC*<sup>D88N</sup> and  $\Delta$ *epsE* mutants and their complemented strains could be readily assessed from the anomeric region of the <sup>1</sup>H NMR spectra following the unequivocal assignment of signals to EPS-1 and EPS-2 (Figure 3.3, 3.4). The wild type, *epsC*<sup>D88N</sup> and its complemented strain produced both EPS-1 and EPS-2, whereas  $\Delta$ *epsE* or its derivative strain containing the wild type gene in the antisense orientation produced only the dextran, EPS-1. However the ability to produce EPS-

2, as well as EPS-1 was restored in the  $\Delta epsE$  strain complemented with the wild type *epsE* gene.

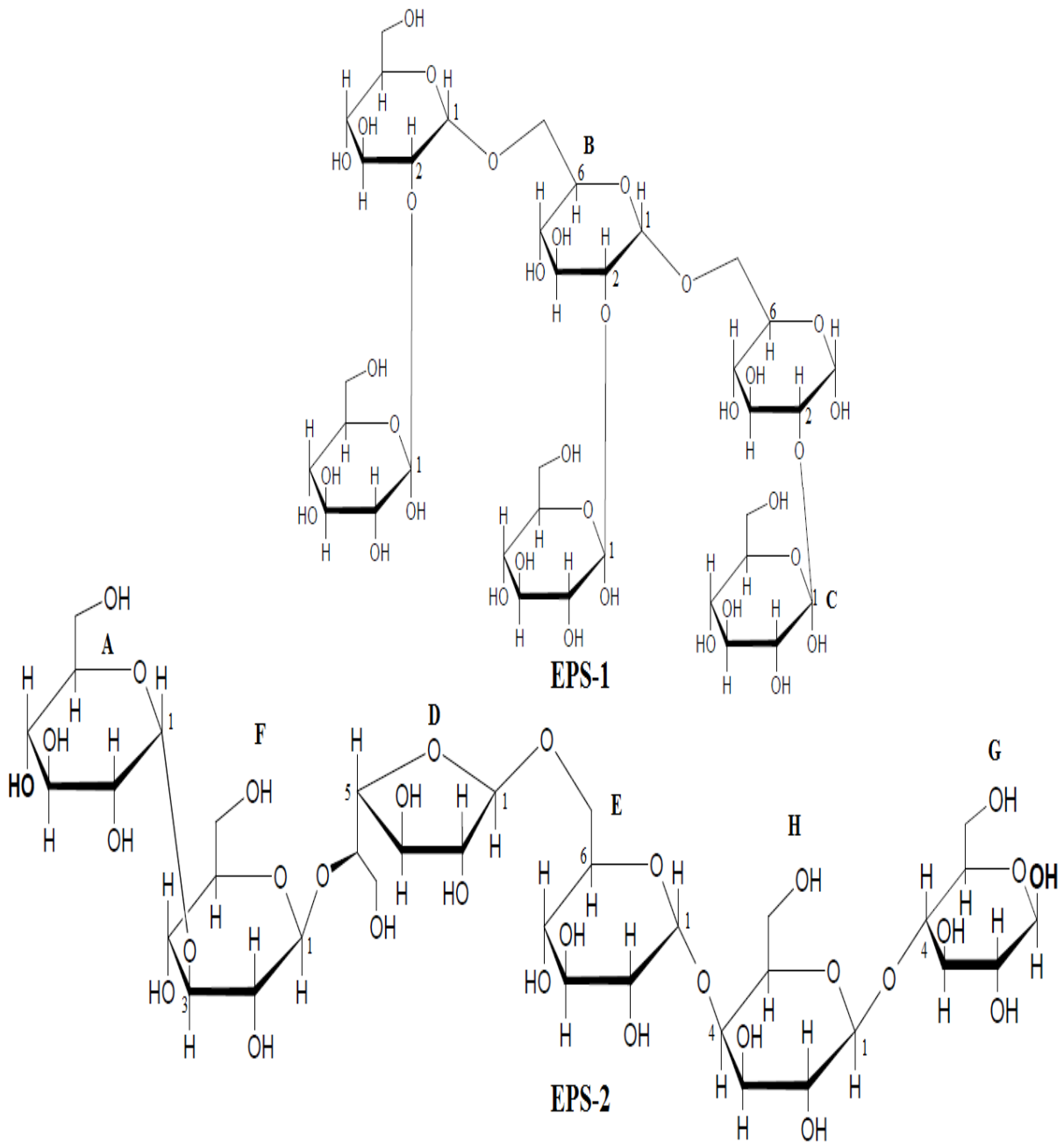


**Figure 3.4.** Structure of exopolysaccharides EPS-1 and EPS-2 produced by *L. johnsonii* FI9785. The letters show the sugar rings for EPS-1 and EPS-2 (A to H) [230].

### 3.3.3 *In situ* localisation of galactose residues on the cell surface

In order to detect and localise the galactose residues of the EPS-2 that covers the cell surface of *L. johnsonii* FI9785 together with EPS-1 which is only composed of glucose residues and also to confirm the lack of galactose containing EPS-2 on the cell surface of  $\Delta epsE$  mutant,

we probed the cell surfaces of live wild type and  $\Delta epsE$  mutant cells in a nanoscale environment using AFM with a galactose specific lectin (PA1) functionalised AFM tip.

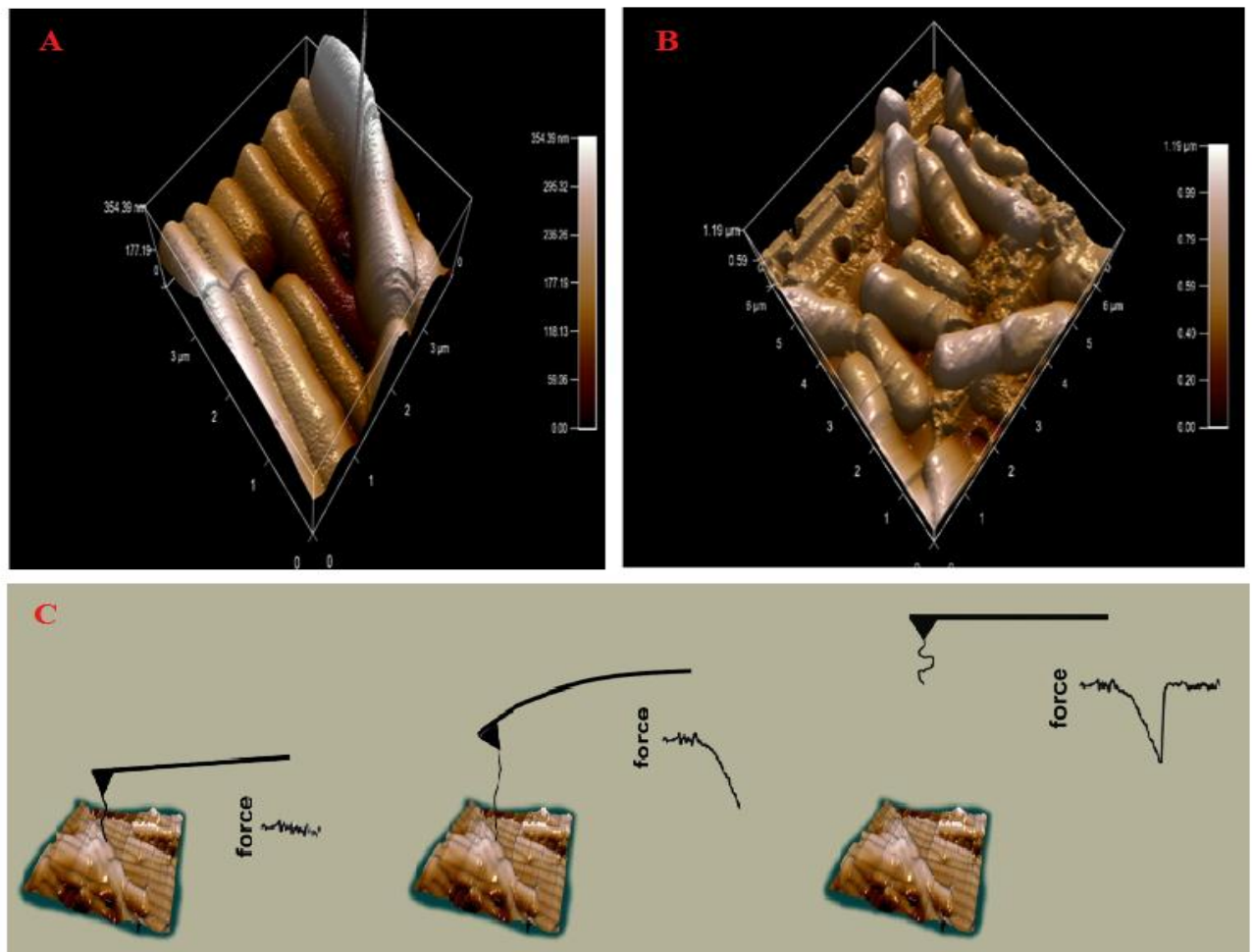


**Figure 3.5.** Imaging wild type (A) and  $\Delta epsE$  mutant cells (B) in their native states by AFM recorded in buffered solution (PBS) and (C) Schematic illustration of the detection of galactose residues on the cell surface by using a lectin-functionalised AFM tip; the functionalised tip binds to the galactose residues on cell surface of *L. johnsonii* FI9785 which results in the firm attachment of the cell to the tip and then a certain force is applied to the target *L. johnsonii* FI9785 cell for adhesion and finally the tip is retracted and this results in a rupture force which is then measured.

This approach allowed an *in-situ* discrimination of the different EPS produced by the wild type which can produce EPS-2 that has galactose residues, and the  $\Delta epsE$  mutant strain which only produces EPS-1 that has no galactose residues (Figure 3.3). Firstly, to investigate the cell surface morphology differences of wild type and  $\Delta epsE$  mutant strain, live bacterial cells were immobilized and imaged in their state using AFM (Figure 3.5A&B). As can be seen from Figure 3.5A, the wild type showed a wavy rough surface morphology, probably due to the accumulation of the EPS on cell surface. In contrast, the cell surface of morphology of

$\Delta epsE$  mutant was clearer and the wave like structures were significantly reduced which was probably due to less EPS accumulation on cell surface (Figure 3.5B). After observing the morphological differences of the wild type and  $\Delta epsE$  mutant strains by AFM, we further detected the galactose residues on cell surface of wild type by using a galactose specific lectin-functionalised AFM tip. Figure 3.5C shows the illustration of the detection of specific molecules by the functionalised AFM tip.

Figure 3.6 shows comparative force-volume images of the wild type and  $\Delta epsE$  mutant strains, allowing the topography of the cells to be compared with the adhesive interactions. The left hand panels depict topography and the right hand panels depict the levels of adhesion encountered by the functionalised AFM tip at each imaging point.

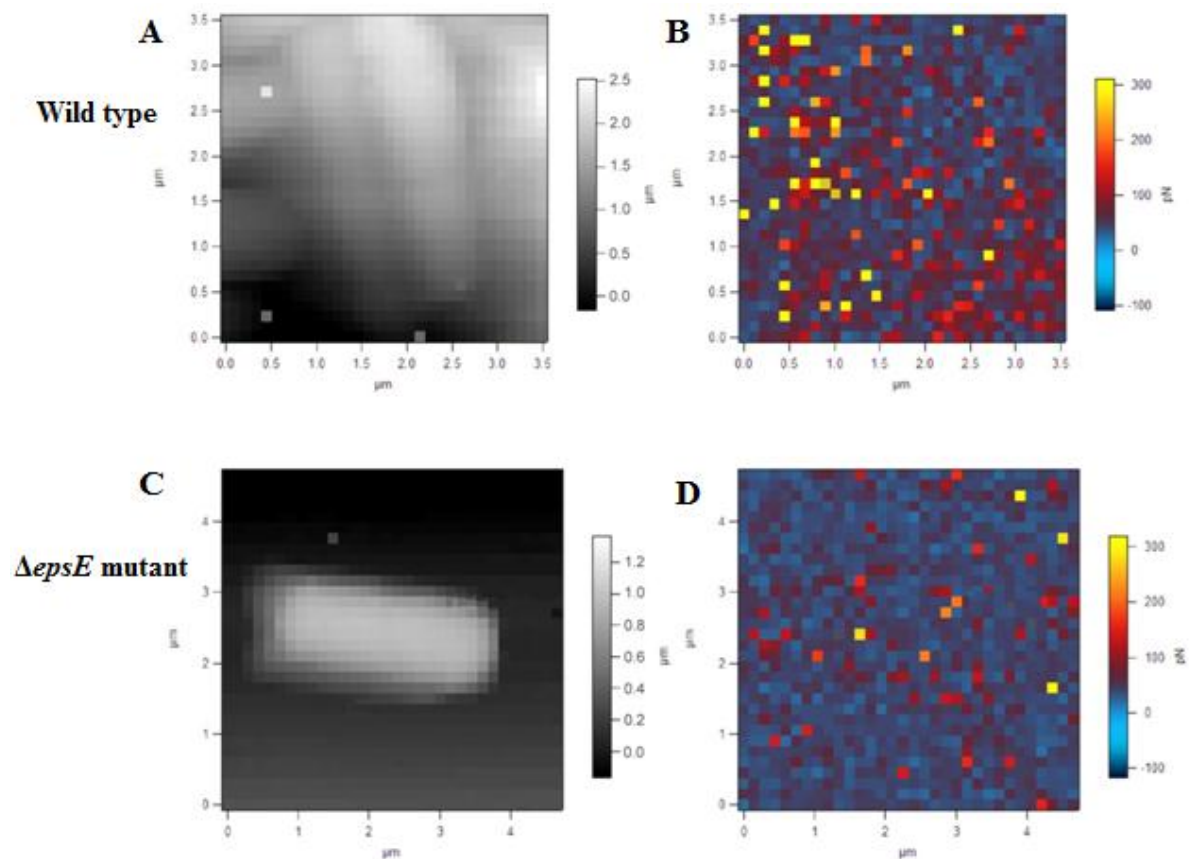


**Figure 3.6.** Force volume images obtained with a PA1 functionalised AFM tip; (A) *L. johnsonii* (wild type) topography and (B) adhesion, (C) *L. johnsonii*  $\Delta epsE$  mutant topography and (D) adhesion.

In Figure 3.6A a close-packed cluster of wild type cells can be seen and in Figure 3.6C a single  $\Delta epsE$  mutant cell is visualised. The adhesion maps reveal that a larger number of the pixels displayed adhesion above the baseline level (approximately 50 pN) for the wild type sample (Figure 3.6B) than the  $\Delta epsE$  mutant sample (Figure 3.6D). Comparison of the

adhesion maps obtained for the wild type which produces EPS-1 and EPS-2 and the  $\Delta epsE$  mutant which only produces EPS-1 reveals a clear difference in the frequency and magnitude of adhesive events captured, with the latter being largely dominated by blue colours (low adhesion) and the wild type adhesion map exhibiting a wider spread of higher value colours (i.e. reds and yellows), agreeing with the loss of a galactose-rich EPS in the  $\Delta epsE$  mutant (Figure 3.6).

Figure 3.7A displays the adhesion data captured on the two samples in graphical form, allowing a quantitative comparison to be made. The modal value for both samples occurs between 50 – 55 pN. Whilst the baseline level of adhesion appears similar for both samples, the wild type data set has a greater proportion of adhesion events in the higher value categories than the  $\Delta epsE$  data set (inset), indicating a higher degree of specific interactions. Adhesion data show that while both strains show adhesion to the tips, a higher frequency of events with a high rupture force is seen for the wild type, and an examination of the rupture distances demonstrated that there was a clear difference between the wild type and the  $\Delta epsE$  mutant, with the latter showing much shorter distances indicative of non-specific interactions. Additionally, the lower baseline adhesion values surrounding the mode in both sets may well be due to non-specific adhesion between the AFM tip and the cell surfaces. This can arise from several sources; one is electrostatic interaction between the tip and cell, although in the current experiment this should be minimal due to the screening action of the buffer solution used.

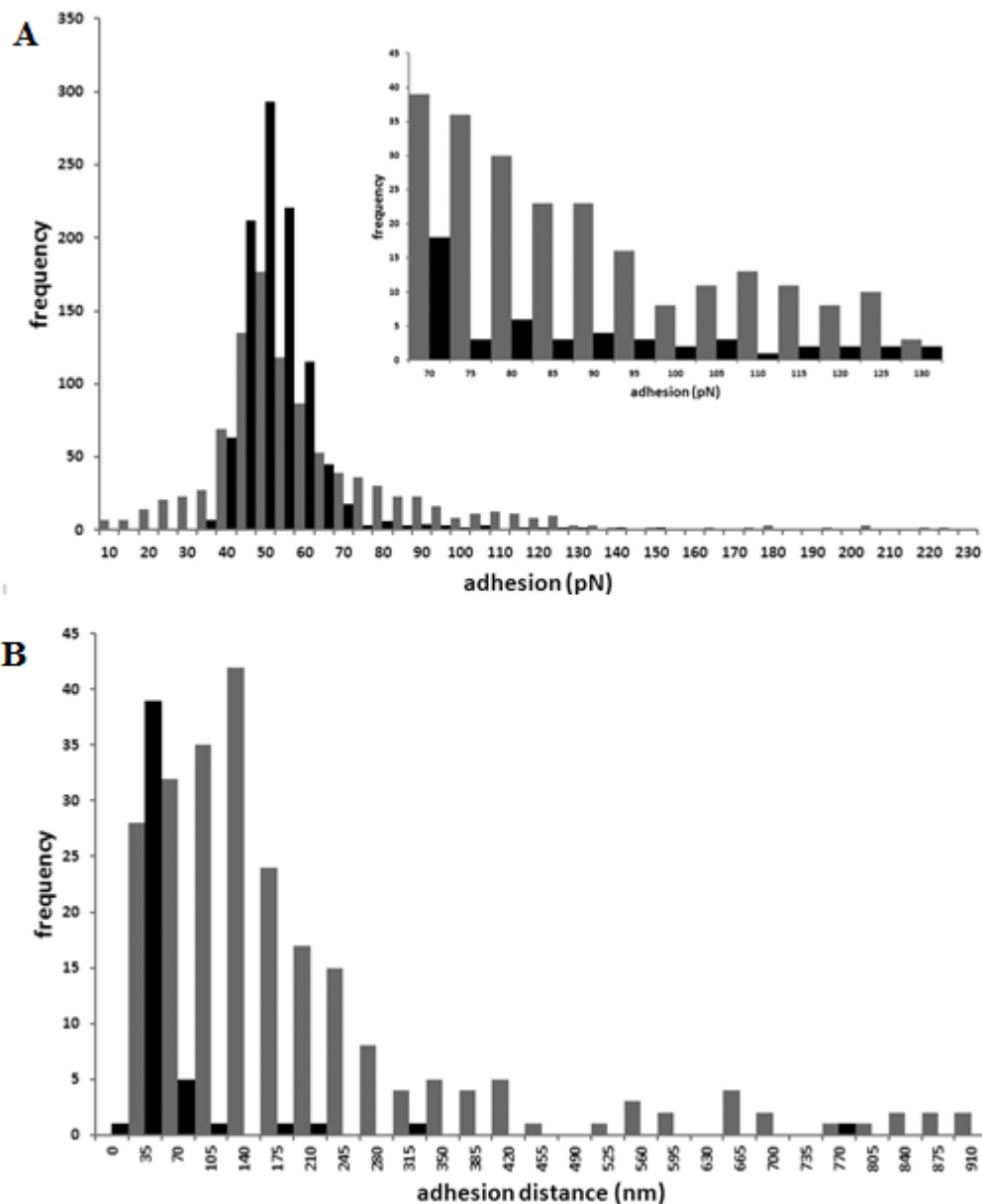


**Figure 3.7.** Adhesion data from force volume data in figure 3.9 depicted as histograms: grey – wild type, black –  $\Delta epsE$  mutant. (A) Distribution of rupture force magnitudes, inset expanded view of data  $> 70$  pN, (B) Distribution of rupture distances.

Another possible source can be penetration of the AFM tip apex into the bacterial cell wall during the approach phase of the measurement. This causes capillary adhesion as the tip is pulled away from the cell surface. In order to minimise this, the maximum loading force was kept to a moderately low value (300 pN) but some penetration or deformation of the cell surface is inevitable considering the sharpness of AFM tips (typical radius of curvature 5-30 nm). Both of these non-specific sources of adhesion tend to occur at (or relatively close to) the tip-sample detachment point (defined as 0 nm in the force-distance curves), whereas specific adhesion between the lectin on the AFM tip and the EPS will occur at distances well

beyond the tip-sample detachment point allowing discrimination of the origins of adhesive peaks in the force spectra. The reason for the shift in position of specific adhesion is due to two factors: the probe molecule (PA1 lectin) is tethered to the AFM tip via a flexible PEG (polyethylene glycol) linker which is approximately 12 nm in length, and the EPS targeted will extend under the load exerted by the retracting AFM tip-cantilever assembly before the ligand and receptor are torn from each other (i.e. the rupture point - arrowed in figure 3.8). This provides a useful means for discrimination of the adhesive forces observed for each sample - comparison of the range of distances at which rupture occurs. Figure 3.7B displays the adhesion data categorised by the distance at which they occurred and shows that the modal values in this case are different for each sample (140 nm for the wild type sample and 35 nm for the  $\Delta epsE$  mutant). This suggests that the adhesion of the functionalised tip to the wild type sample represents specific interactions with the galactose residues of EPS-2.

Figure 3.8 shows three example of force spectra obtained on the wild type sample which exhibit well resolved adhesive interactions on the retract (blue) portion of the force versus distance curves. These can be fitted to a Worm-like chain polymer scaling model [233, 234] to derive two principal characteristic parameters, persistence length,  $L_p$ , and contour length,  $L_c$ . Persistence length is a measure of the flexibility of the polymer chain, and contour length provides a direct measure of the molecular size. The examples chosen are typical of the majority of the adhesive events seen for a PA1 tip probing wild type cells, as are the values derived for persistence and contour lengths. The relatively low value for persistence length indicates that EPS-2 is highly flexible and therefore almost certainly adopts a random coil conformation on the cell surface.

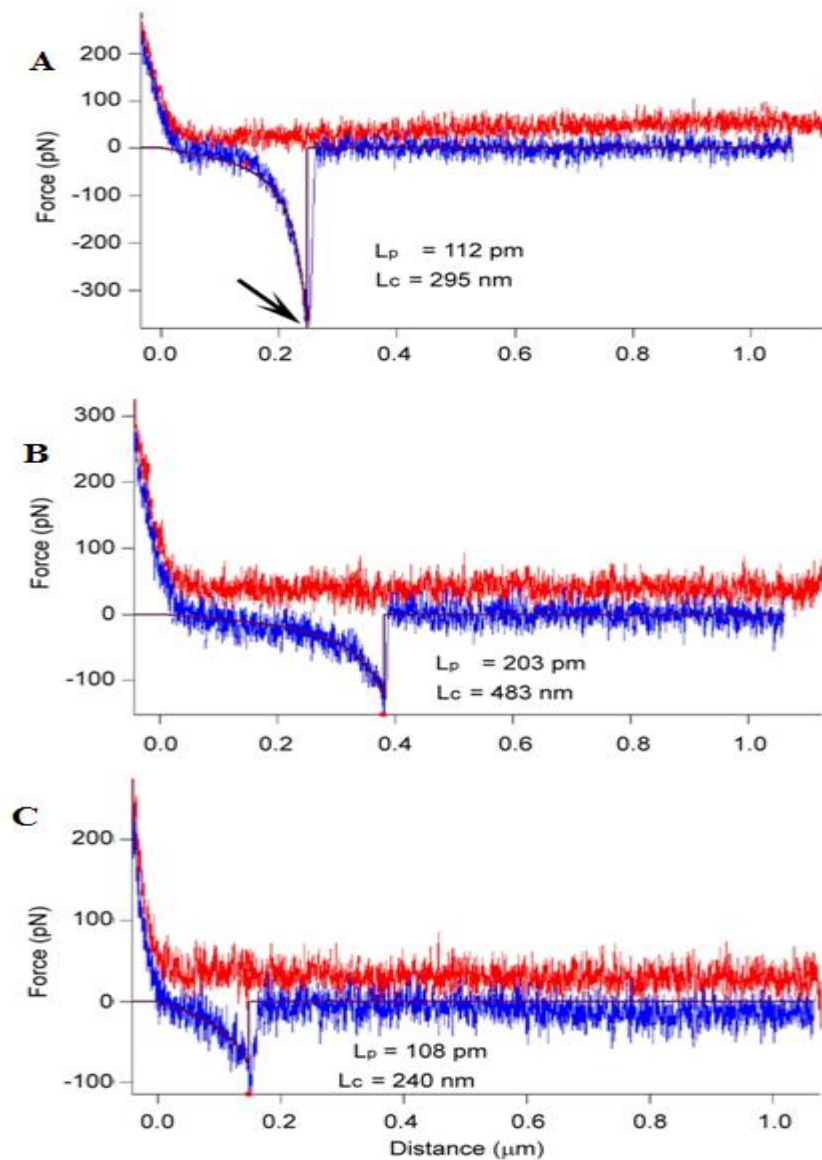


**Figure 3.8.** *In-situ* characterisation of the physical properties of EPS-2 on *L. johnsonii* wild type by fitting example force spectra (A, B, C) to a Worm-like chain model (burgundy line).  $L_c$  derived contour length,  $L_p$  derived persistence length. Arrow indicates the rupture point between the lectin on the AFM tip and the extracellular polysaccharide. Red line – approach, blue line – retract.

Overall, we detected and localised the galactose residues of EPS-2 on cell surface of live *L. johnsonii* cells using AFM. Importantly, we also confirmed the lack of galactose on the EPS-1 that covers the cell surface of  $\Delta epsE$  mutant. We also demonstrated the conformational structure and nature of the EPS-2 chains which showed a Worm-like chain polymer scaling model representing the semi-flexible character of the EPS-2 on cell surface of *L. johnsonii* FI9785.

### 3.3.4 Alterations in EPS structure detected by FTIR analysis

The FTIR spectra of capsular EPS isolated from the wild type and its mutants showed changes in the structural and functional group of this biopolymer after mutations (Figure 3.9).

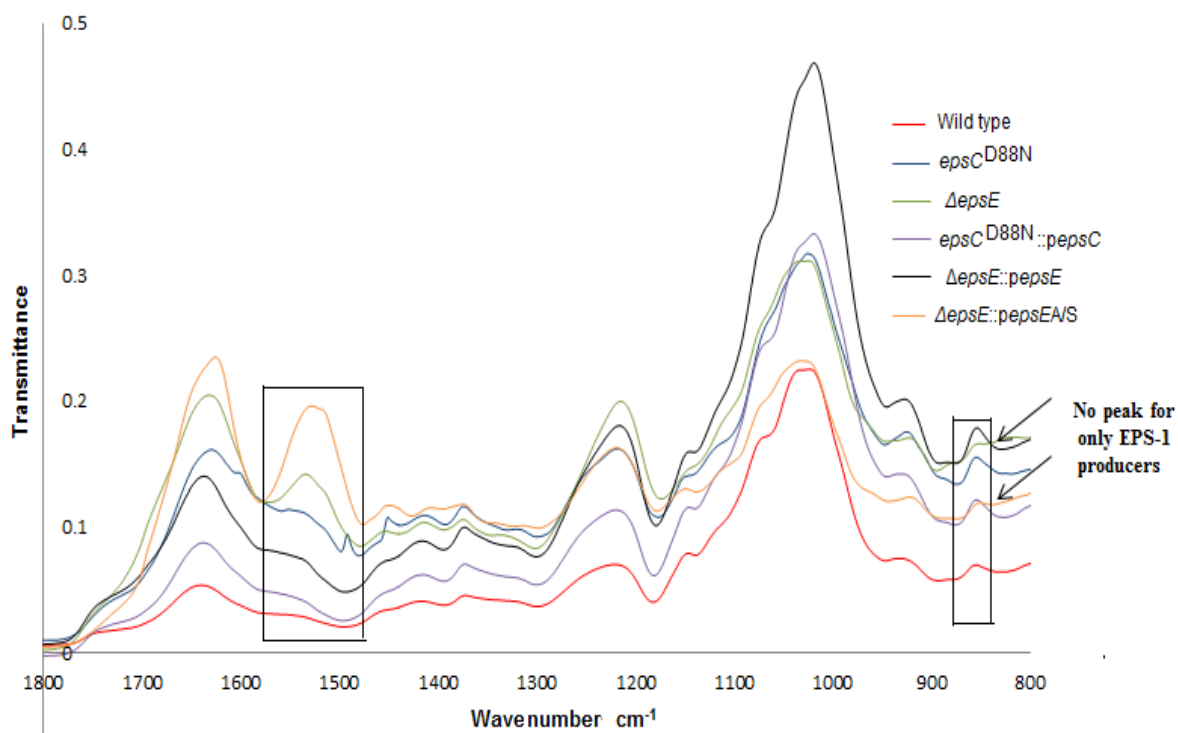


**Figure 3.9.** FTIR spectra of capsular EPS isolated from the wild type and mutants of FI9785. The windows represent the alteration in the spectra of the EPS-1 only producer strains compared to the EPS-1 – EPS-2 producer strains.

All EPS samples showed a wide absorption peak around 3200-3400  $\text{cm}^{-1}$ , indicating typical hydroxyl groups (O-H) of polysaccharides suggesting that all of samples analysed are polysaccharides [19]. The peak from 2800 to 2970  $\text{cm}^{-1}$  showed a weak C-H stretching frequency for all EPS samples [22] (data not shown). The region around 1500-1600  $\text{cm}^{-1}$  showed an intense peak for only EPS isolated from  $\Delta epsE$  and  $\Delta epsE::pepsEA/S$  strains. This peak is assigned to N-H bending and C-N stretching in proteins [235]. The amide C=O stretching and carboxyl groups were detected from the corresponding peak at 1600-1760  $\text{cm}^{-1}$  for all samples. The peak at around 1220-1240  $\text{cm}^{-1}$  that all of EPS samples have, differentiated the bacterial polysaccharides from other types of polysaccharides [19]. All isolated EPS showed an intense peak around 1000  $\text{cm}^{-1}$  which indicated the characteristic C-O bond of polysaccharides [22]. Interestingly, a peak at around 840-860  $\text{cm}^{-1}$  disappeared in samples isolated from  $\Delta epsE$  and  $\Delta epsE::pepsEA/S$  mutants that could only produce the  $\alpha$ -glucan type polysaccharide, whereas all other isolated EPS showed this peak that were

comprising the two polysaccharides, which may show the cross-linking of these two polysaccharides [236]. Another strong possibility in the lack of this peak in  $\alpha$ -glucan samples is the fact that previously it was reported that the peak at around  $800\text{-}900\text{ cm}^{-1}$  was attributed to the presence of the  $\beta$ -glycosidic bonds [237, 238] in which EPS-1 comprises only  $\alpha$ -glycosidic bonds whereas EPS-2 contains  $\beta$ -glycosidic bonds between their monomers.

### 3.3.5 Detection of cell surface alterations

In order to investigate the cell surface changes related to alterations in EPS structures after mutations, FCM and TEM analysis were performed. A polyclonal antibody raised against *L. johnsonii* wild type strain was used and responses to this anti-wild type antibody were detected by using FCM. The viability of *L. johnsonii* cells was assessed by Propidium Iodide (PI) staining and no difference was detected among wild type and mutant's viability (Figure 3.10).

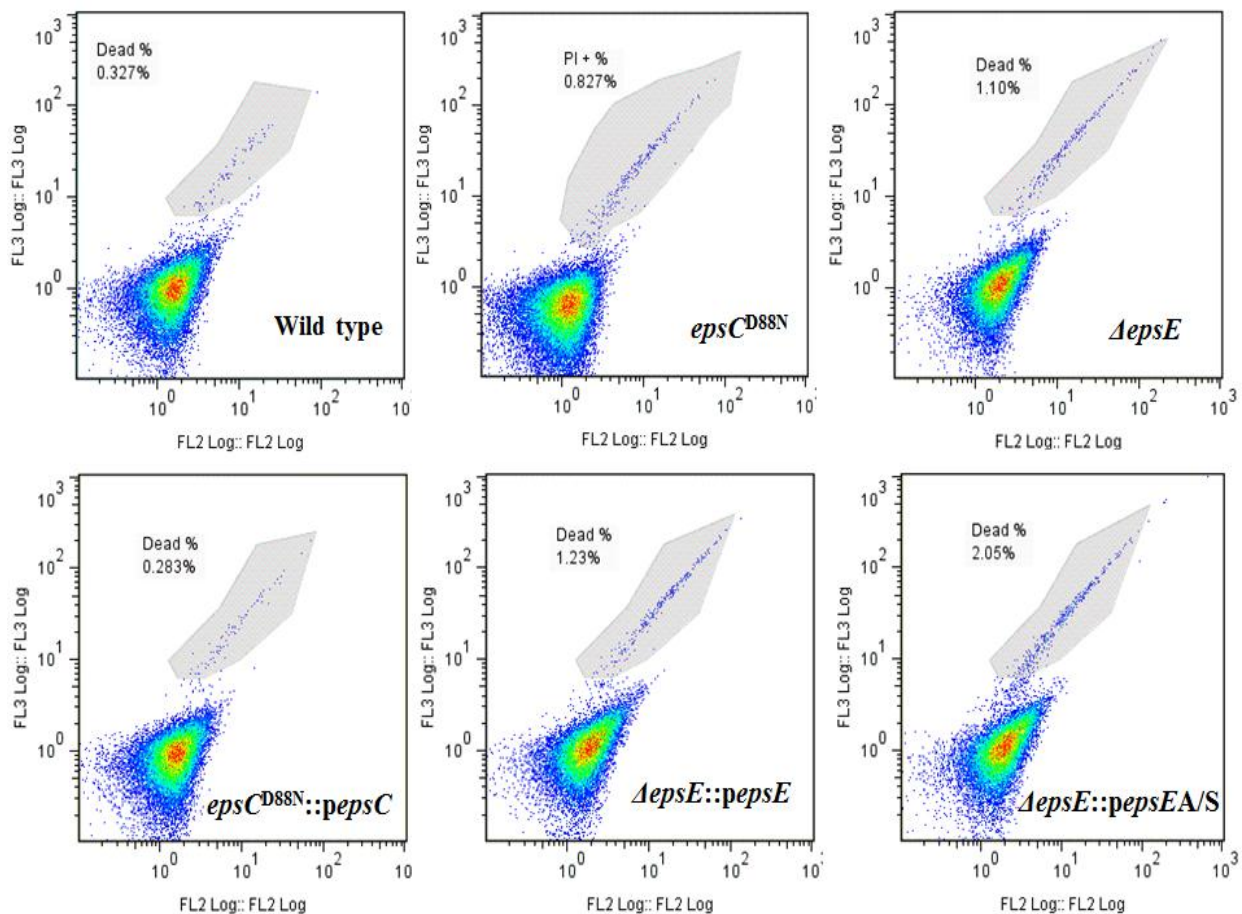


**Figure 3.10.** Viability of stationary phase *L. johnsonii* cells detected by PI staining.

The Median value of the fluorescence signal showed the specific binding of the antibody to each strain. The antibody response to the  $\Delta epsE$  mutant was significantly ( $p < 0.05$ ) higher than to the wild type and the other strains (Figure 3.11). Similar observations were also made in the  $\Delta epsE::pepsEA/S$  mutant which was also statistically different ( $p < 0.05$ ). The inability to produce EPS-2 as a capsular material at the cell surface resulted in the availability of the cell surface epitopes for antibody binding in  $\Delta epsE$  mutant and  $\Delta epsE::pepsEA/S$  mutant strains. As a result of EPS-2 production, the  $\Delta epsE::pepsE$  mutant showed an antibody response more similar to the wild type (Figure 3.11). Despite the increased levels of EPS production in the  $epsC^{D88N}$  mutant and its complemented derivative, the levels of antibody response were similar to the wild type, suggesting that the antibody does not have a large response to EPS-2 itself.

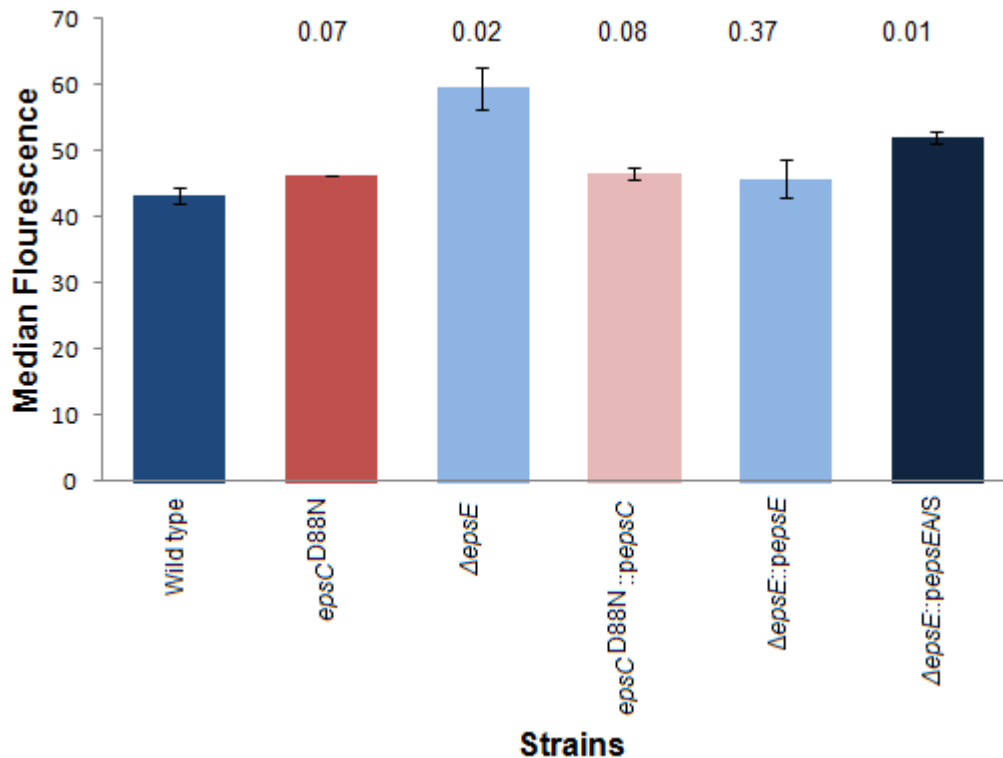


**Figure 3.11.** Anti-wild type antibody responses to the wild type and derivative strains measured by Flow cytometry. Results are the mean of duplicate experiments +/- standard deviation. P values above the bars were determined by an independent t test compared to the wild type.

Additionally, TEM analysis were performed to detect the accumulation of EPS at the cell surface of *L. johnsonii* and also to detect the cell surface alterations after the mutations in *eps* genes. This analysis clearly showed the accumulation of the EPS to the cell surface where they formed a capsule as an outer cell-surface layer in *L. johnsonii* FI9785 (Figure 3.12). An

EPS layer still accumulated at the cell surface of the  $\Delta epsE$  and  $\Delta epsE::pepsEA/S$  mutant strains, consisting solely of EPS-1 (Figure 3.12) which was visually thinner than wild type,  $epsC^{D88N}$  and  $epsC^{D88N}::pepsC$  mutant strains but quite similar to  $\Delta epsE::pepsE$  mutant strain.

These observational differences in the thickness of the EPS layer did not match the yields of EPS measured in GC analysis, suggesting that the preparation procedure resulted in the loss of some EPS from the cell surface (Figure 3.12-3.18). Figure 3.13 to 3.18 show the TEM analysis of wild type,  $epsC^{D88N}$ ,  $\Delta epsE$ ,  $epsC^{D88N}::pepsC$ ,  $\Delta epsE::pepsE$  and  $\Delta epsE::pepsEA/S$  mutant strains, respectively, showing different levels of EPS accumulation on cell surface of *L. johnsonii* strains. Washing with buffers which have no EPS cross-linking potential has been reported to remove capsular EPS [239]; in particular, the  $epsC^{D88N}$  and  $epsC^{D88N}::pepsC$  mutant strains shown to have an increased accumulation of EPS by GC analysis appeared to have a similar or slightly reduced capsule thickness compared to the wild type strain under TEM and this may have implications for the nature of the interactions of the EPS within the capsule and with the cell wall. Similarly, although  $\Delta epsE::pepsE$  restored the EPS-2 production and was able to produce EPS at wild type EPS levels, the thickness of EPS layer was notably reduced in comparison to the thickness of the EPS layer of wild type (Figure 3.12). Overall, TEM analysis confirmed the accumulation of EPS on cell surface of *L. johnsonii* cells and showed some evidences of alterations in the cell surface nature related to the changes of EPS structure of mutant cells, particularly in the  $\Delta epsE$  mutant. Additionally, we demonstrated the removal of EPS from cell surface during the cell preparation steps in TEM analysis which showed that TEM analysis cannot be an indicator alone for the measurement of the EPS thickness.

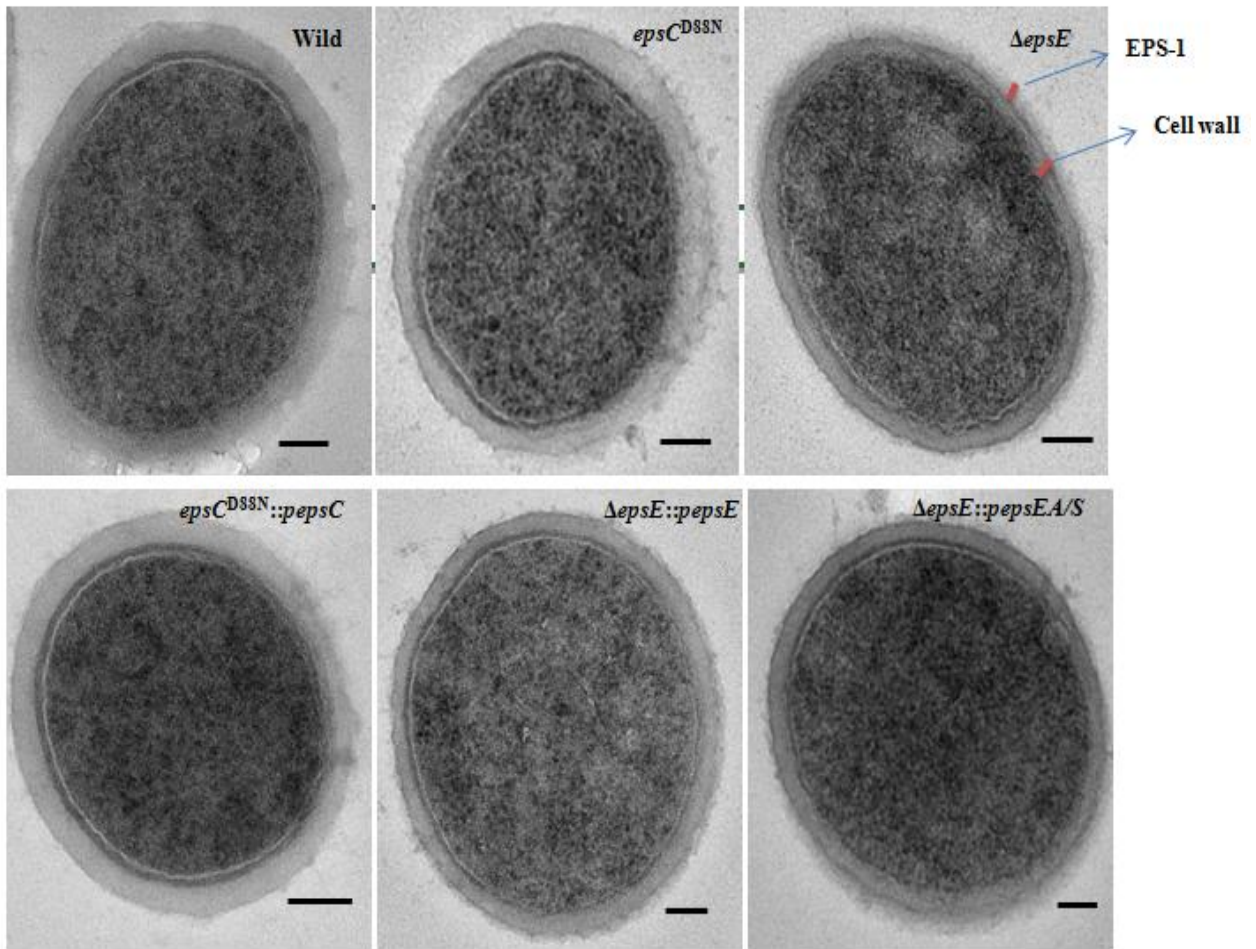


**Figure 3.12.** TEM analysis of *L. johnsonii* FI9785 and its mutants grown in MRS medium showing the capsular EPS accumulation on each strain's cell surface. In each panel the bar represents 100 nm.

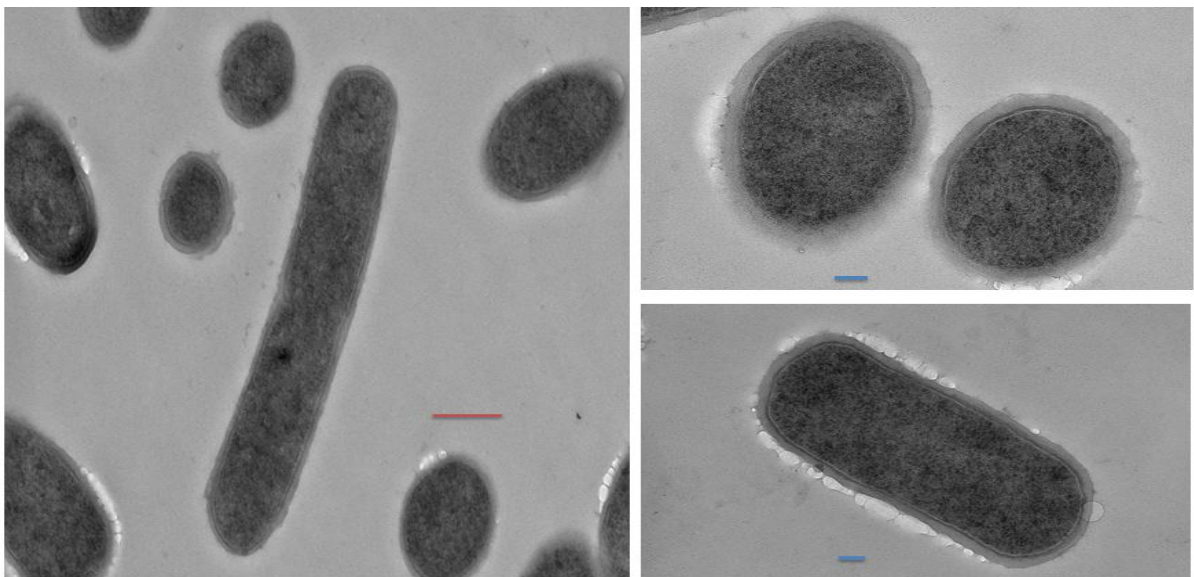


**Figure 3.13.** TEM analysis of *L. johnsonii* FI9785. Red bar and Blue bar represent 500 nm and 100 nm, respectively.

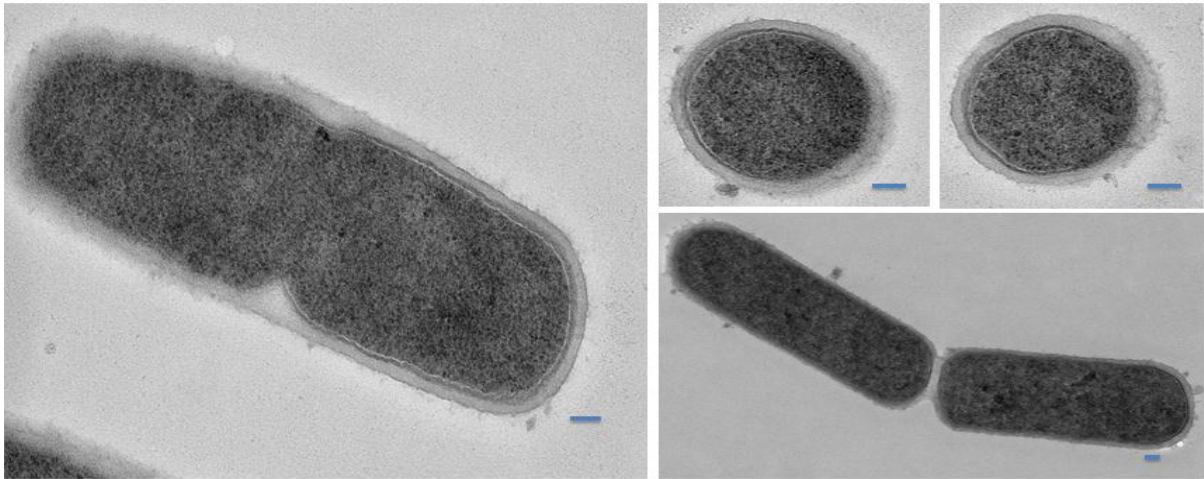


**Figure 3.14.** TEM analysis of *L. johnsonii epsC<sup>D88N</sup>*. Blue bar represents 100 nm in each picture.

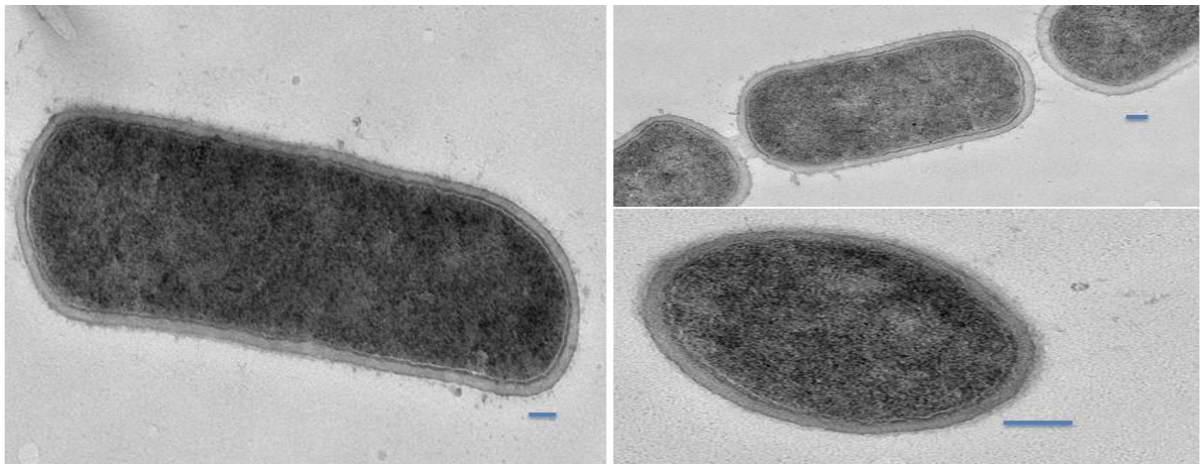


**Figure 3.15.** TEM analysis of *L. johnsonii ΔepsE*. Blue bar represents 100 nm in each picture.

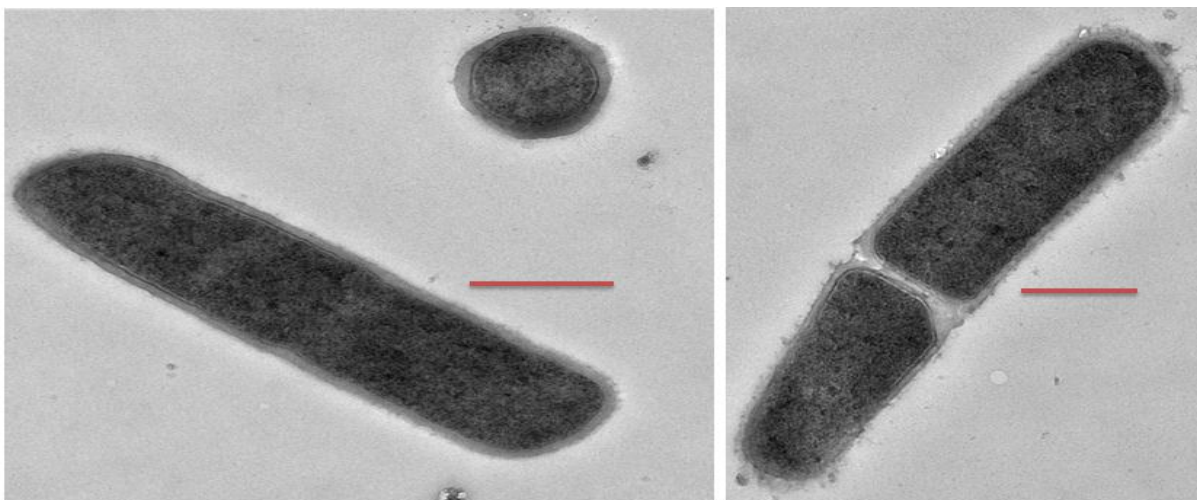


**Figure 3.16.** TEM analysis of *L. johnsonii epsC<sup>D88N</sup>::pepsC*. Red bar represents 500 nm in each picture.

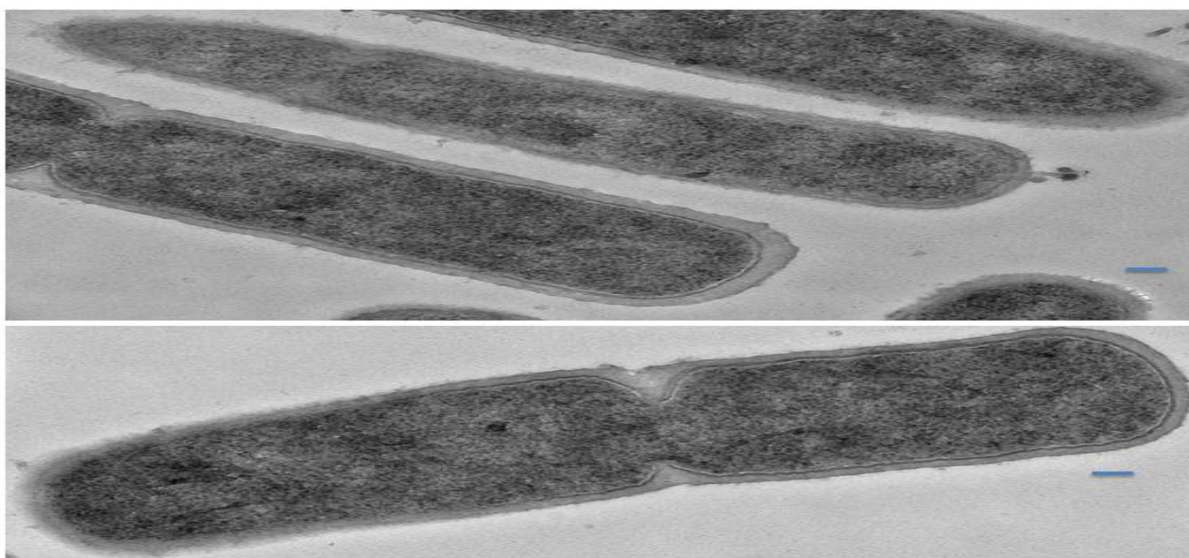


**Figure 3.17.** TEM analysis of *L. johnsonii*  $\Delta epsE::pepsE$ . Blue bar represents 100 nm in each picture.

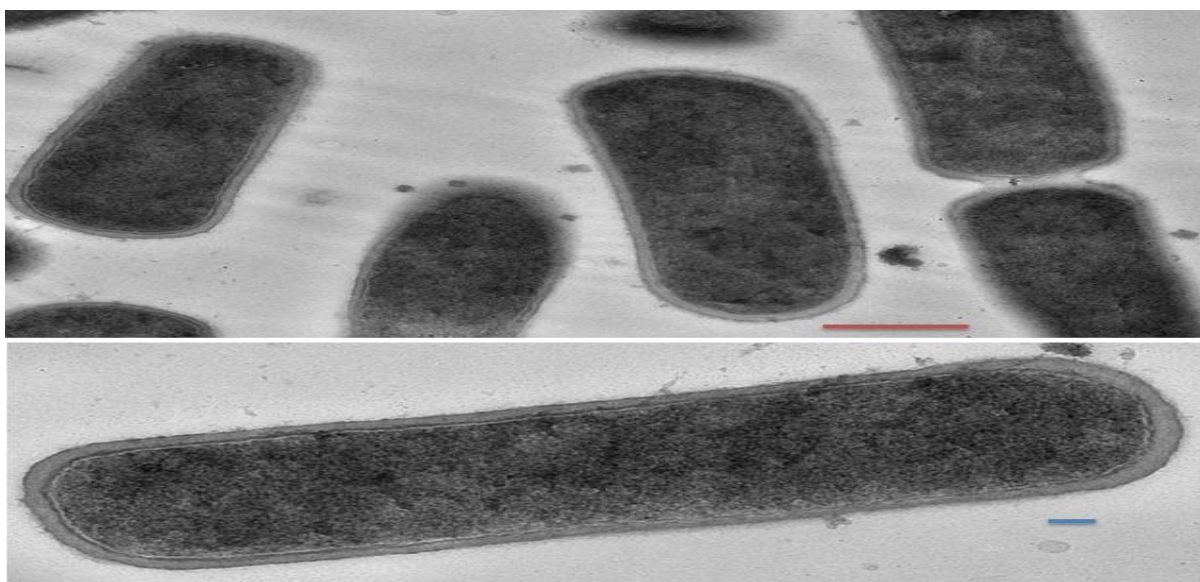


**Figure 3.18.** TEM analysis of *L. johnsonii*  $\Delta epsE::pepsEA/S$ . Red bar and Blue bar represent 500 nm and 100 nm, respectively.

### 3.4 DISCUSSION

Analysis of the total EPS production of wild type and mutant strains revealed alterations in EPS biosynthesis levels after mutations in the *eps* gene cluster although there was no difference among wild type and mutants growth profiles. Furthermore, the smooth variant *epsC*<sup>D88N</sup> showed an increase in EPS biosynthesis levels which demonstrated a link between a smooth colony phenotype and EPS [33]. As described in Chapter 1, the *epsC* gene is predicted to be a tyrosine protein kinase which functions in the chain length determination,

polymerisation and regulation of EPS biosynthesis together with *epsB* and *epsD* genes [33]. The phosphorylation pattern of the *epsC*, *epsD* together with *epsB* was shown to be important to control polymerisation and export of EPS biosynthesis in other *eps* clusters which was explained in detail in Chapter 1 [96, 117]. The role of *cpsD* (a homologue of *L. johnsonii* *epsC*) in capsule formation of *S. pneumoniae* was shown to be crucial for EPS biosynthesis as deletion of this gene or a mutation in the ATP binding domain in this gene (Walker A motif) resulted in acapsular phenotype [96]. The spontaneous mutation in *epsC* gene of smooth variant resulted in a change of the amino acid residue from Aspartic Acid to Asparagine in a conserved area downstream of the Walker A motif which is the ATP binding domain [33, 96]. Similarly, it was shown that this mutation was located only 2 amino acids away from the important area containing aspartate residue that is highly conserved in a range of bacteria [33], which was demonstrated previously as being important for the ATPase activity [240]. Total sugar analysis of this smooth variant showed an increase in EPS content which suggests that this particular mutation may affect the interaction between the *epsB*, *epsC* and *epsD* phosphorylation complex and/or ATP in some way to give increased EPS production and enhanced EPS production might be the reason for the smooth colony morphology in *epsC*<sup>D88N</sup> mutant [33]. Previously it was also reported that the mutation of the tyrosine residues in the carboxy-terminal repeat domain of CpsD (*epsC*) of *S. pneumoniae* resulted in a mucoid phenotype which was suggested to be related with the higher CPS production [96]. Later on researchers produced several tyrosine mutations in this particular domain of CpsD and found that the CPS production was reduced in these mutants but the mucoid phenotype was still observed and it was suggested that the mucoid phenotype was not related with the higher CPS production but it was proposed that the mucoid phenotype might be related with the conformational characteristics of CPS accumulated to the cell surface and its interactions with other surface molecules [95].

The increase in the EPS production levels was also detected for *epsC*<sup>D88N</sup>::*pepsC* mutant that showed a rough colony morphology like wild type in contrast to the smooth morphology of *epsC*<sup>D88N</sup> mutant. The involvement of the tyrosine kinase complexes in the chain length determination of final EPS was shown for several strains [94, 95]. We proposed that not only the quantity but the quality of EPS produced may play an important role in the colony morphology as previously described for pneumococcal CPS [95]. We suggested that variation in the chain length may be responsible for the observed phenotypic changes in these mutants [33]. This type of colony switching was also observed for the polysaccharides of *Vibrio*

*cholerae* O1 where disruption of the *Vpst* gene which is the transcriptional regulator in polysaccharide biosynthesis resulted in smooth colony morphology and complementation of this mutant with the wild type *Vpst* gene caused conversion to rugose phenotype which showed an increased polysaccharide content [241]. The authors showed that there was a 4 fold increase in the expression of *Vpst* gene in the complemented rugose mutant [241]. Similarly, the increase in the expression of the wild type *epsC* gene in the *epsC*<sup>D88N</sup>::*pepsC* mutant might have resulted in an increased EPS production and the formation of the polymerisation and export regulation system in wild type conditions and this may result in rough colony morphology as wild type.

Deletion of the *epsE* gene resulted in a reduction in total EPS biosynthesis compared to the wild type. EpsE is predicted to act as the priming glycosyltransferase in *eps* clusters of LAB that adds the first sugar monomer from an activated sugar nucleotide to the phosphorylated lipid carrier [8, 10, 61, 77, 87, 89, 113, 114]. Deletion of the *epsE* gene, the priming glycosyltransferase gene, resulted in loss of EPS production in several bacterial species [87, 94, 120-122]. Recently it was shown that deletion of *epsE* gene in *L. rhamnosus* GG resulted in the loss of the galactose rich EPS but the glucose rich one was still present on cell surface, suggests that *L. rhamnosus* GG can produce two types of EPS and *epsE* gene can be the priming glycosyltransferase for galactose rich EPS but not for the glucose rich one [61]. The NMR spectroscopy results also confirmed that *L. johnsonii* also produced two types of EPS and  $\Delta$ *epsE* and  $\Delta$ *epsE*::*pepsEA/S* mutant strains were only able to produce one of them which is the reason for the reduction of EPS biosynthesis in these mutants. Additionally, complementation of *epsE* confirmed the important role of this gene in EPS biosynthesis.

The capsular EPS is thought to be involved in the functional properties of probiotic bacteria as described in Chapter 1 in detail [229, 242]. However, there are few reports on the structure determination of commensal gut bacteria such as *L. johnsonii* FI9785. It was interesting to find that *L. johnsonii* FI9785 was capable of producing two different types of capsular EPS: EPS-1 and EPS-2. EPS-1 is a novel dextran (homopolysaccharide) with the unusual feature that every  $\alpha$ -(1,6) linked Glcp backbone residue was substituted at O2 with a terminal  $\alpha$ -Glcp unit. EPS-2 is a heteropolysaccharide which has a unique hexasaccharide repeating unit composed of four glucose and two galactose residues. To the best of our knowledge, the structures of the two EPS are unique among EPS produced by LAB. Previously, the structure of the EPS from *L. johnsonii* 142 has been identified as discussed in Chapter 1, which was a

heteropolymeric pentasaccharide composed of one glucose residues and four galactose residues with the following structure:



Additionally, the accumulation of the EPS to the cell surface of *L. johnsonii* NCC 533 was reported but the structure of the EPS produced by this strain has not been identified yet [62]. More recently, the EPS structure of *L. johnsonii* strain 151 has been identified which was composed of the following structure:



The *eps* gene clusters of these two *L. johnsonii* strains has not been identified yet but the presence of the pentasaccharide EPS repeating units suggests that these *eps* clusters may encode five glycosyltransferases for the biosynthesis of the EPS repeating units. These glycosyltransferases are responsible for the unique EPS structures identified among different species.

The production of more than one EPS has also been demonstrated in other LAB – *Lactobacillus plantarum* EP56 expressed two heteropolysaccharides, one cell bound and one released [221] while the two EPS produced by *Leuconostoc pseudomesenteroides* R2 were both linear dextrans with different characteristics [243]. The heteropolymeric hexasaccharide EPS-2 was also unique containing two galactose residues which were  $\beta$ -galactopyranose and  $\beta$ -galactofuranose, respectively and four glucose residues in  $\alpha$  and  $\beta$  forms. The deletion of the *epsE* gene which is the putative priming glycosyltransferase resulted in complete loss of EPS-2 production but not EPS-1. As we described above as a result of the deletion of the putative priming glycosyltransferase in several other bacteria, the EPS production was abolished [87, 94, 120-122]. In fact the *eps* gene cluster of *L. johnsonii* FI9785 has a similar genetic organisation to identified gene clusters for the biosynthesis of capsular or extracellular heteropolysaccharides which harbour *epsE* as the priming glycosyltransferase [33]. This suggested that the production of EPS-1 could be independent from the *eps* gene cluster of *L. johnsonii* FI9785 and a unique enzyme encoded in the genome of *L. johnsonii* FI9785 can be responsible for the EPS-1 production. Generally, the production of the homopolysaccharides by LAB (glucan or fructan type) is known to be carried out by extracellular glycansucrases using sucrose as the donor substrate [244]. Also, the production of  $\alpha$ -glucan with different linkages is quite common for the genus *Lactobacillus* and

membrane-bound glucosyltransferases that polymerizes glucosyl residues from UDP-glucose encoded by genes defined as *gtf* are commonly responsible for production of these dextran-type EPS [99, 101, 105, 108, 244]. Interestingly, nucleotide and protein BLAST results from several *gtf* genes did not give any correlation with the genes in the *L. johnsonii* FI9785 genome. We suggest that the *L. johnsonii eps* gene cluster which harbours six putative glycosyltransferase genes might be responsible for the biosynthesis of heteropolysaccharide EPS-2; in addition, one of these glycosyltransferases may have a bifunctional role to produce the homopolymer EPS-1 [245]. Potentially, the six monosaccharide units in the heteropolysaccharide EPS-2 might be added by each glycosyltransferase to form the long-chain capsular EPS-2 initiated by the priming glycosyltransferase *epsE*. Another gene supporting the role of the *eps* cluster in EPS-2 production is the *glf* gene, which putatively encodes the UDP-galactopyranose mutase [33]. This has been predicted to convert UDP-galactopyranose to UDP-galactofuranose in *Lactobacillus rhamnosus* GG [61] and may be responsible for the presence of the galactofuranose residues in the repeating unit structure of EPS-2.

In this study, we identified two novel EPS structures produced by *L. johnsonii* FI9785 and confirmed the important role of *epsE* gene in EPS-2 biosynthesis as complementation of the *epsE* gene fully restored the EPS-2 production. We also showed that the increase in the EPS production levels in *epsC*<sup>D88N</sup> and *epsC*<sup>D88N</sup>::*pepsC* mutant strains was not related to the structural changes in the EPS as these mutants were producing EPS-1 and EPS-2 as wild type. It is possible that there was an increase in EPS-2 production levels in these mutants probably resulted in higher final EPS content than the wild type. But it should be noted the colony morphologies of these mutants were different probably due to the conformational characteristics of the EPS-1 and EPS-2 on cell surface in which the relative ratio of these two EPS might play a role.

AFM was used to detect cell surface alterations after changes in EPS structures between wild type and  $\Delta$ *epsE* mutant using a galactose specific lectin functionalised tip. The AFM image showing wild type and  $\Delta$ *epsE* mutant in their native state also supported the reduction in EPS levels in  $\Delta$ *epsE* mutant where surface-wave like structures observed on wild type which was not the case for  $\Delta$ *epsE* mutant. This observation was also in agreement with the previous data showing the surface-wave like structures on wild type *L. rhamnosus* GG which was producing two types of EPS where only one type of EPS producer mutant cells showed non-wavy structure [246]. Although our attempts without functionalised AFM tips was not

successful to investigate the physicochemical role of EPS on cell surface of *L. johnsonii*, these researchers showed the role of EPS on cell wall nanomechanical properties with wild type *L. rhamnosus* GG and its *epsE* gene deleted mutant strain. They demonstrated that EPS plays a very critical role in cell surface nature in terms of elasticity and softness [246]. The stiffness of mutant cell was two times higher than wild type, which suggested that the stiff polymer peptidoglycan was determining the nanomechanical properties of mutant cell whereas the EPS layer which covered the peptidoglycan was the reason of the softness in wild type compared to the mutant strain [246]. We expect the same mechanical properties for wild type and  $\Delta epsE$  mutant strain which may affect their surface characteristics and adhesion properties.

Functionalization of AFM tip with a galactose specific lectin showed the presence of galactose residues on cell surface of wild type and confirmed the lack of this residue on cell surface of  $\Delta epsE$  mutant *in situ*, which was fully consistent with the NMR data. In addition to detecting and spatially locating the galactose-bearing EPS-2 on the wild type sample, further analysis of the force spectra yielded information about the physical properties of the polysaccharide. Force spectra obtained on the wild type sample fitted the Worm-like chain model [233, 234], indicating that EPS-2 adopts a semi-flexible random coil conformation. In summary, these data demonstrated the reduction in EPS levels in  $\Delta epsE$  mutant with the lack of wave-like patterns in this mutant. Additionally, we detected and localised the galactose of EPS-2 on live wild type cells and confirmed the absence of EPS-2 from the cell surface of  $\Delta epsE$  mutant. TEM also confirmed the alterations of cell surface after changes in EPS structures and accumulation levels among wild type and mutant strains but discrepancies between the observed thickness of EPS layer and EPS content assessed by GC analysis suggest this is an inappropriate method for measuring EPS content and that EPS in *epsC*<sup>D88N</sup> mutant may be more loosely attached than in the wild type.

Here we also have detected the cell surface changes after mutations in the *eps* gene cluster using anti-*L. johnsonii* FI9785 antibody responses using flow cytometry. Gorska and co-workers [59] found that the heteropolymeric EPS from *L. johnsonii* 142, isolated from the murine gut, reacted to a whole cell antibody. Interestingly, the  $\Delta epsE$  mutant which could only produce the  $\alpha$ -glucan as a capsular EPS showed a higher antibody response to the *L. johnsonii* whole cell antibody than wild type, while strains producing higher levels of EPS did not show an increased response. The inability to produce EPS-2 as a capsular material at the cell surface may have resulted in the availability and exposure of cell surface epitopes

like surface proteins for antibody binding in  $\Delta epsE$  and  $\Delta epsE::pepsEA/S$  mutants. Another explanation for increased antibody response in these mutants might be that glucose-containing epitopes could be more antigenic than galactose-containing epitopes, as noted previously [247]. Our findings suggest that the gastrointestinal colonisation and recognition by the immune system of the wild type and the  $\Delta epsE$  strains would be different because of the described structural differences. In addition, FTIR results showed the differences of the functional groups that wild type and mutants capsular EPS were containing which may affect the antibody responses and other properties.

In summary, this chapter described two novel EPS structures and the effect of the deletion of the priming glycosyltransferase gene and spontaneous mutation in a putative protein tyrosine kinase gene encoded in *eps* gene cluster on the final EPS structure and the level of EPS production. These alterations was also observed and confirmed with unique techniques such as AFM, FCM, FTIR and TEM. These characterisations will help the understanding the role of cell surface associated EPS in probiotic related properties.

# Chapter 4

---

## Exopolysaccharides and Cell Surface Interactions

## 4.1 INTRODUCTION

The cell surface architecture of probiotic bacteria determine the adhesion properties to the intestinal epithelial cells which is one of the major criteria considered for selection as a probiotic organism [73]. Similarly, it was reported that the adherence capacity of probiotic bacteria to the gastrointestinal tract is a contributing factor for pathogen exclusion [248] and the cell surface characteristics of the probiotic bacteria have been related to these adhesion properties [20, 70, 176, 189]. The cell wall and cell surface envelope of bacteria and the relation of these components with the outer environment affect the bacterial adhesion. These components on cell surface of bacteria can be divided into two groups as specific and nonspecific factors for their functional roles in bacterial adhesion. Specific factors that are affecting the bacterial adhesion are generally cell surface proteins which are specific adhesins for the specific molecules at the epithelial cell environment such as sortase-dependent proteins (for example MUB) and S-layer proteins [162]. The physicochemical characteristics of cell surface such as net charge of bacteria generally determined with Zeta potential, contact angle and cell surface hydrophobicity measurements can also be described as a specific factor affecting the bacterial adhesion in which the composition of cell wall envelope and the molecules on cell surface convey these characteristics [176, 249]. There is no a linear correlation between the net charge or hydrophobicity of a bacterial surface and bacterial adhesion as they are dynamic characteristics depending on the growth phase of bacteria and the pH or the ionic strength of the environment [176].

Nonspecific factors also affect the bacterial adhesion to epithelial cells which include nonspecific adhesins that are located on the bacterial cell surface such as EPS. It has been shown that the level of EPS accumulation and structure of the EPS produced by LAB are important factors for determining the cell surface characteristics of probiotic strains as described in Chapter 1. Furthermore EPS are also involved in colonisation, biofilm formation, autoaggregation and play an important role on physicochemical characteristics of the bacterial cell surface, such as hydrophobicity and Zeta potential, which can affect bacterial adhesion and colonisation. Although there are some contradictive reports about the role of EPS on bacterial adhesion, it was suggested that EPS cover the bacterial adhesins including specific proteins on cell surface and the absence of EPS rather than its presence can be a factor for the increased bacterial adhesion [61].

Biofilm formation which requires the attachment and aggregation of single cells to form a multi-cellular environment is also a contributing factor for bacterial adhesion and probiotic related properties. Furthermore several reports demonstrated the *in vitro* biofilm formations of *Lactobacillus* strains [141, 184-186]. The role of EPS on the biofilm formation of pathogenic bacteria has been studied extensively but only few reports about the role of EPS on biofilm formation of probiotic bacteria are available [141]. Autoaggregation, could also affect the adhesion and colonisation of probiotic strains [189, 190] and EPS may contribute to the aggregation properties of LAB [63]. However the main factor that determines the bacterial autoaggregation properties is cell surface proteins in particular aggregation promoting proteins located at the cell surface [191-193].

The previous chapter describes the alterations in the EPS levels and structure accumulated at the cell surface of *L. johnsonii* strains. In this chapter we describe the effects of alterations in EPS nature of *L. johnsonii* on biofilm formation, physicochemical cell surface properties, autoaggregation, and adhesion to human tissue cells in an *in vitro* model. Understanding the role of the EPS on cell surface characteristics of lactobacilli may provide further knowledge in order to explain the bacteria-bacteria and bacteria-host interactions for probiotic related functions.

## 4.2 MATERIAL AND METHODS

### 4.2.1 Bacterial strains and growth conditions

*L. johnsonii* FI9785 and mutant strains (Table 1.4) and *L. rhamnosus* GG were grown in MRS under the conditions described in section 2.1.2. Additionally, for specific biofilm formation assays, MRS broth without either Tween 80 or salt solution, Lactobacilli broth AOAC medium (Difco) (15 g l<sup>-1</sup> peptonized milk, 5 g l<sup>-1</sup> yeast extract, 10 g l<sup>-1</sup> glucose, 5 g l<sup>-1</sup> tomato juice, 2 g l<sup>-1</sup> dipotassium phosphate, and 1 g l<sup>-1</sup> Tween 80), and Trypticase soy broth (TSB) medium (Oxoid) (17 g l<sup>-1</sup> pancreatic digest of casein, 3 g l<sup>-1</sup> enzymatic digest of soybean, 5 g l<sup>-1</sup> sodium chloride, 2.5 g l<sup>-1</sup> dipotassium hydrogen phosphate, and 2.5 g l<sup>-1</sup> glucose) were used. For strains containing plasmids, chloramphenicol was added to media at 7.5 µg ml<sup>-1</sup> concentration.

### 4.2.2 Biofilm assays and Microscopy

The microscopic analysis of the biofilm formation of *L. johnsonii* FI9785 was conducted based on a previously described method [250]. Briefly a 25-ml volume of sterile MRS broth was inoculated with 250 µl (1%) of an overnight culture. Sterile twin-frosted microscope slides (VWR International) were inserted into the Falcon tubes and cultures were grown statically under aerobic, anaerobic and microaerobic conditions. After 2 to 3 days, slides were removed and washed following with the cleaning of one side and the other side was examined using Nikon Eclipse microscope at magnification of × 400. Similarly the biofilm formation of *L. johnsonii* FI9785 on glass tubes was examined according to the protocol described previously [250]. Overnight grown *L. johnsonii* FI9785 was diluted to OD<sub>600nm</sub> of 1 in fresh MRS broth and 1 ml was added to a sterile borosilicate glass test tube and incubated at 37°C aerobically. For crystal violet staining, tubes were washed with UP H<sub>2</sub>O and then dried at 60°C for 30 min. 1 ml of 1% crystal violet solution was added, and then tubes were incubated on a rocker at RT for 30 min. Unbound crystal violet was washed off with water and tubes were dried at 37°C and bound crystal violet was dissolved in 20% (v/v) acetone in ethanol solution for 10 min and was then poured into the cuvettes and A<sub>590nm</sub> was measured.

Measurement of biofilm formation of *Lactobacillus* strains was based on this method previously described for glass tubes [250] with minor modifications to adapt the method for 96 well format. For each assay a 200 µl single-use glycerol stock, routinely stored at -80°C, was inoculated to fresh MRS broth containing 2% glucose. Cultures were grown aerobically

overnight without shaking at 37°C. The overnight culture was diluted 10 fold with sterile MRS medium and 200 µl was added to 96-well polystyrene plates (Greiner Bio-One Ltd). Plates were incubated aerobically unshaken at 37°C for 72 h. Three replicates for each strain were used for each assay and six independent experiments were conducted.

For crystal violet staining, plates were washed with H<sub>2</sub>O and allowed to stand for 15 min at RT for drying. Two hundred µl of a 1 % (w/v) crystal violet solution was added, and the plates were incubated on a rocker at RT for 15 min. Unbound crystal violet was washed off with water, and the plates were dried at 37°C. Bound crystal violet was dissolved in 20% (v/v) acetone in ethanol for 10 min and A<sub>590nm</sub> was measured with a Thermomax microtitre plate reader (Molecular Devices, US).

Congo red binding to the extracellular material tests were based on the method as previously described [251], with minor modifications. Basically, six 1 µl aliquots of overnight MRS grown cultures were spotted onto MRS agar plates containing 0.04 g l<sup>-1</sup> Congo red and 0.015 µg ml<sup>-1</sup> Coomassie blue. Red or pink colonies on Congo red plates indicated the binding of Congo red to extracellular material around micro-colonies.

TEM analysis was performed on samples after negative staining with uranyl acetate as described before [33].

#### **4.2.3 Measurement of physicochemical cell surface characteristics**

In order to understand the role of EPS on cell surface characteristics of *L. johnsonii* FI9785, zeta potential and adhesion to hydrophobic solvent analysis were performed.

The electrophoretic mobility (zeta potential) measurements were performed according to the previously described protocol [175]. Basically, *L. johnsonii* cells from 20 ml of culture were harvested by centrifugation (6000 x g, 4°C; 10 min) and washed twice with PBS. The pellets were resuspended in 10 mM K<sub>2</sub>HPO<sub>4</sub> to obtain an OD<sub>600nm</sub> ~ 1.0. The pHs of solutions were adjusted to 3, 7 and 10 with 1 M HCl and 1 M NaOH. The electrophoretic mobility was measured using a Zeta master (Malvern Instruments, Malver, UK) instrument. Electrophoretic mobilities were converted to ζ-potential using the Helmholtz–Smoluchowski equation as described elsewhere [175]. All measurements were carried out at 25°C and each sample was analysed in triplicate.

The microbial adhesion to hexadecane (MATH) was carried out largely following the method described previously [176]. Basically, overnight grown cultures were collected by centrifugation (6000 x g, 4°C; 10 min) and resuspended in 5 ml of 10 % (w/v) sucrose solution to obtain an optical density (OD<sub>600nm</sub>) of ~2.5. The cell suspensions of wild type and mutants were then freeze-dried and the resulting cells were washed with PBS and suspended in 10 mM KH<sub>2</sub>PO<sub>4</sub> to obtain an OD<sub>600nm</sub> of ~0.8. The pH of the suspension was adjusted to 3 with 1 M HCl. Two ml of the bacterial cell suspension was then mixed with an equal volume of hexadecane (Sigma) in a 10 ml tube. The mixture was vortexed for 1 min and then left undisturbed for 20 min to allow complete phase separation. After equilibration, the aqueous phase was removed carefully, in order not to disturb the interfacial equilibrium, and the OD<sub>600nm</sub> was measured. The percentage adhesion was calculated using the following equation:

$$\% \text{ Adhesion to hexadecane} = (1 - A_1/A_0) \times 100$$

A<sub>0</sub> is the initial absorbance (OD<sub>600nm</sub>) of the bacterial suspension and A<sub>1</sub> is the absorbance after 20 min of incubation.

#### **4.2.4 Autoaggregation and adhesion to tissue culture assays**

Autoaggregation (i.e., cell clumping and sedimentation) was measured as described previously [250] by monitoring the decrease in OD<sub>600nm</sub> following incubation in a cuvette at RT under aerobic conditions. For autoaggregation assays, overnight MRS-grown cultures were vortexed for 5 min and 1 ml of each strain was removed and left for 4 h at room temperature without any disturbance. Photos were taken with a Coolpix P5100 digital camera (Nikon). Also FCM application was used for the measurement of autoaggregation as described in section 2.1.6.3. Adhesion to HT29 cells experiments were performed by FCM as described in section 2.1.6.4.

### **4.3 RESULTS**

#### **4.3.1 *In vitro* biofilm formation of *L. johnsonii* FI9785**

To investigate the biofilm formation properties of cell surface associated EPS in *L. johnsonii* FI9785, several methods and conditions were examined. TEM showed the accumulation of EPS as a fibre like structure at the cell surface of *L. johnsonii* FI9785 (Figure 4.1). Biofilm formation was tested under two different carbon sources (glucose or sucrose) and using two

different stains crystal violet and Congo red. We also assessed the biofilm formation related to cell surface EPS by using Congo red and coomassie blue in MRS medium agar plates. The micro-colonies of *L. johnsonii* FI9785 and mutant cells appeared to have a dark red layer which shows the Congo red interactions to the cell surface EPS (Figure 4.2). The Congo red binding layer was still visible after 8 days of incubation for all strains (Figure 4.2).

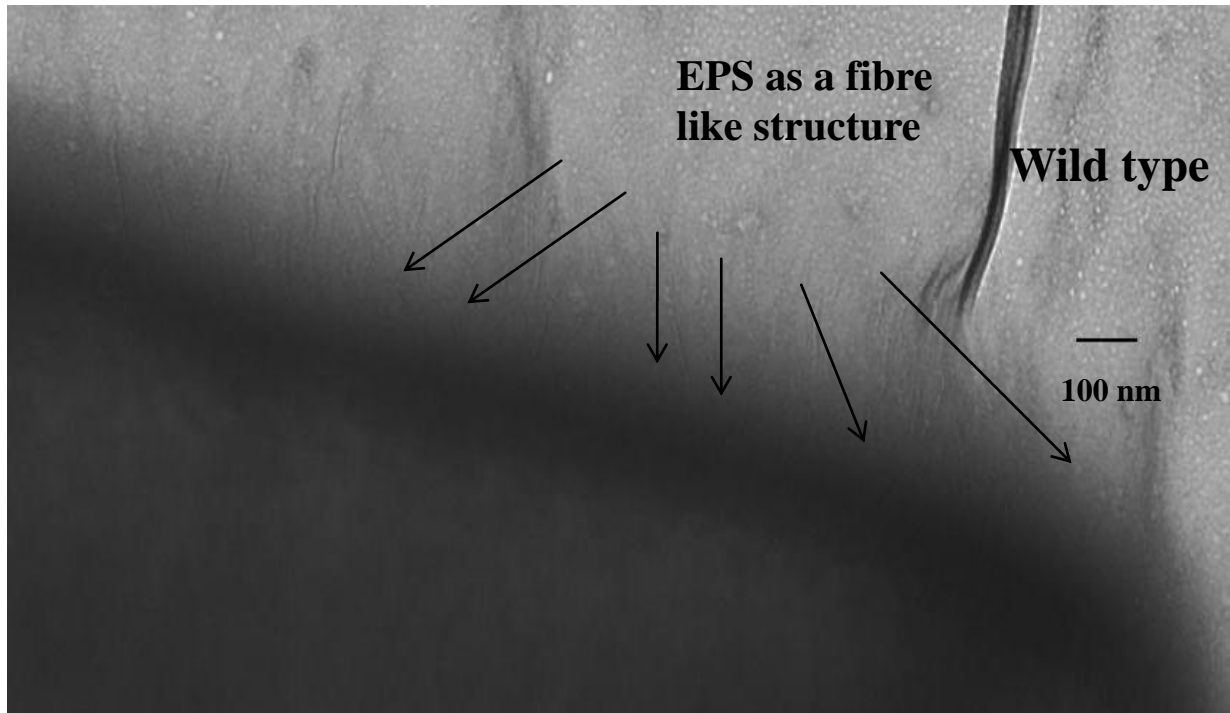


**Figure 4.1.** TEM picture of *L. johnsonii* wild type showing the accumulation of EPS on cell surface as a fibre like structure. Image was produced by Mary Parker (IFR).

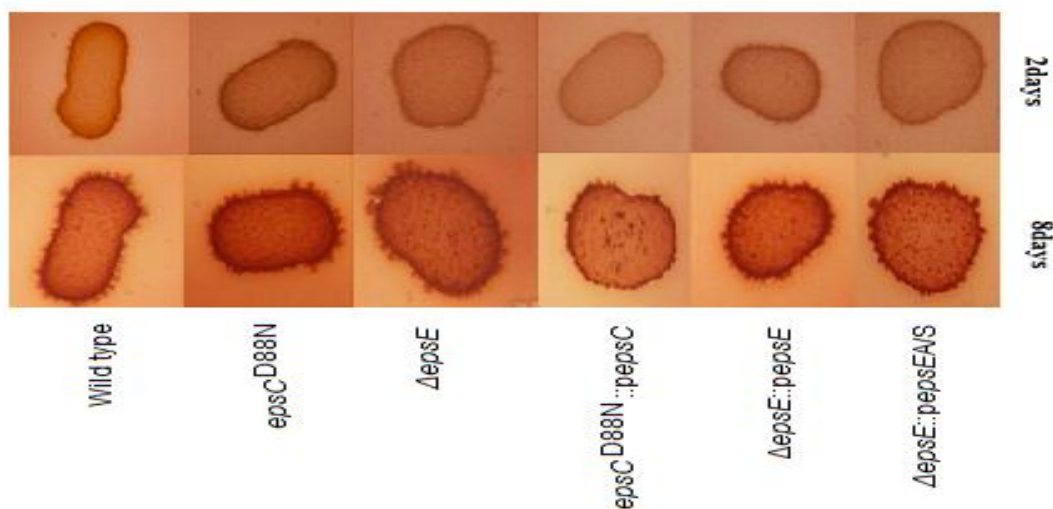


**Figure 4.2.** Congo red binding phenotypes of colonies of wild type and mutants on MRS agar containing Coomassie blue and Congo red.

*L. johnsonii* FI9785 was able to produce biofilms on different surfaces; glass tubes (Figure 4.3d) and on sterile microscope slides under aerobic, microaerobic and anaerobic conditions (Figure 4.3abc, respectively).

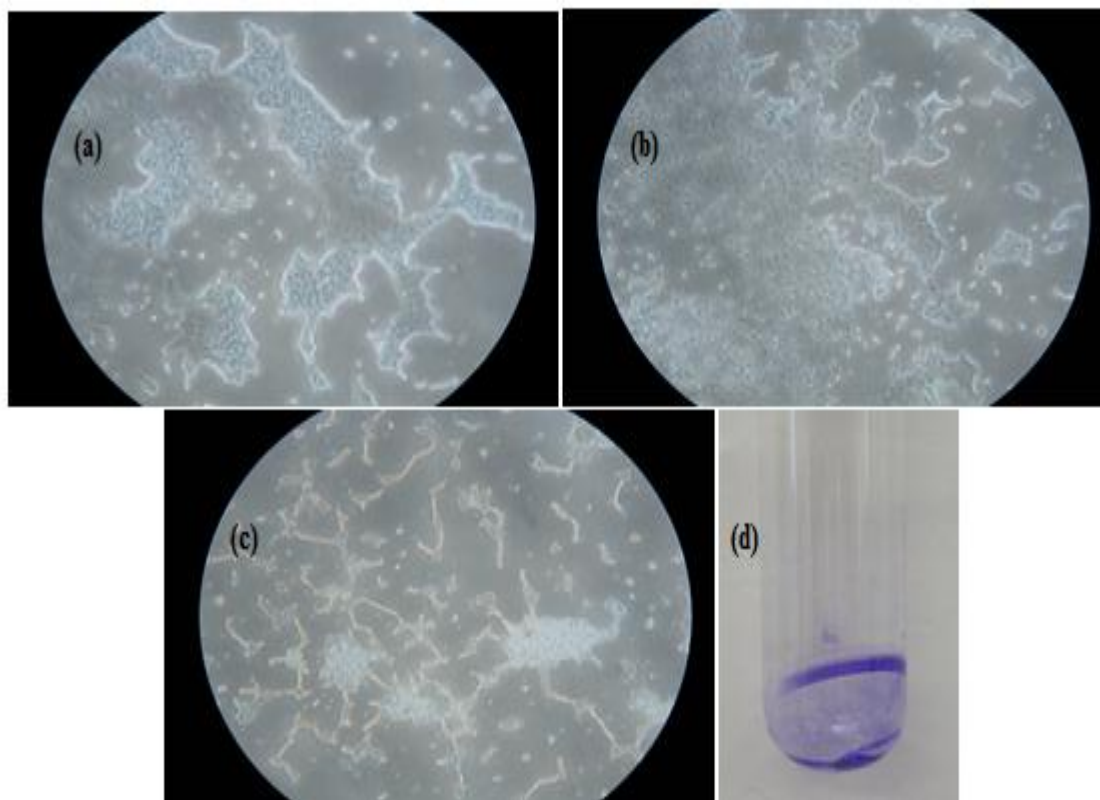


**Figure 4.3.** Biofilm formation of *L. johnsonii* FI9785 on sterile microscope slides under aerobic (a), microaerobic (b) and anaerobic (c) conditions ( $\times 400$  magnification) and biofilm formation of *L. johnsonii* FI9785 on a glass surface (d).

The oxygen limitations did not affect the biofilm formation on sterile microscope slide surfaces (Figure 4.3). Biofilm formation was also seen in polystyrene 96 well plates using crystal violet, on replicate experiments this method was the most reliable one and was selected to measure variations in biofilms between wild type and mutant strains (Figure 4.4). The same method was also used to compare the biofilm formation of *L. johnsonii* FI9785 with the well-known biofilm forming probiotic strain *L. rhamnosus* GG, showing that biofilm formation of these two strains were quite similar (Crystal violet staining  $A_{590\text{nm}}$  of  $0.38 \pm 0.07$  and  $0.3 \pm 0.01$  with sucrose and glucose in MRS medium, respectively).

#### 4.3.2 Comparison of biofilm formation of *L. johnsonii* FI9785 and mutant strains

Examination of biofilm formation of mutants of *L. johnsonii* with varying levels of EPS production indicated that, the alterations in the EPS layer of *L. johnsonii* strains affected

biofilm formation (Figure 4.4). There was not a huge effect of the carbon source utilized by *L. johnsonii* strains in biofilm formation although the effect of sucrose was more consistent. Interestingly, the more EPS producer strains with the same structure, *epsC*<sup>D88N</sup> mutant and its complemented strain showed slightly reduced biofilm formation in comparison to wild type which was statistically significant when they were grown with sucrose.

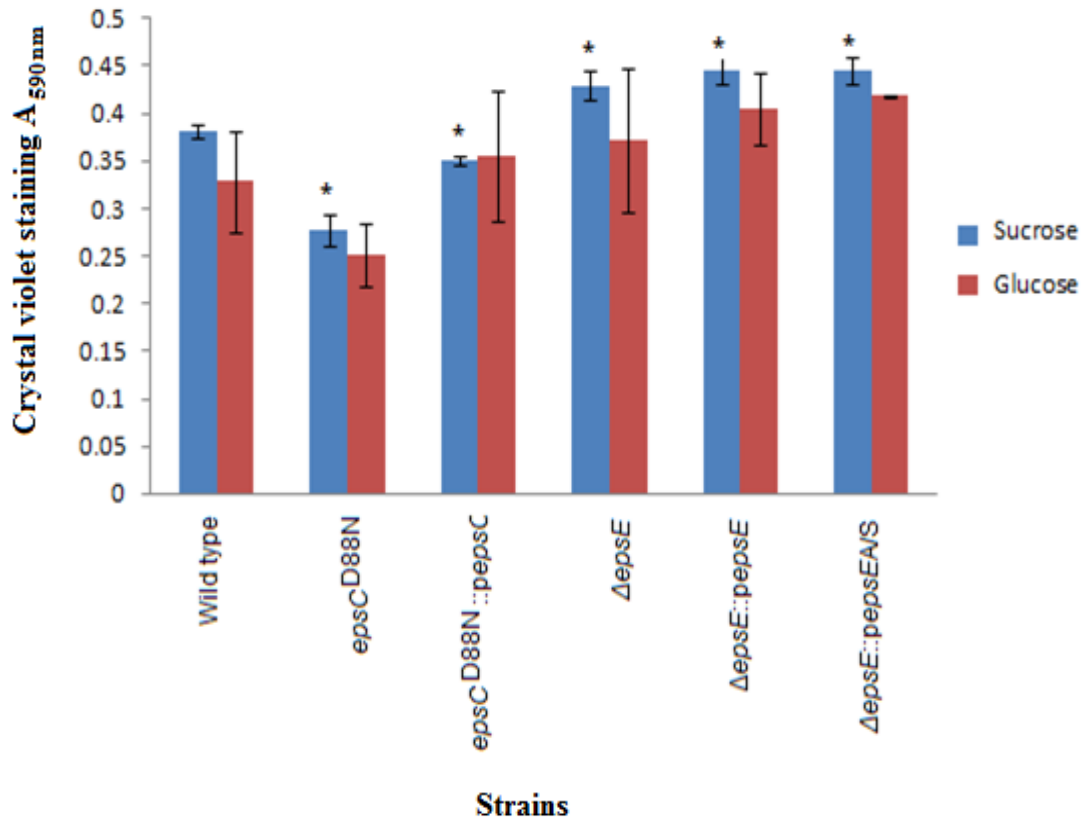


**Figure 4.4.** Influence of EPS on biofilm formation by *L. johnsonii* FI9785. A Crystal violet staining assay was conducted for wild type and mutants grown with (■) sucrose and (■) glucose at a concentration of 2% (w/v) in MRS broth. Results are the mean of triplicate experiments with six replicates per experiment. The description of *L. johnsonii* strains can be found in Table 1.4. \* represents the p values < 0.05 that were determined by an independent t test compared to the wild type.

In contrast, strains with reduced EPS production that only produced EPS-1 (Δ*epsE* and Δ*epsE*::*pepsEA/S*) showed a slight increase in biofilm formation compared to the wild type when grown with sucrose as a carbon source. However, in a range of other tests EPS-1 only producer Δ*epsE* mutant gave similar levels of biofilm formation to the wild type strain (Figure 4.5). Similarly, although overexpression of the *epsE* gene in complemented strain restored the EPS production (EPS-1 and EPS-2), the biofilm formation in Δ*epsE*::*pepsE* mutant was also slightly increased in comparison to wild type in the presence of sucrose. The biofilm formation trend amongst wild type and its *eps* mutants was similar to the sucrose

grown cells in the utilization of glucose as a carbon source but there was however no significant difference in the biofilm formation between wild type and its mutants (Figure 4.4).

### 4.3.3 Influence of medium components on biofilm formation

To investigate the effect of the growth medium and specific key medium components on biofilm formation of *L. johnsonii* FI9785, we used the following EPS producer strains: wild type, the smooth colony mutant with increased EPS and EPS-1 only producer strain  $\Delta epsE$  mutant with the reduced EPS production, in different growth conditions.

The smooth variant consistently formed less biofilm than the other strains in all conditions while biofilm formation of the wild type and  $\Delta epsE$  mutant was broadly similar (Figure 4.5). The biofilm formation in AOAC medium was slightly higher than in standard TSB medium and in MRS medium supplemented with glucose and sucrose as a carbon source.

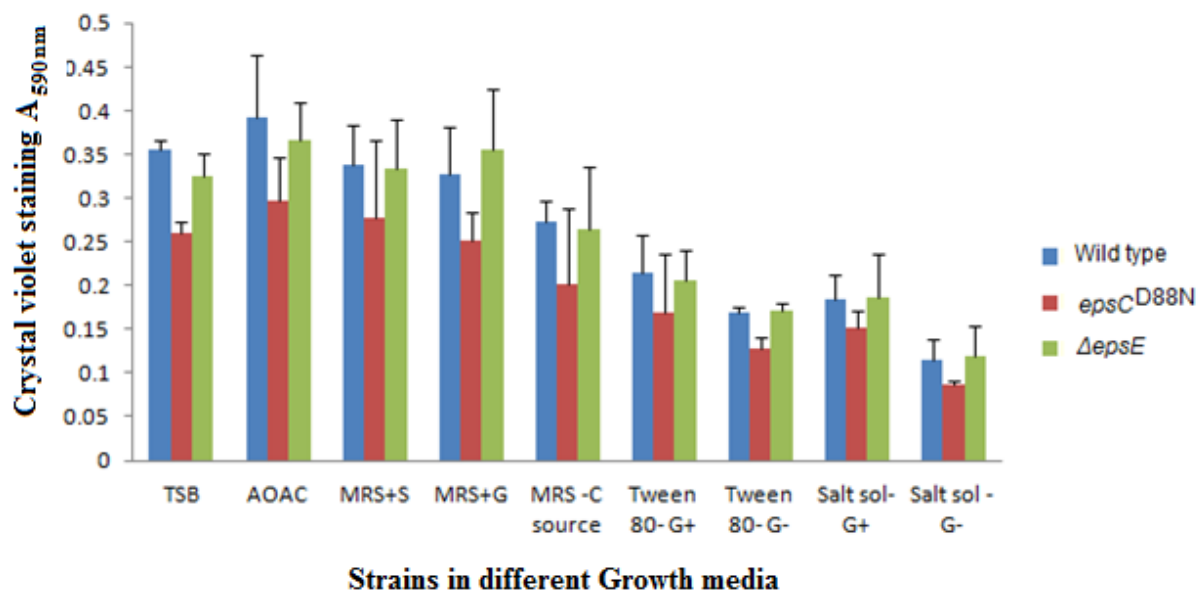


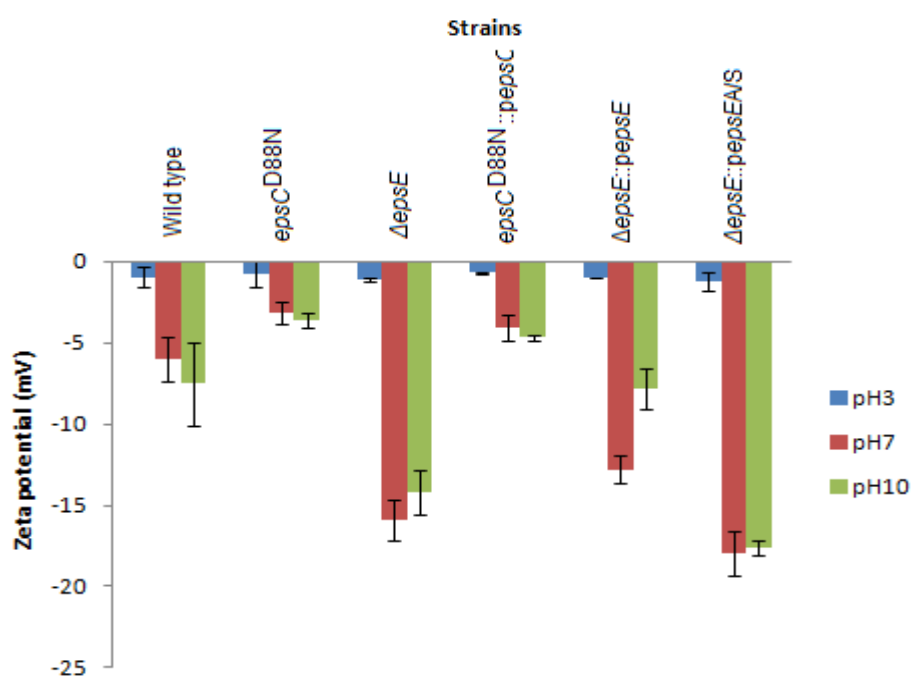
**Figure 4.5.** Effect of medium components on biofilm formation of wild type (■), *epsC*<sup>D88N</sup> (■) and  $\Delta epsE$  (■) mutant. Results are the mean of triplicate experiments with three replicates per experiment + standard deviation. (S: sucrose, G: glucose, C: carbon source and + and - : with or without the supplement).

When glucose or sucrose was omitted from MRS medium which resulted in a low Carbon/Nitrogen ratio, the biofilm formation was slightly reduced but still observable. The lack of surfactant Tween 80 in MRS medium resulted in an approximately 35% reduction in biofilm formation. This reduction was higher when glucose was omitted from the MRS supplemented with Tween 80. In general, LAB require ionic minerals to stimulate the growth. To investigate the role of divalent cations on biofilm formation, we omitted the salts solution

(MgSO<sub>4</sub>, MnSO<sub>4</sub>) from MRS medium either containing glucose or not. The biofilm formation was significantly reduced in the absence of these salts solutions (Figure 4.5).

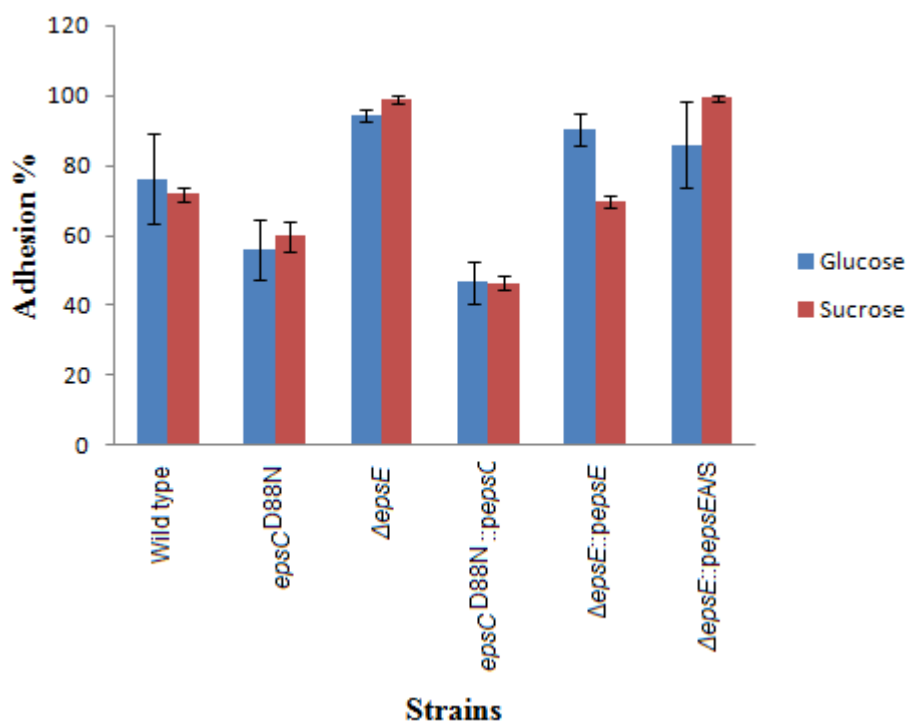
#### 4.3.4 Role of EPS on cell surface properties

To demonstrate the role of cell associated EPS on cell surface characteristics of *L. johnsonii* FI9785, we compared the zeta potential and hexadecane adhesion profile of wild type and mutants. Figure 4.6 depicts the zeta potential profile of different strains as a function of pH. The alterations in the accumulation level and structure of cell-surface associated EPS changed the zeta potential profile (Figure 4.6). It was observed that for all bacterial strains the zeta potential was negative at three pH points. It has to be noted that the isoelectric point of *L. johnsonii* FI9785 cells was close to pH 3. At this pH, the wild type and mutants showed similar zeta potential values at around -1 mV. The zeta potential decreased to different levels for wild type and mutants between pH 3 and pH 7. At pH 7, the zeta potential of low and only one type of EPS producers  $\Delta epsE$  and  $\Delta epsE::pepsEA/S$  mutant was approximately three times lower than the wild type. In these mutants, cell surface proteins might dominate the cell surface characteristics, causing the significant decrease in the zeta potential profile. The zeta potential of the *epsE* complemented strain  $\Delta epsE::pepsE$  was lower than the wild type but higher than  $\Delta epsE$  mutant at pH 7, although it was able to accumulate the same levels of EPS on cell surface as wild type.



**Figure 4.6.** Zeta potential of the *L. johnsonii* FI9785 and mutant strains as a function of pH; (■) pH3, (■) pH7 and (■) pH10, in a 10 mM phosphate solution. The error bars represent standard deviations of triplicates for each strain. The description of *L. johnsonii* strains can be found in Table 1.4.

Different levels of expression of the *epsE* gene (from the chromosome or from an expression plasmid) might lead to alterations in the protein/EPS ratio, resulting in a different ionic composition compared to the wild type and a greater effect of surface proteins in determining the zeta potential profile in this mutant. In contrast, the two strains that were able to produce EPS-1 and EPS-2 with increased levels of accumulation both showed significantly higher zeta potential than the wild type and other mutants at pH 7. The pattern of the zeta potential values at pH 10 were similar to pH 7 except the sense complemented mutant  $\Delta epsE::pepsE$  showed a similar zeta potential to the wild type. Overall, the results indicate that the cell surface charge of *L. johnsonii* FI9785 is heavily determined by cell surface associated EPS.



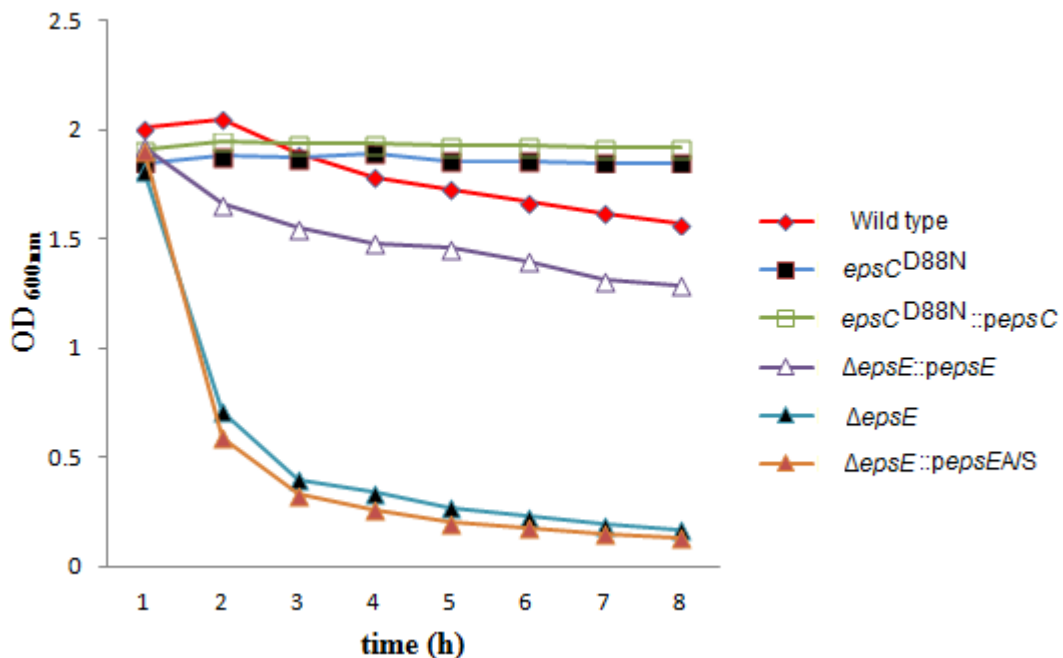
**Figure 4.7.** % Adhesion to hexadecane assays of *L. johnsonii* FI9785 and mutants grown with (■) glucose and (■) sucrose at a concentration of 2% (w/v) in MRS broth. The error bars represent standard deviations of triplicates for each strain. The description of *L. johnsonii* strains can be found in Table 1.4.

Figure 4.7 shows the comparative hexadecane adhesion of *L. johnsonii* FI9785 and its mutants grown under different carbon source. The carbon source did not have a consistent effect on the cell surface hydrophobicity. Cell surface associated EPS were found to alter the cell surface hydrophobicity of *L. johnsonii* FI9785. The percentage of adhesion to

hexadecane increased after deletion of the *epsE* gene, which resulted in less EPS accumulation around cells, and decreased after the mutation in *epsC* gene which resulted in more EPS accumulation compared to the wild type. Complementation of *epsE* deletion failed to fully restore the wild type phenotype when grown in glucose but the adhesion of cells grown in sucrose was similar to that of wild type cells. The changes in cell surface hydrophobicity of wild type and its mutants were quite similar to the pattern of the change in zeta potential values related to EPS.

#### 4.3.5 Effect of EPS on autoaggregation and adhesion to tissue culture cells

The effect of EPS on autoaggregation properties of *L. johnsonii* FI9785 and its EPS mutants was compared by monitoring aggregation at room temperature over an 8 hour period (Figure 4.8), for 4 h (Figure 4.9) and in greater detail by measuring cell aggregates by Flow Cytometry (FCM) after overnight culture (Figure 4.10). The alteration in the cell-surface associated EPS layer changed the aggregation profile of *L. johnsonii* FI9785. Aggregation of the  $\Delta epsE$  and  $\Delta epsE::pepsEA/S$  cells where the cell surface is covered by only EPS-1 was extremely fast, the smooth variant mutant did not aggregate at all during the 8 h time period, and the wild type showed only a low level of aggregation (Figure 4.8).



**Figure 4.8.** OD measurements ( $OD_{600nm}$ ) of *L. johnsonii* FI9785 and mutant strains over an 8 h time period at room temperature; the observed drop in OD values represents autoaggregation. The description of *L. johnsonii* strains can be found in Table 1.4.

Aggregation of the smooth colony mutant expressing the wild type *epsC* (*epsC*<sup>D88N</sup>::*pepsC*) was equivalent to that of the smooth mutant (*epsC*<sup>D88N</sup>), suggesting that the increased level of EPS in these two strains correlated with reduced aggregation phenotype. The *epsE* complemented strain ( $\Delta$ *epsE*::*pepsE*) had a clear decrease in aggregation level over the 8 h period compared to the *epsE* mutant strain ( $\Delta$ *epsE*) but did not reach the same level as the wild type.

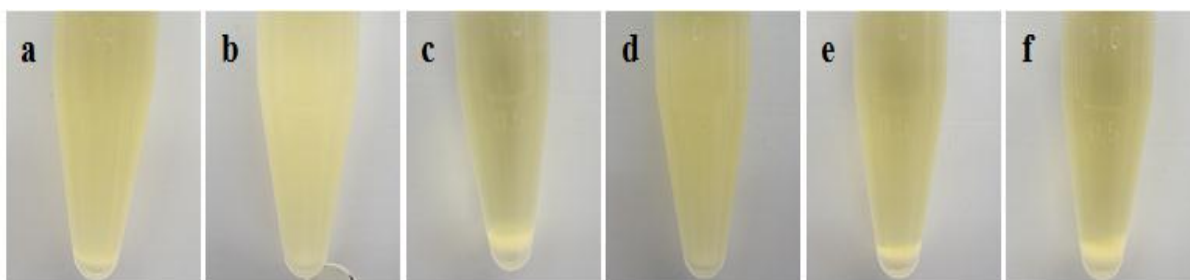


**Figure 4.9.** Autoaggregation of wild type and its mutants: a) WT, b) *epsC*<sup>D88N</sup>, c)  $\Delta$ *epsE*, d) *epsC*<sup>D88N</sup>::*pepsC* e)  $\Delta$ *epsE*::*pepsE* and f)  $\Delta$ *epsE*::*pepsEA/S*. Strains were grown overnight then vortexed 1 min and left 4 h at room temperature without any disturbance.

The turbidity of the  $\Delta$ *epsE* and  $\Delta$ *epsE*::*pepsEA/S* due to the cells in the suspension was no more observed after 4 h incubation at room temperature while the other strains were still turbid due to the lower aggregating properties (Figure 4.9). Also the turbidity of  $\Delta$ *epsE*::*pepsE* mutant was not similar to the wild type turbidity probably due to the reason that the complementation of *epsE* failed to restore the full wild type phenotype.

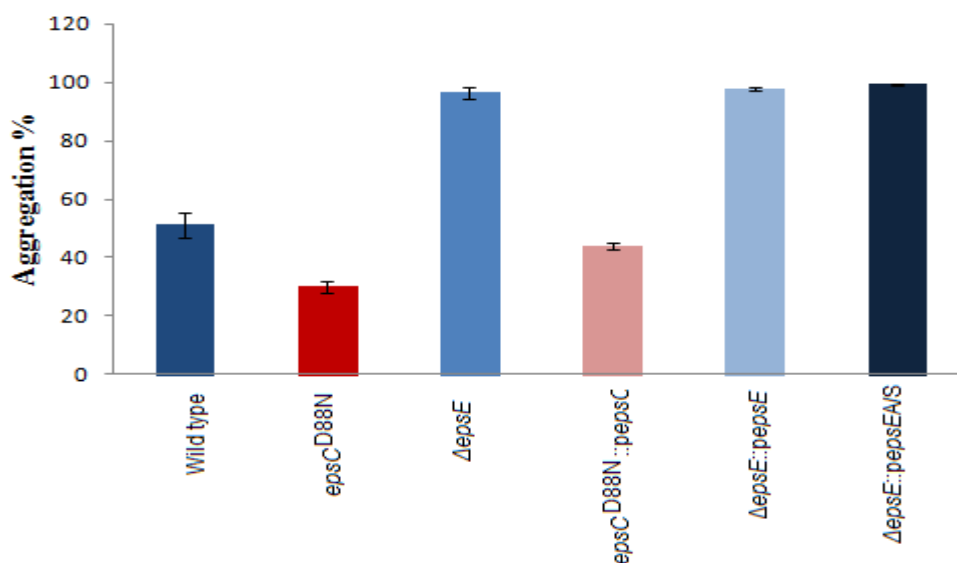


**Figure 4.10.** The aggregation percentage of wild type and mutant strains after overnight incubation (16 h) analysed by FCM. The error bars represent standard deviations of triplicates for each strain. The description of *L. johnsonii* strains can be found in Table 1.4.

FCM observations revealed that nearly 100 % of  $\Delta epsE$ ,  $\Delta epsE::pepsE$  and  $\Delta epsE::pepsEA/S$  mutant cells aggregated during an overnight incubation period at 37°C. In contrast, the aggregation percentage for the smooth variant and its complemented mutant was 29% and 43% respectively, while the wild type showed 50% aggregation after overnight incubation (Figure 4.10). These findings clearly indicated that the accumulation level and the conformational changes in cell-surface associated EPS altered the cell aggregation phenotype of *L. johnsonii* FI9785.

To investigate the impact of cell surface alterations after mutations in *eps* genes on adhesion, the ability of the wild type and mutant strains to adhere HT29 cells was assessed. FCM methodology was used to accurately enumerate bacteria in suspension and bacteria adhering to HT29 cells. The percentage adhesion of the wild type strain was 13.7% of the total bacteria added, whilst the  $epsC^{D88N}$  mutant displayed an adhesion of only 2.3% of the total bacteria added (Figure 4.11).

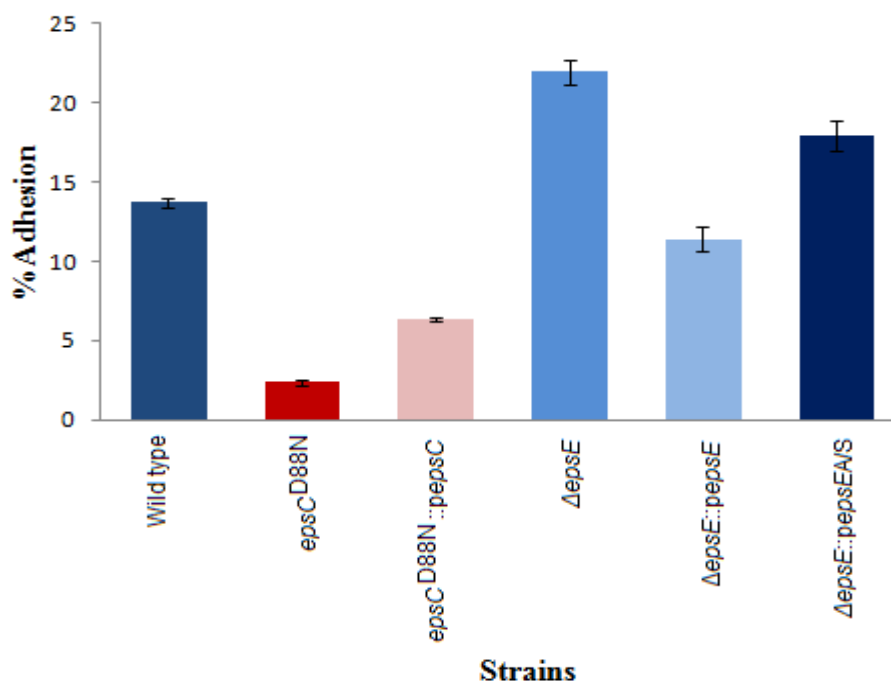


**Figure 4.11.** Adhesion of *L. johnsonii* strains to HT29 monolayers. Results are the mean of triplicate experiments with three replicates per experiment  $\pm$  standard deviation.

Complementation of this mutant ( $epsC^{D88N}::pepsC$ ) gave a slight increase in adhesion, but levels were still less than half of the wild type values. In contrast, EPS-1 only producer  $\Delta epsE$  mutant showed a clear increase in adhesion to approximately 160% of the wild type level. The adhesion level of complemented  $epsE$  mutant ( $\Delta epsE::pepsE$ ), which was able to produce both EPS-1 and EPS-2, showed similar adhesion values to wild type but the negative

control, antisense complemented mutant ( $\Delta epsE::pepsEA/S$ ), producing only EPS-1, maintained higher levels of adhesion than the wild type, although not as high as the  $\Delta epsE$  mutant (Figure 4.11). The FCM figure represents the separation of bacteria-cell population after the adhesion experiments for  $\Delta epsE$  and  $epsC^{D88N}$  mutant as an example of enumeration of adhered bacterial cells in FCM experiments (Figure 4.12).

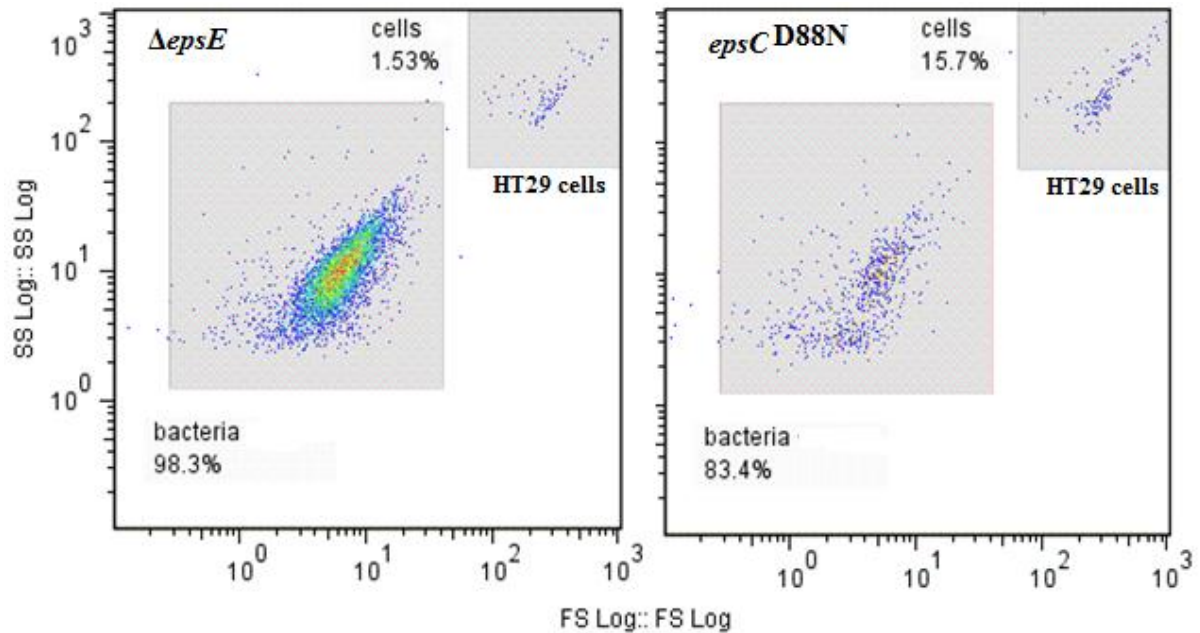


**Figure 4.12.** Adhered bacteria and HT29 cell complex of  $\Delta epsE$  and  $epsC^{D88N}$  mutant detected by FCM. The number of attached bacteria was quantified by distinguishing the number of HT29 cells and bacteria according to their sizes in FSC vs. SSC.

#### 4.4 DISCUSSION

There are numerous reports related to biofilm formation of pathogenic bacteria and the role of EPS on this process. However, the biofilm formation of commensal bacteria, such as *L. johnsonii* FI9785 has not been studied to the same extent. In this study we scanned biofilm formation in *L. johnsonii* FI9785 under different conditions. The level of EPS production as well as the structural composition play a role in process of biofilm formation [154]. As we identified the mutants that have different levels of EPS accumulation as well as different EPS structures, we then further characterized the biofilm formation of these strains. Our experiments showed that increased accumulation of EPS on cell surface with the same structure decreased the biofilm formation of *L. johnsonii* FI9785 and vice versa. The reduction in the biofilm formation of the smooth variant was not surprising as we previously observed the same pattern for resuspending the smooth variant in which distribution of this

mutant in the suspension was easier and faster compared to wild type [33] and the other mutants which were resistant to the resuspension process. Previous studies demonstrated that level of EPS production is an important factor playing enormous roles in biofilm formation especially in pathogenic bacteria affecting different hosts [251-253]. Similarly several studies reported the role of the EPS production in biofilm formation of LAB and EPS was described as a promoting factor for the intracellular interactions and formation of microcolonies depending on the cellular and environmental conditions although the fundamental role of EPS on biofilm formation of probiotic bacteria has yet to be determined [20, 63, 141, 142, 254]. It was reported that the biofilm formation of *L. reuteri* TMW1.106 was reduced after the deletion of the *gtf* and *ftf* genes in comparison to wild type strain on glass surface showing the importance of glucan and fructan like EPS on biofilm formation of this bacterium. However the *in vivo* analysis of the biofilm formation revealed that there was no significant difference in biofilm formation properties of wild type and mutant strains on forestomach epithelial cells [63]. Similarly, in *L. reuteri* 100-21 the *ftf* mutant was able to form biofilms as wild type strain on the forestomach epithelial surface [142]. Disruption of the LamA which is involved in the regulation of the expression of the genes related to cell surface polysaccharides and cell membrane proteins resulted in a reduced biofilm formation in *L. plantarum* WCFS1 on glass substrates [254]. Biofilm formation analysis in *L. rhamnosus* GG demonstrated that EPS can be involved in this process but the effect of EPS in biofilm formation was more likely to be medium dependant [141]. The authors proposed that, not only the level of EPS production but also the compositional and conformational properties of cell surface associated EPS including the polymer size might also affect the biofilm formation. Our data showed that more EPS accumulation at the cell surface of *L. johnsonii* clearly did not increase the biofilm formation in polystyrene surface. It should also be noted that although there was a trend to the increased biofilm formation in EPS-1 only producer mutants but it was not consistent. Overall, EPS is clearly one of the most important components of cell surface of lactobacilli determining the biofilm formation but much remains to be learned about the role of EPS on intracellular interactions and physicochemical characteristics of cell surface determining the biofilm formation of probiotic bacteria.

Several factors including sugar metabolism may also affect this process [255-257]. In *L. johnsonii* FI9785 the carbon source (either glucose or sucrose) did not affect the biofilm formation. Environmental conditions such as nutrient availability are an important factor for biofilm formation [141, 258-260]. We can also conclude that biofilm formation of *L.*

*johnsonii* FI9785 is greatly affected by the medium composition. Previously it was reported that low relative ratio of Carbon/Nitrogen in growth medium increased the biofilm formation in probiotic strain *L. rhamnosus* GG where a suppressive effect of glucose on biofilm formation was also shown [141]. This was contrary to our observations in *L. johnsonii* FI9785; omission of glucose and low relative ratio of Carbon/Nitrogen in growth medium reduced the biofilm formation. The suppressive effect of glucose may be medium dependant or strain specific. Addition of the surfactant Tween 80 in MRS medium decreased the biofilm in *L. rhamnosus* GG but not in *L. johnsonii* FI9785. The removal of salts solution containing  $Mn^{2+}$  and  $Mg^{2+}$  from MRS medium significantly reduced the biofilm formation of *L. johnsonii* FI9785 and its mutants possibly due to the important role of these metal ions in cell metabolism. Previously, it was reported that  $Mn^{2+}$  was essential for stimulating the growth of lactobacilli [141, 261] and increasing the biofilm formation of *L. rhamnosus* GG [141]. In general, salts solution composition appeared to be more influential on biofilm formation than Tween 80 for *L. johnsonii* FI9785.

The effect of cell surface associated EPS on the physicochemical properties of *L. johnsonii* FI9785 was also assessed using mutants with different coverage of EPS. We found that the physicochemical profiles of these cells were completely different. The zeta potential measurements clearly showed that EPS are important components in determining the net cell surface charge. The zeta potential of wild type and mutants was negative for the three pH values indicating that anionic compounds, including lipoteichoic acids, polysaccharides and proteins, dominated the cell surface of *L. johnsonii* FI9785 [175, 176]. The mutations in the *eps* related genes resulted in changes in zeta potential profiles due to the changes of the level and the structure of EPS accumulation. It was interesting to discover that the zeta potential of the smooth colony mutant and its complemented strain was significantly higher than the wild type and other mutants at three tested pH values, which can be the result of enhanced accumulation of EPS on cell surface and their dominant effect on determining the zeta potential. In these mutants, we propose that EPS determined the zeta potential profile, with the higher level of accumulated EPS eliminating the effect of cell surface proteins and other molecules on cell surface and with no obvious effect of the smooth or rough phenotype. In contrast, EPS-1 only producer mutants  $\Delta epsE$  and  $\Delta epsE::pepsEA/S$  with reduced EPS production resulted in lower zeta potential values which may be due to the exposure of acidic compounds dominating the cell surface such as proteins, glycoproteins and phosphate based lipoteichoic acids in these mutants [176]. The physicochemical properties of bacteria as we

assessed by zeta potential measurements and cell surface hydrophobicity can determine the bacterial adhesion to epithelial cells [262]. We demonstrated that the cell surface hydrophobicity of *L. johnsonii* FI9785 was altered after mutations in an *eps* gene cluster. The cell wall and cell surface components including lipoteichoic acids, proteins and specific polysaccharides are responsible for the cell surface hydrophobicity of bacteria [263]. The cell surface hydrophobicity of lactobacilli has been reported in a wide spectrum between 2% to 95% depending on the surface characteristics of each strain [264, 265]. Our study showed the cell surface hydrophobicity of *L. johnsonii* FI9785 was around 75% when it is measured with hexadecane. Previously it was shown that the high hydrophobicity of *Lactobacillus* cells was due to the protein rich surface [266]. The fact that the highest hydrophobicity was obtained for the *epsE* gene deletion mutant ( $\Delta epsE$ ) which produces only EPS-1 and less EPS covers its cell surface compared to the wild type suggested the uncovering of the cell surface proteins and other hydrophobic molecules in this mutant. Several other studies also reported the decrease in hydrophobicity of *Lactobacillus* cells after removal of surface proteins [176, 189]. In contrast, the smooth colony mutant gained a hydrophilic character probably due to the increased EPS production that might have resulted in covering of the other hydrophobic molecules such as proteins on cell surface. No difference was observed in cell surface hydrophobicity of wild type and mutants depending on utilized carbon source.

Autoaggregation can be an important factor for colonisation of gut bacteria and their ability to inhibit the adherence of pathogenic bacteria to the gastrointestinal tract [191, 267]. So far several factors that can affect the aggregation of *Lactobacillus* cells including EPS, and aggregation promoting proteins have been described [63, 189, 192, 193, 268]. Previously, it was shown that the aggregation promoting proteins were also located on the cell surface of *L. johnsonii* [269]. In the light of our results we can confirm that EPS attached to the cell surface are important factors in determining aggregation ability of *L. johnsonii* FI9785. Autoaggregation ability of mutants producing less EPS due to the EPS-1 only production was significantly increased compared to the wild type which produces EPS-1 and EPS-2. The unmasking of surface proteins by reduction of EPS layer or removal of the EPS-2 layer in these mutants may promote aggregation. In contrast, enhanced accumulation of EPS in the smooth colony mutant and its complemented mutant with the same structure of EPS-1 and EPS-2 significantly decreased the autoaggregation indicating masking of surface molecules such as aggregation promoting proteins and lipoteichoic acids. The complemented strain of *epsE* deletion mutant produced similar structure and levels of EPS to the wild type and at 4 h

and 8 h incubation the aggregation levels were also similar to the wild type although there was a tendency for the increased aggregation in this mutant probably due to the fail in complementation process. In addition after 24 h, the aggregation phenotype was similar to the *epsE* deletion strain possibly indicating the failed complementation and a growth phase dependant EPS synthesis in this mutant.

The adhesion profiles of these strains in a tissue culture model were also investigated. We used an HT29 cell line that is a common *in vitro* model for assessing the adhesion of microorganisms to intestinal cells. Importantly, we enumerated the adhered bacterial cells with FCM application which gave us the chance to improve this technique for future studies. The adhesion of *L. johnsonii* to HT29 cells was around 14% which was higher than the adhesion level of well-known probiotic strain of *L. rhamnosus* GG [270]. The mutations in *eps* gene cluster significantly affected the adhesion profile of wild type and mutant strains reflecting the alterations in the structure and accumulation level of EPS which was expected from the physicochemical profiles of these strains. One of the important reason for the adhesion differences may be the changes in aggregation profile of *L. johnsonii* strains that was affected by several factors such as alterations in cell surface properties, possible unmasking of aggregation promoting proteins on cell surface after loss of EPS-2 production. It was suggested that the autoaggregation and adhesion properties could be correlated but also some adhesion differences were found for strains that have same aggregation properties [271, 272]. In general, we can also correlate the aggregation phenotype with adhesion to HT29 cells for *L. johnsonii*. However, the  $\Delta epsE::pepsE$  mutant which showed higher aggregation than wild type had slightly less adhesion than wild type that may show the role of surface characteristics in adhesion properties. Previously, it was reported that hydrophobic/hydrophilic changes of cell membrane could change the adhesion properties of *L. johnsonii* NCC 533 to HT29 cells [273]. We also showed the hydrophobic/hydrophilic changes of cell surface significantly altered the adhesion to HT29 cells of *L. johnsonii* FI9785. Consequently, we showed the role of EPS as a determinant factor on *in vitro* adhesion properties of *L. johnsonii* FI9785. But this adhesion profile may not always reflect the *in vivo* survival and colonisation in the host. Previously it was shown that both *L. johnsonii* NCC 533 and *L. paracasei* strains had similar adhesion profiles to Caco-2 cells *in vitro*, but only *L. johnsonii* strain was able to colonise under *in vivo* conditions [199].

# Chapter 5

---

**Genetics of EPS Biosynthesis in *L. johnsonii***

## 5.1 INTRODUCTION

The identified *eps* gene cluster of *L. johnsonii* FI9785 is a typical *eps* cluster for heteropolymeric EPS production as discussed in previous Chapters, although we showed that *L. johnsonii* is also able to produce a homopolymeric EPS. Deletion of *epsE* gene, which codes for the putative priming glycosyltransferase within the identified *eps* cluster which harbours six glycosyltransferases including with *epsE*, resulted in the loss of EPS-2 biosynthesis that is composed of six sugar residues. This provided further evidence that the *eps* cluster potentially encodes the EPS-2 production. However, none of the genes or predicted proteins from the genome of *L. johnsonii* showed homology with the *gtf* gene or GTF protein which was previously shown to be responsible for the homopolymeric EPS production in the genus *Lactobacillus* as discussed in previous Chapters. It can be speculated that the biosynthesis of these two EPS may be dependent on the identified *eps* cluster in *L. johnsonii* FI9785.

The role of the transcriptional regulator in EPS biosynthesis was demonstrated for *Streptococcus* strains, where deletion of this gene resulted in reduced capsule formation [94, 96, 115]. It was also shown that deletion of a putative transcriptional regulator from the *eps* cluster of a *Lactococcus* strain that was located on a plasmid resulted in the complete loss of EPS biosynthesis [88]. The transcriptional regulation mechanism of succinoglycan biosynthesis which was also composed of two different EPS in the Gram negative soil bacterium *Sinorhizobium meliloti* has been studied extensively and it was reported that several different suppressor or stimulator genes are involved as genetic factors. Also environmental conditions affect the regulation of the EPS production in this strain which results in alteration of the production levels of the two EPS [274, 275]. A considerable number of studies have been reported on EPS of *Lactobacillus* species but data on the transcriptional regulation mechanism and the role of the transcriptional regulators of the *eps* clusters is still lacking. The functional sequences of the *eps* clusters have a similar trend in lactobacilli in which the gene clusters start with a conserved gene responsible for the transcriptional regulation of these clusters [77]. In contrast it was also reported that the putative transcriptional regulator gene was located at the 3' end of the *eps* clusters of *L. rhamnosus* strains [61, 85]. In a comprehensive study on the transcriptional mechanism of *eps* clusters of four *L. rhamnosus* strains, it was demonstrated that these *eps* clusters were organised into five transcriptional units in which the putative transcriptional regulator genes were shown to have their own promoters and showed an opposite transcriptional sense

suggesting their transcription as a separate mRNA. Also the sequence of one of the transcriptional regulators differed from the other three which was proposed to be related to its functional role. Furthermore, the authors suggested that the gene expression regulation mechanism of *L. rhamnosus* might not be related to catabolite repression due to the fact that although the gene clusters of these four strains showed high similarity, the EPS production levels varied remarkably [85]. These results indicate that the regulation mechanism of EPS biosynthesis in LAB is a potential complex system including regulation at the transcriptional level and requires further investigation.

In this study we deleted the entire *eps* cluster and the putative transcriptional regulator of this *eps* cluster in order to understand their functional role in EPS biosynthesis and showed that the EPS production in *L. johnsonii* FI9785 is dependent on this *eps* cluster including the *epsA* gene. Complementation of the *epsA* gene in a  $\Delta epsA$  mutant fully restored both EPS-1 and EPS-2 production and confirmed the essential role of this gene in EPS biosynthesis. Over-expression of this gene in the complemented mutant resulted in doubling the amounts of EPS production compared to the wild type but no difference was observed in the growth profile of this mutant. Furthermore, the loss of the EPS production altered the aggregation and adhesion properties of *L. johnsonii* as well as the anti-wild type antibody responses compared to the capsulated strains.

## **5.2 MATERIAL AND METHODS**

### **5.2.1 Deletion of the *epsA* gene in *L. johnsonii***

Genomic DNA was extracted from *L. johnsonii* FI9785 as described in section 2.2.1 (Figure 5.1). The *epsA* gene was deleted from the *L. johnsonii* FI9785 chromosome using the thermo-sensitive vector pG+host9 [216] which will be described in detail in the results section.

### **5.2.2 Deletion of the whole *eps* gene cluster of *L. johnsonii***

The *eps* cluster was deleted using a previously described method with some modifications which will be described in detail in the results section [62].

### **5.2.3 Complementation of the *epsA* gene**

In order to complement the  $\Delta epsA$  mutant, the *epsA* gene was amplified from the genome of *L. johnsonii* FI9785 and subcloned into a previously engineered plasmid which was originally

isolated from *L. johnsonii* FI9785 [33] which will be discussed in the results section in detail. Primers used in the knock-out studies and complementation process are listed in Table 5.1.

Primer	Sequence (5'- 3')
5epsA_KpnF	AAAG <u>GT</u> ACCAAATTAATAACAAGAG
epsA_R1	CGGTAAGTTAACTTTCATATCTCG
pGhost1	AGTCACGACGTTGTAAAACGACG
pGhostR	TACTACTGACAGCTTCCAAGG
5epsB_XhoF	GACTCGAGAATAGGAAAAAGTGG
epsB_HindIIIR	GCAAAAGCTTGTGACTTTTCTG
1184F	GGGCTT GCTCCTTAAATTG
epsBR1	GTTCTTAAAAGTTTGAGCAACTGC
CAT_XHOF	AACT <u>CG</u> AGCACCCATTAGTTC
CATRSPLICE1170	<u>AGTACTGTCCTTTACTA</u> ACGGGGCAGGT
1170FSPLICECAT	<u>ACCTGCCCCGTTAGTAA</u> AGGACAGTACT
1170_ncR	TATTAAGCTTTCATTTCCTGC
5epsA_NcoI	ATACCATGGATCATAAGAATAGTG
epsANcoI_R	TTCCATGGTTTCCTATTCTCC

**Table 5.1.** Primers used for deletion of *epsA* and *eps* cluster and complementation process. Altered nucleotides underlined throughout in each primer.

#### 5.2.4 Isolation of EPS from new mutants and structural analysis

New mutant strains (*L. johnsonii*  $\Delta$ *epsA*,  $\Delta$ *eps\_cluster* and  $\Delta$ *epsA::pepsA*) were grown under the conditions described in section 2.1.2 and EPS was isolated from wild type and  $\Delta$ *epsA::pepsA* mutant cell pellets and culture supernatants following the method described previously [221] to quantify the total EPS production according to the phenol-sulphuric acid methodology. Briefly, *L. johnsonii* wild type and mutant strains were grown aerobically at 37°C for 2 d. Twenty ml culture samples were centrifuged at 6000 g for 15 min at 4°C. The cell pellet was washed in 5 ml of sterile PBS and then centrifuged at 6000 g for 15 min at 4°C

and the supernatants were retained for further EPS isolation. The viscous pellet was suspended in 5 ml of 1 M NaCl and EPS was dissociated from cells by sonication in a Soniprep 150 (Sanyo, UK) for 5-6 times for 10 seconds at 7-10 amplitude microns using the Small probe (9.6 mm of tip diameter). After each sonication burst samples were cooled on ice for 30 seconds to prevent degradation. Samples were then centrifuged at 6000 g for 30 min at 4°C to eliminate insoluble material. The EPS was precipitated from the supernatant by addition of two volumes of cold ethanol followed by an overnight incubation at 4°C. After centrifugation at 6000 g for 30 min at 4°C, the pellet containing EPS was resuspended in 5 ml of distilled water and dialyzed (12000–14000-Da visking dialysis membrane, Medicell International, UK) against 5 l of distilled water for 2 d with three water changes per day. Similarly supernatants obtained from 20 ml samples at the beginning were treated with trichloroacetic acid (TCA) at a final concentration of 20% (v/v) and incubated for 2 h at 4°C under gentle agitation. Precipitated proteins were removed by centrifugation at 13000 g for 20 min at 4°C. The EPS was precipitated from the supernatant with two volumes of cold ethanol followed by an overnight incubation at 4°C. After centrifugation at 6000 g for 30 min at 4°C the pellet containing the EPS from the supernatant samples were dialyzed as described above. The EPS samples in solutions were stored at 4°C until further use.

For structural studies the EPS from new mutants were isolated according to the method described in section 2.1.4. Then the EPS samples were subjected to NMR and FTIR Spectroscopy analysis using the methods described in section 3.2.2 and 3.2.4, respectively.

### **5.2.5 Quantification of EPS production by phenol-sulphuric acid methodology**

EPS were isolated from the wild type *L. johnsonii* and mutant strains and quantified using the phenol-sulphuric acid method [222] with glucose as a standard. It is a colorimetric carbohydrate assay which includes the breakdown of polysaccharides into monosaccharides by concentrated sulphuric acid and at this step hexoses are dehydrated to hydroxymethyl furfural and then these compounds react with the phenol to produce a yellow-gold color [276]. To measure the total sugar content of EPS samples, standard dilutions between 0 to 200 µg/ml of glucose were used in order to prepare the standard curve for calibration purposes. Using 96-well plates (Grenier), 50 µl of each EPS sample and then 150 µl 98% sulphuric acid were added per well and immediately 30 µl of 5% phenol added for the yellow-gold color development and placed in a plate reader. After 5 min of incubation, the

samples were read at OD<sub>490nm</sub>. The EPS content of each sample was then calculated using the glucose standard curve (Appendix 6).

### **5.2.6 Assessment of Adhesion and Surface alterations by FCM and TEM**

The cell surface characteristics of new mutant cells were determined using the methods described in section 2.1.5 for FCM applications of adhesion, autoaggregation and immunodetection of cell surface alterations and in section 2.1.7 for TEM analysis, respectively.

### **5.2.7 Analysis of *epsA* gene expression by qPCR (Quantitative real-time PCR)**

For qPCR analysis, total RNA was extracted from 3 ml of mid- to late exponential phase cultures of *L. johnsonii* WT,  $\Delta epsA$  and  $\Delta epsA::pepsA$  mutants grown in MRS with glucose as the carbon source. The RNA was stabilized prior to extraction by using RNAprotect Bacteria Reagent (Qiagen, Crawley, UK) according to the supplier's advice. The RNA was then extracted after an enzymatic lysis followed by a mechanical disruption of the cells by bead beating, using the RNeasy Mini Kit (Qiagen) according to manufacturer's instructions. Genomic DNA contamination was removed by DNase treatment using TURBO DNA-free kit (Life Technologies Ltd, Paisley, UK) according to supplier's recommendations. The purity, quantity and integrity of the extracted RNA were assessed before and after DNase treatment, with NanoDrop 1000 UV-Vis Spectrophotometer (Thermo Fischer Scientific, Wilmington, DE). The expression of *epsA* gene in these three strains was quantified using the 16S and *gyrB* genes as housekeeping genes by quantitative real-time PCR (qPCR) on an Applied Biosystems 7500 Real-Time PCR system (Life Technologies Ltd).

One pair of primers was designed for *epsA*, 16S and *gyrB* genes using ProbeFinder version 2.45 (Roche Applied Science, Penzberg, Germany, <http://goo.gl/7WROp2>) in order to have an amplicon around 60-80 bp. The primers were between 18 and 23 nt, with a T<sub>m</sub> of 59-60°C (Table 5.2). Calibration curves were prepared in triplicates for each pair of primers using 2.5-fold serial dilutions of *L. johnsonii* FI9785 genomic DNA. The standard curves showed a linear relationship of log input DNA vs. the threshold cycle (C<sub>T</sub>), with acceptable values for the slopes and the regression coefficients (R<sup>2</sup>) (Appendix 7). The dissociation curves were also performed to check the specificity of the amplicons.

Primer	Sequence (5'-3')	Length	T <sub>m</sub> °C	Amplicon
epsA_1R	TCTTGATCGTTTTAACAGTTTCATCT	26	59	64 bp
epsA_1F	CCAGCTAAGATTAATGCAGCCTA	23	59	
epsA_2R	TCACTAATTTTCATTACTCATCGGATT	26	59	75 bp
epsA_2F	GGTTATTATCGCTTGGCACAAT	22	60	
16S_R	CCGAACTGAGAACGGCTTTA	20	60	61 bp
16S_F	GGTACAACGAGAAGCGAACC	20	59	
gyrB_R	CTTGAAGAACATGGAACAATCG	22	59	74 bp
gyrB_F	CGTCGAAAGTTGTAGTTTCGGTA	23	60	

**Table 5.2.** Primers designed for *epsA*, 16S and *gyrB* genes for qPCR analysis.

One microgram of each DNase-treated RNA was converted into cDNA using QuantiTect® Reverse Transcription kit (Qiagen) according to supplier's advice. Another microgram of DNase-treated RNA was also treated the same way but without addition of the reverse-transcriptase (RT negative control). Each 10 µl-qPCR reaction was then carried out in triplicates with 1 µl of a 20-fold diluted sample (cDNA or RT negative control) and 0.2 µM of each primer, using the QuantiFast SYBR Green PCR kit (Qiagen) according to supplier's advice. Briefly, PCR amplification was initiated at 95°C for 5 min followed by 35 cycles of 95°C for 10 s and 60°C for 30 s. All sample and primer combinations were assessed in triplicate. Control PCR confirmed that there was no background contamination (no-template control) or residual chromosomal DNA. PCR specificity and product detection was checked post amplification by examining the temperature-dependent melting curves of the PCR products.

Generation of quantitative data by real-time PCR is based on the number of cycles needed for amplification generated fluorescence to reach a specific threshold of detection (the C<sub>T</sub> value) for each strain. For relative quantification of *epsA* gene expression in each strain, the *epsA* gene expressions were compared with the housekeeping gene *gyrB* using the 2<sup>-ΔΔCT</sup> methodology. Firstly, the C<sub>T</sub> values for each *epsA* and *gyrB* genes in wild type and mutants were generated with three technical replicates and two biological replicates by qPCR analysis

and then the average  $\Delta C_T$  values of each mutant which is the difference of the average  $C_T$  values of *epsA* gene and *gyrB* gene were calculated (Average  $\Delta C_T = \text{Average } epsA C_T - \text{Average } gyrB C_T$ ). After that for the comparison of the mutants and the wild type *epsA* gene expression  $\Delta\Delta C_T$  values for each biological replicate were calculated from the difference of the average  $\Delta C_T$  values of mutants and average  $\Delta C_T$  value of wild type ( $\Delta\Delta C_T = \text{Average } \Delta C_T epsA::pepsA - \text{Average } \Delta C_T \text{ Wild type}$ ). To calculate the fold change in *epsA* gene expression in mutants compared to the wild type,  $2^{-\Delta\Delta C_T}$  values were calculated.

## 5.3 RESULTS

### 5.3.1 Deletion of *epsA* gene from the genome of *L. johnsonii*

The putative transcriptional regulator, *epsA* gene, was deleted from *L. johnsonii* using thermo-sensitive vector pG+host9 which can replicate at 30°C but not 42°C [216]. Firstly, 390 bp of the *epsA* gene and some upstream sequence was amplified using primers 5epsA\_KpnF and epsA\_R1 from the genomic DNA of *L. johnsonii* giving a 625 bp product (Figure 5.1, 5.2A).

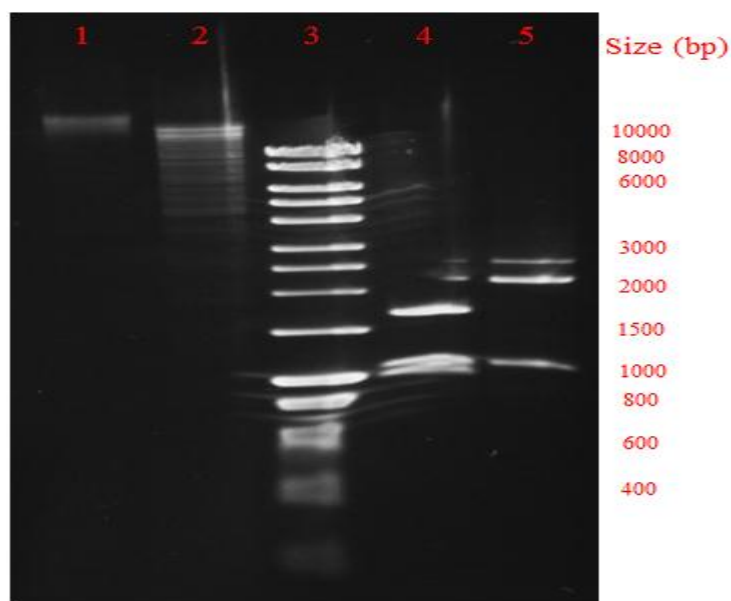


**Figure 5.1.** Agarose gel (0.8 % w/v) was used to separate DNA products. Lane 1- Genomic DNA of *L. johnsonii* FI9785, lane 2- Genomic DNA of *L. johnsonii* FI9785 cut with *BsrBI*, lane 3- HyperLadder 1, lane 4- pG+host9 restricted with *BsrBI* and lane 5- pUK200 restricted with *BsrBI*.

The partial *epsA* product was then restricted using *KpnI* and *XhoI* (New England Biolabs) and subcloned into *KpnI/XhoI* - restricted pG+host9 which had been dephosphorylated with Antarctic phosphatase (New England Biolabs) (Figure 5.2C). The ligation product was

transformed into electro-competent *E. coli* MC1022 and positive colonies were selected with erythromycin (400 µg/ml) and confirmed by colony PCR using GoTaq polymerase (Promega) and primers pGhost1 and pGhostR which target the pG+host9 sequence (Figure 5.2D).

Plasmids were extracted with the plasmid mini kit (Qiagen) and sequenced to confirm the partial *epsA* gene insertion. The positive recombinant plasmid was labelled as pG+host9epsAp. To produce the *epsA* knockout cassette, 539 bp from 5' upstream of the *epsB* gene was amplified and *XhoI/HindIII* sites were created using primers 5epsB\_XhoF and epsB\_HindIIIR giving a 558 bp product (Figure 5.2B). This partial *epsB* product was then restricted using *XhoI/HindIII* sites then subcloned into *XhoI/HindIII* - restricted pG+host9epsAp which had been dephosphorylated with Antarctic phosphatase (New England Biolabs). The ligation product was transformed into electro-competent *E. coli* MC1022 and positive colonies were selected with erythromycin and screened by colony PCR as described before (Figure 5.2D). Plasmids were extracted with the plasmid mini kit and sequenced to confirm the partial *epsB* gene insertion.

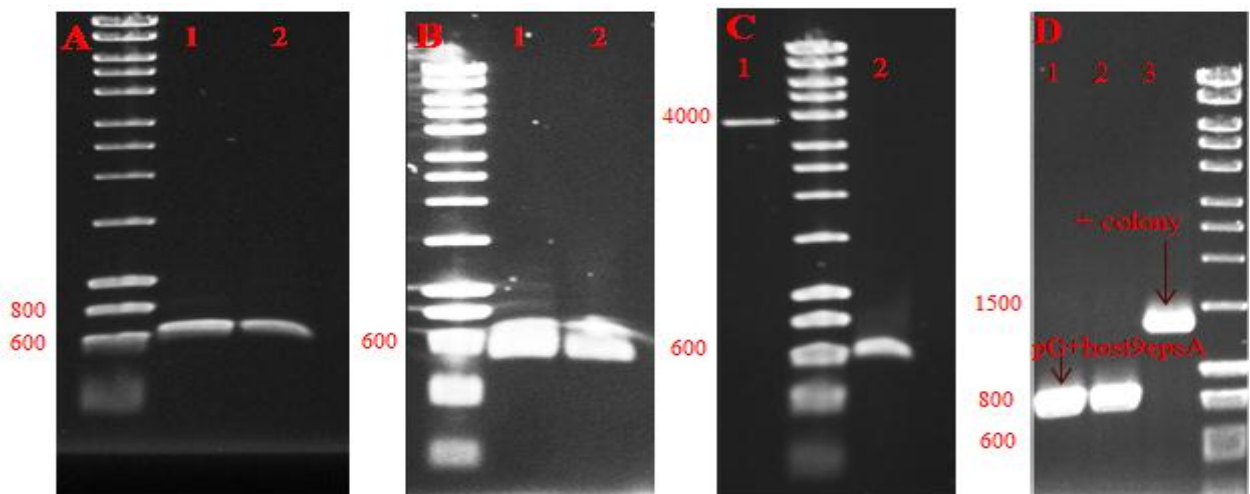


**Figure 5.2.** Agarose gel (0.8% w/v) showing A) lane 1-2, partial *epsA* gene with some of the upstream region amplified from the genome of *L. johnsonii*; B) lane 1-2, partial *epsB* gene amplified from the genome of *L. johnsonii*; C) lane 1-2, *KpnI/XhoI*-restricted pG+host9 and partial *epsA*, respectively; D) Colony PCR of showing pG+host9epsAp (lanes 1-2) and pG+host9epsABp (lane 3), respectively.

Following the sequence confirmation, the deletion plasmid was transformed into *L. johnsonii* FI9785 by electroporation [214] and single and double crossovers were induced as described by Maguin et al., [216] using 30°C as the permissive temperature and 42°C as the non-permissive temperature for the plasmid to replicate which is used to induce integration

(Figure 5.3). Basically, pG+host9epsABp was transformed to electro-competent *L. johnsonii* FI9785 as described in section 2.2.15 and positive colonies were selected with erythromycin (Ery) (10 µg/ml) and grown at 30°C for 2 d and confirmed by colony PCR using GoTaq polymerase (Promega) with primers pGhost1 and pGhostR. Positive colonies were grown overnight in 20 ml MRS supplemented with Ery (10 µg/ml) at 30°C, the same medium (20 ml MRS + Ery) was prewarmed at 42°C and overnight grown sample was used to inoculate the prewarmed media with a dilution series until 10<sup>-6</sup> by taking 2 ml from each dilution. These cultures were grown for 1-2 d at 42°C until good growth (turbid) to induce the chromosomal integration of the plasmid. From the most diluted sample a dilution series up to 10<sup>-6</sup> was made and 100 µl from each dilution was plated in MRS + Ery plates which were prewarmed at 42°C and grown overnight at 42°C (for single colonies 10<sup>-6</sup> is the best one). Then 8-10 colonies were tested by colony PCR with primers 1184F, pGhost1, epsBR1 and pGhostR to confirm single crossovers.

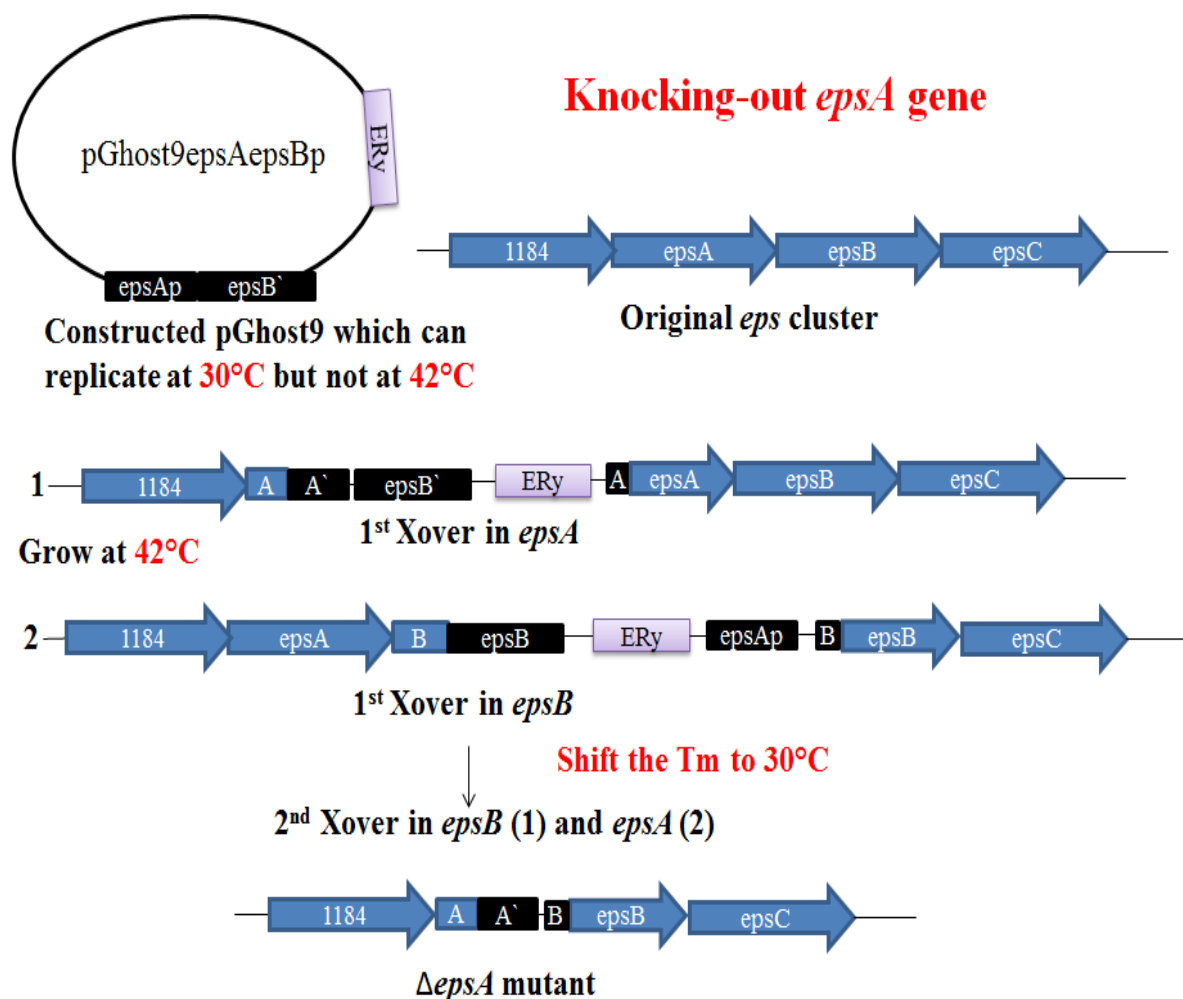


**Figure 5.3.** Schematic representation of *epsA* gene deletion process.

Each orientation was grown in 20 ml MRS + Ery at 42°C overnight and 200 µl from these cultures used for inoculation of 20 ml MRS without Ery and serial dilutions were made until 10<sup>-6</sup> by taking 2 ml from each one and grown at 30°C to encourage the plasmid to come out until good growth (turbid). Similarly, from the most diluted sample a dilution series up to 10<sup>-6</sup> was made and 100 µl from each dilution were plated in MRS plates supplemented with or without Ery which were prewarmed at 42°C and grown overnight at 42°C which resulted in 1 log fold less colony count on +Ery plates than on -Ery plates due to the removal of the plasmid in the previous step. Then the colonies were replica plated to Ery+ and Ery- MRS plates, the colonies that have grown in MRS - Ery but not MRS + Ery were screened by colony PCR to demonstrate the successful double crossover, giving the expected product of 1228 bp with a deletion of 630 bp from the *epsA* gene (*L. johnsonii* Δ*epsA*) (Figure 5.4).

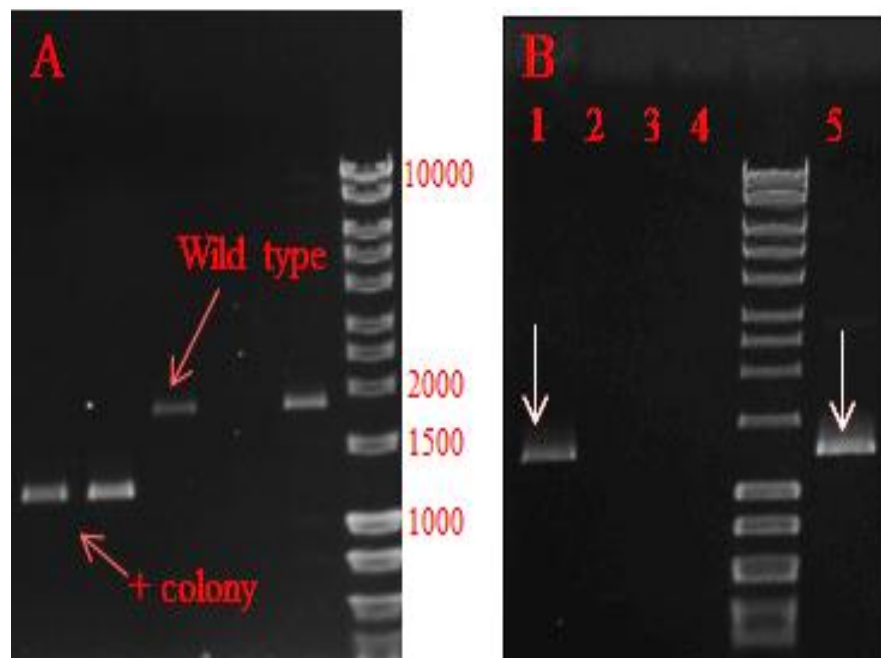


**Figure 5.4.** Agarose gel (0.8% w/v) showing A) the positive colonies showing the successful double crossover, giving the expected product of 1228 bp with a deletion of 630 bp from the *epsA* gene (*L. johnsonii* Δ*epsA*) and the colonies that reverted back to the wild type phenotype after the second crossover; B) The positive colonies screened by colony PCR using GoTaq polymerase (Promega) and primers 1184F and *epsBR1* (lane 1 and lane 5) and same colonies checked with primers pGhost1 and pGhostR (lane 2-3-4) showing no bands which confirms the removal of the plasmid.

To get the final mutant, a large number of colonies have to be screened due to the tendency of the *L. johnsonii* FI9785 to reverse its chromosome to the original form after the first cross over step (Figure 5.4). The removal of the plasmid was confirmed by colony PCR with the primers pGhost1 and pGhostR which did not give any product as expected (Figure 5.4). After

the confirmation of the deletion and removal of the plasmid the mutant strains were grown at 37°C and no difference was observed in the growth of *L. johnsonii*  $\Delta epsA$  cells compared to the wild type strain (Figure 5.5).

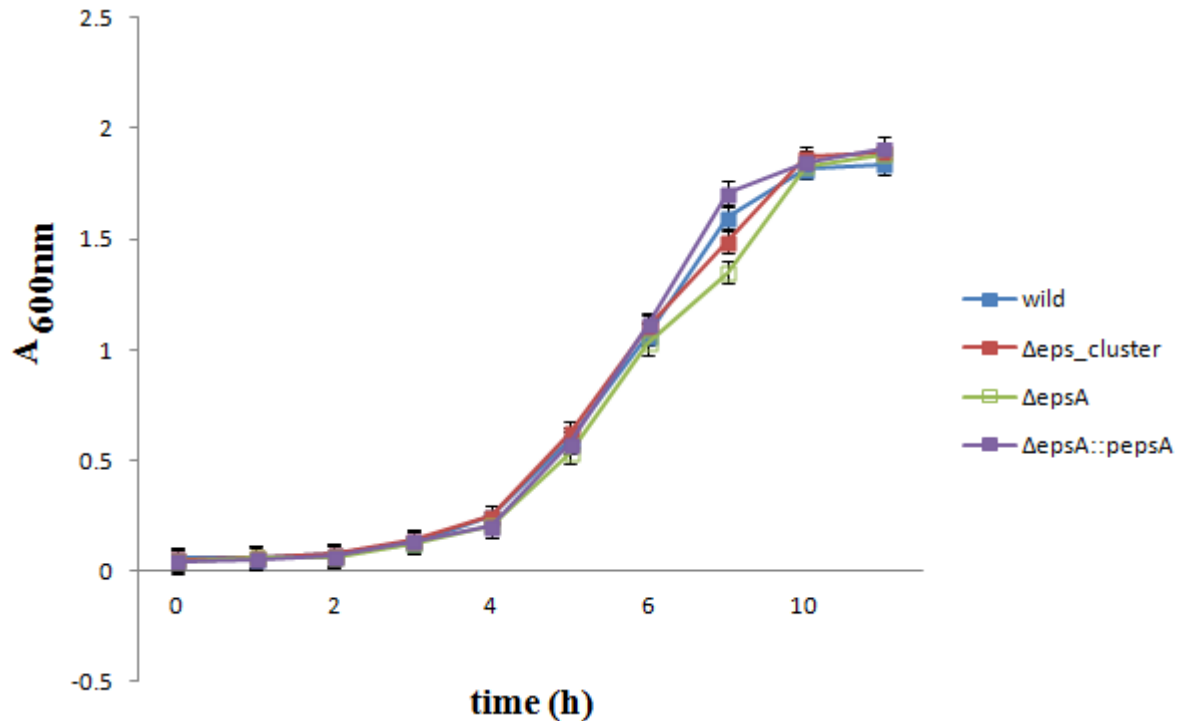


**Figure 5.5.** The growth curve of wild type and new mutant strains during the 11 h period.

### 5.3.2 Deletion of the *eps* gene cluster from the genome of *L. johnsonii*

The identified *eps* gene cluster was deleted from the *L. johnsonii* FI9785 using a previously described methodology which includes replacement of a target region with an antibiotic resistance gene [62]. For this purpose the partial upstream and partial downstream of the target region were amplified with the introduction of the overlap regions with the antibiotic resistance gene (chloramphenicol) and then a final deletion product were PCR constructed which is formed by partial upstream gene, antibiotic resistance gene in the middle and the partial downstream gene (Figure 5.6). This includes preparing a construct that consists partial *epsA* gene as upstream region of the *eps* cluster, chloramphenicol resistance gene in the middle and partial *FI9785\_1170* gene as downstream region of the *eps* cluster. Finally the deletion process was carried out with the thermo-sensitive vector as described above.

The plasmid pG+host9epsAp that harbours the first 390 bp of the *epsA* gene and some upstream sequence with *XhoI/HindIII* restriction sites was constructed as described previously (Figure 5.2). To prepare the final construct for the deletion of *eps* cluster,

chloramphenicol resistance gene and partial *FI9785\_1170* gene PCR spliced with introducing a *XhoI* and a *HindIII* site to each end, respectively.

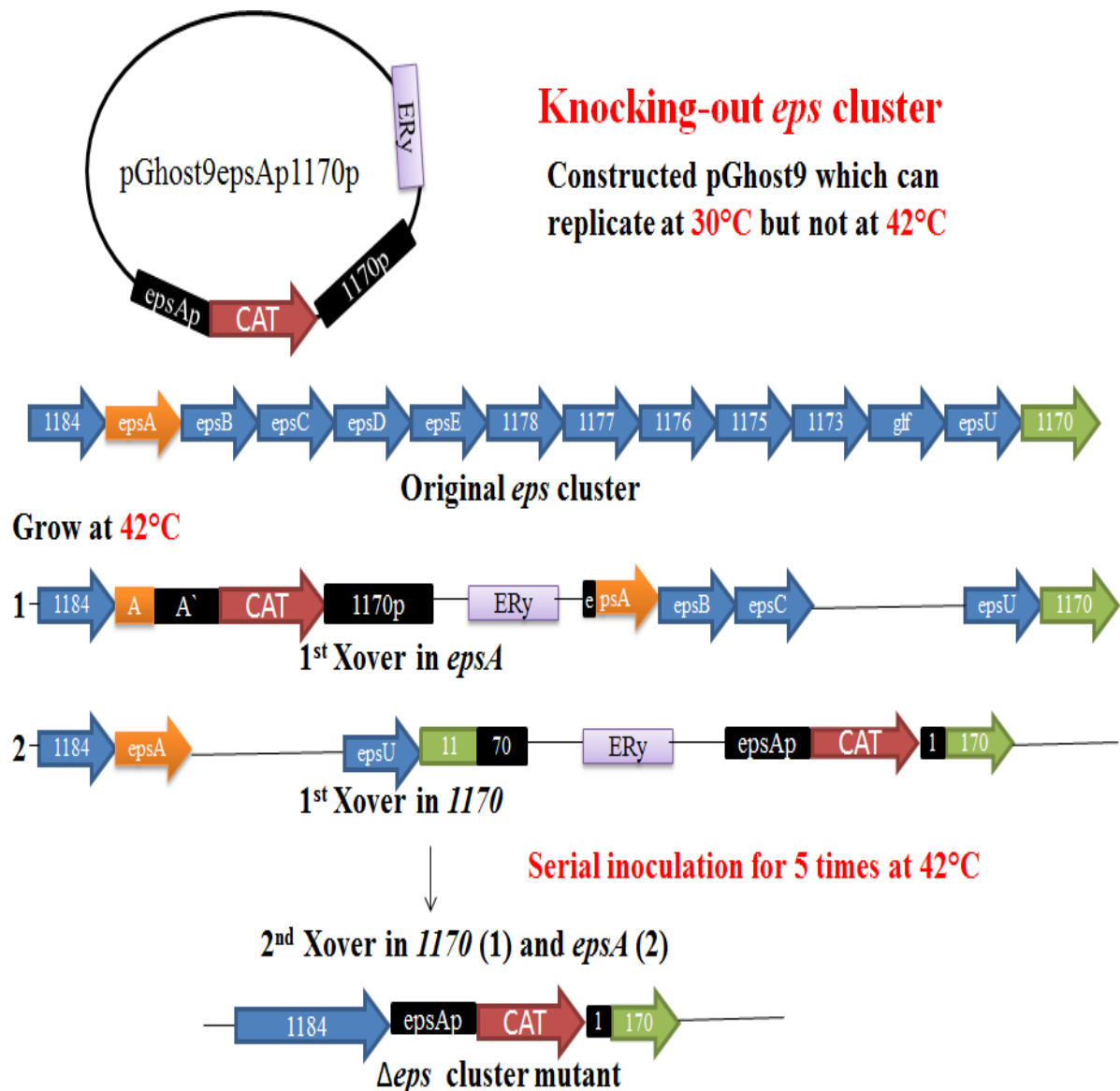


**Figure 5.6.** Schematic representation of *eps* gene cluster deletion process.

Firstly, the chloramphenicol resistance gene from plasmid pUK200 [217] was amplified using Phusion polymerase (Finnzymes) with primers CAT\_XHOF and CATRSPLICE1170, introducing a *XhoI* restriction site and a tail for splice overlap extension PCR with sequence from the *FI9785\_1170* gene (Figure 5.7).

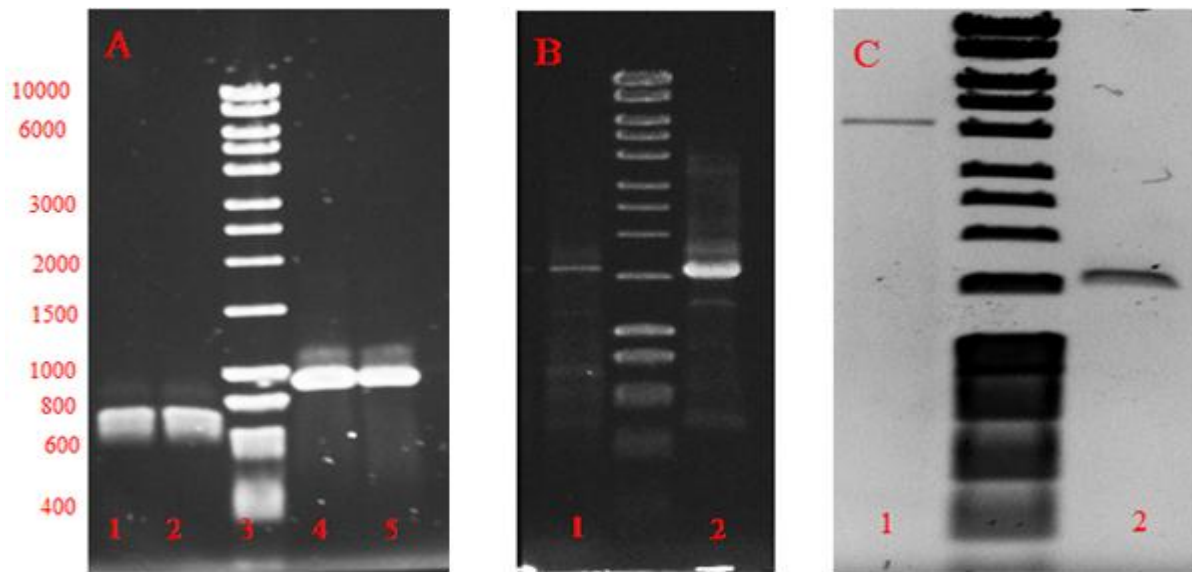


**Figure 5.7.** Agarose gel (0.8% w/v) showing A) lane 1-2; *FI9785\_1170* gene with a splice tail to *CAT*, lane 3; ladder, lane 4-5; *CAT* gene with a splice tail to *FI9785\_1170*, B) lane 1-2 splice PCR product of *FI9785\_1170* and *CAT* genes resulted as CATsplice1170, C) lane 1; Cut vector pG+host9epsAp and lane 2; cut insert CATsplice1170.

To amplify the partial *FI9785\_1170* gene with 280 bp of non-coding region, primers 1170FSPLICECAT and 1170\_ncR were used, introducing a tail for the splice overlap extension PCR with the chloramphenicol resistance gene product and incorporating a *HindIII* restriction site, respectively. The products from these two reactions were then used as templates for splice overlap extension PCR together with the primer pair CAT\_XHOF and 1170\_ncR to produce a 1585 bp product (Figure 5.7). This was then digested with *XhoI* and *HindIII* and subcloned into pG+host9epsAp digested with *XhoI* and *HindIII*. The ligation product was transformed into electro-competent *E. coli* MC1022 and positive colonies were selected with erythromycin (400  $\mu\text{g/ml}$ ) and confirmed by colony PCR using GoTaq polymerase (Promega) and primers pGhost1 and pGhostR (Figure 5.8).

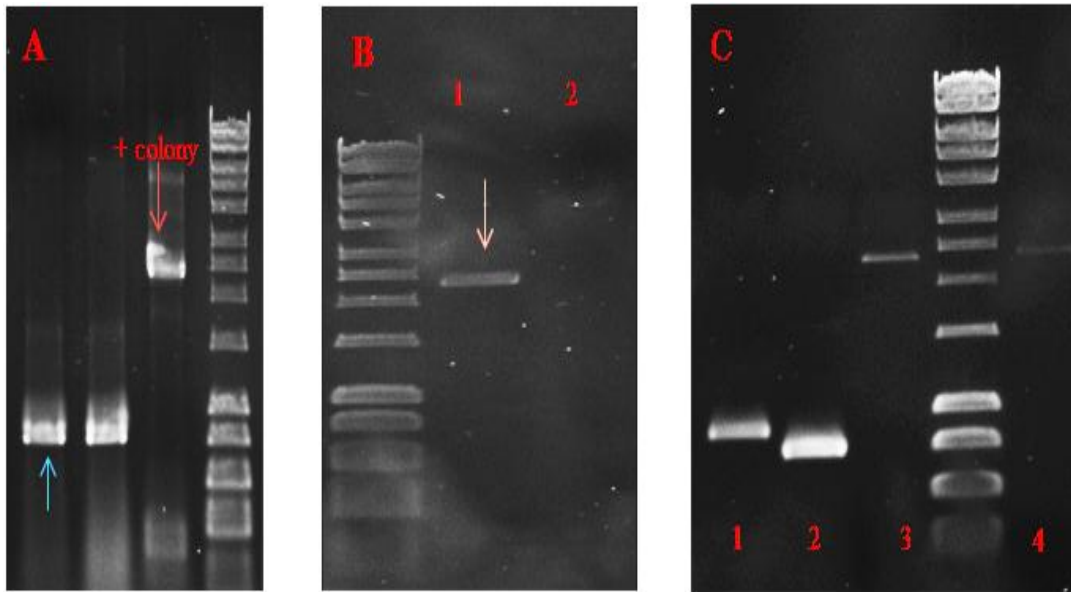


**Figure 5.8.** Agarose gel (0.8% w/v) showing A) Red arrows show the confirmation of the positive colonies having the pG+host9epsApCATsplice1170 by colony PCR using GoTaq polymerase (Promega) and primers pGhost1 and pGhostR, blue arrow shows the self-ligated or uncut vector pG+host9epsAp, B) lane 1; the positive colonies showing the successful double crossover, giving the expected product of 2315 bp with the deletion of *eps* gene cluster confirmed with colony PCR using GoTaq polymerase (Promega) and primers 1184F and 1170ncR2 (*L. johnsonii*  $\Delta$ *eps*\_cluster), lane 2; control in which a *L. johnsonii* FI9785 colony was used as a DNA template for colony PCR which did not show any band as expected, C) Confirmation of the  $\Delta$ *eps*\_cluster mutant; lane 1; colony PCR using GoTaq polymerase (Promega) and primers CATF1 and 1170ncR2 with the expected size of 890 bp, lane 2; colony PCR using GoTaq polymerase (Promega) and primers 1184 and CATPR1 with the expected size of 782 bp, lane 3-4; colony PCR using GoTaq polymerase (Promega) and primers 1184F and 1170ncR2 with the expected size of 2315 bp (*L. johnsonii*  $\Delta$ *eps*\_cluster).

Following sequence confirmation the deletion plasmid was transformed into *L. johnsonii* FI9785 by electroporation [214] and the method of gene replacement was performed as described by Denou et al., [62] (Figure 5.6). The transformants were selected on MRS plates supplemented with chloramphenicol and grown at 30°C which is the permissive temperature for plasmid replication. For the insertion of the plasmid construct to the genome of *L. johnsonii*, the overnight grown positive transformants were used to inoculate MRS broth supplemented with chloramphenicol (7.5 µg/ml) and grown at 42°C which is the non-permissive temperature for plasmid replication. This inoculation was serially proceeded for five passages for the removal of the plasmid construct from the genome of *L. johnsonii*. After the fifth passage, the culture was diluted and plated on MRS containing chloramphenicol at 42°C to obtain single colonies that were replica streaked onto plates containing MRS with chloramphenicol and MRS with erythromycin to identify erythromycin-sensitive, chloramphenicol-resistant clones. A positive clone was selected and the deletion of the *eps*

cluster was confirmed by PCR (*L. johnsonii*  $\Delta eps\_cluster$ ) (Figure 5.8). The growth of the new mutant was not altered after the mutation (Figure 5.5).

### 5.3.3 Complementation of *epsA* gene

For complementation purposes, the *epsA* gene was PCR amplified from FI9785 genomic DNA using the primer pair 5*epsA*\_NcoI and *epsA*NcoI\_R to produce a 1023 bp product with the *NcoI* sites. This product was then digested with the corresponding enzyme and ligated together in the expression vector pFI2560 [33] digested with *NcoI* following with the transformation of the ligated construct to *L. johnsonii*  $\Delta epsA$  strain (*L. johnsonii*  $\Delta epsA::pepsA$ ) (Figure 5.9). Similar to the other mutants there was no difference in the growth profile of the  $\Delta epsA::pepsA$  mutant in comparison to the wild type strain (Figure 5.5).

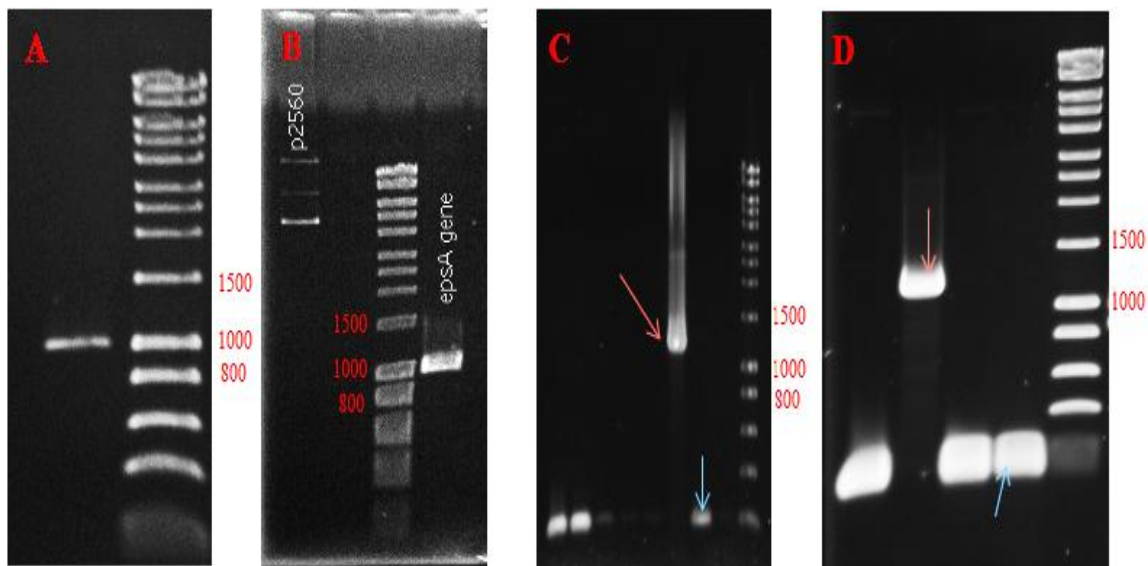


**Figure 5.9.** Agarose gel (0.8% w/v) showing A) Amplification of *epsA* gene from the genome of *L. johnsonii* by PCR using Phusion polymerase (Finnzymes) with primers 5*epsA*\_NcoI and *epsA*NcoI\_R, B) Digestion of pFI2560 and *epsA* gene with *NcoI*, C) Red arrow shows the positive colony after the transformation of the ligated plasmid into *L. johnsonii*  $\Delta epsA$  strain, but the sequence was checked and showed that it was not in the right orientation (antisense), D) Red arrow shows the positive colony after the transformation of the new ligated vector into  $\Delta epsA$  mutant; its sequence confirmed the sense orientation, Blue arrow shows the transformants with the re-ligated or uncut vector.

### 5.3.4 Loss of EPS production after deletion of *epsA* gene and *eps* gene cluster

*L. johnsonii* FI9785 is able to produce two structurally different EPS as we described in Chapter 3: EPS-1 and EPS-2 (Figure 3.6). To demonstrate the role of the *eps* cluster with 14 genes related to EPS production in *L. johnsonii* FI9785 and the *epsA* gene, which is the putative transcriptional regulator of this cluster, in the EPS biosynthesis, mutant strains were

produced where the whole *eps* cluster and the *epsA* gene had been deleted by deletion mutagenesis. The cell surface associated EPS were then isolated from both mutant strains and were subjected to NMR spectroscopy to analyse the alterations in EPS structure after deletion of the *eps* cluster and the *epsA* gene, respectively. Interestingly, both mutants were unable to produce either EPS-1 or EPS-2 (data not shown). Both mutants showed acapsular phenotypes (Figure 5.10). Furthermore, the complementation of the *epsA* gene resulted in the production of these two EPS indicating the essential role of this gene in EPS biosynthesis mechanism of *L. johnsonii* FI9785.

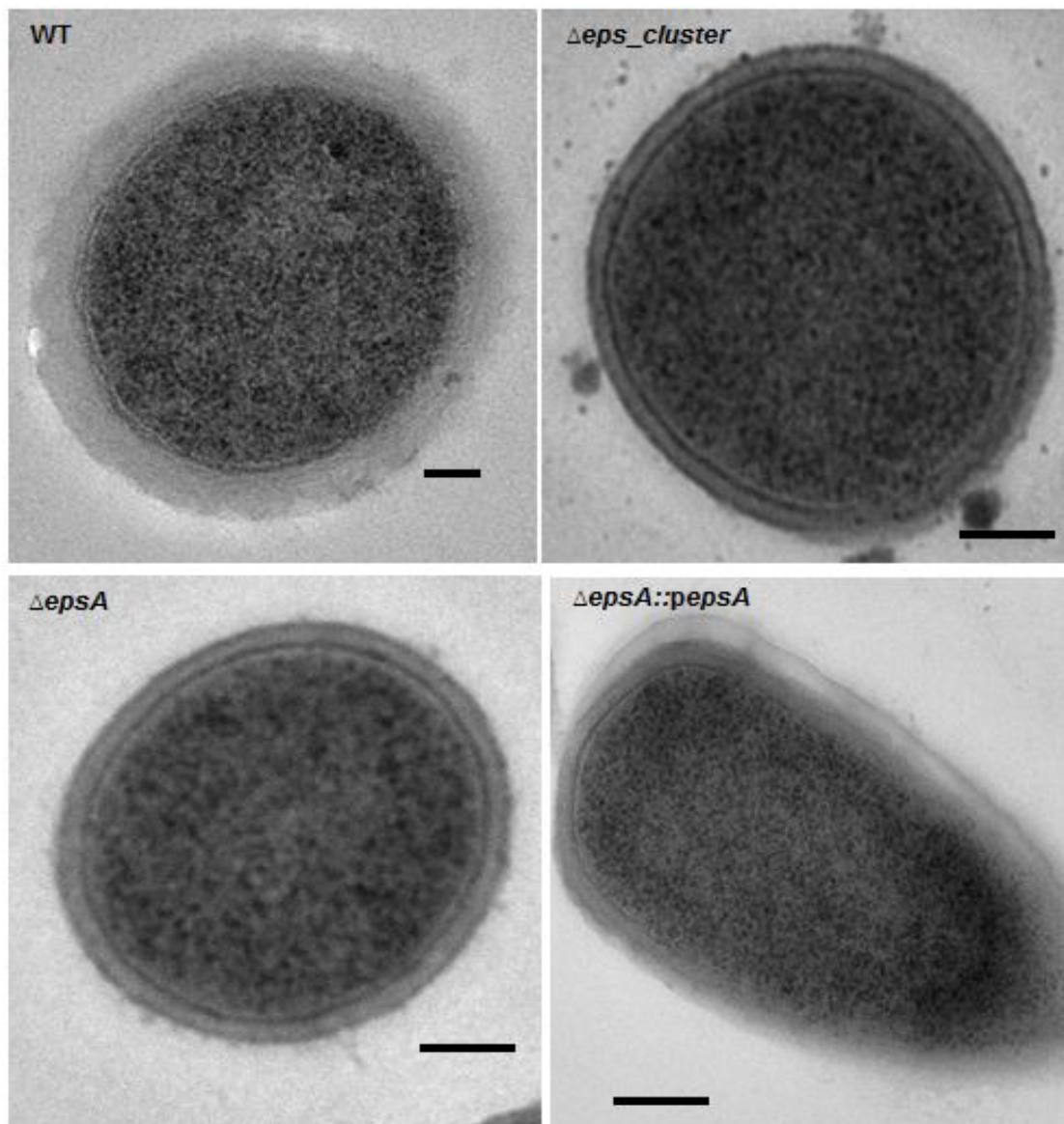


**Figure 5.10.** TEM analysis of *L. johnsonii* wild type and  $\Delta eps\_cluster$ ,  $\Delta epsA$  and  $\Delta epsA::pepsA$  mutants showing the capsular EPS accumulation on cell surface of wild type and  $\Delta epsA::pepsA$  mutant and showing the acapsular  $\Delta eps\_cluster$  and  $\Delta epsA$  mutants. The bar represents 100 nm.

TEM analysis showed the capsular EPS layer as an outer cell surface layer accumulated at the wild type but this EPS layer was absent in  $\Delta epsA$  and  $\Delta eps\_cluster$  mutant strains which shows the non-EPS production in these mutants and finally the  $\Delta epsA::pepsA$  restored the accumulation of EPS on cell surface of *L. johnsonii* (Figure 5.10).

### 5.3.5 Structural analysis revealed the complementation of *epsA* gene

In order to confirm the role of *epsA* gene in EPS production, the *epsA* knock-out strain was complemented with the wild type *epsA* gene in sense orientation. The structural analysis of EPS showed that complementing the *epsA* gene ( $\Delta epsA::pepsA$  mutant) had fully restored the biosynthesis of EPS in *L. johnsonii* FI9785. The  $^1H$  NMR spectrum of the  $\Delta epsA::pepsA$  mutant (Figure 5.11) showed the presence of both EPS, EPS-1 (~30%) and EPS-2 (~70%).

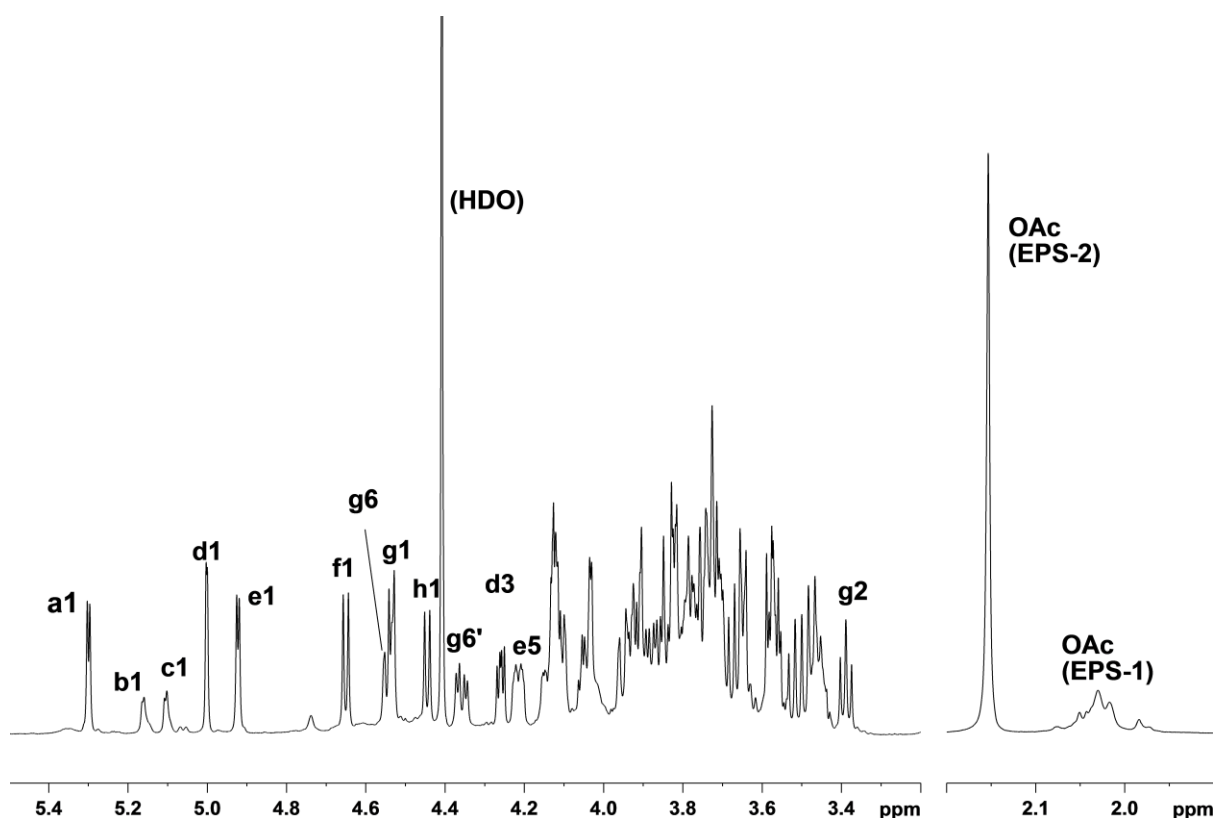


**Figure 5.11.** 600 MHz  $^1H$  NMR spectrum (338<sup>0</sup>K, D<sub>2</sub>O) of  $\Delta epsA::pepsA$  mutant of *L. johnsonii* FI9785. The same labels are used as previously [230], i.e. sugar residues *b*, *c* are from EPS-1 and residues *a* and *d-h* from EPS-2.

This contrasted with the composition of the mixture obtained from the WT (also isolated from the bacterial cell pellet) in which EPS-1 was the major polysaccharide. It was mentioned previously that both polysaccharides are acetylated [230]. The acetyl group in the hexasaccharide repeating unit of EPS-2 gives rise to a sharp singlet at 2.15 ppm in the  $^1H$

spectrum (Figure 5.11); by integration there is one acetyl group per repeating unit. The other signals at ~2.0 to 2.05 ppm are associated with EPS-1 and although integration shows that there is approximately one acetyl group per disaccharide repeating unit the presence of multiple peaks means that these groups must be distributed across several locations.

label	unit		Chemical shift (ppm)						
			1	2	3	4	5	6	OAc
<i>a</i>	(1,6) $\alpha$ Glc $p$ →3	H	5.30	3.58	3.74	3.52	4.14	3.88, 4.11	
		C	101.94	74.43 <sup>a</sup>	75.75 <sup>b</sup>	72.27	73.80	71.43	
<i>f</i>	(1,3) $\beta$ Glc $p$ →5	H	4.65	3.45	3.65	3.65	3.47	3.74, 3.92	
		C	104.85	74.79	85.81	72.76	78.27	63.56	
<i>d</i>	(1,5) $\beta$ Gal $f$ →6	H	5.00	4.13	4.26	4.11	4.05	3.82	
		C	110.41	83.63	79.02	84.42	80.60	63.99	
<i>e</i>	(1,6) $\alpha$ Glc $p$ →4	H	4.92	3.57	3.74	3.48	4.22	3.72, 3.95	
		C	102.86	74.50 <sup>a</sup>	75.53 <sup>b</sup>	72.37	73.80	69.24	
<i>h</i>	(1,4) $\beta$ Gal $p$ →4	H	<b>4.44</b>	3.57	3.72	4.03	3.79	3.84, 3.91	
		C	106.29	73.70	75.02	80.31	78.19	63.05	
<i>g</i>	(1,4) $\beta$ Glc $p$ →6	H	4.53	3.39	3.67	3.71	<b>3.80</b>	<b>4.36, 4.55</b>	2.15
		C	105.51	75.64 <sup>b</sup>	77.06	81.94	<b>75.02</b>	<b>65.73</b>	23.05

<sup>a</sup> <sup>13</sup>C assignments may need to be interchanged

<sup>b</sup> <sup>13</sup>C assignments may need to be interchanged

**Table 5.3.** <sup>1</sup>H and <sup>13</sup>C chemical shifts of  $\Delta$ *epsA::pepsA* repeating unit. The residues are listed in the order in which they occur in the linear repeating unit of the acetylated EPS-2, i.e. *a* is linked to *f*, *f* to *d* etc and *g* to *a*. The repeating unit is acetylated at C6 of residue *g*. Shifts which differ most from the previously reported [230] non-acetylated EPS-2 are indicated in bold.

A detailed study of the 2D NMR spectra showed that in this preparation EPS-2 was acetylated at just one position: C6 of the (1,4)-linked  $\beta$ -Glc $p$  residue, *g*. The <sup>1</sup>H and <sup>13</sup>C chemical shifts of EPS-2 are listed in Table 5.3. The data reported previously [230] referred to non-acetylated EPS-2 which was the predominant component in the sample analysed there. The location of the acetyl group in acetylated EPS-2 is revealed by the downfield displacement, compared with non-acetylated EPS-2, of the *g*6 signals to  $\delta$ 4.36/4.55 from  $\delta$ 3.84/4.00 (<sup>1</sup>H) and to  $\delta$ 65.73 from  $\delta$ 63.04 (<sup>13</sup>C). Shifts of neighbouring atoms (*h*1, *g*5) are also affected by the presence of the acetyl group as indicated in Table 5.3; the remaining shifts are essentially unchanged.

The FTIR spectra of capsular EPS isolated from the  $\Delta epsA::pepsA$  mutant also confirmed the complementation of the biosynthesis of EPS-1 and EPS-2 in this mutant and showed the structural and functional group changes of this biopolymer after complementation (Figure 5.12).

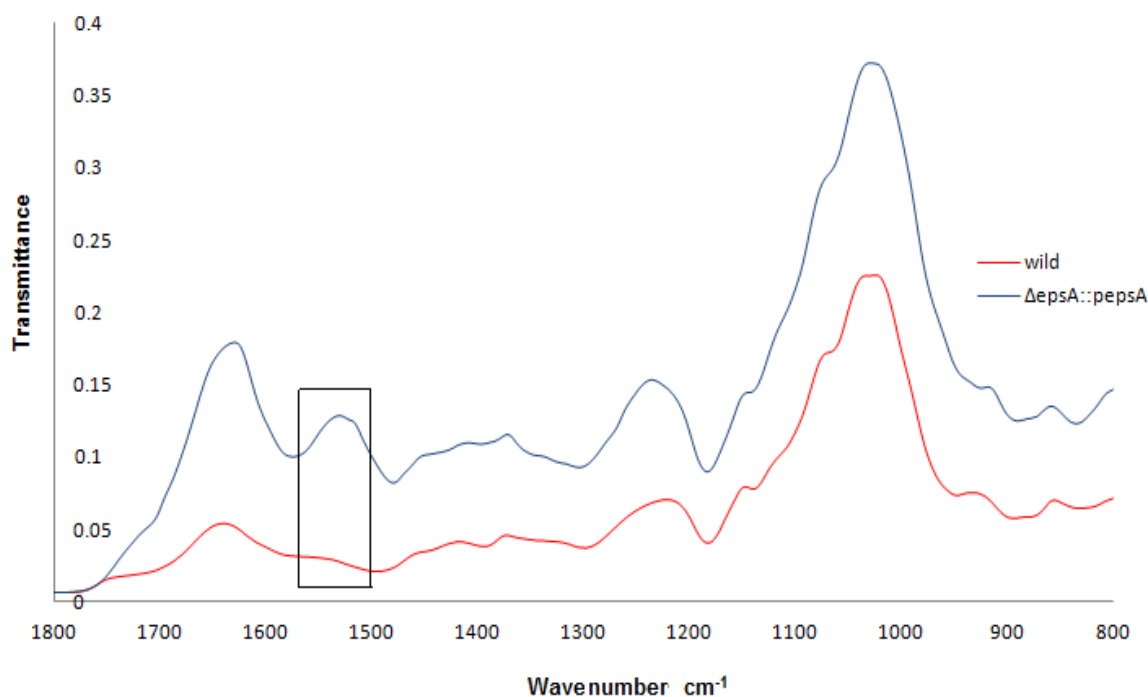


**Figure 5.12.** FTIR spectra of capsular EPS isolated from the wild type and the  $\Delta epsA::pepsA$  mutant. The window represents the alteration in the spectra of the  $\Delta epsA::pepsA$  mutant compared to the wild type strain.

The only difference in the FTIR spectra of wild type and  $\Delta epsA::pepsA$  mutant was the peak at the region  $1500\text{-}1600\text{ cm}^{-1}$  which is assigned to N-H bending and C-N stretching in proteins which was also previously observed for EPS isolated from  $\Delta epsE$  and  $\Delta epsE::pepsEA/S$  strains (Figure 3.12).

These results suggest that the *eps* cluster is responsible for the production of both EPS in *L. johnsonii* FI9785 and *epsA* gene as a putative transcriptional regulator is essential for EPS production in *L. johnsonii* FI9785 which has been shown for the first time in genus *Lactobacillus*.

### 5.3.6 Adhesion and cell surface alterations after the loss of the EPS layer

EPS play an important role on cell surface characteristics of *L. johnsonii* FI9785 as we reported in previous chapter. Furthermore in this study we generated mutants that were not

capable of EPS production and also complementation of *epsA* gene resulted in restoring the EPS accumulation to the cell surface of *L. johnsonii* FI9785. The role of EPS on cell surface characteristics related to probiotic concept such as autoaggregation, adhesion to human cells and immunomodulatory properties was further investigated with these acapsular and capsular strains.

Firstly, the autoaggregation of wild type and new mutants was evaluated by FCM after overnight incubation at 37°C. The loss of the EPS layer in  $\Delta epsA$  and  $\Delta eps\_cluster$  strains resulted in significantly higher aggregation levels compared to the wild type. But the ability to form EPS as a capsular layer in the  $\Delta epsA::pepsA$  mutant as well as higher EPS production than wild type (Figure 5.16) resulted in a sharp decrease in aggregation levels compared to the wild type (Figure 5.13). FCM observations revealed that nearly 100 % of  $\Delta epsA$  and  $\Delta eps\_cluster$  mutant cells aggregated during the overnight incubation period at 37°C. In contrast, wild type showed 50% aggregation at overnight incubation and only 13% of  $\Delta epsA::pepsA$  mutant cells showed aggregation during this incubation period. These findings confirm the role of capsular EPS layer in determining the aggregation properties of EPS producing bacteria.

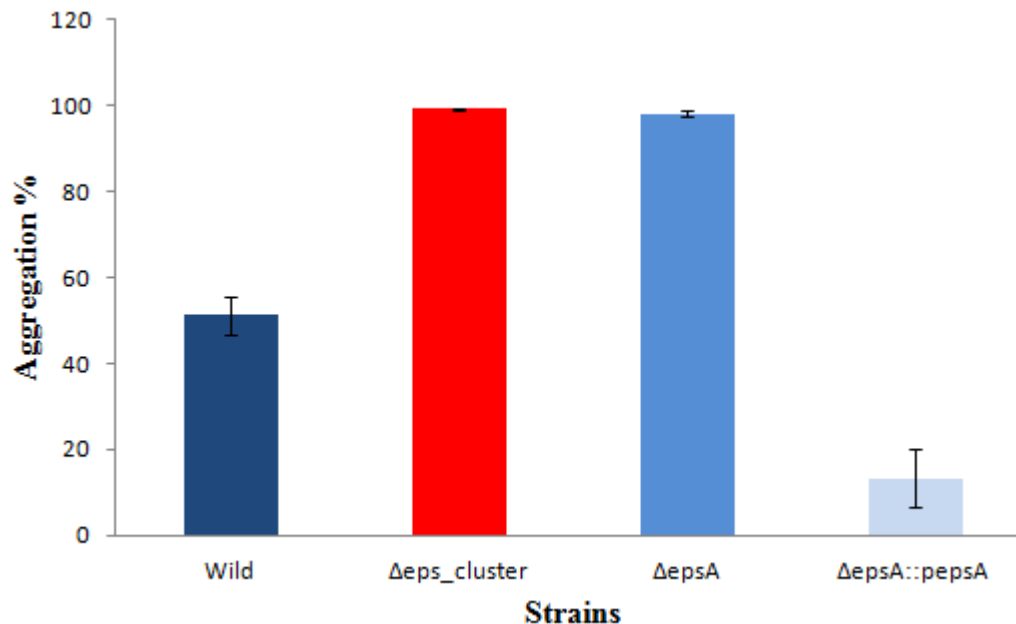


**Figure 5.13.** The aggregation percentage of wild type and mutant strains after overnight incubation (16 h) analysed by FCM. The error bars represent standard deviations of triplicates for each strain.

Secondly, to understand the role of the EPS layer in antibody responses, FCM immunodetection of cell surface alteration analysis were conducted for new mutant strains.

The acapsular strains,  $\Delta epsA$  and  $\Delta eps\_cluster$  mutants, showed significantly higher responses to anti-wild type polyclonal antibody compared to the wild type and  $\Delta epsA::pepsA$  mutant. The anti-wild type antibody responses in these mutants were around three times higher than the antibody response to wild type cells. The exposure of the cell surface epitopes after the loss of the EPS layer resulted in a significant increase in antibody responses. In contrast the  $\Delta epsA::pepsA$  mutant revealed nearly the same antibody response as wild type (Figure 5.14).

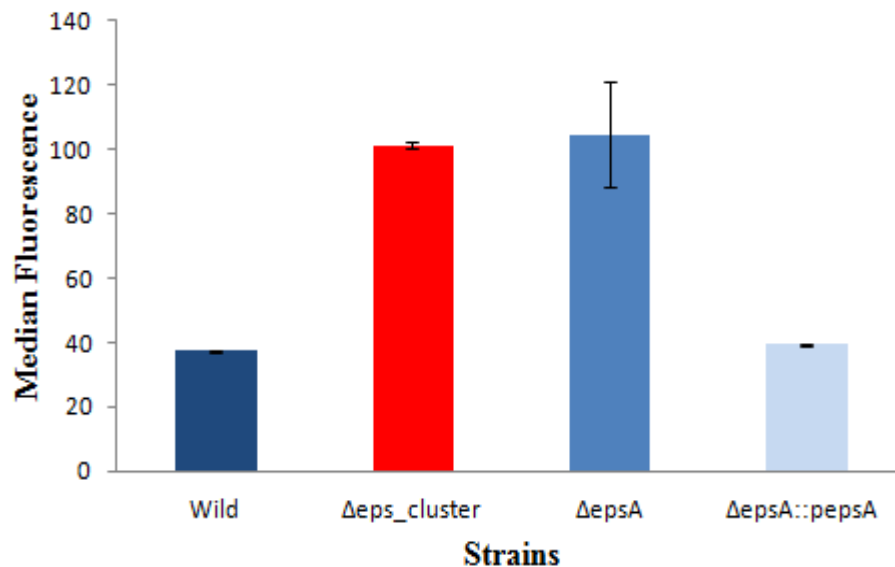


**Figure 5.14.** Anti - wild type antibody responses to the wild type and derivative strains measured by FCM. Results are the mean of duplicate experiments +/- standard deviation.

When the cell surface was surrounded by the EPS layer again, the antibody responses to this mutant was reduced because of the unavailability of the these epitopes in this mutant. These results further suggest that cell surface EPS may play a role in the immunomodulatory mechanism of probiotic bacteria.

Lastly, adherences to HT29 cells experiments were performed using FCM to confirm the role of the EPS layer on adhesion properties of *L. johnsonii* FI9785. The loss of capsular EPS layer altered the adhesion level of *L. johnsonii* FI9785 cells (Figure 5.15). The adhesion level of the wild type strain was c. 14% of the total bacteria added (Figure 4.18) while adhesion level of  $\Delta epsA$  and  $\Delta eps\_cluster$  mutants was 25% and 40% higher than wild type levels, respectively.

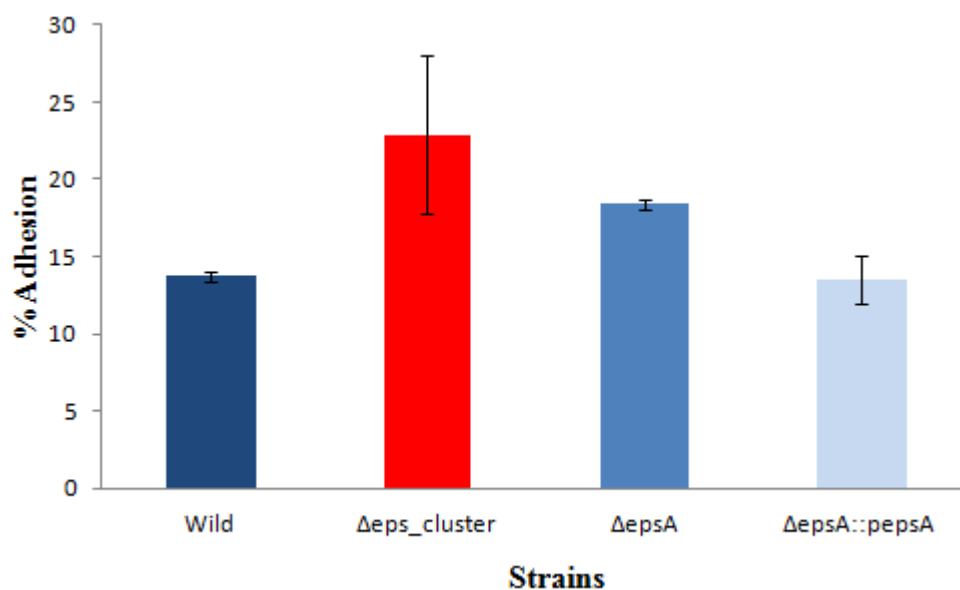


**Figure 5.15.** Adhesion of *L. johnsonii* strains to HT29 monolayers. Results are the mean of triplicate experiments with three replicates per experiment +/- standard deviation.

Complementation of  $\Delta epsA$  mutant restored the adhesion level to the wild type levels after restoring the ability to form the capsular EPS layer (Figure 5.15). These results clearly showed the impact of the cell surface associated EPS on *in vitro* adhesion properties of *L. johnsonii* FI9785.

### 5.3.7 Quantification of EPS production and qPCR analysis *epsA* gene expression

In order to understand the effect of complementation of the deleted *epsA* gene with a plasmid that allows the constitutive expression of this gene on EPS production levels, total EPS production of wild type and  $\Delta epsA::pepsA$  mutant were determined by phenol-sulphuric acid methodology as a quantity of EPS production per  $10^7$  cells.

Total EPS production analysis showed that over-expression of the *epsA* gene in  $\Delta epsA::pepsA$  mutant resulted in significantly increased levels of EPS production in this mutant compared to the wild type (Figure 5.16). The EPS production was nearly doubled after complementation which also affected the final ratio of the EPS-2 in EPS mix in which the ratio of the EPS-2 was 70% in  $\Delta epsA::pepsA$  mutant whereas the ratio of EPS-2 in wild type EPS was 50% (Based on NMR signals). To confirm the role of *epsA* gene expression on increased EPS production compared to the wild type, we performed qPCR analysis to compare the *epsA* gene expression levels in wild type,  $\Delta epsA::pepsA$  and  $\Delta epsA$  mutant cells.

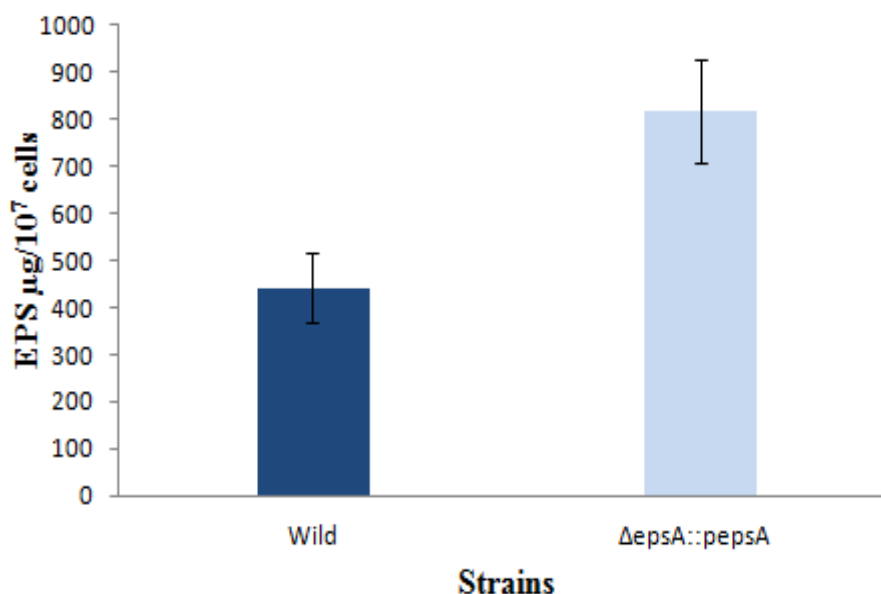


**Figure 5.16.** Total sugar content of *L. johnsonii* wild type and  $\Delta\text{epsA}::\text{pepsA}$  mutant strain. Results are the mean of the triplicate measurements with three technical replicates per measurement +/- standard deviation.

The expression of the *epsA* gene in the  $\Delta\text{epsA}$  could not be detected in qPCR analysis as expected (data not shown). In contrast, complementation of *epsA* gene in  $\Delta\text{epsA}::\text{pepsA}$  mutant resulted in  $1.99 \pm 0.34$  fold increase in *epsA* gene expression level compared to the wild type *epsA* gene expression level. These results clearly show that increased expression of the putative transcriptional regulator gene resulted in nearly double the amount of EPS production in *L. johnsonii* FI9785.

## 5.4 DISCUSSION

In this study, we show that *L. johnsonii* FI9785, a probiotic organism is able to produce two different EPS, a homopolymeric and a heteropolymeric EPS, although it has a typical *eps* gene cluster related to the heteropolymeric EPS production [33]. By deleting the *eps* gene cluster we wanted to show the role of this *eps* cluster in biosynthesis of these two EPS, although we were expecting to see only an abolishment in EPS-2 biosynthesis as deleting the priming glycosyltransferase from the *eps* cluster which harbours six putative glycosyltransferases including *epsE* resulted in loss of EPS-2 biosynthesis which is also composed of six sugar residues. But, interestingly, deletion of the *eps* cluster resulted in the loss of not only EPS-2 but also EPS-1 biosynthesis in *L. johnsonii* FI9785. This was in agreement with the previous observation where the deletion of the *eps* gene cluster in another *L. johnsonii* strain resulted in an acapsular phenotype although the structure of the EPS

produced by this strain is not yet determined [62]. Furthermore considering the data from Chapter 3, we still suggest that this gene cluster which harbours six putative glycosyltransferase genes might be responsible for the biosynthesis of heteropolysaccharide EPS-2; in addition, one of these glycosyltransferases may have a bifunctional role to produce the homopolymer EPS-1 [245]. But a stronger possibility is a novel gene located elsewhere in the genome of *L. johnsonii* FI9785 may be involved in EPS-1 production in conjunction with a gene/s in the identified *eps* cluster. Another interesting observation was the complete loss of the EPS production after the deletion of *epsA* gene from the *eps* cluster which is the putative transcriptional regulator [33] of this cluster. To the best of our knowledge, we can confirm that this study is the first to show the crucial role of the transcriptional regulator in EPS biosynthesis of *Lactobacillus* strains. To date several *eps* clusters and numerous numbers of EPS structures have been identified for LAB but the transcriptional regulation mechanism of the EPS metabolism has not been determined in detail. A recent review on the regulatory factors of the transcription of the *eps* clusters and EPS biosynthesis in Gram negative *Rhizobium* spp., describes the complexity of the regulatory pathways which includes several intrinsic factors such as proteins which suppress or stimulate the transcription and EPS biosynthesis and several extrinsic factors including the presence or the lack of carbon source or non-carbon nutrients or stress and starvation conditions [275].

A recent study on the transcriptional analysis of the *eps* clusters of *B. breve* strains demonstrated that only two genes encoding the putative priming glycosyltransferase and the putative chain length regulation protein were transcribed by a separate promoter, monocistronically and apart from these two genes the identified *eps* clusters were transcribed by a single promoter polycistronically [66]. Similarly it was reported that the transcription of fifteen genes in the *eps* clusters of *L. rhamnosus* strains which harboured eighteen genes occurred as a single mRNA transcript where three different promoter sites were detected within these fifteen genes and also the putative transcriptional regulator was suggested to be transcribed separately and shown to have its own promoter [85]. It was also shown that Gram negative human commensal bacterium *B. fragilis* can alter its cell surface structure and one of the proposed mechanisms for this modification is the control of the transcription of the genes responsible for the polysaccharide biosynthesis by a unique DNA invertase that modulates the expression of these genes. This ON-OFF mechanism results in the production of at least eight different capsular polysaccharide in *B. fragilis* [277]. Similarly it was reported that over-expression of the transcriptional regulator of the polysaccharide biosynthesis in *V.*

*cholerae* O1 caused a colony switch which was found to be related with the increased polysaccharide production [241]. In a previous study the *eps* gene cluster of *L. lactis* NIZO B40 strain which has a similar genetic orientation with the *eps* cluster of *L. johnsonii* was shown to be transcribed as a polycistronic single mRNA [87]. Deletion of the putative transcriptional regulator *epsA* gene resulted in the loss of the EPS biosynthesis and furthermore based on the BLAST analysis, *epsA* protein of *L. johnsonii* is the only protein in the *eps* cluster that contains conserved domains associated with the transcriptional regulator proteins (Table 1.3). Similarly prediction of the promoters in the *eps* gene cluster of *L. johnsonii* FI9785 analysis by online tool BPROM (<http://goo.gl/AdGkF>) showed the highest possibility for the promoter region in the beginning of the *epsA* gene (data not shown). Based on these results it can be speculated that the *epsA* gene is probably the transcriptional regulator of the EPS biosynthesis and the transcription of the *eps* cluster occurs as a single polycistronic mRNA in *L. johnsonii* FI9785. But the transcriptional regulation mechanism is a complex process that is affected by genetic and environmental conditions and future studies are definitely required in order to underline the exact mechanism of this regulation in *L. johnsonii* FI9785 and other organisms.

The complementation of *epsA* gene resulted in a mutant that had fully restored the production of both EPS, confirming the essential role of the transcriptional regulator in EPS biosynthesis of *L. johnsonii* FI9785. Furthermore, the two - fold increase in *epsA* gene expression levels in the complemented *epsA* mutant strain resulted in nearly two - fold increase in EPS production levels of *L. johnsonii* FI9785. As previously discussed, it was shown that three - fold increase in the expression level of the plasmid encoded *eps* gene cluster in *L. lactis* NIZO B40 resulted in four - fold increase in the final EPS production level but the growth rate of the over-expression strain was lower than the wild type *L. lactis* NIZO B40 strain [123] due to the fact that the sugar nucleotides are common source of bacteria which are used in not only EPS production but also for bacterial metabolic activities [123, 127, 134]. Previously it was also suggested the inhibition in the growth rate can even be expected when higher EPS production occurs due to less cell wall polymer synthesis and availability of the components for the EPS production that may compete with the cell wall biosynthesis metabolism [124]. We did not observe any difference in growth profile of the  $\Delta epsA::pepsA$  mutant although the EPS production has been doubled which can be also related to the nutrient availability of the growth environment and conditions and cellular organisations of each bacteria. In a previous study, over-expression of the priming glycosyltransferase in *L. lactis* NIZO B40 strain resulted

in 15% increase in EPS production levels [135]. Similar over-expressions to improve the final EPS yield have been shown also in other LAB [81]. Similarly, higher transcription level of the priming glycosyltransferase resulted in higher EPS production in *Bifidobacterium longum* subsp. *longum* CRC 002 strain [129]. In a recent study, it was shown that the expression levels of the *cpsA* gene of *Streptococcus pneumoniae* altered in different medium conditions and the increase in the expression level resulted in higher capsule formation [278] which is also in agreement with our observation. Overall, this study together with the previous studies show the potential of the over-expression of target genes in *eps* clusters to increase the EPS production levels not only to impact the cell surface characteristics but also to improve the technological properties of products that EPS producing bacteria are used.

As we previously discussed, EPS mediated the autoaggregation properties of *L. johnsonii* FI9785. Our hypothesis was that less EPS around cells resulted in the unmasking of aggregation promoting proteins which are located on the cell surface of *L. johnsonii* [269] and increased the aggregation properties and vice versa; more EPS on cell surface decreased the autoaggregation properties of *L. johnsonii* FI9785. In the present study we confirmed our hypothesis; the lack of EPS layer around *L. johnsonii* FI9785 resulted in higher aggregation levels in both  $\Delta epsA$  and  $\Delta eps\_cluster$  mutants compared to the wild type and the mutant expressing the *epsA* gene resulted in nearly non-aggregating phenotype possibly due to the more EPS production than wild type strain which also supports this hypothesis. These findings clearly confirm the role of EPS on determining the autoaggregation properties of the probiotic strain of *L. johnsonii* FI9785. Similarly, the adhesion to HT29 cell profiles of acapsular mutants increased in the same extent as we discussed in Chapter 4 and confirmed the role of EPS on adhesion properties probably due to the its role in uncovering of the surface adhesins on cell surface of *L. johnsonii* [62]. It should also be noted that there was no difference in the adhesion and autoaggregation properties of acapsular mutants in comparison to EPS-1 only producer  $\Delta epsE$  mutant suggesting that EPS-1 itself can be a determinant factor in bacterial aggregation and adhesion or the thickness of the EPS-1 layer is not sufficient to cover the proteinaceous components promoting the bacterial aggregation and the surface adhesins as latter being a strong possibility. Additionally, the increased EPS producer  $\Delta epsA::pepsA$  mutant which showed less aggregation properties than increased EPS producer *epsC*<sup>D88N</sup> mutant, showed similar adhesion properties as wild type which suggests that autoaggregation or cell surface adhesins are not the only factors determining the adhesion

properties of lactobacilli and the accumulation of the EPS layer as well as the EPS nature play a role in adhesion process.

We also examined the alterations of the antibody (AB) responses after the loss of the EPS layer to the anti-wild type polyclonal antibody using FCM. Notably, we observed a significant increase in AB responses after the loss of EPS layer around cells *in vitro* and this response dropped to the wild type's response levels after ability to form EPS layer in *epsA* complemented mutant. This result was previously proposed by some *in vitro* and *in vivo* studies showing the immune-silencing and suppressive effect of capsular polysaccharides for other bacteria as we discussed previously [60, 65, 66, 279]. The EPS layer probably masks the surface antigens in *L. johnsonii* FI9785 which are now available in EPS<sup>-</sup> mutants which resulted in a massive increase in AB responses in these mutants. Similarly not only the EPS-1+EPS-2 complex but also EPS-1 alone was also sufficient to mask the surface antigens in *L. johnsonii* FI9785 as we observed a slight increase in AB response levels in EPS-1 only producer mutant strains in comparison to the wild type strain. But there was no difference in adhesion and aggregation properties of acapsular and EPS-1 only producer mutant strains as we previously mentioned suggesting that the surface molecules promoting the adhesion and aggregation might not be the most important surface epitopes determining the overall antigenicity of *L. johnsonii* FI9785 and these epitopes are still covered by EPS-1 layer in EPS-1 only producer mutant strains. Overall, using FCM antibody application we clearly showed and confirmed the indisputable role of EPS on antibody responses of *L. johnsonii* FI9785.

The FTIR spectra of the EPS from *epsA* complemented mutant also confirmed the complementation process and the role of *epsA* gene in EPS biosynthesis mechanism. Notably, the spectra was significantly similar to the spectra of EPS of wild type except the peak around 1500-1600 cm<sup>-1</sup> shows the glycoproteins after over-expressing the *epsA* gene in this mutant [235]. Previously it was shown that changes in a sugar transferase related to sugar biosynthesis in *Campylobacter jejuni* affected the glycosylation process of the lipooligosaccharides in this bacterium [280]. Changes in the transcriptional mechanism of the *eps* cluster in *L. johnsonii* FI9785 after over-expressing the *epsA* gene, the transcriptional regulator, in  $\Delta epsA$  mutant, might have led the addition of protein like structures to the EPS in the biosynthesis process. Overall, our results may suggest that over-expressing the *epsA* gene may result in some structural alterations of some functional groups of EPS as mentioned in NMR Spectroscopy results.

In conclusion, the study described in this chapter confirmed that *epsA* and the *eps* cluster are required for both EPS-1 and EPS-2 biosynthesis in *L. johnsonii* FI9785. The inability to produce EPS after these mutations in *L. johnsonii* FI9785 gave the advantage to show the biological and immunological relevance of EPS accumulated at the cell surface of this bacterium.

# Chapter 6

---

## Physiological role of the Exopolysaccharide Layer

## 6.1 INTRODUCTION

In the previous chapters we demonstrated the alterations in the EPS production levels and final EPS structures accumulated at the cell surface of *L. johnsonii* FI9785 by generating several mutants in the *eps* cluster. These are valuable tools that we can use to study the biological function of the EPS layer of probiotic *L. johnsonii* FI9785. The viability and the survival of probiotic bacteria during transit and gut colonisation is crucial in order to provide their therapeutic functions [281, 282]. EPS may be the one of important factors contributing the survival and protection of probiotic bacteria under different environmental conditions. The EPS layers in a number of different bacteria are shown to be protective against desiccation, antibiotics, bacteriophages, metal ions, antimicrobials such as nisin and lysozyme, osmotic stress, phagocytosis and macrophages [10, 139, 140]. Similarly, another physiological role of the EPS layer is its protective function under harsh conditions such as acid and bile conditions [281]. The survival ability of probiotic bacteria under the low pH of the stomach which ranges between pH 2.5 to pH 3.5 [283] is essential for their entry to the intestinal tract for colonisation purposes. Similarly, bile salts which are secreted to the small intestine destroy the bacterial membranes affecting the bacterial viability and so resistance to bile salts under concentration of 0.15-0.30% is an important criterion for selecting probiotic bacteria; EPS from yogurt starter bacteria was shown to be protective under these conditions [210, 281]. Previously, It was also shown that EPS produced by *L. lactis* was required for the protection of cells against bacteriophages, lysozyme and the antimicrobial nisin whereas EPS did not show any protective effect against increased temperature, freezing, freeze-drying as well as the antibiotics penicillin and vancomycin [139]. Similarly, the EPS layer of *B. breve* UCC2003 was shown to have a protective role against low pH and bile salts conditions which was also the case for yogurt starter bacteria mentioned previously [66, 281]. Although, there are numerous reports about the identification of new EPS structures and their technological and biological functions, the potential protective role of EPS of LAB against harsh conditions has not yet been assessed in detail.

Colonisation ability of probiotic bacteria is also crucial for their health benefits including immune-modulation, pathogen inhibition and modifying the gut microbiota [284]. In the previous chapters, we clearly showed that an increase in EPS layer decreased adhesion to human cells *in vitro* while EPS-1 only producer or acapsular mutants had increased adhesion. There are other reports showing contrary results regarding the role of EPS in colonisation and persistence of EPS producing bacteria. The loss of the capsular EPS layer in *L. johnsonii*

NCC 533 resulted in a slightly increased persistence in the murine gut in comparison to the EPS producing parental strain [62]. In contrast, it was shown that the EPS mutant of *L. rhamnosus* GG which has a reduced EPS layer compared to the wild type strain showed a reduced persistence in the murine GIT. In this study researchers also demonstrated the protective role of EPS to the human defence factors such as LL-37 [67]. Similarly, Bifidobacterial EPS was shown to be important for stress tolerance and this EPS promoted the *in vivo* persistence but not the initial colonisation [66]. As described in Chapter 1 modification of the gut microbiota after the supplementation of diet with probiotic organisms is one of the proposed mechanisms of how probiotic bacteria show health benefits to their host [285]. Several potential mechanisms for modification of gut microbiota by probiotic organisms have been described so far including the competitive exclusion of other bacteria by probiotic bacteria by competing for binding sites, production of growth substrates by probiotic bacteria (for example, EPS or vitamins), reduction of inflammation by probiotic bacteria, thus altering intestinal properties for colonization and persistence within and stimulation of innate immune responses by probiotic bacteria (by unknown mechanisms) [285]. In this concept the EPS layer of *L. johnsonii* may be one of the important factors playing a role in gut microbiota modification due to its potential role determining the adhesion properties, as a carbon source that may stimulate the growth of a specific bacterial group/groups, and possibly altering the innate immune responses which may also cause modification of the gut microbiota composition. Apart from the possible protective function of the EPS layer of *L. johnsonii*, these potential roles of the EPS layer in the modification of gut microbiota will be discussed in this chapter.

Overall, the aim of the study described in this chapter was to identify the physiological role of the EPS produced by *L. johnsonii* in order to understand its protective role under *in vivo* and *in vitro* conditions. Furthermore, additional function of the EPS layer in colonisation and persistence of *L. johnsonii* was assessed using a mouse model. Finally, microbiota alteration analysis after dosing the mice with the wild type and the  $\Delta eps\_cluster$  mutant was performed in order to understand the possible role of the EPS in the gut microbiota composition modification.

## 6.2 MATERIAL AND METHODS

### 6.2.1 Minimum Inhibitory Concentration (MIC) of nisin and antibiotics

The Antibiotic Susceptibility tests of *L. johnsonii* FI9785 were performed as described in section 2.1.3.2 and *L. johnsonii* was found to be mildly sensitive to the following antibiotics: Erythromycin (Sigma, MW; 733.9), Ampicillin (Melford, MW; 371.4), Tetracycline (Boehringer Mannheim GmbH, MW; 480.9) and Furazolidone (Sigma, MW; 225.16). Further, MIC of these antibiotics was assessed for the wild type, *epsC*<sup>D88N</sup>,  $\Delta$ *epsE* and  $\Delta$ *eps\_cluster* mutant strains in order to show the potential protective role of the EPS layer. Wild type and mutant strains were grown overnight as described in section 2.1.2. Standard MRS medium with the following antibiotic concentrations were prepared: 0.5 µg/ml and 1.0 µg/ml Erythromycin; 1 µg/ml and 2 µg/ml Ampicillin; 1 µg/ml and 4 µg/ml Tetracycline and 15 µg/ml and 30 µg/ml Furazolidone and the growth of each strain after 1% inoculum was monitored using a Bioscreen (Section 2.1.3) in triplicate in honeycomb plates at 37°C. Similarly, the MIC of nisin was assessed with the Bioscreen methodology using 0.25 µg/ml, 0.5 µg/ml, 1 µg/ml, 2.5 µg/ml, 5.0 µg/ml, 10 µg/ml and 20 µg/ml concentration of nisin (Aplin and Barret, resuspended in dilute HCl pH 3) in MRS medium. The experiments were performed in triplicate with three technical replicates.

### 6.2.2 Cell survival tests of wild type and mutant cells

*L. johnsonii* strains were grown as described in section 2.1.2 and harvested by centrifugation (4000 g for 10 min at 4°C). The harvested cells were then washed twice with PBS. Following the second wash, the cells were resuspended in phosphoric acid buffer (100 mM) at pH 2.00 for 90 min (acid shock). Similarly, for heat shock analysis cells were resuspended in PBS and incubated at 50°C and 60°C for 5 min, respectively. The cell survival was monitored during acid and heat shock analysis. Before and after acid and heat shock, serial dilutions of each strain were plated to MRS agar in order to determine CFU counts for each strain to calculate the survival of each strain. The experiments were performed as duplicates with three technical replicates.

### 6.2.3 Survival in bile salts and simulated *in vitro* digestion

*L. johnsonii* strains were grown in MRS media overnight and diluted in fresh MRS media containing 0.3% (wt/vl) bile salts (Bovine bile; Sigma) to an OD<sub>600nm</sub> of 0.1. The growth of *L. johnsonii* strains was monitored over 24 h at 37°C using the Bioscreen instrument as

described in section 2.1.3. Growth experiments were performed in triplicate and values were used to calculate average OD<sub>600nm</sub>.

*In vitro* digestion tests of *L. johnsonii* strains were performed as described by Nueno-Palop et al., [286]. Strains were grown in MRS media overnight and harvested by centrifugation (4000 g for 10 min at 4°C). The harvested cells were then resuspended in PBS to obtain an OD<sub>600nm</sub> ~ 1.0. To simulate gastric digestion, each sample was adjusted to pH 3.0 and Pepsin (Sigma) was added to a final concentration of 5% (w/v). The mix was incubated at 37°C for 90 min with agitation at 110 rpm. To create intestinal digestion conditions, the sample was adjusted to pH 6.0 and solutions of pancreatin (Sigma) and bile salts at a final concentration of 0.1% and 0.3% (w/v) respectively were added. Samples were incubated for 150 min at 37°C with agitation (110 rpm). Samples were removed for determination of cell count before and after gastric and intestinal digestion. An aliquot was serially diluted and then plated on MRS agar in triplicate. The plates were incubated under aerobic condition at 37°C for 48 h.

#### **6.2.4 *In vivo* Colonisation Studies**

Mouse experiments were conducted in order to investigate the role of EPS on colonisation and persistence of *L. johnsonii* strains on three separate occasions. In each period of study C57BL/6 mice were obtained from Charles River UK Ltd and used at 6 – 8 weeks of age. Mice were maintained in the Disease Modelling Unit (DMU) at the University of East Anglia and were fed a diet of standard rodent chow and normal drinking water *ad libitum*. All mouse studies were authorised by the Home Office under the Animals Act 1986 by a Home Office registered personal license holder (Dr Kevin Hughes, IFR). The first period of the mouse study was performed using the wild type, *epsC*<sup>D88N</sup>,  $\Delta$ *epsE* and  $\Delta$ *eps\_cluster* mutant strains with 3 mice per group of strain as a preliminary experiment. In this period of study, *L. johnsonii* strains were selected on MRS plates using neomycin. *L. johnsonii* is naturally resistant to neomycin (personal communication, Dr Arjan Narbad, IFR), also the resistance of *L. johnsonii* derivatives were checked and all strains were observed to be resistant to neomycin at 10 µg/µl concentration (data not shown). To dose the mice, all strains had been grown to late stationary phase (24 h) aerobically in MRS medium supplemented with 10 µg/µl neomycin at 37°C and then centrifuged at 4000 g for 10 min at 24°C and resuspended in PBS to 10<sup>9</sup> cfu/ml. These amounts of cells were obtained by setting the 10<sup>-1</sup> dilution of the cell suspension to OD<sub>600nm</sub> of 0.6. Serial dilutions were plated on MRS plates supplemented with 10 µg/µl neomycin to check the bacterial concentrations in each suspension. In order to

dose the mice with *L. johnsonii* strains, C57BL/6 mice received 500 µl of 10<sup>9</sup> cfu/ml of each strain by gavage for 3 consecutive days. Before the dosing process faecal materials were collected from each mice group as the controls. After the dosing of the mice with each of strains, faecal samples were planned for collection at 3, 7, 10, 14, 17, 21 and 24 d after the first gavage for each time point. Faecal pellets were collected and resuspended in PBS (1:10 w/v) and homogenised using the Pellet Pestle (Sigma, UK) homogeniser and ten - fold serial dilutions were prepared up to 10<sup>-5</sup> dilution factor for each strain. From each dilution series 20 µl aliquots were plated out onto MRS plates containing 10 µg/µl neomycin with three replicates per dilution series and plates were grown for 2 d at 37°C and colonies counted. Additionally, the mice were sacrificed at 24 d after the first gavage by cervical dislocation and their GIT was isolated. Subsequently, colon, small intestine and caecum were collected and resuspended in 9 times volume of the organ weight in PBS and replica-plated as described for the faeces samples then the colony counts were calculated.

In the second period of mouse study, 20 female C57BL/6 mice were ordered from Charles River UK Ltd and used at 6 – 8 weeks of age and the experiments were conducted under the same licences and conditions described previously. This period of study was performed with the selection of *L. johnsonii* strains with a chloramphenicol (CAT) marker. For this purposes, the plasmid pFI2431 which is the original plasmid isolated from *L. johnsonii* [214] engineered to carry the CAT gene (by Nikki Horn, IFR), was transformed into the wild type and the *epsC*<sup>D88N</sup> mutant following the protocol described in section 2.2.15. Interestingly, after the transformation with the pFI2431, the *epsC*<sup>D88N</sup> mutant altered its phenotype which resulted in cell aggregation (data not shown). Due to that reason we decided to use *epsC*<sup>D88N</sup>::*pepsC* mutant which contains pFI2660 (Table 1.4) that also carries a CAT marker, which also produces higher levels of EPS than wild type strain (Figure 3.2). Finally, the last strain in the second mouse study was the acapsular strain,  $\Delta$ *eps\_cluster* mutant, which also carries the *CAT* gene in its genome introduced during the cluster deletion process (see section 5.3.2). The second period of study has therefore conducted with the wild type, *epsC*<sup>D88N</sup>::*pepsC* and  $\Delta$ *eps\_cluster* mutants with 6 mice per group with the addition of 2 mice as a control group which did not receive any *L. johnsonii*. The dosing process was performed as described previously and the CFU counts were counted in MRS plates supplemented with 7.5 µg /ml chloramphenicol.

The target of the mouse study was to identify the role of EPS on passage and persistence of *L. johnsonii*. The wild type with plasmid pFI2431 and the  $\Delta$ *eps\_cluster* mutant strain were used

with 5 mice per strain with the selection of chloramphenicol over 3 d of experimental period. For this purpose, mice were dosed with  $5 \times 10^8$  CFU of each strain by gavage for 3 consecutive days. Faecal samples were collected at 6, 24, 32, 48, 54 and 72 h after the first gavage and replica-plated on MRS + chloramphenicol. Additionally, the mice were sacrificed at 48 h after the last gavage by cervical dislocation and their GIT was isolated. Subsequently, colon, small intestine and caecum samples were collected and resuspended in 9 times volume of the organ weight in PBS and replica-plated as described for the faecal samples, then the colony counts were calculated on MRS + chloramphenicol plates.

### **6.2.5 Analysis of microbiota composition by 454 pyrosequencing**

In order to understand if the EPS layer of *L. johnsonii* FI9785 has a role on gut microbiota alterations, a pyrosequencing methodology for taxonomic analysis of the bacterial community present before and after the dosage with *L. johnsonii* strains was conducted using the samples from second experimental period. For this purpose total DNA of the faecal materials from the control mice group (n=2), mice groups dosed with wild type *L. johnsonii* (n=6) and  $\Delta eps\_cluster$  mutant (n=6), respectively, was extracted from day 0 and day 7 faecal samples of each group. DNA was extracted from 0.2 g of faecal material using a FastDNA Spin Kit for Soil (MPbio, UK) according to the manufacturer's instructions but with one modification: the bacterial cells were disrupted with a Fast Prep instrument 3 times at 6.5 m/s for 60 s. The isolated DNA was quantified using Nanodrop (Thermo Scientific) and stored at -20°C until examined.

The amplification and high-throughput sequencing of 16S rRNA regions in the extracted DNA samples were conducted by Dr Richard Ellis (AHVLA). Basically, the extracted DNA were amplified with the universal primers for the variable V4 and V5 regions of the 16S rRNA gene using the primers U515F (5'-GTGYCAGCMGCCGCGGTA) and U927R (5'-CCCGYCAATTCMTTTRAGT) which were designed to amplify bacterial ribosomal gene regions with the best possible taxonomic resolution based on published information [287, 288]. Forward fusion primers included the GS FLX Titanium primer A and the library key (5'-CCATCTCATCCCTGCGTGTCTCCGACTCAG) bearing a suite of eight 10 base multiplex identifier sequences (MID) (Roche Diagnostics Ltd, UK). Reverse fusion primers consisted of the GS FLX Titanium primer B and the library key (5'-CCTATCCCCTGTGTGCCTTGGCAGTCTCAG). Amplification was performed with FastStart HiFi Polymerase (Roche Diagnostics Ltd, UK) using the following cycling

conditions: 94°C for 3 min; 30 cycles of 94°C for 30 s, 55°C for 45 s, 72°C for 1 min; followed by 72°C for 8 min. Amplicons were purified using Ampure XP magnetic beads (Beckman Coulter) and the concentration of each sample was measured using the fluorescence-based Picogreen assay (Invitrogen). Concentrations were normalized before pooling samples in batches of up to 16, each of which would be subsequently identified by its unique MID. Pooled samples were then subjected to unidirectional sequencing from the forward primer on the 454 GS FLX Titanium platform according to the manufacturer's instructions (Roche Diagnostics).

The data analyses of the 454 sequences were performed by Dr Adrian Tett (IFR). Raw 16S rDNA sequences were processed in QIIME [289] version 1.6.0 using default parameters unless otherwise stated. Sequences were removed from the analysis if <350 and >450, of low quality, contained ambiguous bases and if there were mismatches in the barcode or forward sequencing primer. Both forward and reverse sequencing primers were removed and the remaining sequences clustered into operational taxonomic units (OTUs) using UCLUST [290] at 97% sequence identity. A representative sequence for each OTU was chosen and assigned taxonomy using the RDP classifier [287] and Greengenes [291] release October 2012. Each representative sequence was aligned by PyNAST [292] to the Greengenes core reference alignment. Sequences were rarefied to 2940 sequences to remove bias due to heterogeneity in the number of sequences for each sample. A phylogenetic tree was generated in Fast Tree [293] and shown as a taxonomy summary.

## 6.3 RESULTS

### 6.3.1 EPS layer of *L. johnsonii* protects against antibiotics and nisin

The growth profiles of the wild type, higher EPS producer (*epsC*<sup>D88N</sup>), EPS-1 only producer ( $\Delta$ *epsE*) and non-EPS producer ( $\Delta$ *eps\_cluster*) strains were monitored. As noted previously there was no difference in growth between the strains when grown without antibiotics (Figure 3.1&5.5). Firstly, an antibiogram test was conducted and four different antibiotics were selected due to the relative sensitivity of *L. johnsonii* FI9785 to these four antibiotics for the MIC analysis of *L. johnsonii* strains.

Among these four antibiotics no growth was observed when *L. johnsonii* strains were grown with erythromycin at concentrations tested (data not shown). When *L. johnsonii* strains were grown at 1 µg/ml ampicillin concentration, the wild type and the *epsC*<sup>D88N</sup> mutant strain showed similar growth rates, while EPS-1 only producer  $\Delta$ *epsE* and non-EPS producer  $\Delta$ *eps\_cluster* exhibited significantly reduced growth rates and reached a lower end point

OD<sub>600nm</sub> compared to the wild type and *epsC*<sup>D88N</sup> mutant strain (Figure 6.1). Notably, the growth of the  $\Delta eps\_cluster$  mutant was also largely lower than the  $\Delta epsE$  mutant strain, presumably due to the loss of the EPS layer.

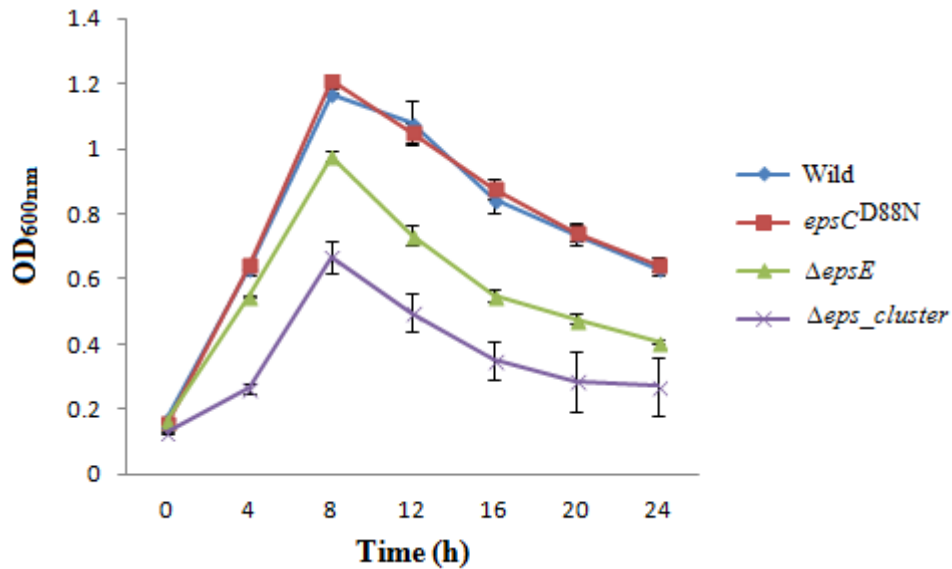


**Figure 6.1.** Growth curve of wild type, *epsC*<sup>D88N</sup>,  $\Delta epsE$  and  $\Delta eps\_cluster$  mutant strains of *L. johnsonii* in MRS supplemented with 1  $\mu\text{g/ml}$  ampicillin. Cells were grown aerobically at 37°C.

Similarly, the protective role of EPS was also clear when the ampicillin concentration was doubled. At 2  $\mu\text{g/ml}$  ampicillin concentration, the *epsC*<sup>D88N</sup> mutant showed higher growth rates than the wild type and the growth of the  $\Delta epsE$  mutant was reduced compared to the wild type. Furthermore, the non-EPS producer  $\Delta eps\_cluster$  mutant did not show any growth at this ampicillin level indicating the protective role of EPS in a dose dependant manner against this antibiotic (Figure 6.2). The growth of the  $\Delta epsE$  mutant was similar to the wild type during the first period (8 h) of incubation due to the EPS-1 production but then a significant reduction in its growth profile was observed in comparison to the wild type and the growth rate was no longer different from  $\Delta eps\_cluster$  mutant.

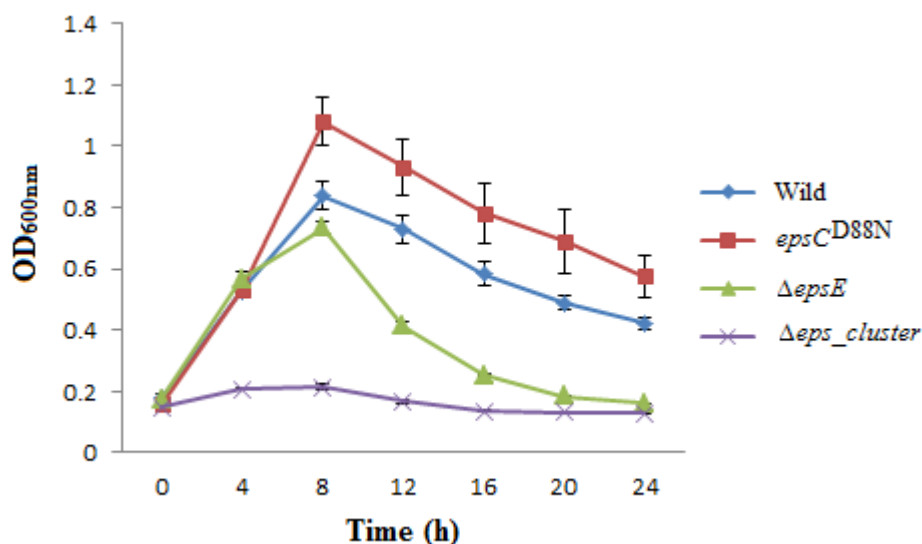


**Figure 6.2.** Growth curve of wild type, *epsC*<sup>D88N</sup>,  $\Delta$ *epsE* and  $\Delta$ *eps\_cluster* mutant strains of *L. johnsonii* in MRS supplemented with 2  $\mu$ g/ml ampicillin. Cells were grown aerobically at 37°C.

Several different concentrations of tetracycline were tested ranging between 1-50  $\mu$ g/ml concentrations but only at 1  $\mu$ g/ml concentration, the growth of *L. johnsonii* strains was observed (Figure 6.3). The EPS layer showed a protective role against tetracycline at 1  $\mu$ g/ml concentration similar to the other antibiotics tested. At the first half of the 24 h growth period only little growth was observed for all the strains.

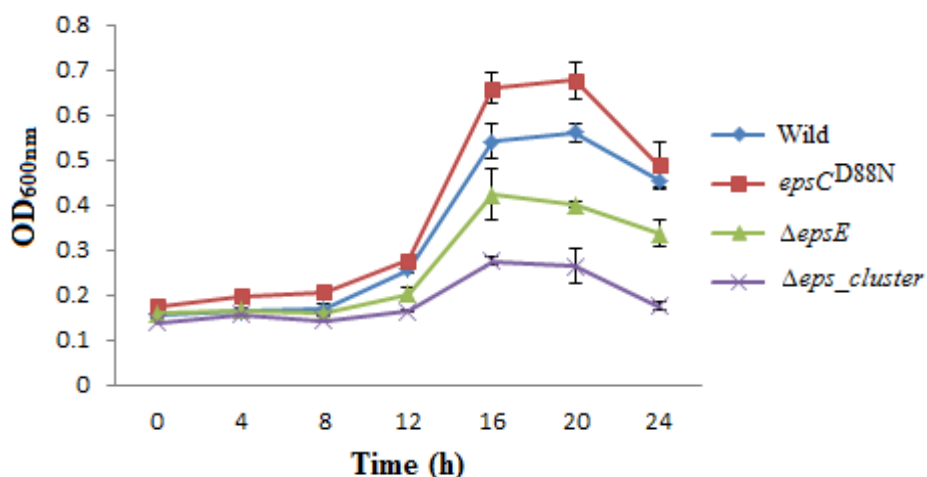


**Figure 6.3.** Growth curve of wild type, *epsC*<sup>D88N</sup>,  $\Delta$ *epsE* and  $\Delta$ *eps\_cluster* mutant strains of *L. johnsonii* in MRS supplemented with 1  $\mu$ g/ml tetracycline. Cells were grown aerobically at 37°C.

In the second half of the growth period probably after adaptation for the presence of tetracycline all strains showed an exponential growth rate for a 4 h period. Following this exponential growth, all strains exhibited a stationary phase for 4 h and finally all strains showed a decline in their optical density (Figure 6.3). It should be noted that the higher EPS

producer *epsC*<sup>D88N</sup> mutant showed the highest growth rates at 1 µg/ml tetracycline concentration compared to the other strains. Similar to other antibiotics,  $\Delta epsE$  and  $\Delta eps\_cluster$  mutant strains showed much lower growth rates than wild type where the growth of the non-EPS producer  $\Delta eps\_cluster$  mutant was the lowest at 1 µg/ml tetracycline (Figure 6.3).

We also tested different concentrations of furazolidone. At 15 µg/ml furazolidone, the growth of the wild type and the *epsC*<sup>D88N</sup> mutant strain was quite similar although the *epsC*<sup>D88N</sup> mutant reached higher OD<sub>600nm</sub> values compared to the wild type (Figure 6.4). The reduction or the lack of the EPS layer resulted in reduced growth rates in  $\Delta epsE$  and  $\Delta eps\_cluster$  mutant strains with the absence of EPS layer in  $\Delta eps\_cluster$  mutant causing further reduction in cell growth (Figure 6.4).

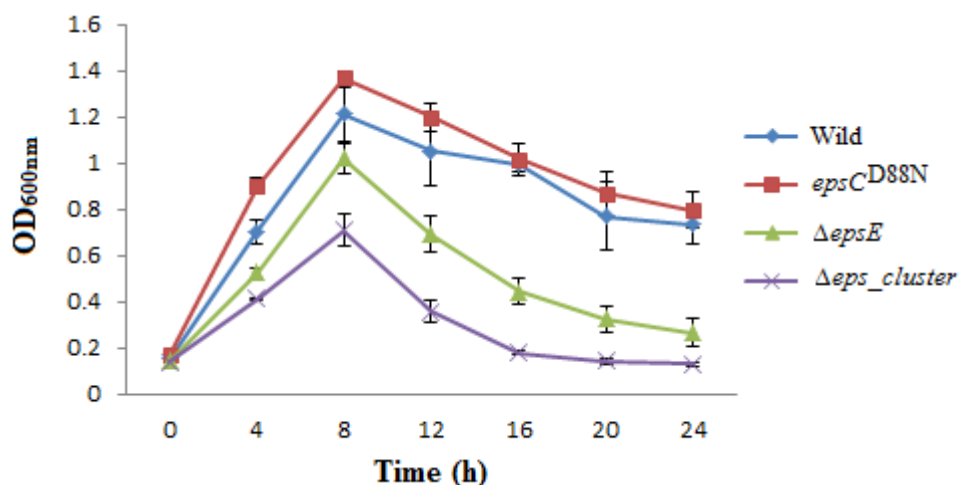


**Figure 6.4.** Growth curve of wild type, *epsC*<sup>D88N</sup>,  $\Delta epsE$  and  $\Delta eps\_cluster$  mutant strains of *L. johnsonii* in MRS supplemented with 15 µg/ml furazolidone. Cells were grown aerobically at 37°C.

When the concentration of furazolidone was increased to 30 µg/ml, the protective role of EPS was more effective as the *epsC*<sup>D88N</sup> mutant showed a largely higher growth than the wild type (Figure 6.5). At the first 8 h of the growth period ability to accumulate EPS-1 to the cell surface in  $\Delta epsE$  mutant, an increased growth in comparison to the non-EPS producer mutant was observed (Figure 6.5). But later on the presence of furazolidone caused a significant drop in the optical density of both  $\Delta epsE$  and  $\Delta eps\_cluster$  mutants which reached the same OD<sub>600nm</sub> values at the end of the 24 h incubation period. Overall these results confirm the important protective role of EPS against different antibiotics in a dose dependant manner.

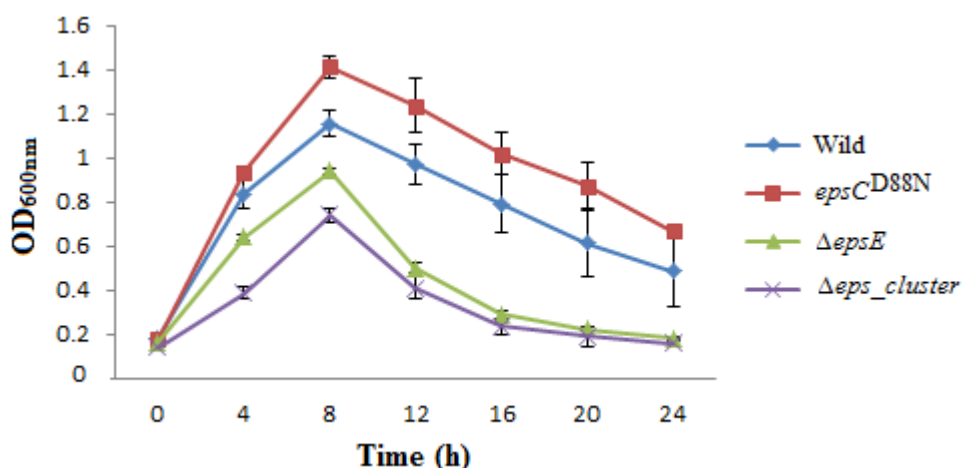


**Figure 6.5.** Growth curve of wild type, *epsC*<sup>D88N</sup>,  $\Delta epsE$  and  $\Delta eps\_cluster$  mutant strains of *L. johnsonii* in MRS supplemented with 30  $\mu\text{g/ml}$  Furazolidone. Cells were grown aerobically at 37°C.

We also investigated the role of EPS against the antimicrobial compound nisin at different concentrations. *L. johnsonii* was able to grow at up to 250 ng/ml nisin (Figure 6.6) and we conducted the growth comparison of wild type and mutant strains at this nisin concentration.

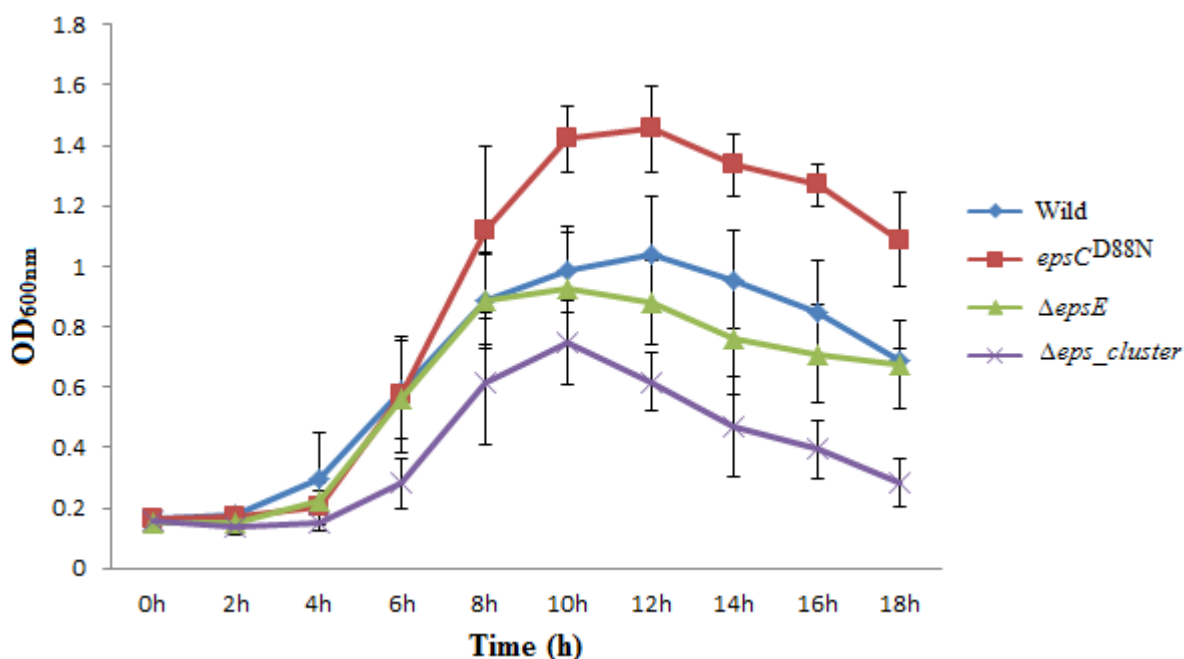


**Figure 6.6.** Growth curve of wild type, *epsC*<sup>D88N</sup>,  $\Delta epsE$  and  $\Delta eps\_cluster$  mutant strains of *L. johnsonii* in MRS supplemented with 250 ng/ml nisin. Cells were grown aerobically at 37°C.

Interestingly, the higher EPS producer *epsC*<sup>D88N</sup> mutant exhibited a significantly higher growth rate and reached a higher end-point of OD<sub>600nm</sub> compared to the wild type and other mutants (Figure 6.6). In contrast, the growth rate of non-EPS producer  $\Delta eps\_cluster$  mutant

was significantly lower than wild type and other strains as a result of the acapsular phenotype (Figure 6.6). The accumulation of EPS-1 at the cell surface of  $\Delta epsE$  mutant resulted in similar growth profile in comparison to the wild type although there was a slight reduction in its survival. Similarly  $\Delta epsE$  mutant showed slightly higher growth rates than acapsular mutant and reached a higher end-point of OD<sub>600nm</sub>. These results show that EPS layer has a protective role against the antimicrobial compound nisin.

### 6.3.2 Protective role of EPS layer in cell survival under stress conditions

In order to understand the physiological role of EPS layer under temperature and acid stress conditions, heat and acid shock experiments were performed. *L. johnsonii* is a probiotic organism and production of probiotic supplements includes several technical applications such as high temperatures, temperature changes and mechanical damages which may cause loss of viability of probiotic bacteria. So, we assessed the heat stress tolerance of *L. johnsonii* wild type,  $epsC^{D88N}$ ,  $\Delta epsE$  and  $\Delta eps\_cluster$  mutant cells by exposing them to 50°C and 60°C for 5 min and survival of *L. johnsonii* strains were monitored by CFU counts on MRS plates.

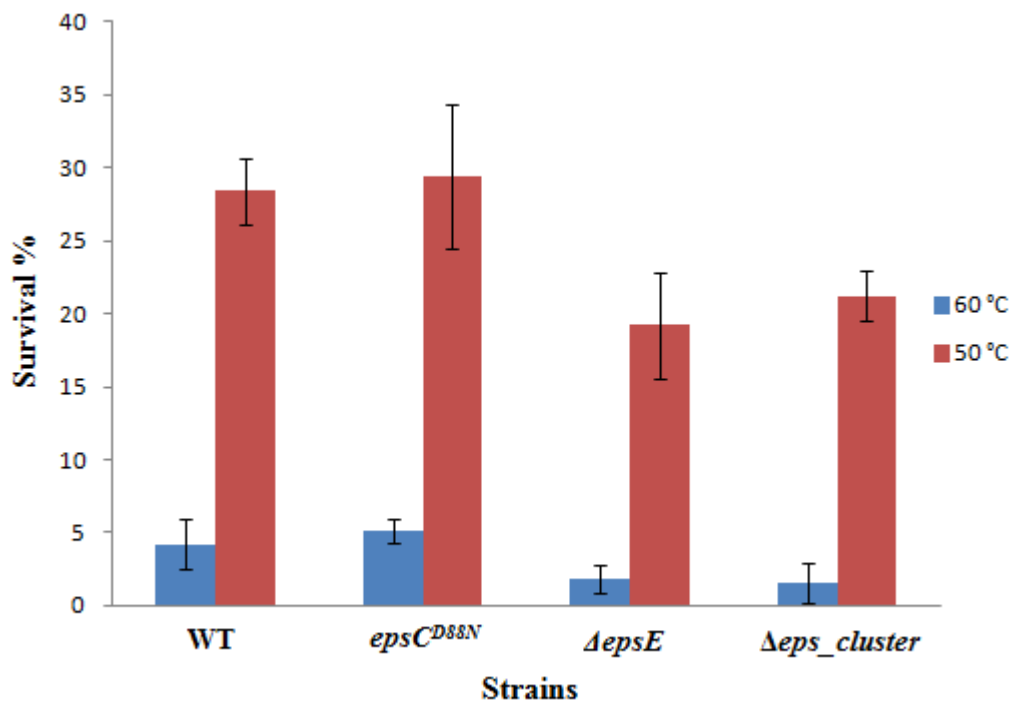


**Figure 6.7.** Percentage of survival of *L. johnsonii* strains after a 5-min heat shock at 50°C and 60°C. 100% represents approximately 10<sup>8</sup> CFU for each strain.

The results demonstrated that there was no difference in survival between wild type and  $epsC^{D88N}$  mutant following 5 min of heat shock at 50°C and 60°C (Figure 6.7). However, there was a reduction in the survival of  $\Delta epsE$  and  $\Delta eps\_cluster$  mutant strains compared to

wild type and *epsC*<sup>D88N</sup> mutant. Similarly, the survival of  $\Delta epsE$  and  $\Delta eps\_cluster$  mutant strains was similar which indicates there was no additional effect of EPS-1 accumulation in the survival of *L. johnsonii* under high temperature conditions.

The ability of probiotics to survive in the low pH of stomach is essential in order to pass through the GIT before their colonisation. Wild type and mutant strains were exposed to the pH 2.0 for 90 min. Viability after the acid shock was monitored using CFU counts (Figure 6.8).

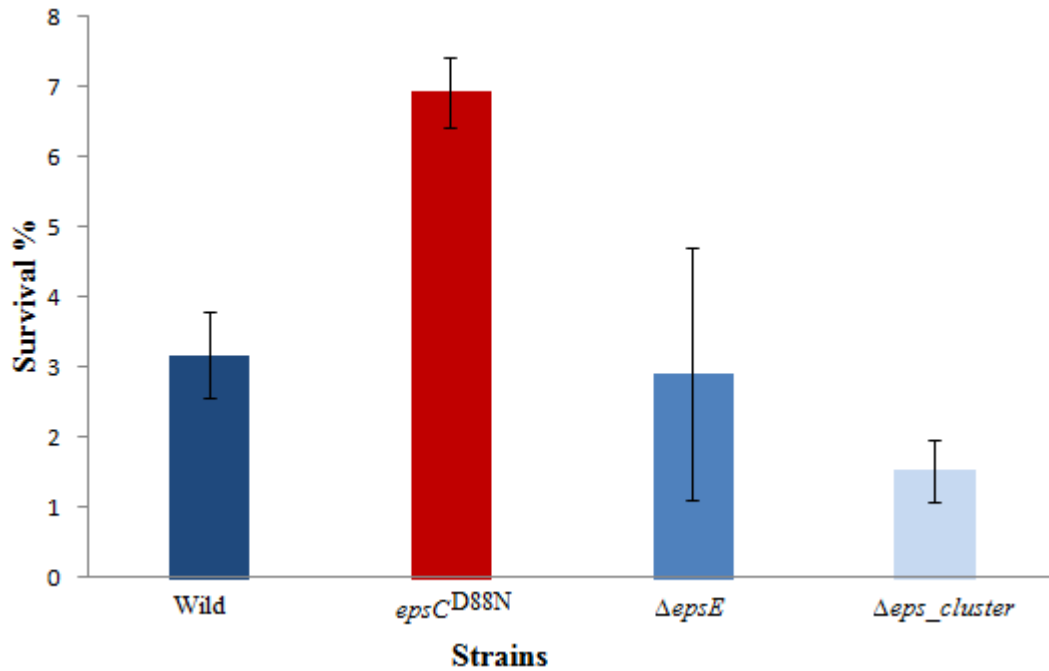


**Figure 6.8.** Percentage of survival of *L. johnsonii* strains after a 90 min exposure to pH 2. 100% represents approximately  $10^8$  CFU for each strain.

As can be seen in Figure 6.8, nearly double amounts of *epsC*<sup>D88N</sup> mutant cells survived after acid shock in comparison to wild type due to the more EPS accumulation at the cell surface. However there was no large difference between wild type and EPS-1 only producer  $\Delta epsE$  mutant in terms of survival after acid shock (Figure 6.8). In contrast the survival percentage of  $\Delta eps\_cluster$  was around 1.5% which was significantly decreased compared to the wild type due to the loss of the entire EPS layer. Overall, these results show the protective role of EPS layer under low pH and high temperature conditions.

### 6.3.3 Survival in bile salts and simulated *in vitro* digestion

To investigate the relationship between EPS production and survival in bile salt environments, the growth profiles of the wild type, *epsC*<sup>D88N</sup>,  $\Delta epsE$  and  $\Delta eps\_cluster$  mutants were monitored at 37°C for 24 h. As in to the other conditions tested, the EPS layer

was also protective against bile salts (Figure 6.9). The growth profile of the wild type and higher EPS producer strain the *epsC*<sup>D88N</sup> mutant was similar in this bile salts concentration. In contrast, the growth rate of  $\Delta epsE$  mutant was significantly decreased due to the reduced EPS layer in this mutant in comparison to the wild type. Furthermore, the lowest OD<sub>600nm</sub> values were detected for  $\Delta eps\_cluster$  mutant emphasizing the essential role of the EPS layer in protection against bile salts.

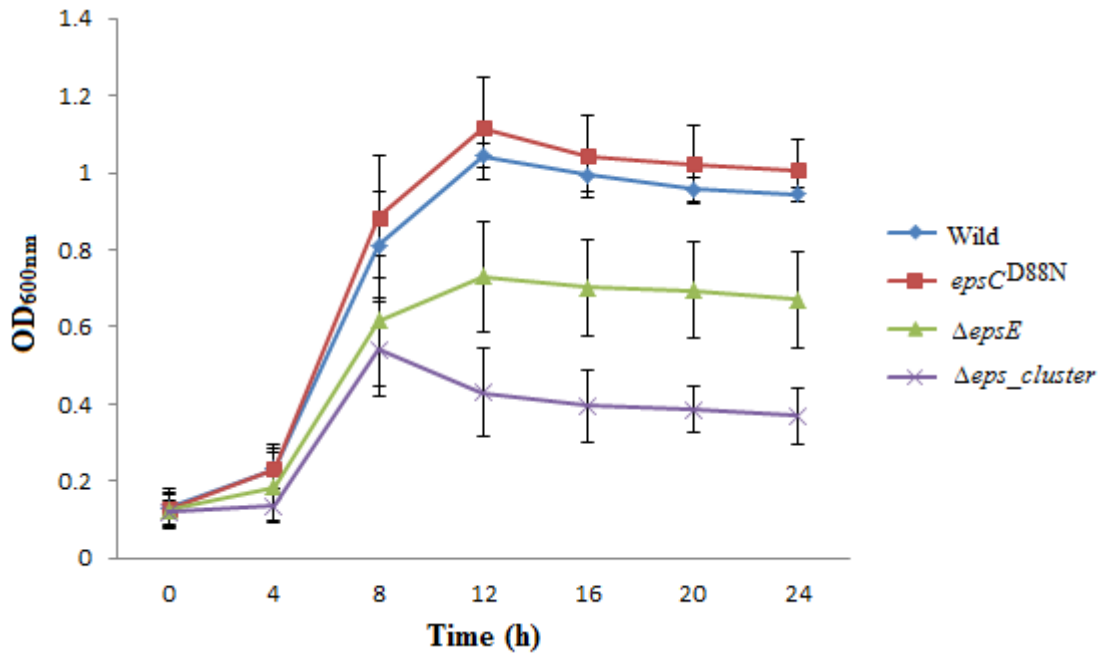


**Figure 6.9.** Growth curve of wild type, *epsC*<sup>D88N</sup>,  $\Delta epsE$  and  $\Delta eps\_cluster$  mutant strains of *L. johnsonii* in MRS supplemented with 0.3% bile. Cells were grown aerobically at 37°C.

The ability to survive in the GIT is one of the crucial characteristics required for probiotic bacteria. In order to understand the role of the EPS layer in passage through the GIT an *in vitro* digestion test was performed. The survival rate of *L. johnsonii* was around 20% after the *in vitro* digestion conditions (Figure 6.10). The survival of the *epsC*<sup>D88N</sup> mutant was slightly increased indicating the protective role of EPS layer under these conditions (Figure 6.10). Similar to the acid shock results there was no difference in the survival rate of wild type and  $\Delta epsE$  mutant under *in vitro* digestion therefore the accumulation of EPS-1 on cell surface of *L. johnsonii* was still providing a protective role. In contrast the lack of the EPS layer in  $\Delta eps\_cluster$  mutant resulted in only 10% survival rate which was half of the survival rate of wild type.

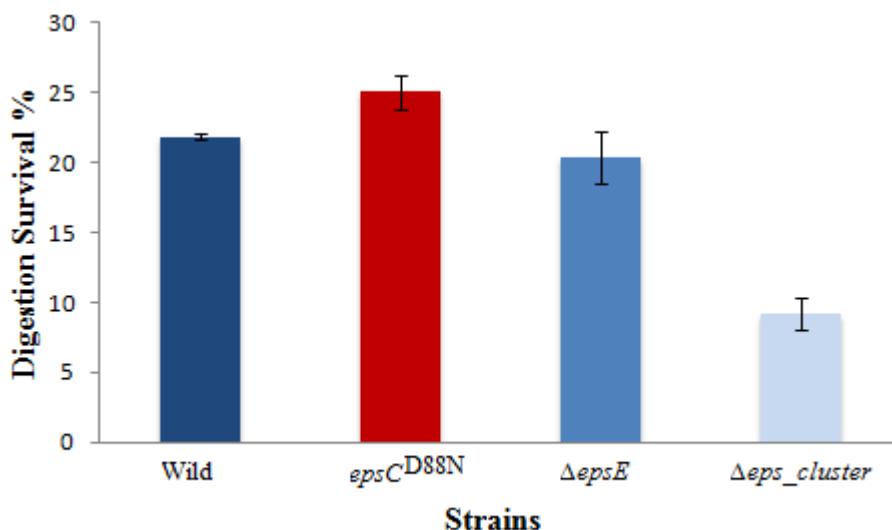


**Figure 6.10.** Percentage of survival of *L. johnsonii* strains after the *in vitro* digestion conditions. 100% represents approximately  $2 \times 10^8$  CFU for each strain.

These results clearly showed the protective effect of the EPS layer against bile salts and under *in vitro* digestion conditions.

#### 6.3.4 Colonisation analysis of wild type and mutant cells in mice model

In order to establish the role of EPS accumulation in colonisation ability and persistence of *L. johnsonii* under *in vivo* conditions, wild type and *eps* mutant strains were tested in a mouse model system. Due to the variability of results during the experimental models, the mice study was repeated three times to optimise the detection of *L. johnsonii* cells by altering the antibiotic selection as described in section 6.2.4. The first period of the study was the preliminary analysis of *L. johnsonii* strains which was conducted with the wild type, *epsC*<sup>D88N</sup>,  $\Delta epsE$  and  $\Delta eps\_cluster$  mutants with three mice per strain over 21 d after dosing mice with these strains for three consecutive days. The preliminary data confirmed the presence of the *L. johnsonii* strains in the murine GIT as we recovered *L. johnsonii* colonies from the faecal materials until day 21 and the identity of *L. johnsonii* was confirmed by colony PCR analysis (data not shown). But in terms of comparing the wild type and mutant colonies, the data were a bit problematic due to the other colonies that were also resistant to neomycin and morphologically similar to the *L. johnsonii* colonies, which were already abundant in the GIT of mice. We might have distinguished the *L. johnsonii* strains by colony PCR but it did not succeed always with a positive band even in the positive control sample due the accumulation of lactic acid after 2 d of growth (personal communication, Dr Melinda Mayer IFR). So, it was not possible to count individual *L. johnsonii* colonies and compare them to understand the role of EPS on persistence and colonisation of *L. johnsonii*. Similarly

we could not distinguish the colonies recovered from the intestinal organs of the mice at the end of this period of study. Nevertheless, the first period of mouse experiments demonstrated the presence of *L. johnsonii* colonies in the faeces for a period of time.

The second mouse experiment was repeated with the selection of *L. johnsonii* strains using a chloramphenicol resistance marker to eliminate the other *Lactobacillus* species that were already presented in the GIT of mice. The second period of the study was performed with wild type containing pFI2431, *epsC*<sup>D88N</sup>::*pepsC* and  $\Delta$ *eps\_cluster* mutants which were carrying the *CAT* resistance gene. After dosing the mice with these strains bacteria were recovered from faecal pellets by plating dilutions of these pellets on MRS + chloramphenicol plates. Interestingly, we could not recover any colonies from *epsC*<sup>D88N</sup>::*pepsC* strain even in day 3 (data not shown). The plasmid might have been lost from this strain during the passage under harsh conditions which potentially resulted in the absence of this strain on MRS + chloramphenicol plates. Another possibility can be that *epsC*<sup>D88N</sup>::*pepsC* mutant could not resist the harsh conditions although we recovered the wild type and  $\Delta$ *eps\_cluster* mutant from faecal pellets at day 3. The colony counts for wild type and  $\Delta$ *eps\_cluster* mutant at day 3 were  $5.85 \pm 0.07$  and  $5.88 \pm 0.08$  log<sub>10</sub> cfu/g, respectively, whereas there was no colony recovery at day 7 for any of these strains (data not shown). These results suggest that the mouse model might not be a suitable model for *L. johnsonii* FI9785, as it was originally isolated from chicken GIT, or that the dosage given to mice at day 0 was not sufficient for *L. johnsonii* FI9785 in order to colonise mice gut. Also this result was contrary to our previous observation where *L. johnsonii* FI9785 was recovered from mouse faeces at day 21. It can also be due to the chloramphenicol marker as we have seen some phenotypic differences in the *epsC*<sup>D88N</sup> mutant after transformation with pFI2431 (data not shown), or the *in vivo* GIT conditions of mice at this period. Nevertheless, it was observed that there was no difference in the colony numbers of wild type and  $\Delta$ *eps\_cluster* mutant at day 3 which was still informative in order to understand the role of EPS in passage and short term residence under *in vivo* conditions. We also isolated the total DNA from bacterial pellets of control and treatment groups of day 0 and day 7 samples (Figure 6.13) and subjected it to 454 phylogenetic analyses in order to understand the effect of dosing mice with EPS<sup>+</sup> and EPS<sup>-</sup> *L. johnsonii* strains on the mice microbiota which will be discussed later.

The last period of the mouse study was planned in order to understand the role of the EPS layer accumulated at the cell surface of *L. johnsonii* in survival during the passage and persistence in the mice model using the wild type containing pFI2431 (*CAT* resistance) and

the  $\Delta eps\_cluster$  mutant. In general, there was a fluctuation in the of number colonies recovered at each time point during the 4 days of experimental period due to dosing mice with *L. johnsonii* strains for 3 consecutive days (Figure 6.11). Also, some variations in the faecal counts between individual mice were observed probably due to the differences in the transit time of *L. johnsonii* strains in individual mice. In the first time point after the oral gavage the number of the  $\Delta eps\_cluster$  mutant colonies was slightly lower than the wild type colony numbers. The number of colonies of both wild type and  $\Delta eps\_cluster$  mutant dropped nearly 1 log<sub>10</sub> unit 24 h after the first gavage but in contrast to the 6 h samples the number of the  $\Delta eps\_cluster$  mutant colonies was similar to the wild type colony numbers (Figure 6.11). At time 32 h, the numbers of colonies for both strains were increased around 2 log<sub>10</sub> units due to the second oral dosage, but there was no difference in the numbers of wild type and  $\Delta eps\_cluster$  mutant. Similar fluctuations were observed for 48 h and 54 h samples with no difference in colony numbers of wild type and  $\Delta eps\_cluster$  mutant. There was however, a slight increase in the number of the  $\Delta eps\_cluster$  mutant colonies compared to the wild type colony numbers at the end of the experimental period. Overall, no significant reduction in the number of  $\Delta eps\_cluster$  mutant strain was observed during the 4 days of experimental period. These results show that the loss of the EPS layer in this mutant did not affect its survival and persistence in the mouse model system.

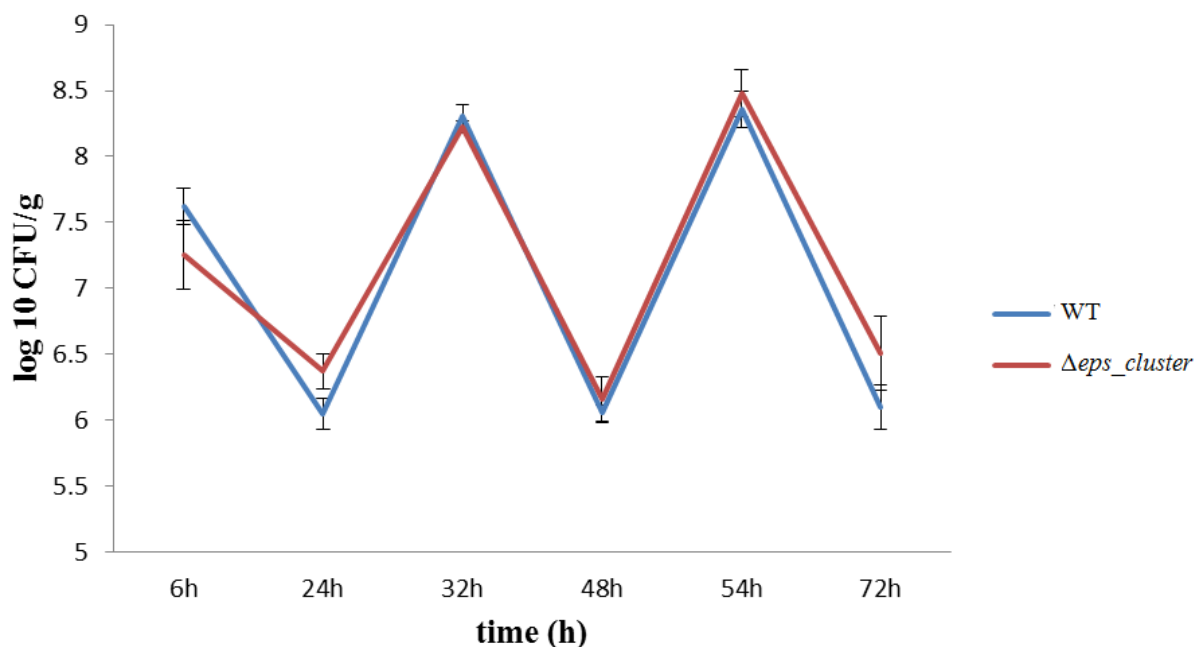


**Figure 6.11.** C57BL/6 mice were treated orally with  $5 \times 10^8$  CFU of wild type and  $\Delta eps\_cluster$  mutant strain on 3 consecutive days (0, 24, 48 h) and bacterial numbers (CFU) in faecal material were determined at each time point (Data represent log<sub>10</sub> of colony counts  $\pm$  SD, n=5).

In order to understand the interaction between the presence of the *L. johnsonii* cells in the faeces and the *in vivo* adhesion properties, the last experimental group of mice were sacrificed 48 h after the last gavage and tissue samples were collected from small intestine, caecum and colon of mice GIT and replica-plated to MRS plates supplemented with chloramphenicol. Interestingly, *L. johnsonii* cells were undetectable in the small intestine by viable counts (data not shown) but colonies were recovered from caecum and colon samples although the numbers were significantly lower than the recovery of the colonies from faecal samples (Figure 6.12). The results demonstrated that although there was a slight increase in the numbers of  $\Delta eps\_cluster$  mutant cell numbers in both caecum and colon samples compared to the wild type but this increase was not statistically significant (Figure 6.12), supporting the observations from the studies with faecal samples.

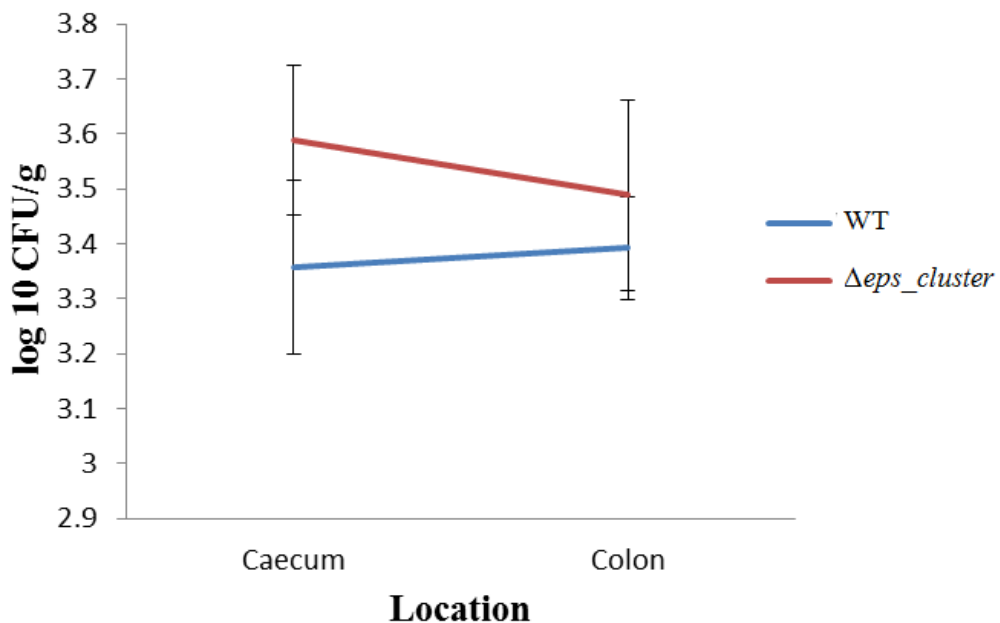


**Figure 6.12.** C57BL/6 mice were treated orally with  $5 \times 10^8$  CFU of wild type and  $\Delta eps\_cluster$  mutant strain on 3 consecutive days and mice were sacrificed 48h after the last gavage and the bacterial numbers (CFU) in caecum and colon samples were determined (Data represent  $\log_{10}$  of colony counts  $\pm$  SD, n=5).

Unfortunately, the colonisation experiments in mice model were not conclusive therefore it was not pursued further.

### 6.3.5 Role of EPS layer on gut microbiota alterations

In order to understand the effect of dosing the mice with EPS<sup>+</sup> and EPS<sup>-</sup> *L. johnsonii* on the overall mice gut microbiota with respect to the role of EPS, total DNA was isolated from control and treatment groups of the second experimental period samples at day 0 and day 7 (Figure 6.13) and total bacterial community analysis was performed by clustering the control and treatment samples according to their bacterial taxonomy as found by the Qiime analysis.

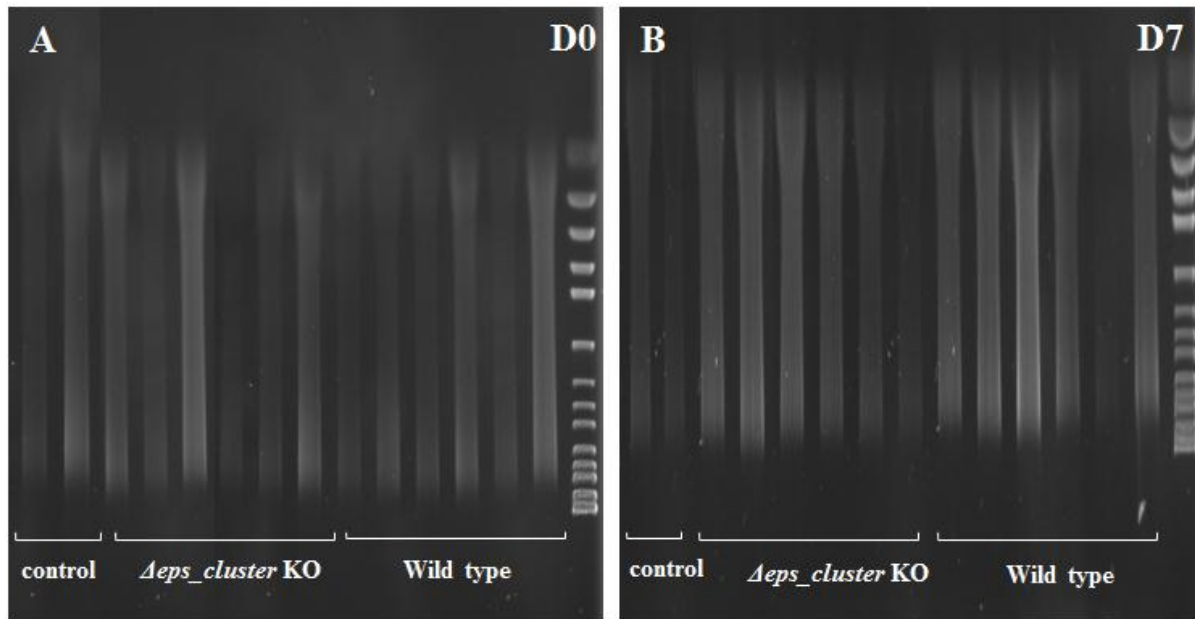


**Figure 6.13.** Agarose gel showing the isolation of the total DNA from the faecal materials collected from control mice group (no *L. johnsonii* inoculation, 2 mice),  $\Delta eps\_cluster$  mice group (received *L. johnsonii*  $\Delta eps\_cluster$  mutant, 6 mice) and wild type mice group (received *L. johnsonii* wild type, 6 mice) at day 0 (A) and day 7 (B) after inoculation.

In total six bacterial phyla were identified in pooled libraries before the treatments in faecal samples where Gram positive *Firmicutes* and Gram negative *Bacteroidetes* established nearly 60% and 35% of the bacterial community, respectively (Figure 6.14). Although there was not a huge diversity in mice microbiota before dosing with *L. johnsonii*, phylum *Firmicutes* where genus *Lactobacillus* belongs was the most abundant group in mice faecal materials (Figure 6.14). However the intake of *L. johnsonii* did not result in a further increase in the relative abundance of phylum *Firmicutes* in mice microbiota from treated groups whereas there was a spontaneous increase in the proportion of this phylum in control samples (Figure 6.14).

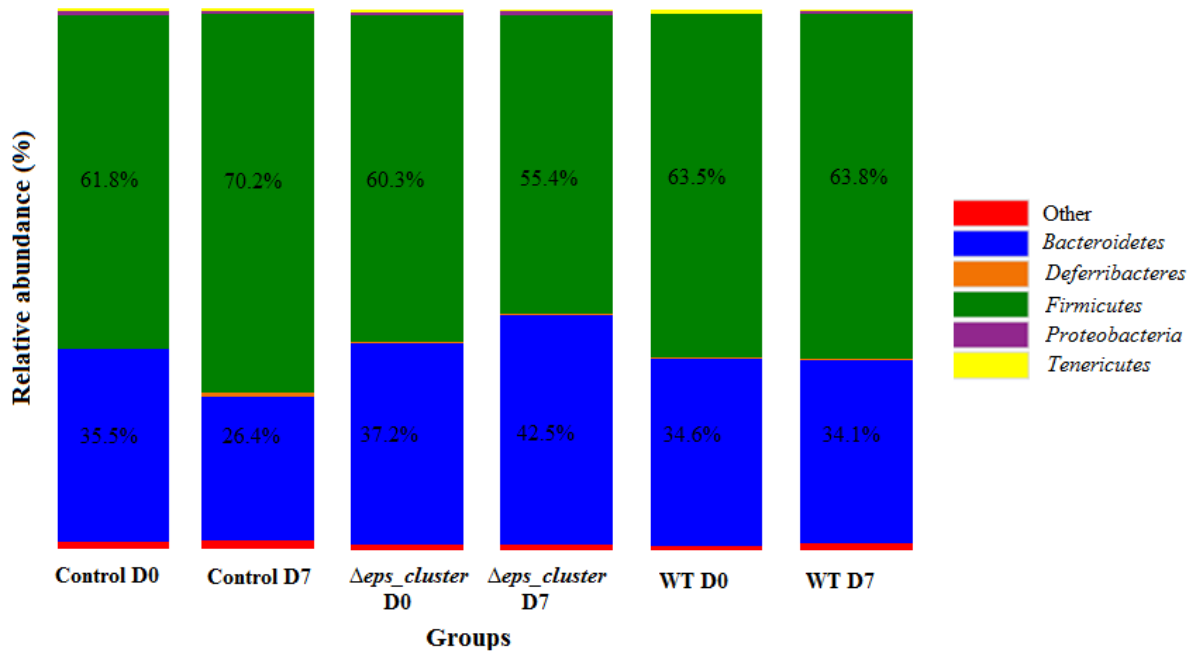


**Figure 6.14.** Relative abundances of bacterial phylums determined by 454 pyrosequencing of the V4 and V5 regions of 16S rRNA gene in fecal bacterial DNA from control mice group (no bacterial inoculation, 2 mice),  $\Delta eps\_cluster$  mice group (received *L. johnsonii*  $\Delta eps\_cluster$  mutant, 6 mice) and wild type mice group (received *L. johnsonii* wild type, 6 mice) at day 0 and day 7 after inoculation.

Comparison of the abundances of the bacterial order in the mice microbiota before and after the treatment showed some alterations related to the intake of *L. johnsonii* strains, though several trends were observed (Figure 6.15). Although all day 0 samples as a control demonstrated the same bacterial orders in the microbial community, the relative abundances of these groups were significantly different. Interestingly, the proportion of order *Lactobacillales* in day 7 faecal samples of the  $\Delta eps\_cluster$  mice group increased around 33% in comparison to the day 0 samples due to the intake of *L. johnsonii*  $\Delta eps\_cluster$  mutant whereas there was a 15% reduction in the proportion of the *Lactobacillales* order in day 7 samples of the wild type mice group which suggested that the intake of wild type did not result in the proliferation of this order (Figure 6.15). Although there was no difference in the colony numbers of wild type and  $\Delta eps\_cluster$  mutant in treatment groups at day 3 samples, the enrichment of the *Lactobacillales* was only observed for the  $\Delta eps\_cluster$  mice group. The only difference in these groups is the presence of the EPS layer in wild type and this may explain the non-altered *Lactobacillales* numbers in wild type treated mice group which might be due to the potential proliferation of an order related to use of EPS as a nutrient. Nevertheless, there were also some common alterations in the bacterial communities of both treated groups which were not observed in the control group where no *L. johnsonii*

was received (Figure 6.15). An important observation in both treatment groups was the suppression of the order *Clostridiaceae* which comprises several genera including *Clostridium* in the mice microbiota whereas the abundance of this order increased nearly 40% in the control group (Figure 6.15).

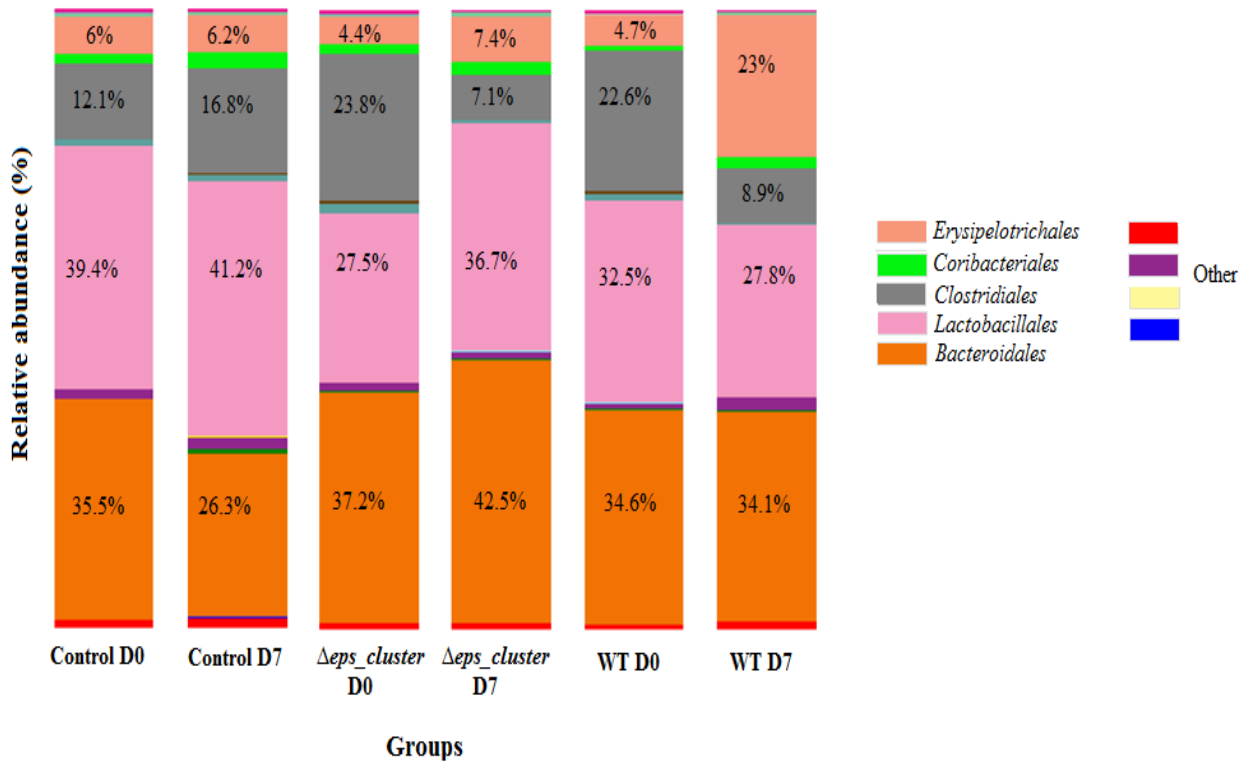


**Figure 6.15.** Relative abundances of bacterial orders determined by 454 pyrosequencing of the V4 and V5 regions of 16S rRNA gene in fecal bacterial DNA from control mice group (no bacterial inoculation, 2 mice),  $\Delta eps\_cluster$  mice group (received *L. johnsonii*  $\Delta eps\_cluster$  mutant, 6 mice) and wild type mice group (received *L. johnsonii* wild type, 6 mice) at day 0 and day 7 after inoculation.

The intake of *L. johnsonii*  $\Delta eps\_cluster$  mutant and the wild type reduced the proportion of the *Clostridiaceae* order approximately 70% and 60%, respectively. This was in agreement with the fact that probiotic bacteria may alter the gut microbiota in order to exclude specific microorganism groups especially pathogenic organisms. However the reduction of this order was observed both EPS<sup>+</sup> and EPS<sup>-</sup> *L. johnsonii* strains suggesting there was no specific effect of the EPS accumulation on this process. Similarly, the proportion of the order *Erysipelotrichales* increased only 68% in the  $\Delta eps\_cluster$  mutant treated group in one week period where this increase was around 6 times in mice group that received the wild type cells. There was no alteration in the proportion of this order in the control group (Figure 6.15). The proportion of the Gram negative order *Bacteroidales* decreased in the control group in one

week period while there was an increase of around 15% in this order in the *Δeps\_cluster* mutant mice group. In contrast the proportion of this group did not change in one week period for the wild type mice group (Figure 6.15). Although there was no colony recovery from day 7 samples in both groups the overall microbiota altered due to the intake of *L. johnsonii* strains (Figure 6.15). Additionally the microbiota analysis of the faecal samples confirmed the high abundance of *Lactobacillales* in mice microbiota which caused some unexpected problems during the colony recovery using neomycin as a selection marker. It was also interesting to find out that even in 6-8 weeks period the microbiota of mice have been formed with a clear diversity. Overall these results suggest that there was no clear effect of EPS production in *L. johnsonii* in terms of *in vivo* passage and persistence. Similarly there was not a huge difference between the wild type and the *Δeps\_cluster* mutant treated group in terms of microbiota alteration though several different patterns were observed.

#### 6.4 DISCUSSION

Cell surface associated EPS are thought to be crucial for the protection of cells against desiccation, antibiotics, bacteriophages, metal ions, antimicrobials, osmotic stress, phagocytosis, macrophages due to their function as a capsular layer [10, 139, 140]. Similarly, the role of the cell surface associated EPS from commensal bacteria on host-bacteria interactions related to immune functions and colonisation have been shown for several bacteria as we discussed in Chapter 1. Furthermore, EPS were shown to be protective under harsh conditions such as acidic environments and presence of bile salts [66]. In this study, we used the wild type which produces EPS-1 and EPS-2 as an EPS layer, the *epsC*<sup>D88N</sup> mutant which also produces both EPS with a higher level of accumulation than the wild type, the *ΔepsE* mutant as EPS-1 only producer and the *Δeps\_cluster* mutant strain as non-EPS producer strain to investigate the potential protective role of the EPS layer of *L. johnsonii* against different antibiotics and nisin as an antimicrobial compound and to investigate the role of the EPS layer for cell integrity of *L. johnsonii* under different environmental conditions. Furthermore, we tested the role of the EPS layer on the survival of *L. johnsonii* under *in vitro* GIT mimicking conditions and against bile salts. Finally, we analysed the role of EPS layer in passage and persistence of *L. johnsonii* under *in vivo* conditions using a mouse model.

The surface polysaccharides of the Gram negative cell envelope as an outermost layer such as LPS directly interact with the surrounding environment and play a crucial role in response to different molecules including antibiotics [294]. It was reported that LPS in Gram negative

cell envelope reduces the permeability of the hydrophobic antibiotics on the outer membrane probably due to its role in cell hydrophilicity and the presence of LPS results in the increase of the resistance to these antibiotics [294]. EPS of *L. johnsonii* also constitute an outer layer and play an important role in cell surface hydrophobicity and an increase in the EPS layer resulted in an increase in cell surface hydrophilicity as we previously reported (Chapter 4). Furthermore, the availability of different mutants with different degree of EPS enabled us to test the role of this layer in antibiotic resistance. Several antibiotics were tested but *L. johnsonii* showed no resistance to chloramphenicol, rifamycin, vancomycin and erythromycin. Previously, *L. plantarum* and *L. casei* strains were shown to be resistant to vancomycin and several *L. lactis* strains were shown to be resistant to rifampicin but none of the LAB tested were resistant to chloramphenicol, erythromycin and tetracycline [295]. In this study the presence of the antibiotic resistance genes for different antibiotics to which bacteria were shown to be resistant were analysed, but in general the antibiotic resistance genes were not detected and the authors proposed that the antibiotic resistance in these bacteria were due to their intrinsic resistance to these antibiotics [295] which is one of the mechanisms of bacteria to resist antibiotics [296]. *L. johnsonii* showed resistance to ampicillin, tetracycline and furazolidone in a dose dependant manner. When we ran the BLAST analysis for related antibiotic genes for their presence in the genome of *L. johnsonii* FI9785, we found a putative tetracycline gene, *FI9785\_97* which encodes for a putative tetracycline resistance protein, but there was no sign for the presence of antibiotic resistance genes for ampicillin and furazolidone according to BLAST analysis. These suggest that for the latter antibiotics *L. johnsonii* shows an intrinsic resistance property. The antibiotic susceptibility analysis for *L. johnsonii* strains demonstrated that EPS was a protective factor against those antibiotics.

Ampicillin, which is a hydrophilic compound, like several other antibiotics damages the bonds between the polymers which constitutes the cell wall of bacteria which results in cell lysis [297]. Although more EPS layer covered the *epsC*<sup>D88N</sup> mutant, resulting in more hydrophilicity, this mutant was more resistant to ampicillin than the others. It can be proposed that the EPS layer was sufficient enough to protect the cells from the penetration of the ampicillin to the cell wall molecules rather than hydrophilic interactions. Another antibiotic molecule which EPS also showed protection against was tetracycline, which is a hydrophobic antibiotic that blocks a lot of enzymatic reaction in cell metabolism especially in protein biosynthesis [298]. As mentioned above *L. johnsonii* FI9785 harbours a putative tetracycline resistance gene but the presence of the EPS layer increased the resistance ratio to

this antibiotic which can be related to the role of hydrophilic EPS in order to decrease the permeability of the hydrophobic tetracycline to the cell surface. EPS prevented the passage of the active tetracycline molecules to the cytoplasm of *L. johnsonii* which resulted in an increased growth in the *epsC*<sup>D88N</sup> mutant in comparison to the  $\Delta$ *eps\_cluster* mutant. *L. johnsonii* was also grown in the presence of furazolidone which is also a hydrophobic antibiotic that cross-links with DNA that causes the lysis of the bacterial cells [299]. The potential mechanism of EPS for furazolidone resistance can be similar to its contribution for tetracycline resistance however the concentration of the furazolidone that *L. johnsonii* was able to grow was higher than the other antibiotics tested, probably related to its structure and the low molecular weight of this antibiotic than others. Previously, it was reported that negatively charged EPS produced by *Lactococcus lactis* did not show any protective effect against antibiotics penicillin and vancomycin [139]. Nevertheless, the authors suggested that EPS can prevent the passage of active antibiotics to the cell cytoplasm which can be the role of EPS in protection against different antibiotics [139]. Based on our observations, we can also suggest that EPS as an outer layer can be a protective factor against different antibiotics. The mechanism behind this protection can be related to the physicochemical characteristics of the cell surface in which EPS is a crucial factor and it can also be related to the level of EPS accumulation as a barrier to prevent the penetration of antibiotics to the cell wall. A recent report demonstrated that surface polysaccharides of *Campylobacter jejuni* contribute to resistance to the hydrophobic antibiotic erythromycin due to their role in increasing the surface hydrophobicity [300]. Future studies are required to investigate the molecular mechanism of interactions between EPS and antibiotic substances and AFM can be a powerful tool for this aim.

Similarly, the EPS layer of *L. johnsonii* was protective against the bacteriocin nisin which is a positively charged small antimicrobial peptide produced by *L. lactis* strains, that is active against a wide range of Gram positive bacteria [139]. Nisin inhibits the bacterial growth by targeting the permeabilisation of the cytoplasmic membrane which results in leakage of the crucial cytoplasmic components to the outside of the cell and causes lysis of the cell [301]. The presence of the EPS layer as well as its increased accumulation in *L. johnsonii* cells resulted in protection against nisin. Previously, the protective role of the EPS layer against nisin was also reported for the *L. lactis* NZ4010 strain. The authors suggested that the EPS produced by *L. lactis* NZ4010 was negatively charged due to the presence of the phosphate groups in its structure which was proposed to be the main reason for the protection of the EPS molecule against positively charged nisin: the negatively charged EPS cleaned the

positively charged nisin from the cell surface of bacteria [139]. We also showed that negatively charged molecules dominated the cell surface of *L. johnsonii* together with EPS but the increase in the EPS layer in *epsC*<sup>D88N</sup> mutant provided a positively charged nature as we reported in Chapter 4. Furthermore, negatively charged molecules dominated the cell surface of the  $\Delta epsE$  mutant as a result of the reduction in the EPS layer but the decrease of the growth in the presence of nisin increased in this mutant. Taken this together, we suggest that the negative charge of the EPS can be a factor for the protection against nisin as proposed previously but the role of the EPS layer of *L. johnsonii* was probably due to its inhibition for nisin to penetrate to the cell wall and due to its blocking effect to nisin in order to bind to the membrane components of *L. johnsonii*. Overall, the EPS layer gives the advantage to *L. johnsonii* to grow in the environments containing antimicrobials such as nisin.

Another physiological role of cell surface associated EPS is their protective role under harsh conditions such as temperature changes, acid and bile conditions. Our results confirmed the protective role of EPS against high temperatures when the higher EPS producer *epsC*<sup>D88N</sup> mutant and non-EPS producer  $\Delta eps\_cluster$  mutant were compared. There was no difference between wild type-*epsC*<sup>D88N</sup> and  $\Delta epsE$ - $\Delta eps\_cluster$  mutants, possibly due to the shortness of duration of the heat shock which was not enough to record the difference among strains. Previously, it was reported that there was no difference in the viability of *L. johnsonii* NCC 533 strains which have different membrane composition due to the shortness of the heat application period [273].

Gastric acidity is one of the most important antimicrobial stress factors affecting the survival and colonisation properties of probiotics inside the host [20, 302, 303]. Previously it was reported that there was no difference between the survival of the *L. rhamnosus* GG and its mutant which lacks the galactose rich EPS on its surface, during the acid shock application for 30 min and 90 min, respectively [67]. In fact, our results also support this finding; there was no difference in the survival of wild type and the  $\Delta epsE$  mutant strain which also lacks the galactose rich EPS on its surface. But based on their results, the authors proposed that EPS does not give any advantage to cells in terms of their survival ability under gastric conditions [67] which is not the fact when we look the whole picture. The survival rate of the *epsC*<sup>D88N</sup> mutant under the gastric conditions was around 4 times higher than the non-EPS producer strain of  $\Delta eps\_cluster$  mutant which clearly indicates the protective role of the EPS layer. Based on our data we can confirm the protective role of the EPS layer under the low pH conditions.

The probiotic bacteria also have to overcome bile salts that are one of the biological barriers in the GIT that probiotic bacteria has to resist [304]. In this study we found that EPS layer of *L. johnsonii* can be protective against bile salts. EPS layer provides tolerance to the bile salts which is an adverse environmental condition found in the GIT. Recent reports also confirm that EPS are protective against bile salts environment [66, 281]. Furthermore, a recent study reported that bile salts stimulated the EPS production in a *Bifidobacterium animalis* strain which indicates a clear strategy of probiotic bacteria in order to increase its resistance to the harsh environments [305].

The survival ability of probiotic bacteria during their passage through the upper digestive tract in order to reach the colon where they are expected to show beneficial effects to their host is prerequisite for the probiotic action [302, 306]. If probiotic bacteria survive after their exposure to the gastric acid and bile conditions, another requirement to show their probiotic effects is their adherence ability to the intestinal mucosa and mucus layer for colonisation to protect their removal from the colon by peristalsis [286]. Previously, we have reported the role of the EPS layer in adhesion to the colon cells *in vitro*: the reduction or the absence of the EPS layer increased the adherence ability of *L. johnsonii* and vice versa. But as mentioned above, before the adherence to the colon cells *L. johnsonii* should survive under the gastric acidity, pepsin and pancreatin conditions. In order to understand the role of EPS layer under these conditions we performed an *in vitro* simulated digestion analysis for wild type and mutant strains. The comparison of the survival of the *epsC*<sup>D88N</sup> mutant and the  $\Delta$ *eps\_cluster* mutant clearly demonstrated that the EPS layer increased the survival capacity of *L. johnsonii*. But this effect was not clear when we compare wild type and  $\Delta$ *epsE* mutant which suggests the presence of the EPS-1 layer alone can still be protective under these conditions, although the thickness of the EPS layer is reduced. Nevertheless, the *in vitro* conditions do not always mimic the *in vivo* conditions, for this reason we investigated the role of the EPS layer of *L. johnsonii* in a mouse model.

Although *L. johnsonii* FI9785 was originally isolated from chicken GIT, the *in vivo* experiments were conducted in a mouse model due to the accessibility of the mouse model system and previous studies also showed the colonisation of the *L. johnsonii* FI9785 to the mouse GIT (personal communication, Dr Arjan Narbad IFR). Unexpectedly the mice experiments were problematic for long term colonisation studies but we managed to investigate the role of EPS layer on the persistence and passage of *L. johnsonii* FI9785. There was no difference between the wild type and acapsular  $\Delta$ *eps\_cluster* mutant in terms of persistence and passage through the mice GIT during the 3 days of the experimental period.

This result was contrary to our *in vitro* observations where the survival rate of the wild type was higher than the acapsular mutant. Previously, it was reported that the loss of the EPS layer in *L. johnsonii* NCC 533 slightly increased the gut persistence time of this strain and the authors proposed that this would even be expected due to the removal of the negatively charged EPS molecules which might have increased the binding of this strain to the receptors on the mucosal membrane [62]. The *in vitro* adhesion of *L. johnsonii* FI9785 to the human colonic cells and its autoaggregation significantly increased after the loss of the EPS layer which was in agreement with the proposed mechanism of EPS on the increased gut persistence of *L. johnsonii* NCC 533 but there was no difference in the recovery of wild type and  $\Delta eps\_cluster$  mutant from colon and caecum samples. It should be noted that we could not recover any *L. johnsonii* FI9785 from the small intestine; this part of the GIT has been reported to have limited bacterial numbers and diversity due to the fast transit time and continuous digestive secretions such as bile acids [307]. Nevertheless, our *in vitro* survival tests exposed the importance of the EPS layer under harsh and *in vivo* mimicking conditions. The lack of EPS layer might have increased the adhesion of the *L. johnsonii*  $\Delta eps\_cluster$  mutant compared to the wild type but less mutant cells might have survived under the harsh conditions in comparison to wild type cells which might be the reason for the similar persistence rates in mice model. In contrast, Lebeer et al., showed that the accumulation of the long galactose rich EPS on cell surface of *L. rhamnosus* GG promoted the survival and persistence of this strain in the mice GIT compared to the *L. rhamnosus* GG mutant strain which does not have the long galactose rich EPS on its surface [67]. Additionally, it was shown that the production of the homopolymeric fructan in *L. reuteri* 100-23 assisted the colonisation of this strain to the murine GIT compared to the mutant strain which was unable to produce this fructan. Researchers also showed that EPS played a protective role under high sucrose-containing *in vitro* conditions but the *in vivo* biofilm formation properties of wild type and its EPS deficient mutant were indistinguishable [142]. In another study, the EPS production by *B. breve* UCC2003 resulted in 100 - fold increased persistence rate in comparison to the EPS<sup>-</sup> mutant strains in the mice GIT through the 31 days of experimental period but there was no difference in the first 10 days of initial colonisation period for wild type and EPS<sup>-</sup> mutant strains [66]. The authors suggested that the reduction in the numbers of the EPS<sup>-</sup> mutant strains was due to the immune-modulatory effect of EPS, where this layer prevented *B. breve* UCC2003 from its removal by host defence mechanisms [66]. Overall, the early passage and persistence properties of *L. johnsonii* FI9785 was not affected by the EPS layer but to characterise its biological function more studies are required including

colonisation tests and assessing its role in a chicken model where *L. johnsonii* FI9785 was originally isolated. Additionally, drawing a general picture for the *in vivo* role of the EPS layer related to the probiotic action can be too speculative because the structure of the EPS layer in different probiotic strains and its conformation on cell surface is frequently different which results in unique adhesion, colonisation and immune response properties in different bacteria even at strain level.

Although we observed no difference in the recovery of the wild type and EPS<sup>-</sup> mutant strain from mice organs and faeces, we performed microbiota analysis in order to investigate the impact of oral administration of *L. johnsonii* strains on the gut microbiota as well as to investigate the role of the EPS layer. In recent years the regulation of gut microbiota with probiotic bacteria such as *Lactobacillus* and *Bifidobacterium* strains or prebiotic ingredients gained special interest due to the potential roles of gut microbiota in host homeostasis [308]. For instance a recent study showed that administration of *L. johnsonii* N6.2 resulted in the mitigation of the development of type 1 diabetes and the authors suggested that modifying gut microbiota might modulate the development of this disorder [309]. One of the reasons to use probiotics is to modify the gut microbiota to exclude pathogenic bacteria in order to maintain host homeostasis [66]. Gut microbiota can also be modified by the availability of prebiotic fermentable carbohydrates reaching the colon including EPS [308, 310]. To date several prebiotics and their beneficial effects have been shown to increase the populations of desired bacteria in GIT especially bifidobacteria and lactobacilli, but the role of EPS has not been determined yet to the same extent [308]. Several *in vitro* studies demonstrated that EPS produced by lactobacilli and bifidobacteria could modulate the microbiota in a positive way [144, 310-312] but another *in vitro* study with the EPS from *L. rhamnosus* RW-9595 showed that EPS was not degraded by the infant microbiota although there was a reduction in the lactobacilli and staphylococci counts in comparison to the FOS (Fructooligosaccharide) containing batch cultures [313]. In another study an oat-based product fermented with EPS producer *Pediococcus parvulus* 2.6 stimulated the Bifidobacteria flora in humans whereas this effect was not recognised without EPS which can be due to the usage of EPS as a substrate by different groups of the gut microbiota [314]. Recently, a comprehensive *in vivo* study was conducted with the purified EPS ( $\beta$ -glucan) from *P. parvulus* 2.6 and *P. parvulus* 2.6 cells in order to understand their functional role on gut microbiota in a mouse model [308]. Both purified EPS and the live EPS producing strain altered the mice microbiota but not in a similar pattern. There was no bifidogenic effect of the  $\beta$ -glucan EPS whereas the

Bifidobacteria population decreased in the EPS treated group. But it was shown that there was a significant increase in *Akkermansia* group probably due to the usage of EPS by this group as a substrate [308]. This increase was also detected in the live *P. parvulus* 2.6 group but not in the control group which suggests the role of EPS. Furthermore live *P. parvulus* 2.6 group decreased the *Enterobacteriaceae* group without disturbing the homeostatis of the faecal microbiota which suggests the complexity of the microbiota alterations [308]. We assessed the microbiota alterations with wild type and its EPS deficient mutant in which the microbiota may alter due to the role of the bacterial strain, where the adhesion and strain specific properties can play a role, or the microbiota may alter as a result of the selection pressure of EPS that only presents in wild type treatment group. The microbiota analysis demonstrated that *L. johnsonii* strains did not alter the diversity but there were some differences in the treated groups between them in comparison to the control group. Interestingly, the administration of *L. johnsonii* wild type did not induce an increase in the proportion of *Lactobacillales* order while the proportion of this order in the  $\Delta eps\_cluster$  mutant treated group significantly increased as can be expected. The comparison of these two groups also showed that the proportion of the *Erysipelotrichales* order in the wild type treatment group increased 6 times whereas this increase was not observed in the  $\Delta eps\_cluster$  mutant treated group. The increase in the *Erysipelotrichales* observed in the present study may have resulted from a selection toward the *Erysipelotrichales* by the EPS when used as the substrate. The polysaccharides and fibers including prebiotics within the colon are fermented by gut microbiota which results in the formation of SCFAs such as acetate and butyrate [315]. Previously it was reported that the *Erysipelotrichales* can be a key phylotype that contributes to the separation of the intestinal lumen microbiota in colorectal cancer patients in comparison to healthy individuals and this phylotype is associated with energy metabolism [316]. Similarly this group was also correlated with the butyrate production mainly from polysaccharides within the colon in obese individuals [315]. Overall it can be speculated that the increase in *Erysipelotrichales* in wild type treated group might be related with the role of EPS as a substrate used by this group which resulted in the proliferation of this group in comparison to the EPS<sup>-</sup> samples due to the symbiotic effect of EPS from *L. johnsonii* FI9785. The diverse chemical and structural composition of EPS produced by different bacteria results in various biodegradability properties but to date several homopolymeric and heteropolymeric EPS were reported to be used by several bacteria [317-320] and they were also shown to alter the gut microbiota [308, 320, 321]. It was reported that the glycosidic linkages between the disaccharide molecules could affect the prebiotic

index of different carbohydrates and disaccharides with 1-2, 1-4 and 1-6 glycosidic linkages, of which EPS of *L. johnsonii* FI9785 are composed, was reported to generate a high prebiotic index score compared to the other linkages [322]. Nevertheless it was also reported that EPS can somehow affect the microbiota composition without being degraded [313]. Our observations in microbiota alterations may be related with the EPS but more *in vitro* and *in vivo* studies are required in order to determine the role of EPS, including EPS-1 and EPS-2 from *L. johnsonii* FI9785, with different chemical structures as a carbon source for gut microbiota and individual bacterial groups.

In conclusion, this chapter described the protective role of EPS layer of *L. johnsonii* FI9785 against different antibiotics and antimicrobial nisin, acid and bile salts conditions, temperature changes and mimicking human digestion under *in vitro* conditions. Interestingly, this protective effect was not recognised under *in vivo* conditions as the recovery rate of EPS<sup>+</sup> wild type and EPS<sup>-</sup> mutant strain in early persistence was almost identical in the mice model. Furthermore, an alteration in gut microbiota was also reported which can be influenced by the presence of the EPS.

# Chapter 7

---

**Characterisation of Glycosyltransferases involved in EPS biosynthesis of *L. johnsonii***

## 7.1 INTRODUCTION

The biosynthesis of the EPS repeating unit occurs by the activity of the specific glycosyltransferases (GTFs) encoded in the *eps* clusters of *Lactobacillus* strains for heteropolymeric EPS production or by the activity of a single glycosyltransferase encoded in the genome separately from the *eps* clusters for the homopolymeric EPS production as described in Chapter 1. The substrate specificity, structure and activity of the glycosyltransferases result in unique EPS structures containing different sugar monomers with different glycosidic linkages [10, 89]. To date several glycosyltransferases encoded in the *eps* clusters of LAB have been biochemically characterised for their role in the EPS repeating unit biosynthesis, their sugar specificities and their role in the formation of specific glycosidic linkages between the sugar monomers forming the EPS repeating unit [86, 89, 135]. But the number of the biochemically characterised glycosyltransferases related to EPS repeating unit biosynthesis is still a small proportion of the potential glycosyltransferases available as putative glycosyltransferase genes identified with the genome projects of *Lactobacillus* strains and the projects for the determination of *eps* genes based on their similarity with the identified glycosyltransferases after gene or protein BLAST analysis. Notably, glycosyltransferases cover 1-2% of gene products of bacteria which shows their great abundance in bacterial genomes [92]. The vast majority of the biochemically characterised bacterial glycosyltransferases are from human pathogenic bacteria and their similarity to those from LAB resulted in the identification of several putative glycosyltransferases [323]. In general, glycosyltransferases can be described as an enzyme group which catalyzes the transfer of activated sugar moieties from glycosyl donor molecules to specific acceptor molecules thereby forming an  $\alpha$  or  $\beta$  glycosidic bond depending on the structure of the glycosyltransferases [323, 324]. More detailed information about all the classification and biochemical properties of glycosyltransferases can be found in the CAZY (Carbohydrate-Active enZymes) database at <http://www.cazy.org>. This database includes the classification of the glycosyltransferases into 94 different families based on the amino acid sequence similarities; the number has been growing in recent years due to the application of genomics and in the future this trend will continue [92]. There are several excellent reviews on mechanism, function and structural biology and engineering of glycosyltransferases [92, 323, 325-327] which will not be discussed in detail as it is not the main scope of this thesis.

Glycosyltransferases can be divided into two main groups depending on the donor molecules they use in the glycosyl transfer reaction. The first group is the glycosyltransferases that

belong to the Leloir pathway (sugar nucleotide-dependent) which use the activated sugar nucleotides such as UDP-Glucose and UDP-Galactose as a glycosyl donor. This group is also classified as Leloir enzymes due to the first discovery of the sugar nucleotide by Luis F. Leloir which brought him the Nobel Prize in chemistry in 1970 [92]. The second group is the glycosyltransferases belong to the non-Leloir pathway which use either sugar phosphates such as glucose-1-phosphate or the disaccharide sucrose or other oligosaccharides as glycosyl donor molecules [323]. The acceptor molecules can also vary depending on the biochemical conditions, generally, the acceptor molecule is the growing carbohydrate chain but it can also be a membrane lipid carrier or other organic compounds such as proteins or lipids that are covalently modified by glycosylation process [90]. Furthermore, glycosyltransferases can be divided into two further groups depending on their activity mechanism: processive glycosyltransferases that transfer sugar residues successively to the acceptor molecule, which is the case for the homopolymeric EPS production, and non-processive glycosyltransferases which transfer only a single sugar residue to the acceptor molecule which can be the case for the biosynthesis of the growing EPS repeating unit in heteropolymeric EPS production [90]. The specificity of the enzymes regarding the Leloir or non-Leloir pathways for the donor and the acceptor molecules and their mode of action as being processive or non-processive result in unique carbohydrate structures.

Finally, according to the catalytic functional mechanism, glycosyltransferases can also be divided into two groups: “retaining enzymes” which form an  $\alpha$  glycosidic bond between an  $\alpha$  linked donor such as UDP-glucose, UDP-galactose and the acceptor molecule and “invertase enzymes” which form a  $\beta$  glycosidic bond between the  $\alpha$  linked donor and the acceptor molecule [90, 323]. Previously it was reported that bacterial glycosyltransferases involved in the biosynthesis of EPS repeating unit are often unique or show little homology to the others except the priming glycosyltransferase which shows high homology within Gram positive bacteria [86, 87, 328]. In theory, the glycosyltransferases encoded in the *eps* clusters add their sugar monomer to the lipid carrier-sugar complex sequentially to form the EPS repeating unit [8] which means that for the heteropolymeric EPS structures one glycosyltransferase is required for the one sugar monomer in the EPS repeating unit. Alternatively, it was proposed that some glycosyltransferases may have bifunctional roles which give them the ability to add different monomers to the acceptor substrates [245]. Moreover, several other bacterial glycosyltransferases which play a role in the cell wall biosynthesis of bacteria were shown to have bifunctional roles [329, 330]. The numbers of the identified EPS structures produced by

LAB is increasing rapidly but the numbers of the biochemically characterized glycosyltransferases which are responsible for the biosynthesis of different EPS repeating units are still low. In future, more research in this field is required in order to engineer the EPS structures to develop novel approaches related to bacteria-bacteria and bacteria-host interactions.

The bacterial cell surface polysaccharides are generally composed of hexose units that are formed by either five or six-membered rings [331]. The hexose units of EPS-2 produced by *L. johnsonii* FI9785 also consists both galactopyranose (Galp) which is the six-membered ring form of the galactose and galactofuranose (Galf) that is the five-membered ring form of the galactose in its repeating unit structure. The Galp form of the galactose exists in all life forms while the Galf does not occur in mammalian glycans including human [331]. Previously it was reported that the conversion of the pyranose form to furanose form does not occur either at free-sugar or sugar-phosphate level [332]. Later on the structure of the O Antigen of *E. coli* K-12 which was shown to have galactofuranose residues and the responsible *rbf* gene cluster has been identified and it was speculated that a candidate gene designated as *orf6* might encode the enzyme which was described as a UDP-galactopyranose mutase that might be responsible for the conversion of galactopyranose to galactofuranose at the sugar nucleotide level [333]. Following this study, this candidate gene was subcloned, expressed and enzyme activity assays confirmed the function of this gene product for the conversion of the UDP-galactopyranose to UDP-galactofuranose and the responsible gene that encodes this UDP-galactopyranose mutase was described as *glf* [334]. Based on the homology results, several putative Glf mutases have been identified in many bacteria including LAB. Previously, the Glf mutase had been predicted to convert UDP-galactopyranose to UDP-galactofuranose in *L. rhamnosus* GG [61]. The *eps* cluster of *L. johnsonii* FI9785 harbours a putative *glf* gene and the Glf enzyme may also be responsible for the presence of the galactofuranose residues in the repeating unit structure of EPS-2 as was discussed previously. The two identified EPS structures from two other *L. johnsonii* strains also contain galactofuranose residues [56, 59] which may reflect the conserved presence of the mutase encoding *glf* genes in *L. johnsonii* strains. Previously, it was proposed that this enzyme is crucial for the viability of many pathogens including *Mycobacterium tuberculosis* due to its role in the formation of D-galactofuranose (Galf) residues in cell wall biosynthesis of this pathogenic bacterium and the absence of this enzyme in humans increased the interest in this enzyme as a potential therapeutic target [335]. Although there

are several publications related to the occurrence of the galactofuranose residues in the EPS structures of LAB, the role of the putative *glf* genes has not yet been determined for LAB.

The primary objectives of the work in this chapter were to delete all putative glycosyltransferases (except *epsE* which had been previously deleted, see section 1.11) encoded in the *eps* cluster of *L. johnsonii* FI9785 in order to determine their role in the EPS repeating unit biosynthesis of *L. johnsonii* FI9785 and to investigate the resulting alterations in the EPS structures and production levels.

The second objective of the work was to over-express putative glycosyltransferases, purify them and characterise their enzymatic activity by *in vitro* assays related to the EPS repeating unit structure of *L. johnsonii* FI9785.

## 7.2 MATERIAL AND METHODS

### 7.2.1 Deletion of the putative glycosyltransferase genes from the *eps* gene cluster

To delete the putative glycosyltransferases (GTFs) from the *eps* cluster of *L. johnsonii* the deletion strategy which was described in section 5.3.2 were followed with some modifications and thermo - sensitive vector pG+host9 was used for deletion studies (see section 5.3.1). These five putative glycosyltransferases are labelled as *gtf1* to *gtf5* starting from the downstream of *epsE* gene in order to simplify the context of this chapter (Figure 7.1).

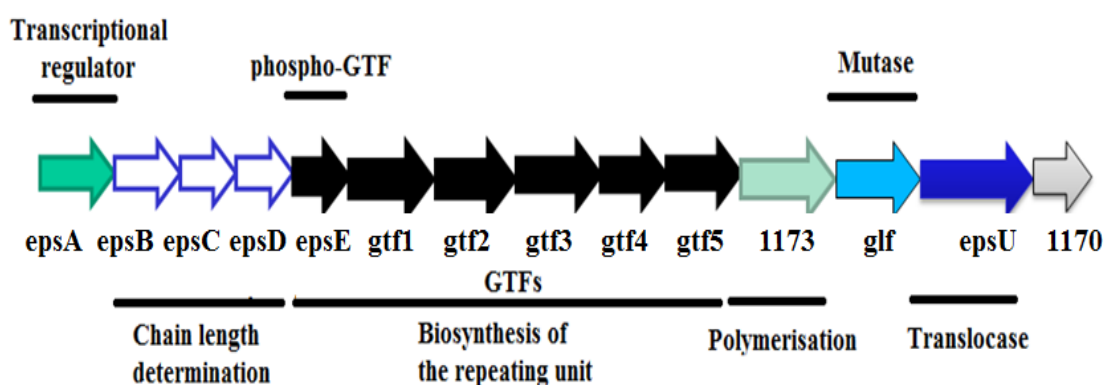


**Figure 7.1.** Molecular organisation of the *eps* cluster of *L. johnsonii* FI9785; the putative glycosyltransferases located downstream of *epsE* gene are re-labelled as *gtf1*, *gtf2*, *gtf3*, *gtf4* and *gtf5* which correspond to 1178, 1177, 1176, 1175 and 1174, respectively.

The strategy used is illustrated in Figure 7.2 for the deletion of second putative glycosyltransferase gene, *gtf1* (1178), which is based on replacing the target gene with a chloramphenicol (CAT) resistance gene. Primers used in the deletion process of the putative *gtf* genes are listed in Appendix 2. Firstly, partial *epsE* gene was amplified with primers 5epsE\_KpnF and epsERspliceCat which incorporated a *KpnI* restriction site and introduced a tail for splice overlap extension PCR with the chloramphenicol resistance gene, respectively. The chloramphenicol resistance gene from plasmid pUK200 [217] was amplified with primers CatFspliceepsE and CatR splice1177, introducing two tails to the 5' end and 3' end for splice overlap extension PCRs with products from the *epsE* gene and *gtf2* gene, respectively. The products from these two reactions were then used as templates for splice overlap extension PCR together with the primer pair 5epsE\_KpnF and CatRsplice1177 to produce the construct for the splice PCR reaction with the product of the third PCR reaction which was the amplification of the partial *gtf2* gene with primers 1177FspliceCat and 1177\_HindR, incorporating a tail with the chloramphenicol resistance gene and introducing a *HindIII* site, respectively. The products of the second and the third PCR reactions were then used as templates for splice overlap extension PCR using the primer pair 5epsE\_KpnF and 1177\_HindR. This final construct was then digested with *KpnI* and *HindIII* and ligated into pG+host9 digested with same restriction enzymes.

The ligation product was then introduced into electro-competent *E. coli* MC1022 by transformation and positive colonies were selected with erythromycin and confirmed by colony PCR using primers pGhost1 and pGhostR. This plasmid construct was labelled as pG+host9gtf1 (pG+host91178). The same strategy was followed for the deletion of the following four putative glycosyltransferases, *gtf2*, *gtf3*, *gtf4* and *gtf5* using the primers listed in Appendix 2: amplifying the partial upstream gene with introducing a *KpnI* site to the 5' and incorporating a tail to the *CAT* gene, then amplifying the *CAT* gene introducing tails to the both ends for the partial upstream gene and the partial downstream gene of the target gene and finally amplifying the downstream gene with incorporation of a tail to the *CAT* gene and introducing a *HindIII* site to the 3' for splice overlap PCR reactions. When required the specific bands from the gel were excised and DNA extracted using the Qiaex II Gel Extraction Kit (Qiagen, UK) according to the manufacturer's protocol and recommendations.

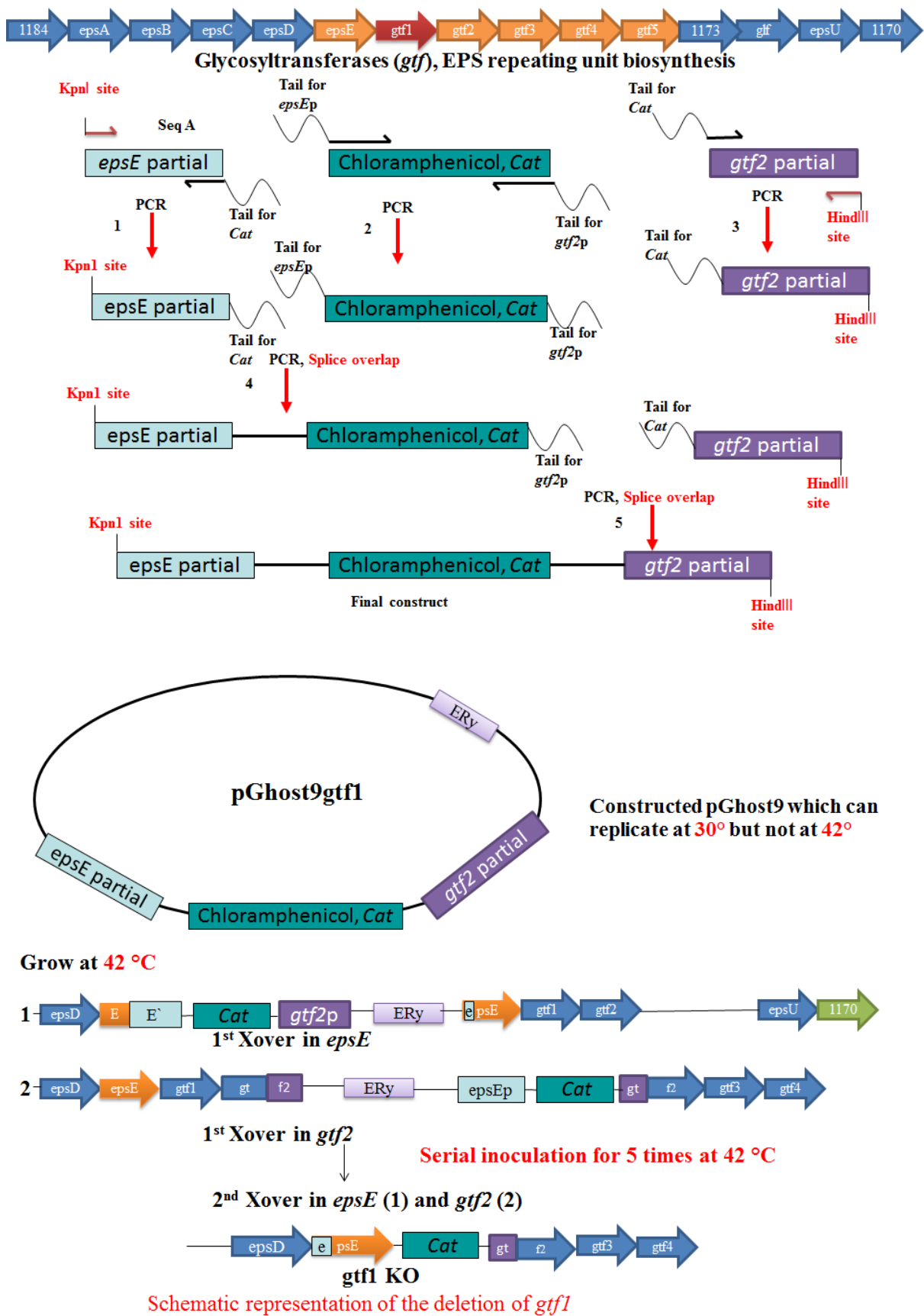


**Figure 7.2.** An illustration of the gene replacement process for *gtf1*.

After constructing all products for the gene replacement process, the deletion vectors pG+host9gtf2, pG+host9gtf3, pG+host9gtf4 and pG+host9gtf5 were prepared as described above. Following sequence confirmation, the deletion plasmids were transformed into *L. johnsonii* FI9785 by electroporation (see 2.2.15) and the method of gene replacement was performed as described in Chapter 5. The transformants were selected on MRS plates supplemented with chloramphenicol at 30°C as the permissive temperature for plasmid replication followed by inoculation in MRS broth supplemented with chloramphenicol (7.5 µg/ml) at 42°C as the non-permissive temperature for five serial passages. The cultures were diluted and plated on MRS + chloramphenicol at 42°C to obtain single colonies that were replica streaked onto plates containing MRS + chloramphenicol and MRS + erythromycin to identify erythromycin-sensitive, chloramphenicol-resistant clones. The gene deletions were identified by PCR reactions by comparing the wild type genome and the expected products after the gene replacements as described in Table 7.2. The deletion strategies and attempts for all four putative glycosyltransferases are explained in results section in detail.

### **7.2.2 Isolation of EPS from new mutants and analysis of EPS structure and production levels**

New deletion strains (*L. johnsonii*  $\Delta$ gtf1 and  $\Delta$ gtf3) were grown under the conditions described in section 2.1.2 and the EPS were isolated from new strains according to the method described in section 2.1.4. Then the EPS samples were subjected to NMR and FTIR Spectroscopy analysis using the methods described in section 3.2.2 and 3.2.4, respectively. Similarly, the EPS were isolated from the new mutant strains with the method described in section 5.2.4 for the quantification of the EPS production by phenol-sulphuric acid methodology described in section 5.2.5.

### **7.2.3 Subcloning of two potential glycosyltransferases: gtf1 and gtf3**

In order to understand the role of gtf1 (1178) and gtf3 (1176) as putative glycosyltransferases, these genes were subcloned into the expression vector pET15b (Novagen) which will be explained in detail in the results section. The pET15b vector carries an N-terminal His•Tag sequence which is composed of 6-Histidine residues which can be used for subsequent protein purification. The pET15b vector harbours a T7 RNA polymerase promoter sequence from T7 bacteriophage which inhibits the recognition of this sequence by the *E. coli* host cells and a *lacI* gene from the lac operon of *E. coli* that codes for the *lac*

repressor and a ribosome binding site which are located in front of the three cloning sites which are NdeI, XhoI and BamHI, respectively for the cloning of the target gene (Figure 7.3).

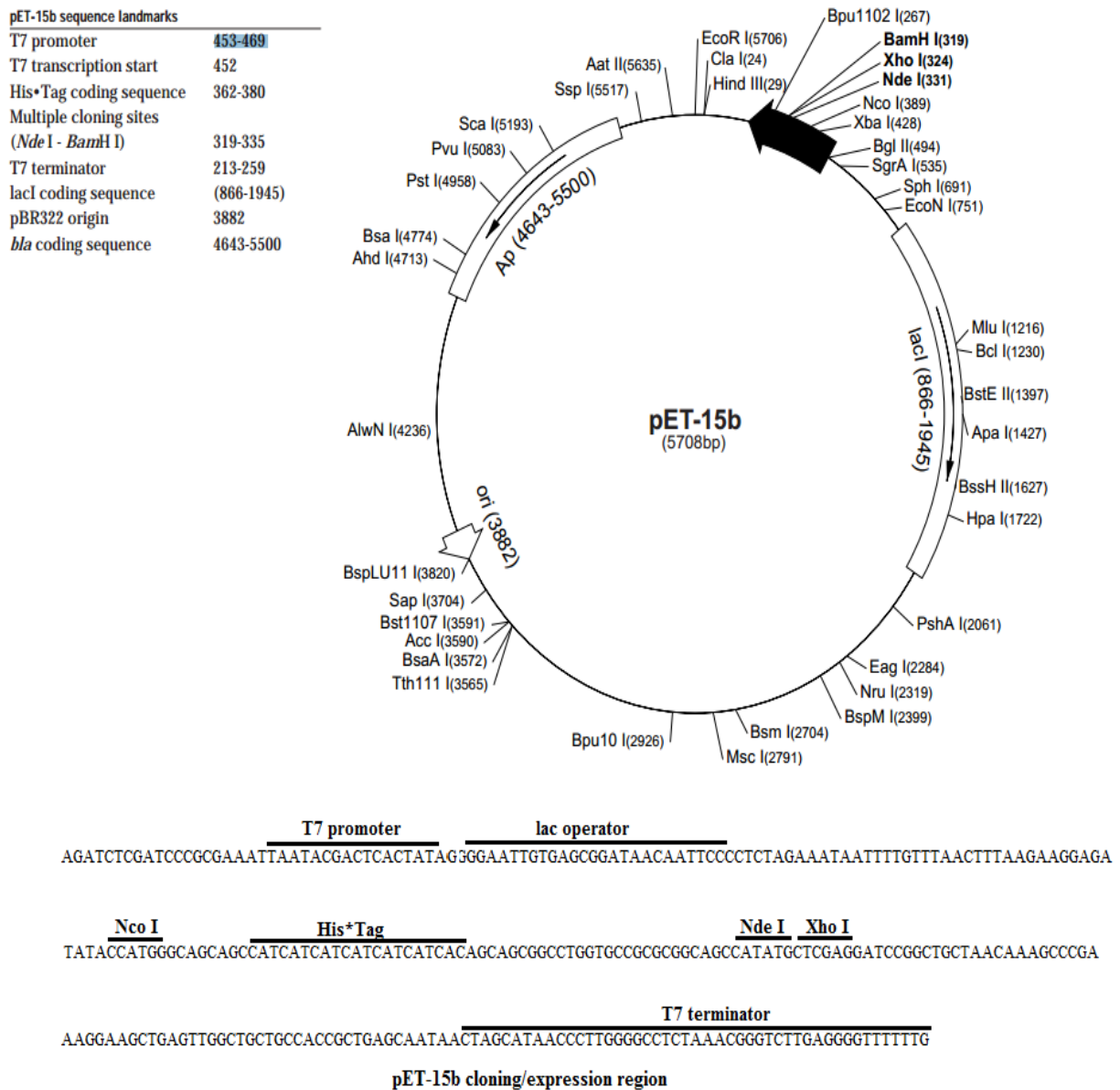


**Figure 7.3.** The scheme of pET15b and the detailed sequence of the expression region (Novagen).

For the transcription of our target gene firstly the *lac* repressor should fall off and a T7 RNA polymerase should be introduced and recognise the T7 promoter sequence in pET15b. Once IPTG is added to the environment the LacI falls off and T7 RNA polymerase binds to the promoter region in front of our target gene and transcribes our gene which results in a bulk production of our target protein.

#### 7.2.4 Protein expression, analysis and purification

*L. johnsonii* FI9785 harbours six putative glycosyltransferase genes starting with *epsE* and a putative *glf* mutase in the identified *eps* cluster as described in section 1.10. In order to understand the role of rest of the putative glycosyltransferase genes (except *epsE*) and the putative *glf* mutase, these genes (*gtf2*, *gtf4*, *gtf5* and *Glif*) were subcloned into the pET15b vector by Dr Melinda Mayer (IFR). All target proteins including the empty vector pET15b as a control, were expressed using pET15b constructs in *E. coli* BL21 (DE3) cells (Invitrogen) with the IPTG induction and cells were lysed and proteins were extracted as described in 2.3.1. For the insoluble fractions BugBuster Protein Extraction Reagent (Novagen) was used, following the manufacturer's protocol.

After the extraction process the concentration of the proteins were measured with the protocol described in section 2.3.2. The molecular weight of the target proteins *gtf1*, *gtf2*, *gtf3*, *gtf4*, *gtf5* and *Glif* were calculated using Editseq software (DNASTAR, USA) and the proteins were separated according to their size by SDS-PAGE as described in section 2.3.3 and the target His-tagged proteins were detected with anti-His-tag monoclonal antibodies (Novagen) by Western Blotting as described in section 2.3.4.

Crude protein extracts were produced from IPTG-induced *E. coli* BL21 (DE3) containing pET15b*gtf1*, pET15b*gtf2*, pET15b*gtf3*, pET15b*gtf4*, pET15b*gtf5*, pET15b*Glif* or pET15b in buffer 2 (20 mM Tris-HCl, 50 mM NaCl pH 7.5) as described above. His-*gtf1*, His-*gtf2*, His-*gtf3*, His-*gtf4*, His-*gtf5* and His-*Glif* were partially purified from *E. coli* using the nickel-nitrilotriacetic acid (Ni-NTA) Fast Start kit (Qiagen).

An alternative method was also carried out for the partial purification of the expressed proteins using FPLC. Briefly, cell pellets from 2 l cultures induced with IPTG, were thawed and resuspended into 50 ml of lysis buffer (50 mM HEPES pH 7.5, 100 mM NaCl, 1 x complete, EDTA-free Protease Inhibitor Cocktail Tablet (Roche), 0.02 mg/ml DNaseI). Cells were lysed using a cell disruptor (one shot mode, 25 kpsi, Constant Systems, UK) and the cell debris was removed by centrifugation at 30000 g for 30 min. Protein was purified at 4°C using an ÄKTA Xpress FPLC system (GE Healthcare). The supernatant was passed through a HiTrap Ni-NTA column (5 ml, GE Healthcare), washed with wash buffer (50 mM Tris-HCl pH 8.0, 0.5 M NaCl, 0.03 M imidazole) and eluted with elution buffer (50 mM Tris-HCl pH 8.0, 0.5 M NaCl, 0.5 M imidazole (BioUltra)). Further purification was performed by gel filtration on a Superdex S75 26/60 column (GE Healthcare) using Gel Filtration buffer (50

mM HEPES pH 7.5, 150 mM NaCl) at a flow rate of 3.2 ml/min. After the purification, the eluates were further purified with the centrifugal filters with a MW cut off of 30 kDa (Amicon Ultra-15, Merck Millipore; UK) and stored at -20°C for the enzyme assays.

### 7.2.5 Glycosyl transfer activity assays

Four different reactions (ED-1, ED-2, ED-3 and ED-4) were planned depending on the EPS structure and the availability of the donor and the acceptor molecules which are listed in Table 7.1.

Reaction	Donor	Acceptor	Target unit in EPS structure
ED-1	<b>UDP-<math>\alpha</math>-D-Glucose</b>	<b>Octyl <math>\beta</math>-D-Lactoside</b>	$\alpha$ -Glc $p$ -(1 $\rightarrow$ 4)- $\beta$ -Gal $p$ (1 $\rightarrow$ 4)- $\beta$ -Glc $p$ -(1 $\rightarrow$ 6) (EPS-2)
ED-2	<b>UDP-<math>\alpha</math>-D-Glucose</b>	<b>Octyl <math>\beta</math>-D-glucofuranoside</b>	$\alpha$ -Glc $p$ -(1 $\rightarrow$ 3)- $\beta$ -Glc $p$ (EPS-2)
ED-3	<b>UDP-<math>\alpha</math>-D-Galactose</b>	<b>Octyl <math>\beta</math>-D-glucofuranoside</b>	$\beta$ -Gal $p$ (1 $\rightarrow$ 4)- $\beta$ -Glc $p$ (EPS-2)
ED-4	<b>UDP-<math>\alpha</math>-D-Glucose</b>	<b>Octyl <math>\alpha</math>-D-glucofuranoside</b>	$\alpha$ -Glc $p$ -(1 $\rightarrow$ 2)- $\alpha$ -Glc $p$ or $\alpha$ -Glc $p$ -(1 $\rightarrow$ 6)- $\alpha$ -Glc $p$ (EPS-1)

**Table 7.1.** The donor and acceptor molecules used for each reaction mixture for crude and purified GTFs and their potential products in EPS repeating unit structure.

Figure 7.4 illustrates the schematic of the glycosyltransferase activity in reaction ED-1. The donor molecules UDP- $\alpha$ -D-Glucose (MW 566.0550) and UDP- $\alpha$ -D-Galactose (MW 566.0550) were purchased from CalbioChem (Merckmillipore, UK) and the acceptor molecules that are used in this study were Octyl  $\beta$ -D-Lactoside (MW 454.2414, Toronto Chemicals, Canada), Octyl  $\beta$ -D-glucofuranoside (MW 292.1886, Sigma, UK) and Octyl  $\alpha$ -D-glucofuranoside (MW 292.1886, Sigma, UK), respectively.

## ED-1

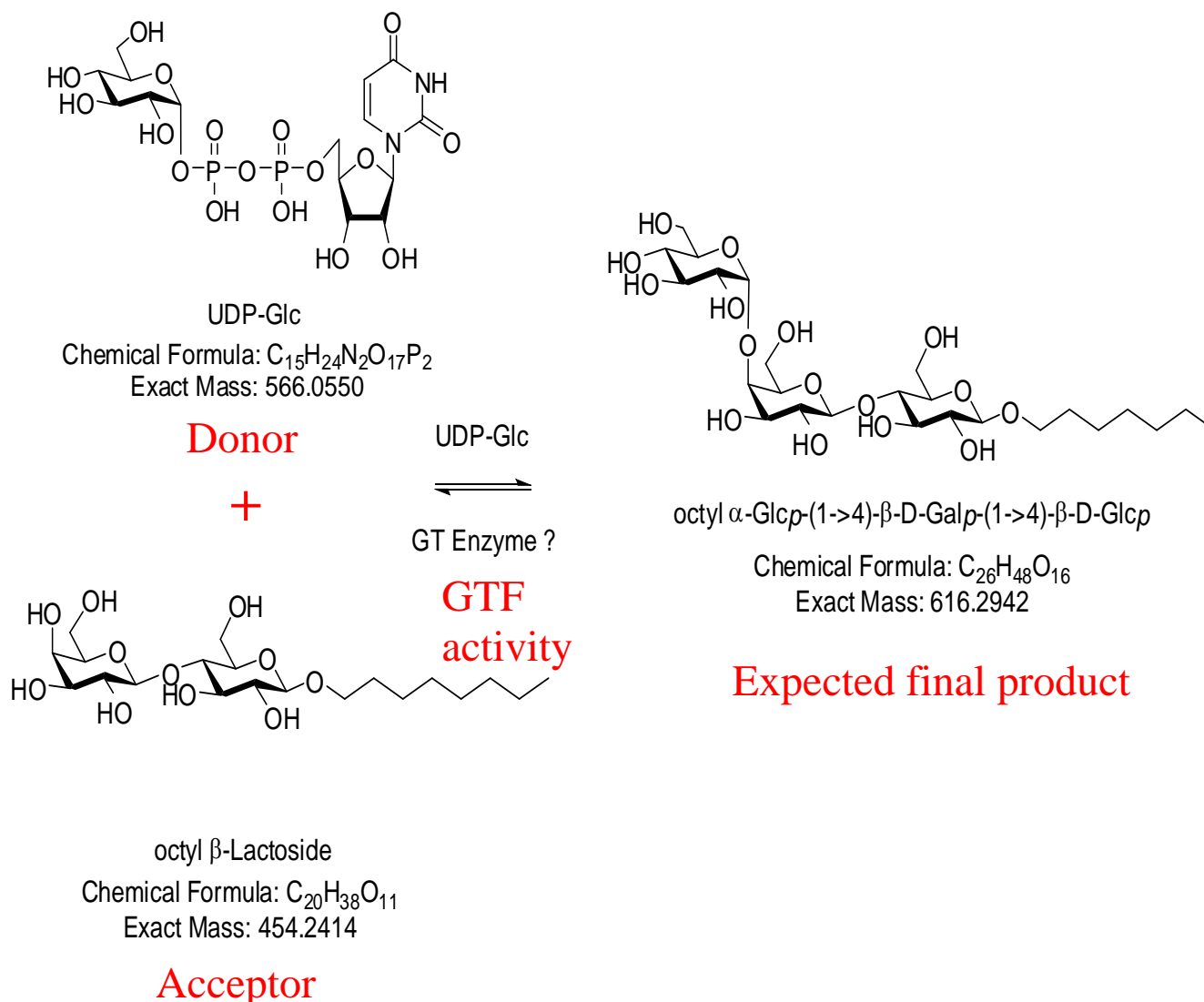


**Figure 7.4.** ED-1 reaction mixture and expected final product after the GTF activity.

Reaction mixtures were prepared in reaction buffer containing 50 mM Tris pH 8, 10 mM  $MgCl_2$  and 0.1 mM dithiothreitol which was added shortly before starting the reaction. Then donor and acceptor molecules for each reaction mixtures were added at final concentrations of 5 mM. The reactions were carried out in 100  $\mu$ l final volumes and 30  $\mu$ l of crude or purified recombinant putative glycosyltransferases were added and then incubated at 37°C for 4 to 16 h. The reactions were stopped by adding 50  $\mu$ l of ethanol and for the removal of the charged molecules from the reaction mixture ion exchanger TMD-8 hydrogen and hydroxide (Sigma) were added and incubated for 1 h at RT, the reaction mixture was centrifuged at 10000 rpm (eppendorf, 5415D) for 3 min and the supernatants were collected for further

analysis. Reactions were monitored by TLC (Thin-Layer Chromatography) using silica gel precoated aluminium TLC plates (Sigma, UK), run in chloroform: methanol: water (65:25:4.1). Compounds were detected with an orcinol solution (20 mg of orcinol dissolved in 10 ml of 70% sulphuric acid) by heating at 100°C. Spots containing sugars appeared pink-violet on a white background. The resulting TLC was scanned as a JPG file.

To confirm the presence of the expected products in reaction mixtures, the Ultra performance liquid chromatography-Quadrupole time-of-flight mass spectrometer system (UPLC-QToF Synapt-2 MS) (Waters Corp., Milford, MA, USA) was used and data recorded with MassLynx software (Waters Corp.) Samples from the reaction mixtures were run using an HSS-T3C18 column (2.1 mm × 50mm, 1.8 μm particle size Waters Corp.). Chromatographic separations were performed at a flow rate of 0.4 ml/min. The column was eluted with 0.1% acetic acid in water (A) and 0.1% acetic acid in acetonitrile (B). Samples (5 μL) were injected onto the column at 100% A, held for 1 min and subsequently ramped to 90% B over 10 min, held for 2 min before a rapid return to 100% A and an equilibration for 2 min. Centroided mass spectra were acquired in the mass range of 80-1200 amu using the mass spectrometer in negative electrospray mode with a scan time of 0.3 sec per channel. Data were obtained in the MassLynx.

### 7.2.6 Glf mutase activity assay

The crude and the purified putative Glf, UDP-galactopyranose mutase, activities were tested following the method described before with some modifications [336]. Assay mixtures contained 50 mM MOPS and 2 mM magnesium chloride pH 7.5, with the addition of sodium dithionite to a final concentration of 10 mM shortly before the experiment. Then 30 μl of the crude and purified Glf were added to the assay mixture and incubated for 10 min. After the incubation the substrate 5 mM UDP-galactopyranose (MW 610.27) was added to the 700 μl of final mixture and incubated for 1-6 h at 37°C. The same reactions conditions were also prepared for purified recombinant *Klebsiella pneumoniae* mutase as a positive control and the crude extract of *E. coli* expressing the pET15B vector only as a negative control. Reactions were monitored by NMR Spectroscopy. <sup>1</sup>H NMR spectra were recorded on a Bruker Avance III spectrometer at 400 MHz. Chemical shifts of <sup>1</sup>H NMR signals recorded in D<sub>2</sub>O are reported with respect to residual HDO at δ<sub>H</sub> 4.70 ppm.

## 7.3 RESULTS

### 7.3.1 Deletion of putative glycosyltransferases from the *eps* cluster

One of the aims of this chapter was to delete the potential glycosyltransferases from the *eps* cluster of *L. johnsonii* in order to understand their function in EPS repeating unit biosynthesis. These glycosyltransferases were labelled as gtf1, gtf2, gtf3, gtf4 and gtf5 corresponding to 1178, 1177, 1176, 1175 and 1174, respectively as described in material and methods. The deletion of the individual gtf genes was performed as illustrated in Figure 7.2 for gtf1. In the final step the colonies were checked for the gene replacement by colony PCR using the primers listed in Table 7.2.

Target gene	Primer set for clone check	Original size (bp)	Expected size (bp)
gtf1 (1178)	epsEFclone, 1177Rclone	1699	1463
	1177FspliceCat, 1177Rclone	-	293
gtf2 (1177)	1178Fclone, 1176Rclone	1570	1495
	1176FspliceCat, 1176Rclone	-	305
gtf3 (1176)	1177Fclone, 1175Rclone	1610	1483
	1175FspliceCat, 1175Rclone	-	315
gtf4 (1175)	1176Fclone, 1174Rclone	1384	1487
	1174FspliceCat, 1174Rclone	-	246
gtf5 (1174)	1175Fclone, 1173Rclone	1618	1482
	1173FspliceCat, 1173Rclone	-	295

**Table 7.2.** The primer set for the final clone check of the *gtf* genes and their original and expected sizes after the deletion process.

The partial upstream and downstream sequences of the target genes (for instance target gene is gtf1 and partial upstream and downstream sequences are *epsE* partial and gtf2 partial, respectively) were amplified using the genomic DNA of *L. johnsonii*, introducing a *KpnI* site to the upstream genes and a *HindIII* site to the downstream genes and incorporating a tail

from both ends for the splice overlap reactions with the chloramphenicol resistance gene (Figure 7.5). Similarly the chloramphenicol resistance gene was amplified from pUK200 plasmid with adding the tails for the related up and downstream sequences (Figure 7.5C).

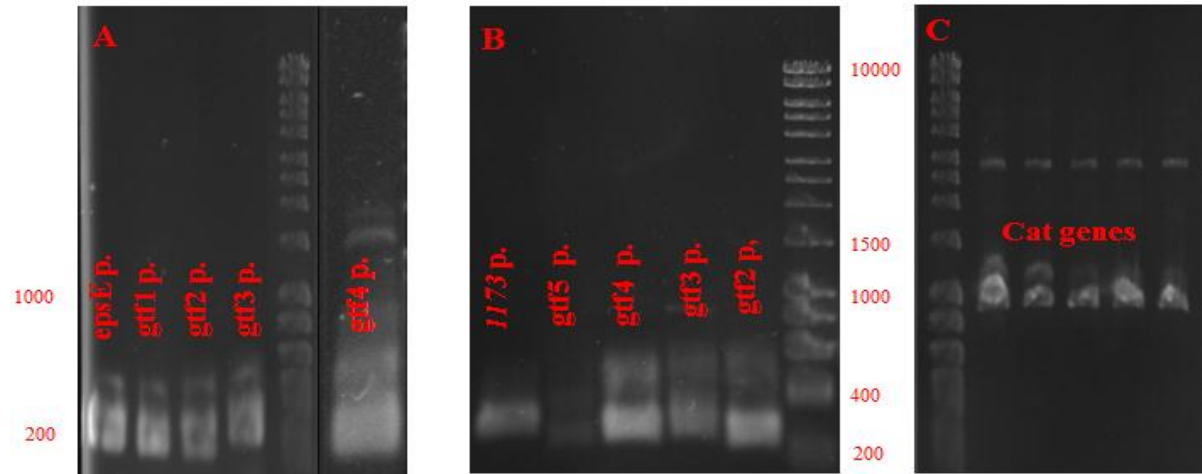


**Figure 7.5.** Agarose gel (0.8% w/v) showing A) partial (p.) upstream sequences of gtf genes from the genome of *L. johnsonii* with a tail to the CAT gene; B) partial downstream of gtf genes from the genome of *L. johnsonii* with a tail to the CAT gene; C) CAT genes with the tail in both ends to the corresponding gtf.

Then the first splice overlap PCR reactions were performed using the amplified DNA products from the upstream genes and related CAT genes, respectively (Figure 7.6A).

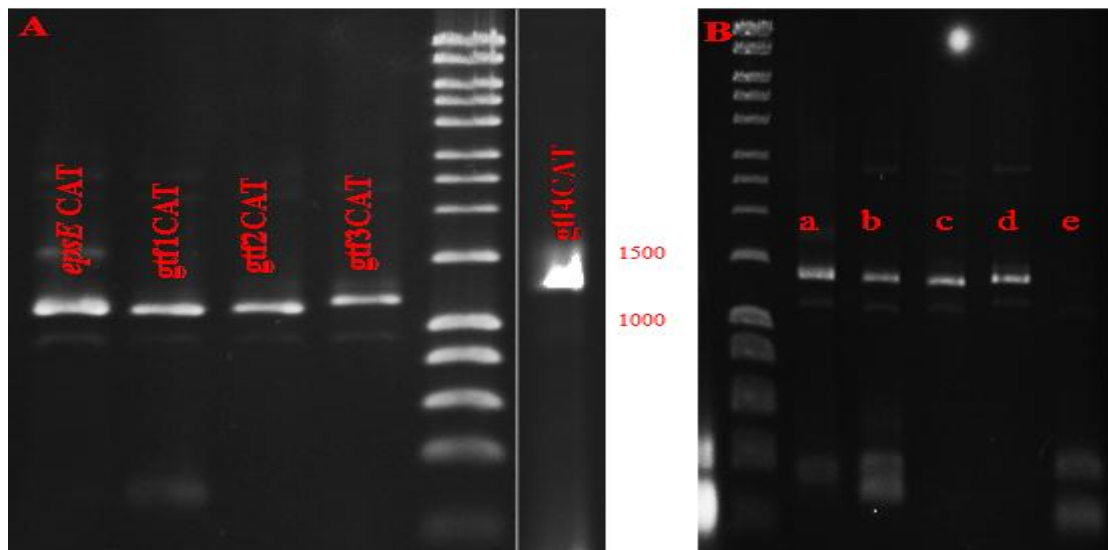


**Figure 7.6.** Agarose gel (0.8% w/v) showing A) splice PCR product of the upstream gtf genes with the CAT gene resulted as epsECAT, gtf1CAT, gtf2CAT, gtf3CAT and gtf4CAT; B) splice PCR product of the first splice products (from panel A) with the downstream sequences of each gtf genes (see Figure 7.5B); Lanes a-d describing final constructs for gtf1, gtf2, gtf3 and gtf4 respectively, lane e negative PCR result for gtf5 construct.

The PCR products from the first splice reactions were then used with the downstream gene products for the second splice overlap PCR reactions to prepare the final construct for the gene replacement process (Figure 7.6B). As a result of the second PCR reactions the final constructs were successfully prepared for the replacement of *gtf* genes except for the *gtf5* (Figure 7.6B).

To prepare the construct for *gtf5* several splice overlap PCRs were performed but several secondary products were also amplified in all different PCR reactions (Figure 7.7A).

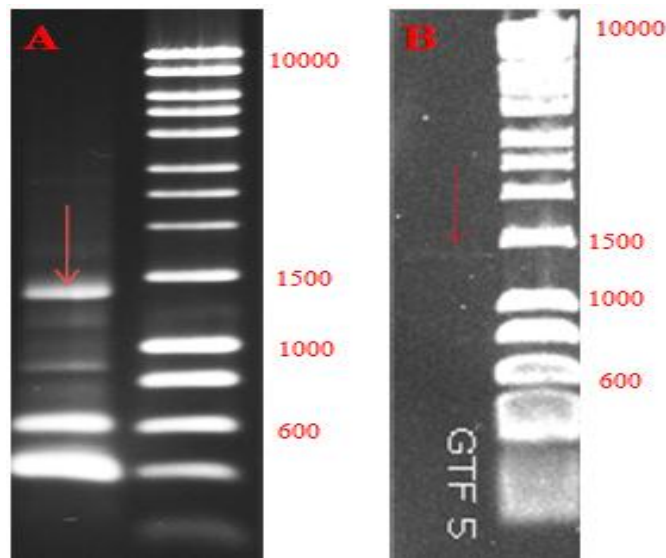


**Figure 7.7.** Agarose gel (0.8% w/v) showing A) splice PCR product of the *gtf4*CAT and partial *1173* with a tail to *CAT* to prepare final construct for *gtf5*; B) The excised band of the *gtf5* construct from the gel shown in A.

To overcome this problem the expected splice product were excised from the agarose gel successfully (Figure 7.7B).

The first 4 GTF constructs and the deletion vector pG+host9 were cut with *KpnI* and *HindIII* and the ligation reactions were performed with the inserts and vector individually for all four constructs and the ligation mix were checked by ligation PCR with primers from pG+host9 and if positive ligation product were amplified the transformation to *E. coli* MC1022 were carried out and the positive colonies were selected (data not shown).

Then the positive colonies were grown in L Broth supplemented with erythromycin (400  $\mu$ g/ml) overnight at 37°C and the plasmids were isolated and then transformed into *L. johnsonii* after the sequence confirmation and grown overnight in MRS broth supplemented with 10  $\mu$ g/ml erythromycin at 37°C. The overnight grown cultures were then subcultured at

42°C in MRS broth supplemented with chloramphenicol (7.5 µg/ml) which resulted in the integration of the related plasmids to the chromosome of *L. johnsonii* FI9785 (Figure 7.8A). For the removal of the plasmids these cultures were serially subcultured for 5 consecutive days at 42°C in MRS broth supplemented with chloramphenicol.

Following the procedure described in material and methods several colonies were tested for each construct and positive colonies were detected for the replacement of the *gtf1* gene with *CAT* gene in the first attempt (Figure 7.8B). The removal of the plasmid from the genomic content of this strain was also confirmed and this new mutant was entitled as *L. johnsonii*  $\Delta$ *gtf1* (Figure 7.8C).

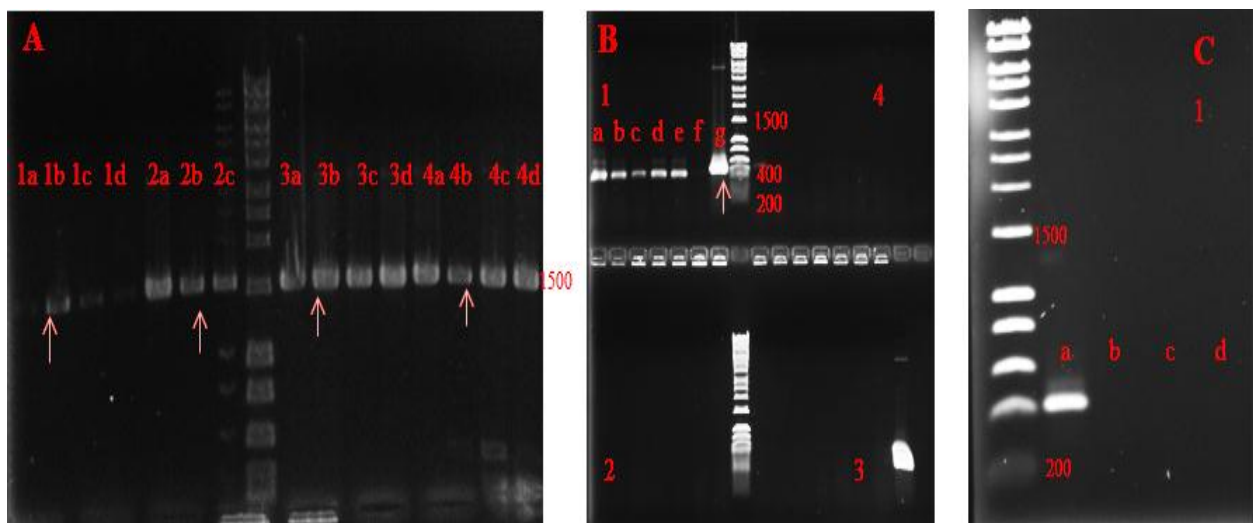


**Figure 7.8.** Agarose gel (0.8% w/v) showing A) Colony PCR showing the integration of the pG+host9+constructs for 4 *gtf* to the genome of *L. johnsonii* after forcing the vector to integrate by growing the *L. johnsonii* mutants at 42°C: Each number represents related *gtf* construct and each letter shows different colonies; B) Confirmation of the  $\Delta$ *gtf1* mutant with primers 1177FspliceCat and 1177Rclone for *gtf1*: Lane a, b, c, d, e shows positive colonies after 5 serial dilutions of the integrated mutants at 42°C, then replica-plating to MRS plates containing Ery and CAT, respectively. The colonies that were checked grew in the presence of CAT but not Ery; lane 1f, negative result; lane 1g shows the colony did not grow with Ery but a band at (6 kb) showed that in some cells the plasmid was still integrated to the chromosome of *L. johnsonii*. The other 3 *gtf* sets of colonies did not result in the gene replacement after the deletion process, they all returned to the wild type's genome except the colony in *gtf3* which showed the integration of the plasmid to the *L. johnsonii* genome; C) Confirmation of the  $\Delta$ *gtf1* mutant: lane a; colony PCR with primers 1177FspliceCat and 1177Rclone showing the replacement of the *gtf1* gene with the chloramphenicol resistance gene, lane b; same colony checked with primers pGhost1 and pGhostR showing the removal of the plasmid from the genome of *L. johnsonii*, lane c-d; colony PCR of wild type with primer sets 1177FspliceCat and 1177Rclone and pGhost1 and pGhostR showing no bands as a negative control.

The gene replacement processes for the other three constructs were repeated several times but only the third construct resulted in the deletion of the *gtf3* gene (Figure 7.9A), the other constructs always failed in the mutation process (data not shown). The removal of the plasmid from the genomic content of the new mutant was confirmed and this mutant was entitled as *L. johnsonii*  $\Delta$ *gtf3* (Figure 7.9B).

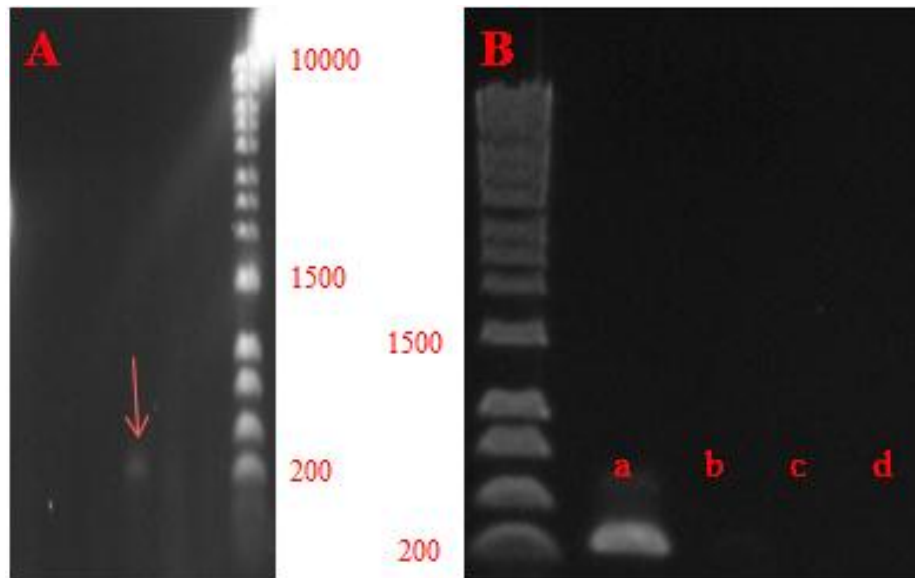


**Figure 7.9.** Agarose gel (0.8% w/v) showing A) Colony PCR showing only one positive colony which demonstrates the deletion of the *gtf3* gene after the same applications described above, B) Confirmation of the  $\Delta$ *gtf3* mutant: Lane a; Colony PCR with primers 1175FspliceCat and 1175Rclone showing the replacement of the *gtf3* gene with the chloramphenicol resistance gene, lane b; same colony checked with primers pGhost1 and pGhostR showing the removal of the plasmid from the genome of *L. johnsonii*  $\Delta$ *gtf3*, lane c-d; Colony PCR of wild type with primer sets 1177FspliceCat and 1177Rclone and pGhost1 and pGhostR showing no bands as a negative control.

Although, different conditions was applied in the subculturing process of the failed two constructs, such as increasing the number of subculturing up to 10 cycles or starting with little amounts of inoculum (10  $\mu$ l), the mutation in *gtf2* and *gtf4* genes could not be achieved (data not shown).

The last construct *gtf5* was also ligated with the deletion vector pG+host9 and the transformation to *E. coli* MC1022 were carried out and the positive colonies were selected (Figure 7.10).

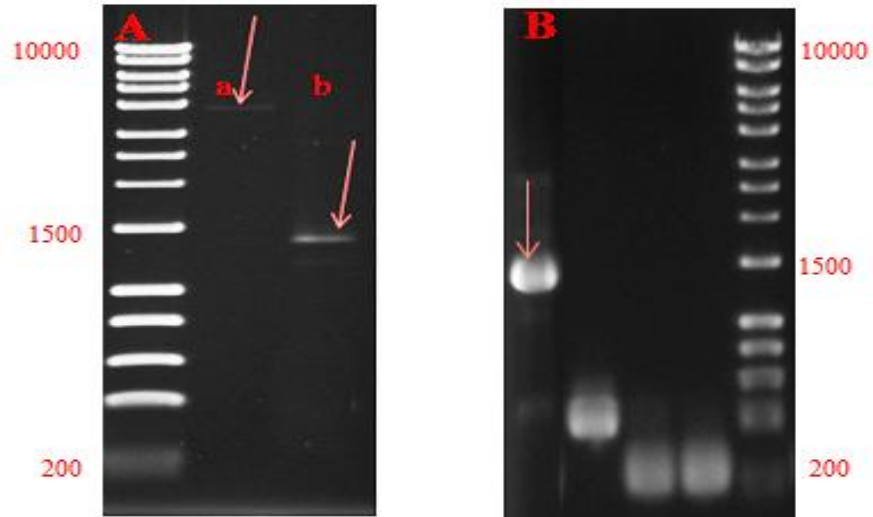


**Figure 7.10.** Agarose gel (0.8% w/v) showing A) Lane a; pG+host9 cut with *KpnI* and *HindIII*, respectively, lane b; *gtf5* construct cut with *KpnI* and *HindIII*, respectively; B) Colony PCR of ligation of pG+host9 and construct *gtf5* transformed into *E. coli* MC1022: Red arrow shows the positive colony PCR product amplified with pGhost1 and pGhostR, the other products are related to the self-ligated products and some unexpected ligation products.

Then the positive colony was grown in L Broth supplemented with erythromycin overnight at 37°C and the plasmid were isolated and then transformed into *L. johnsonii* after the sequence confirmation (Figure 7.11) and same processes were applied for the mutation as described above. But, unfortunately any of the colonies were positive in terms of the gene replacement in *gtf5* (data not shown).

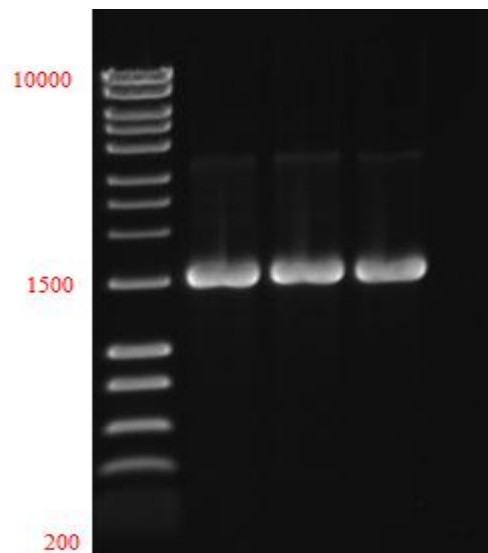


**Figure 7.11.** Agarose gel (0.8% w/v) showing colony PCR with primers pGhost1 and pGhostR showing the integration of the pG+host9+*gtf5* construct to the genome of *L. johnsonii* after forcing the vector to integrate by growing the *L. johnsonii* mutants at 42°C.

### 7.3.2 Quantification of EPS production and structural analysis

In total, only *gtf1* and *gtf3* were deleted from the *eps* cluster of *L. johnsonii* FI9785. To understand the role of these two genes in EPS biosynthesis mechanism, EPS were isolated from the new mutant strains, *L. johnsonii*  $\Delta$ *gtf1* and *L. johnsonii*  $\Delta$ *gtf3* and subjected to total sugar and structural analysis. Interestingly, the total sugar analysis of new mutant strains demonstrated that there was no difference between wild type and the new mutant strains in terms of EPS production levels (Figure 7.12).

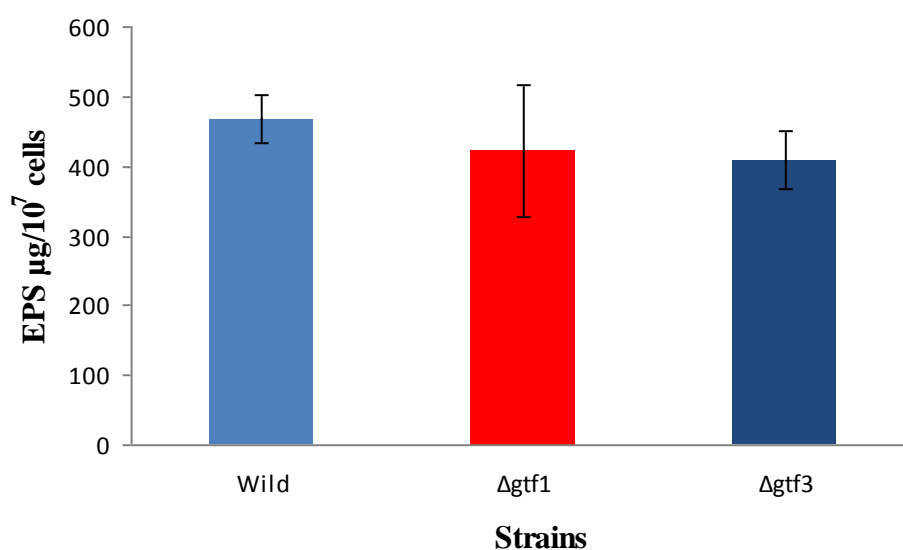


**Figure 7.12.** Total sugar content of *L. johnsonii* wild type,  $\Delta$ *gtf1* and  $\Delta$ *gtf3* mutant strains determined by phenol-sulphuric acid test. Results are the mean of the triplicate measurements with three technical replicates per measurement  $\pm$  standard deviation.

Similarly, deletion of the either *gtf1* or *gtf3* did not change the EPS structure accumulated at the cell surface of *L. johnsonii* FI9785. Both mutants were still producing EPS-1 and EPS-2 EPS mixture like the wild type strain (Figure 7.13, see Figure 3.3 for the NMR spectra of wild type). The only difference detected in NMR spectroscopy analysis was the alteration of the EPS-1 and EPS-2 ratios in  $\Delta$ *gtf3* and  $\Delta$ *gtf1* mutant's EPS samples; The EPS-1 was higher than the EPS-2 in the capsular EPS mixture of  $\Delta$ *gtf1* mutant strain whereas the two EPS samples were equal in the capsular EPS mixture of  $\Delta$ *gtf3* mutant strain (analysed by Dr Ian J. Colqhoun) which could be the effect of the deletion of the putative glycosyltransferases.

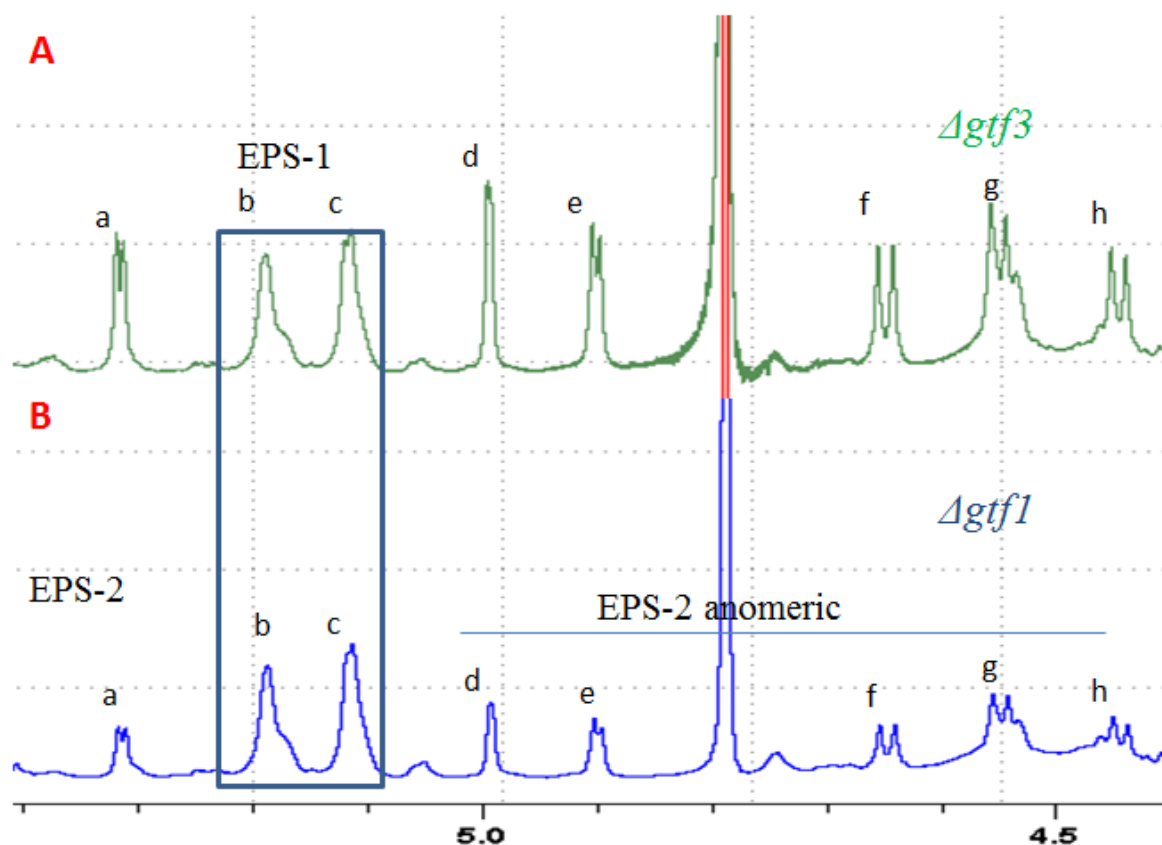


**Figure 7.13.** 600 MHz  $^1\text{H}$  NMR spectra (anomeric region, 338 K,  $\text{D}_2\text{O}$ ) of EPS produced by *L. johnsonii* A)  $\Delta\text{gtf3}$  and B)  $\Delta\text{gtf1}$  mutants. Sugar units *b* and *c* are from EPS-1 and units *a* and *d-h* from EPS-2 [230].

The FTIR spectra of the EPS samples isolated from new mutant strains also confirmed the unchanged EPS composition compared to the wild type strain (Figure 7.14). The only difference in the FTIR spectrum of wild type and new mutant strains were the peak at the region  $1500\text{-}1600\text{ cm}^{-1}$  which is assigned to N-H bending and C-N stretching in proteins which was also previously observed for EPS isolated from  $\Delta\text{epsE}$ ,  $\Delta\text{epsE}::\text{pepsEA/S}$  and  $\Delta\text{epsA}::\text{pepsA}$  strains (Figure 3.12, 5.11).

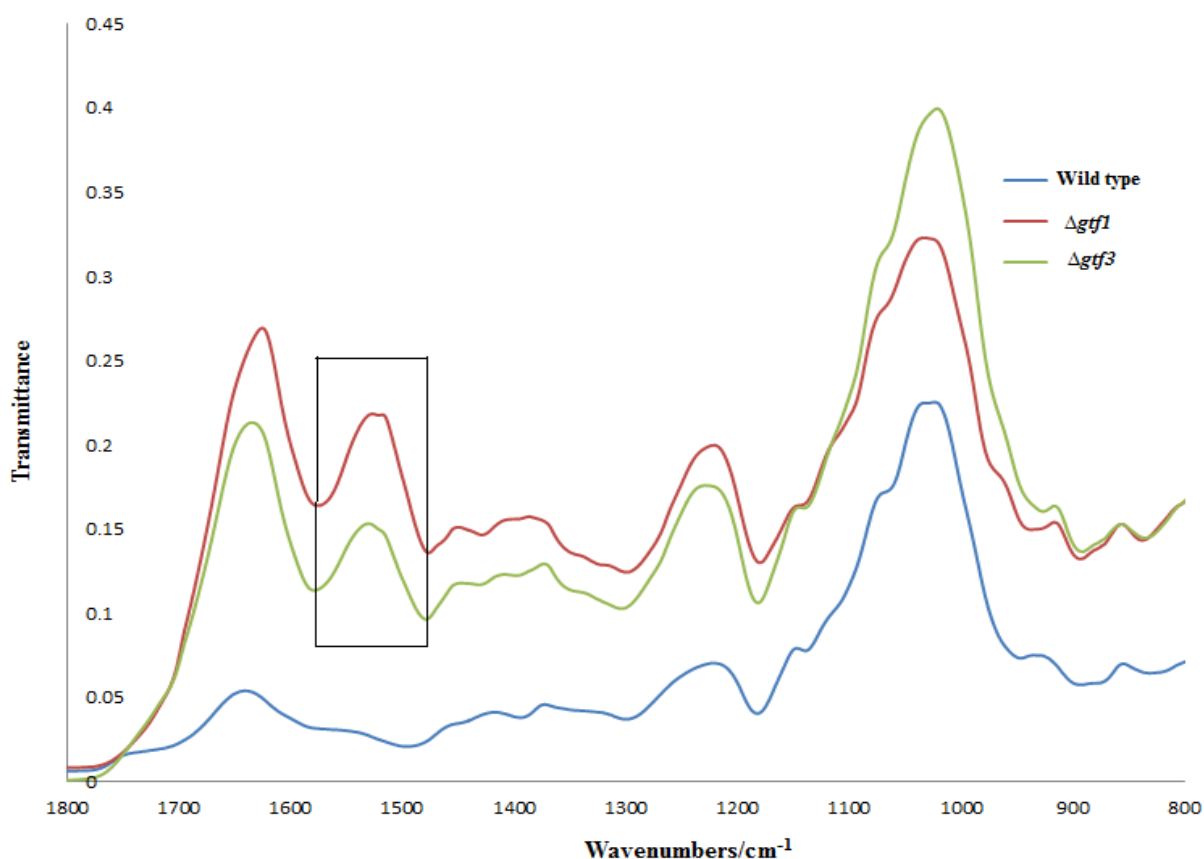


**Figure 7.14.** FTIR spectra of capsular EPS isolated from the wild type,  $\Delta gtf1$  and  $\Delta gtf3$  mutants. The window represents the alteration in the spectra of the new mutants compared to the wild type strain.

Overall, the deletion of the second and the fourth putative glycosyltransferases of the *eps* cluster of *L. johnsonii* FI9785 revealed no alteration in the basic EPS structure of *L. johnsonii* FI9785, especially in EPS-2, which might be due to the fact that the other glycosyltransferases may compensate the function of the deleted glycosyltransferases in the EPS repeating block biosynthesis.

### 7.3.3 Glycosyltransferases and Gtf mutase expression and GTF activity tests

In order to express two putative GTFs, these two genes (*gtf1* and *gtf3*) were amplified from the genome of *L. johnsonii* FI9785 with the introduction of *NdeI* and *BamHI* sites with the primers 1178\_NdeF and 1178\_BamR for *gtf1* and 1176\_NdeF and 1176\_BamR (see Appendix 2 for primer details) for *gtf3* to facilitate the subcloning into the expression vector pET15b (Figure 7.15A). The amplified products were purified using SureClean (Bioline), restricted with *NdeI* and *BamHI* and ligated into *NdeI* - *BamHI* restricted and dephosphorylated vector pET15b (Figure 7.15B).

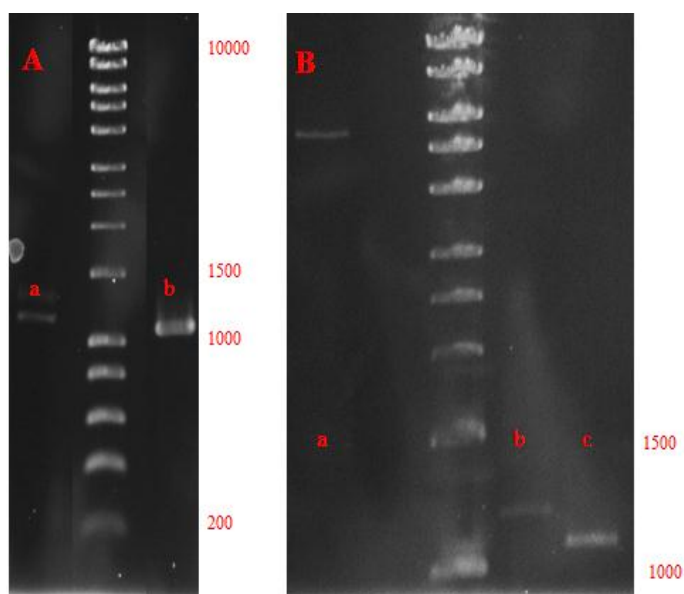


**Figure 7.15.** Agarose gel (0.8% w/v) showing A) Lane a and b; *gtf3* and *gtf1* amplified from the genome of *L. johnsonii*, respectively; B) Lane a; restricted with *NdeI* and *BamHI* and dephosphorylated vector pET15b, lane b-c; *gtf3* and *gtf1* restricted with *NdeI* and *BamHI*, respectively.

Ligation products were transformed into chemically competent *E. coli* TOP10 cells (Invitrogen) and transformants selected with ampicillin (100 µg/ml) and positive colonies (Figure 7.16A, B) were grown overnight in L broth supplemented with ampicillin at 37°C under shaking conditions for both constructs.

The plasmids were then isolated from these colonies and the insertion of *gtf* genes were checked by restriction with *HindIII* for pET15b*gtf3* which was expected to give two bands at 803 bp and 5920 bp and *XhoI* and *NdeI* for pET15b*gtf1* which was also expected to give two bands at 895 bp and 5952 bp which confirmed the insertion process (Figure 7.16C) and these plasmids were then checked by sequencing and after the sequence confirmation the positive colonies and the empty vector were grown in *E. coli* TOP10 cells as described above (Figure 7.16D).

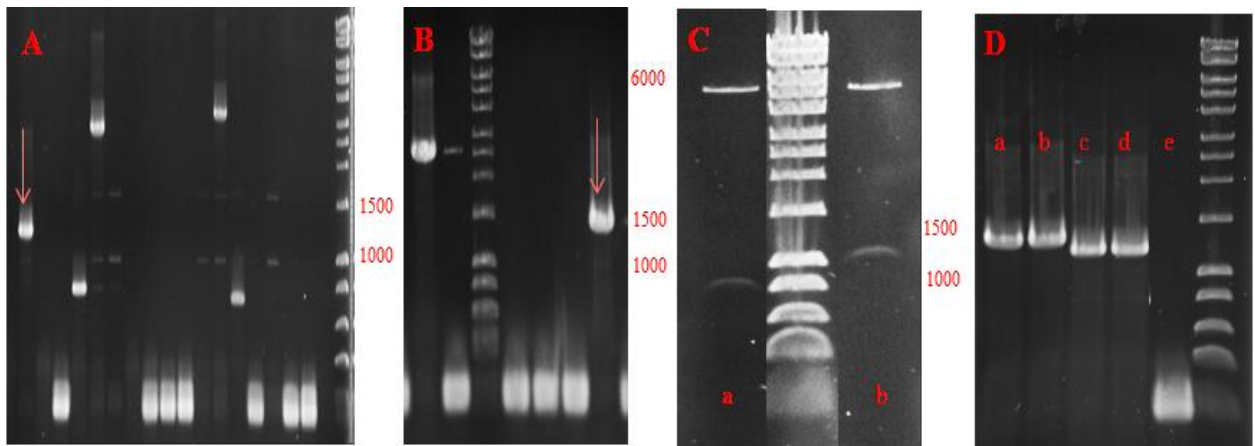


**Figure 7.16.** Agarose gel (0.8% w/v) showing A-B) Red arrows shows the positive transformants of *E. coli* TOP10 cells for the ligation of *gtf3* and *gtf1* into pET15b, respectively; C) Lane a; Restricted pET15b*gtf3* with *HindIII*, lane b; Restricted pET15b*gtf1* with *XhoI* and *NdeI*, D) Colony PCR of *E. coli* TOP10 cells which confirms the presence of right constructs; lane a-b) pET15b*gtf3*, lane c-d) pET15b*gtf1* and lane e) pET15b.

These constructs, pET15b*gtf3* and pET15b*gtf1* (Figure 7.17A) and the empty vector (negative control) and pET15bCD27L [337] as a positive control were transformed for expression into chemically competent *E. coli* BL21 (DE3) cells (Invitrogen) (Figure 7.17B). Additionally, pET15b*gtf2*, pET15b*gtf4*, pET15b*gtf5* and pET15b*Glf* were subcloned into pET15b by Dr Melinda Mayer (IFR) and transformed into *E. coli* BL21 (DE3) cells for the expression purposes.

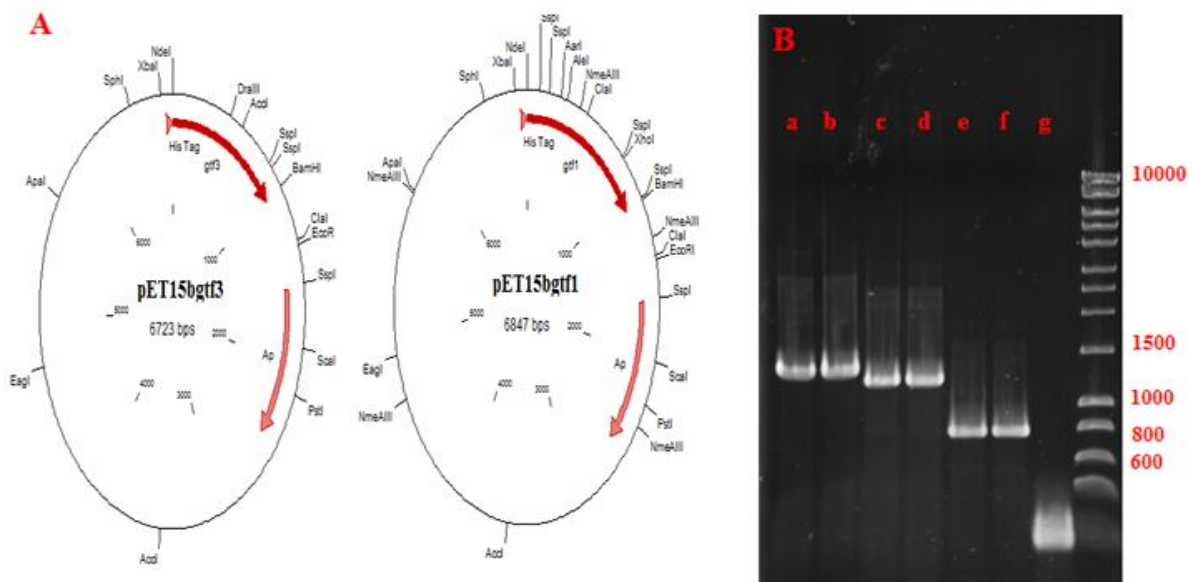


**Figure 7.17.** A) Scheme of the pET15b*gtf3* and pET15b*gtf1*; B) Agarose gel (0.8% w/v) showing colony PCR after the transformation of lane a-b, pET15b*gtf3*; lane c-d, pET15b*gtf1*; lane e-f, pET15bCD27L as a positive control; lane g, pET15b into *E. coli* BL21 (DE3) cells with primers T7P2 and T7T.

These two proteins, gtf3 and gtf1, were then expressed in *E. coli* as His-tagged proteins, giving a product of c. 41.2 kDa and c. 45.2 kDa, respectively which were not identifiable in the crude extracts (Figure 7.18A). In order to optimise the production of these two putative glycosyltransferases, *E. coli* cells were induced for different time points, in different final volumes and several different methods including sonication and using extraction reagent were applied for the extraction of these proteins (Figure 7.18C & 7.19).

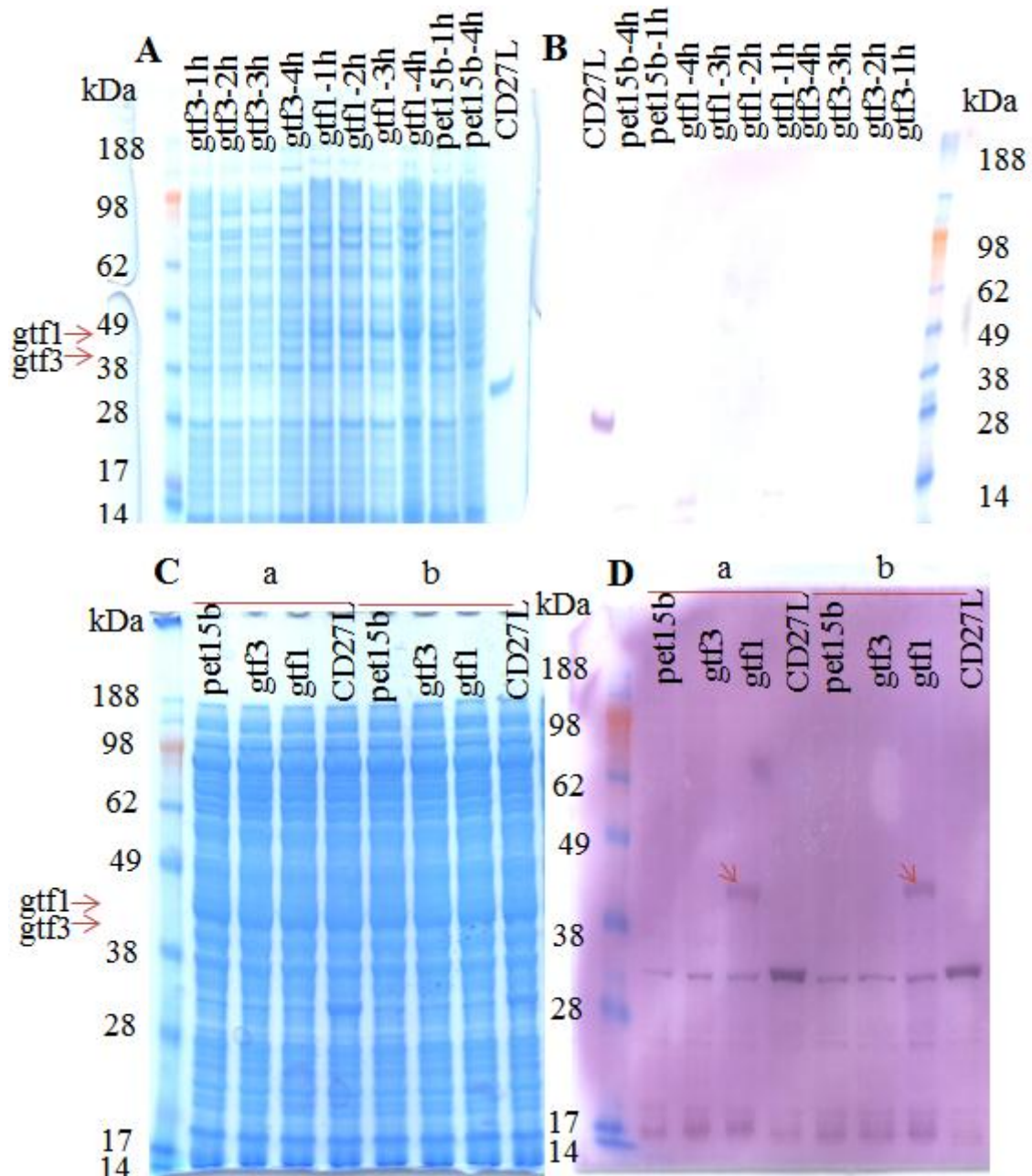


**Figure 7.18.** (A) Expression of gtf3 and gtf1 in *E. coli*. SDS-PAGE analysis of the crude protein lysates (10  $\mu$ l) from *E. coli* expressing pET15bgtf3, pET15bgtf1 and empty pET15b as a negative control induced for 1 to 4 h with the purified protein of CD27L as a positive control after extraction with 20 mM Tris-HCl pH 7.5, 50 mM NaCl (Buffer 2),

(B) Western analysis of the crude extracts from panel A with 6x-His antibody, (C) Same constructs with panel A but crude proteins were extracted by sonication from *E. coli* cells which were induced for 4 h a; 10  $\mu$ l, b; 20  $\mu$ l loaded, (D) Western analysis of the crude extracts from panel C with 6x-His antibody. Red arrows show the His-tagged gtf1.

But none of them were successful in terms of yield improvement and observe them as a visible protein band in the SDS-PAGE protein gels. Similarly, Western analysis of the 1 to 4 h induced samples showed no positive response to these proteins after the hybridization with the anti-His-tag antibody but the positive control, purified CD27L, showed a positive signal showing that the Western hybridization method was working (Figure 7.18B). These negative results suggested that the bead-beating extraction method may not be suitable for the maximal extraction of these proteins after lysing *E. coli* cells, so we replaced this method with the sonication methodology. Similar to the bead-beating method for the extraction of the proteins, there was no difference in the protein gel after sonication between the negative control and the putative glycosyltransferases expressed samples suggesting the poor expression of these proteins (Figure 7.18C) in comparison to the efficiently expressed CD27L. But, the expression of the gtf1 was confirmed by the positive signals in the Western analysis of crude proteins from different starting volumes after hybridization with the His-tag antibody when proteins were extracted by sonication (Figure 7.18D). In contrast, there was no positive signal to a His-tag protein from *E. coli* cells expressing gtf3.

In order to eliminate the problems in the expression of these putative glycosyltransferases, *E. coli* cells were induced with a fresh stock of IPTG solution and an overnight induction was performed at 37°C in 20 ml and 100 ml final volumes and proteins were extracted by sonication (Figure 7.19). Another approach to eliminate the extraction problems was taking account the possibility of these expressed proteins to be insoluble in cell cytoplasm and using the Bugbuster protein extraction reagent which is suitable for preparing high purity inclusion bodies during the extraction process (Figure 7.19). Nevertheless, there was no difference in the protein gels regardless of the methods used and the proteins were still not visible (Figure 7.19A). However, probing these crude proteins with the His-tag antibody in Western analysis showed a positive signal to gtf1 but not gtf3 when the overnight expression occurred in 20 ml final volume while the positive signal was observed to gtf3 but not gtf1 in 100 ml final volume (Figure 7.19B). Additionally, there was no positive signal to these proteins in the Western analysis of the crude proteins extracted with the Bugbuster protein extraction reagent (Figure 7.19B). Overall, several different approaches and techniques were performed to confirm and optimise the expression of these putative glycosyltransferases in *E. coli* cells and

these results showed that these proteins were expressed as His-tagged proteins and they were soluble in the extraction conditions but their yields were low.

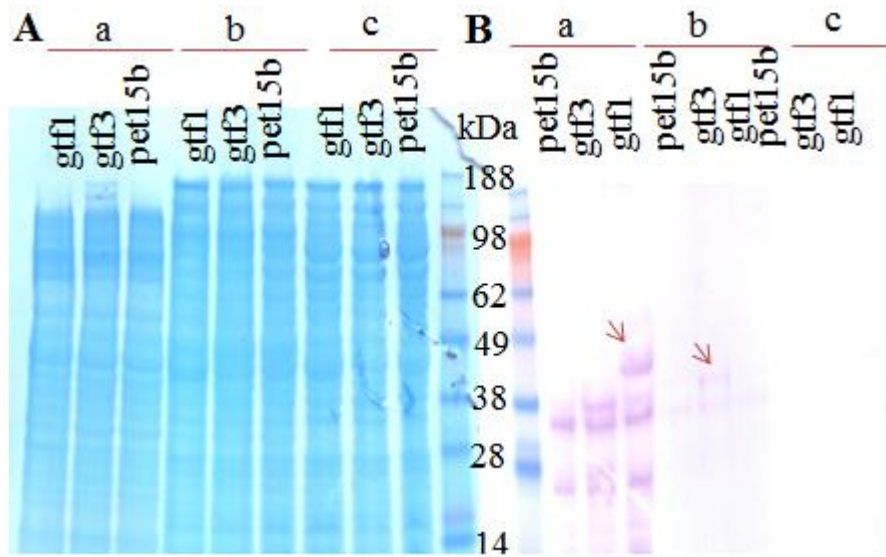


**Figure 7.19.** (A) SDS-PAGE analysis of the crude protein lysates *E. coli* expressing pET15b1176, pET15b1178 and empty pET15b as a negative control extracted from overnight induced cells in 20 ml (a) and 100 ml (b) final volumes by sonication and with BugBuster Protein Extraction Reagent (c), (B) Western analysis of the crude extracts from panel A with 6x-His antibody.

Furthermore, the constructs that were prepared for the other three putative glycosyltransferases gtf5, gtf4 and gtf2 and the Glf mutase were expressed in *E. coli* as His-tagged proteins, giving an expected product of c. 41.33 kDa, c. 33.205 kDa, c. 41.5 kDa and c. 44.6 kDa, respectively (Figure 7.20A). The resulting proteins displayed an apparent molecular weight consistent with that predicted for the His-tagged proteins which were visible in the crude extracts and hybridized to a His-tag antibody (Figure 7.20B).

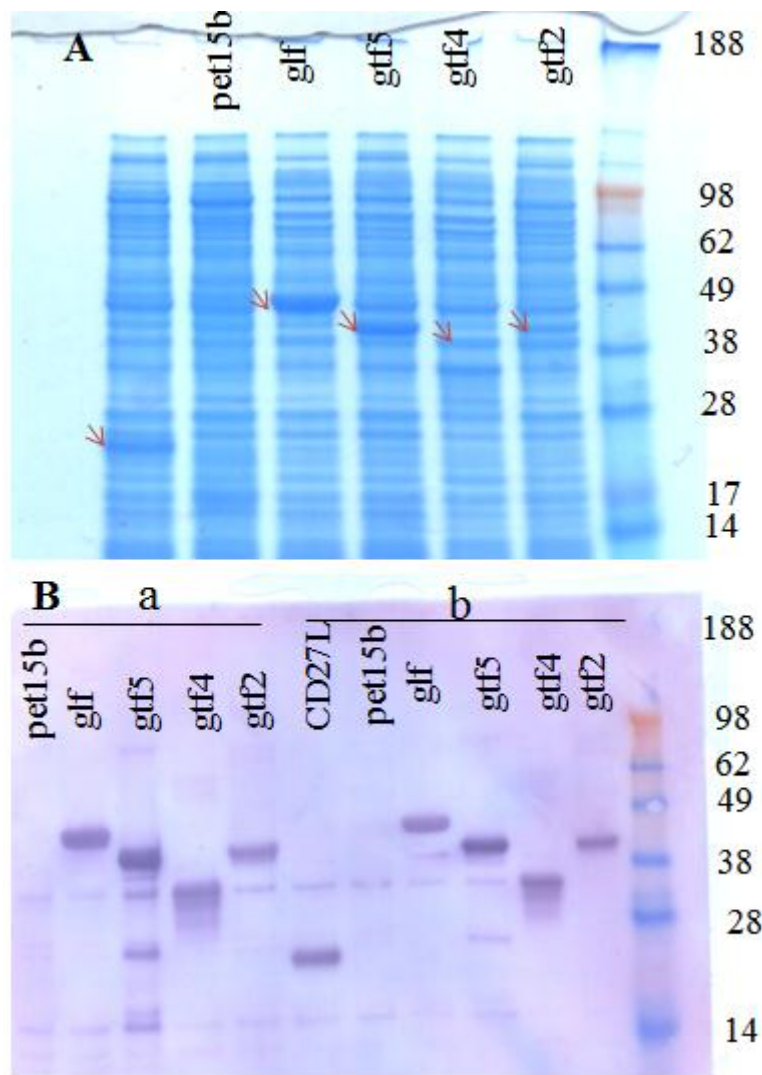


**Figure 7.20.** (A) Expression of gtf2, gtf4, gtf5 and Glf in *E. coli* induced for 4 h at 37°C, cells were lysed by sonication for protein extraction. SDS-PAGE analysis of the crude protein lysates from *E. coli* expressing pET15bgtf2, pET15bgtf4, pET15bgtf5, pET15bGlf and pET15bCD27L as a positive control or empty pET15b as a negative control. Red arrows show the expected proteins. (B) Western analysis of the crude extracts from panel A with 6x-His antibody; a, b, 20, 10 µg of protein lysates were used, respectively.

In order to partially purify the Hig-tagged proteins from the *E. coli* crude extracts, Ni-NTA columns were used (Figure 7.21A-D). The Ni-NTA-purification methodology resulted in the partial purification of gtf5, gtf2 and gtf1 but the rest of the expressed proteins (gtf4, gtf3 and Glf) were not visible in the final eluates although they were visible in the lysates and flow through fractions (Figure 7.21A-D). To further purify the proteins and increase the concentrations of the partially purified proteins, FPLC methodology was used as an alternative approach as described in Material and Methods (see section 7.2.4). Several attempts were performed in 2 l cultures in order to purify these six proteins by FPLC, but

only in three of them (Glf, gtf4 and gtf1) the final FPLC chromatogram showed the protein peaks related to the His-tagged proteins and these proteins were collected (Appendix 8). These three proteins were then visualised in a protein gel but only Glf and gtf4 were visible as partially purified proteins but not gtf1 (Figure 7.21E).

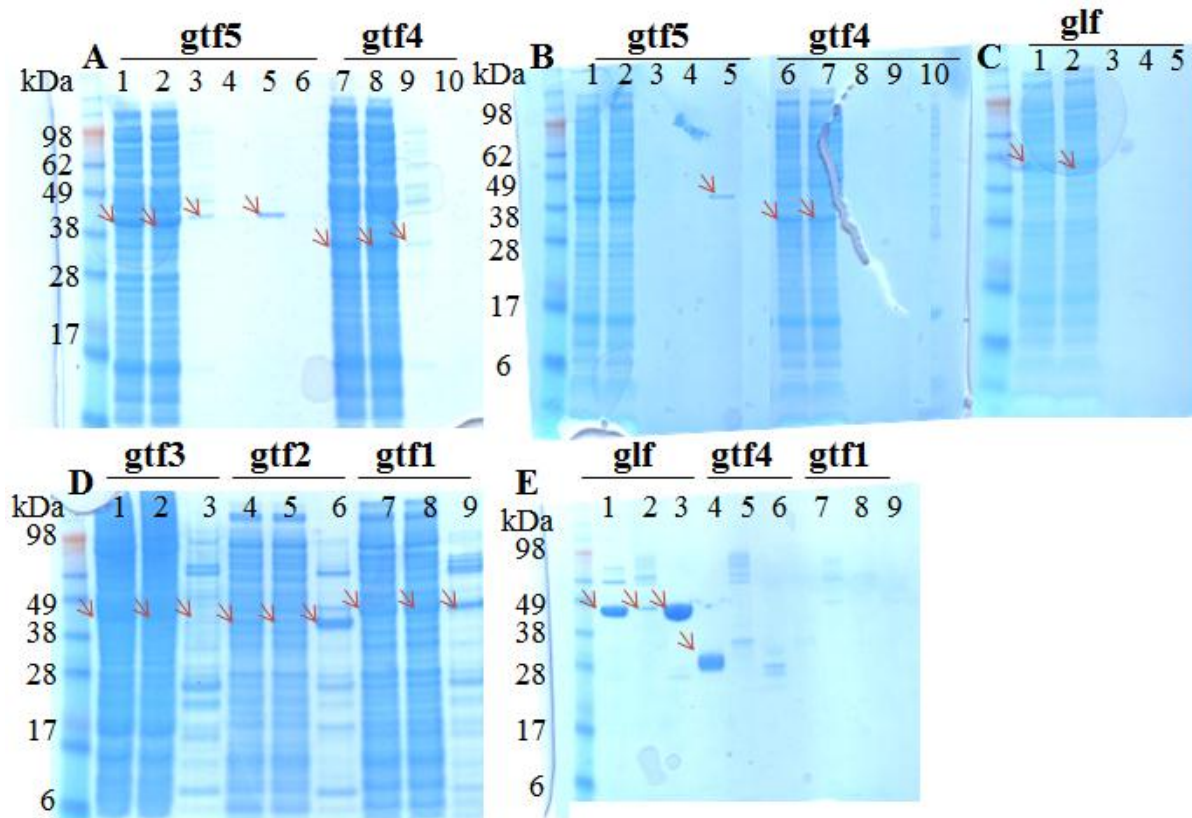


**Figure 7.21.** Expression of putative glycosyltransferases in *E. coli*. SDS-PAGE analysis of NiNTA-purified protein lysates from *E. coli* expressing pET15bGtf and pET15bGlf constructs; A) Lane 1, lysate; lane 2, flow through fraction; lanes 3-4 wash fractions, lanes 5-6 eluates from *E. coli* expressing pET15bgtf5, lanes 7-10; unsuccessful purification of gtf4; B) SDS-PAGE analysis of NiNTA-purified protein lysates from panel A except sonication was used for the extraction of the proteins; C) unsuccessful purification of Glf protein with the NiNTA column method; lane 1, lysate; lane 2, flow through fraction; lanes 3-4 wash fractions, lane 5 eluate; D) Lane 1, lysate; lane 2, flow through fraction; lane 3 eluate from *E. coli* expressing pET15bgtf3; Lane 4, lysate; lane 5, flow through fraction; lane 6 eluate from *E. coli* expressing pET15bgtf2; Lane 7, lysate; lane 8, flow through fraction; lane 9 eluate from *E. coli* expressing pET15bgtf1; E) SDS-PAGE analysis of FPLC purified protein lysates; lanes 1-2-3, final eluates from *E. coli* expressing pET15bGlf; lanes 4-5-6, final eluates from *E. coli* expressing pET15bgtf4; lanes 7-8-9 final eluates from *E. coli* expressing pET15bgtf1. Red arrows show the expected proteins in each panel.

Although the peaks related to the His-tagged proteins were present in the chromatograms of the other three proteins (gtf5, gtf3 and gtf2) but their presence could not be detected via SDS-PAGE. The partial purification of these proteins was not pursued further.

### 7.3.4 Glf mutase activity tests

Glf mutase is thought to be involved in the conversion of the UDP-Galp to UDP-Galf (Figure 7.22). An *in vitro* enzyme assay was performed in order to understand the role of the putative Glf protein with purified Glf and crude Glf extracts.

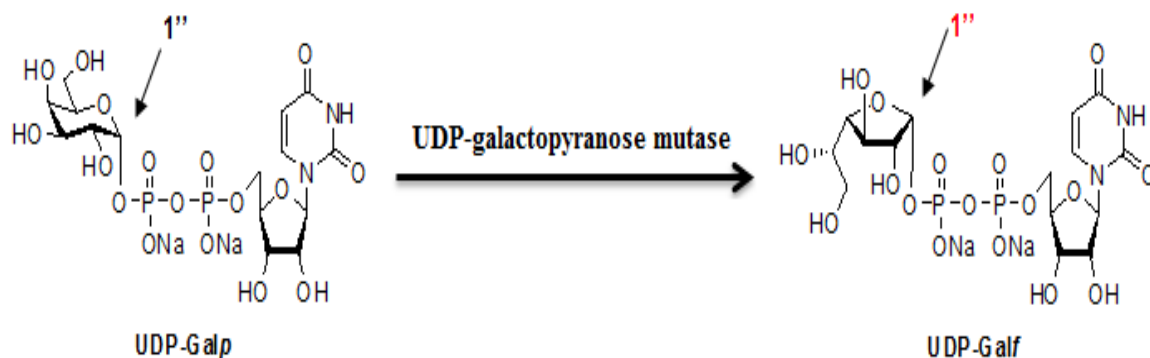


**Figure 7.22.** Conversion of the UDP-Galp to UDP-Galf by Glf mutase. 1'' indicates the conversion of the pyranose form to furanose form.

The conversion of the commercial UDP-Galp to UDP-Galf was monitored by  $^1\text{H}$  NMR spectra after incubation of enzyme reaction at  $37^\circ\text{C}$  at different time points. A shift in the  $^1\text{H}$  NMR spectra of the UDP-Galp was expected due to the resonance of the H atom after the formation of 5-membered ring form from the 6-membered pyranose ring and this shift was monitored at different time points. Additionally, a mutase from *K. pneumoniae* which was confirmed by *in vitro* assays previously [338] was used as a positive control in these enzyme assays.

There was no difference in the  $^1\text{H}$  NMR-spectra of the control sample and the enzyme assay sample containing the crude Glf mutase after 4 h incubation at  $37^\circ\text{C}$  (Figure 7.23). The substrate UDP-Galp was not converted at all with the crude Glf mutase. Additionally, the concentration of the Glf mutase in the enzyme assay was doubled and the enzyme assay was performed overnight at  $37^\circ\text{C}$  and the  $^1\text{H}$  NMR-spectra was recorded but similarly there was still no conversion of the substrate UDP-Galp (data not shown). Similarly, the enzyme reactions were performed with the purified mutase from *K. pneumoniae* (positive control), but there was also no sign of the conversion of galactopyranose to galactofuranose after incubation overnight at  $37^\circ\text{C}$  (data not shown).

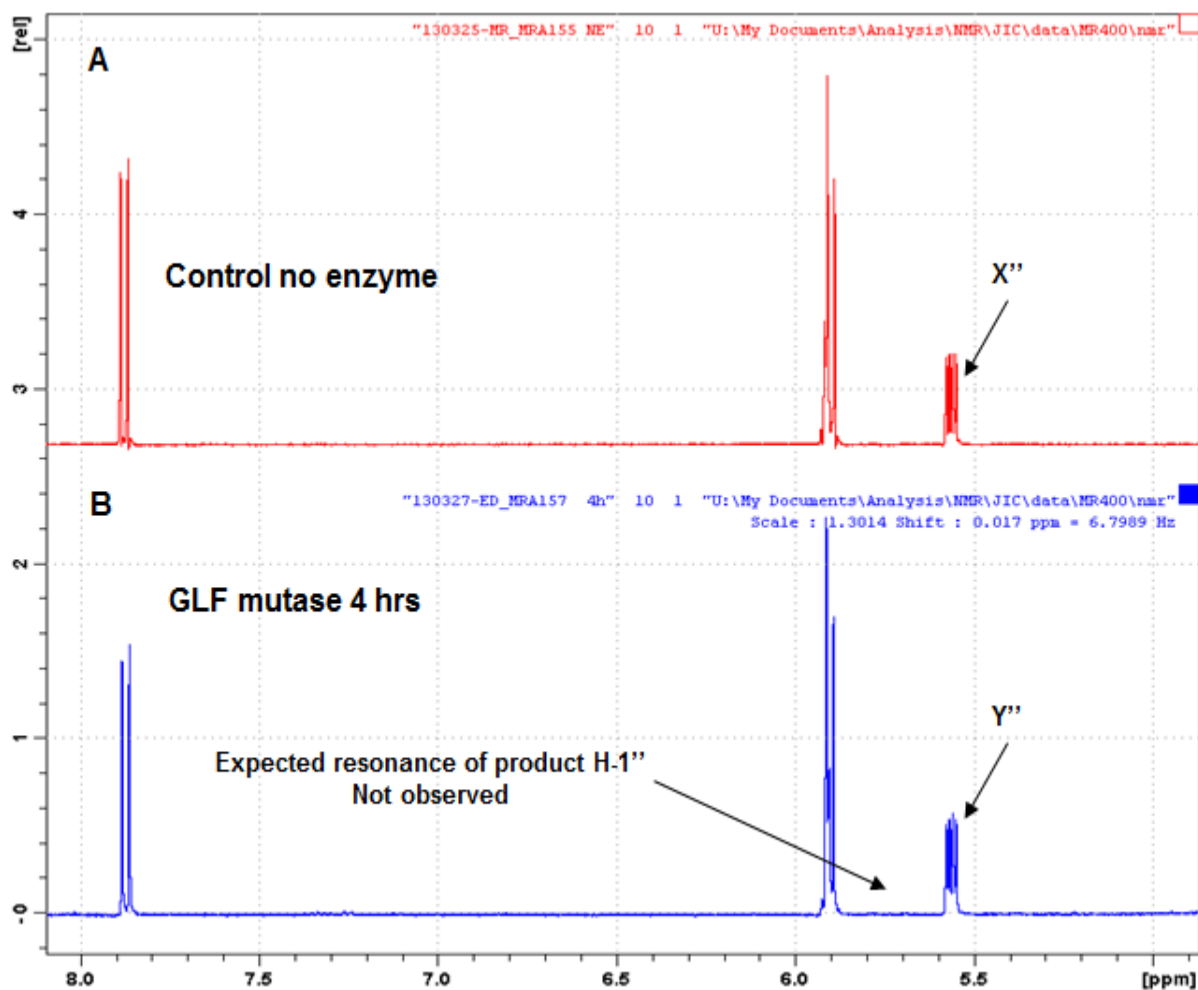


**Figure 7.23.**  $^1\text{H}$  NMR-spectra of the reaction products of the UDP-galactopyranose mutase assays; A) negative control with no enzyme, B) Enzyme assay with the crude Glf mutase after 4 h incubation at  $37^\circ\text{C}$ . (X, Y'' indicates the signal of the UDP-Galp).

The mutase assay was also performed with the purified mutase (Figure 7.24). Analysis of the purified mutase by SDS-PAGE revealed a single protein with a molecular mass of approximately 44.6 kDa (Figure 7.21E). The purified protein was incubated with UDP-galactopyranose for 0.5 and 6 hours and the potential conversion was analysed by NMR spectroscopy. After 6 h incubation there was around 4% shift in the spectra of the UDP-Galp (Figure 7.24A). But this shift was also detected in the negative control sample which only contains the substrate UDP-Galp (Figure 7.24B). The spectra of the enzyme reactions from the purified protein and the negative control were almost identical (Figure 7.24B). We proposed that this alteration in the spectra of UDP-Galp may have originated from the spontaneous intraconversion of UDP-galactose to galactose-1-phosphate (Figure 7.24A). The result of the mutase activity test was inconclusive and the enzyme assays were not pursued further.

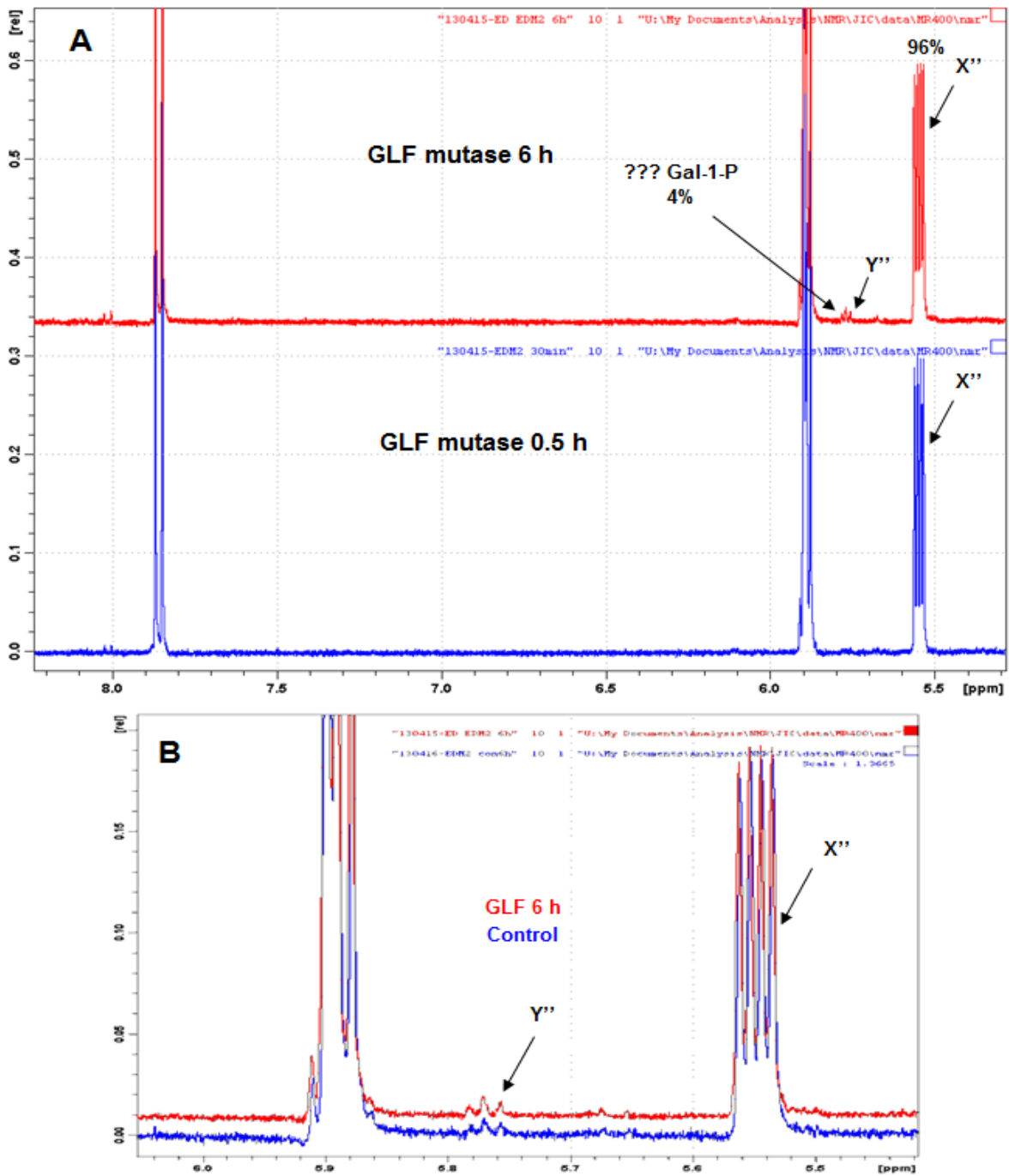


**Figure 7.24.** A)  $^1\text{H}$  NMR-spectra of the reaction product of the purified UDP-galactopyranose mutase assays after 0.5 h and 6 h incubations at  $37^\circ\text{C}$ ; B) Comparison of the  $^1\text{H}$  NMR-spectras of the purified UDP-galactopyranose mutase assay incubated for 6 h and the negative control incubated 6 h at  $37^\circ\text{C}$ . (X'' indicates the signal of the UDP-Galp and Y'' indicates the 4% chemical shift in the signal of UDP-Galp which was also detected in the control sample).

### 7.3.5 Biochemical characterisation of putative glycosyltransferases

To investigate the function of the putative glycosyltransferases in the biosynthesis of the EPS repeating units, *in vitro* enzyme assays were performed with the available donor and acceptor substrates. The first reaction was ED-1 (see 7.2.5) where UDP- $\alpha$ -D-Glucose and Octyl  $\beta$ -D-Lactoside were the donor and the acceptor molecules, respectively, with the expected product trisaccharide:  $\alpha$ -Glc $p$ -(1 $\rightarrow$ 4)- $\beta$ -Gal $p$ (1 $\rightarrow$ 4)- $\beta$ -Glc $p$ -(1 $\rightarrow$ 6). The crude *E. coli* BL21 (DE3) cell extracts of each construct which were induced to overproduce 6 $\times$ His-GTFs and the pET15b vector control were used for the enzyme reactions. All five crude constructs plus the purified gtf4 protein (by Ni-NTA) and the negative control (pET15b vector only) together with the donor and the acceptor molecules were incubated at 37 $^{\circ}$ C for different time points and 5  $\mu$ l of each reaction mixtures were subjected to thin-layer chromatography (TLC) analysis. Incubation of the crude GTF proteins gave a potential new product in comparison to the no enzyme control and crude extract from the negative control harbouring pET15b only (Figure 7.25, spot c).

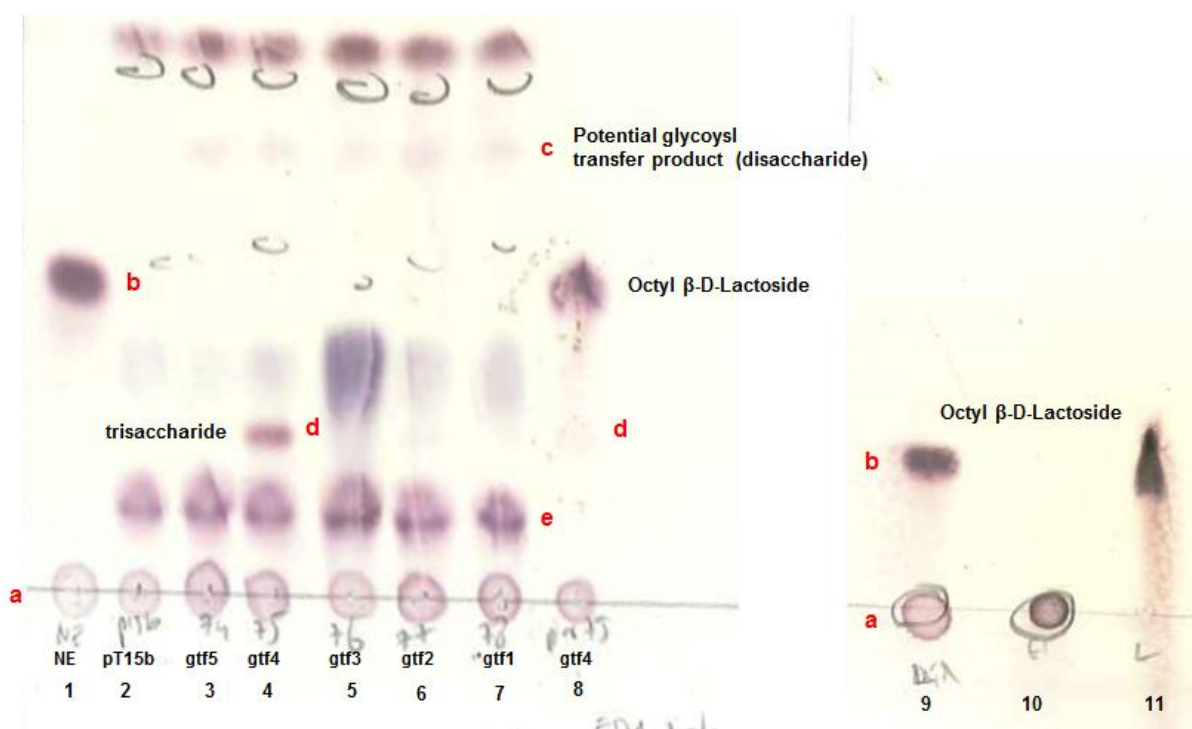


**Figure 7.25.** TLC analysis of ED-1 reactions with putative GTFs. Lane 1; reaction mixture with no enzyme showing the spots for (a) UDP-Glc and (b) octyl-lactoside. Lanes 2-8: ED-1 reaction mixtures with crude cell extracts of pET15b (negative control), gtf5, gtf4, gtf3, gtf2, gtf1 and purified gtf4, respectively; spots (c) show the potential glycosyl transfers (to form a potential disaccharide) that were observed in reactions of crude cell extracts of each protein except pet15b negative control and the purified gtf4, all *E. coli* cell extracts also showed spots (e) related to the contaminants originating from *E. coli* cells. A strong (d) spot occurred

only in the reaction mixture of gtf4 crude protein (lane 4), this spot (d) was also very weak but still observable in the reaction mixture of purified gtf4 which can be the expected trisaccharide, also the acceptor (b) octyl-lactoside was observed in the reaction mixture of purified gtf4 but with a significantly lower intensity than the control sample (lane 8). Lane 9: no enzyme control with donor and acceptor molecules only. Lane 10: UDP-Glucose. Lane 11: octyl-lactoside. Activity assays were performed at 37°C for 20 h.

The aim of TLC analysis was to observe the formation of the trisaccharide in ED-1 reaction which has lower retention factor ( $R_f$ ) value than the disaccharide acceptor Octyl  $\beta$ -D-Lactoside (Figure 7.25, spot b). This new product (spot c) ran further than the acceptor molecule suggesting that it may be another disaccharide molecule but not the expected trisaccharide. From this TLC plate, we speculated that this product may show the glycosyl transfer from the donor UDP-Glucose to the monosaccharide glucopyranoside which occurred as a product after the hydrolysis of Octyl  $\beta$ -D-Lactoside by the host *E. coli* galactose hydrolase enzyme. Figure 7.26 summarizes the potential enzymatic activities in the reaction mixtures of crude protein extracts examined here.

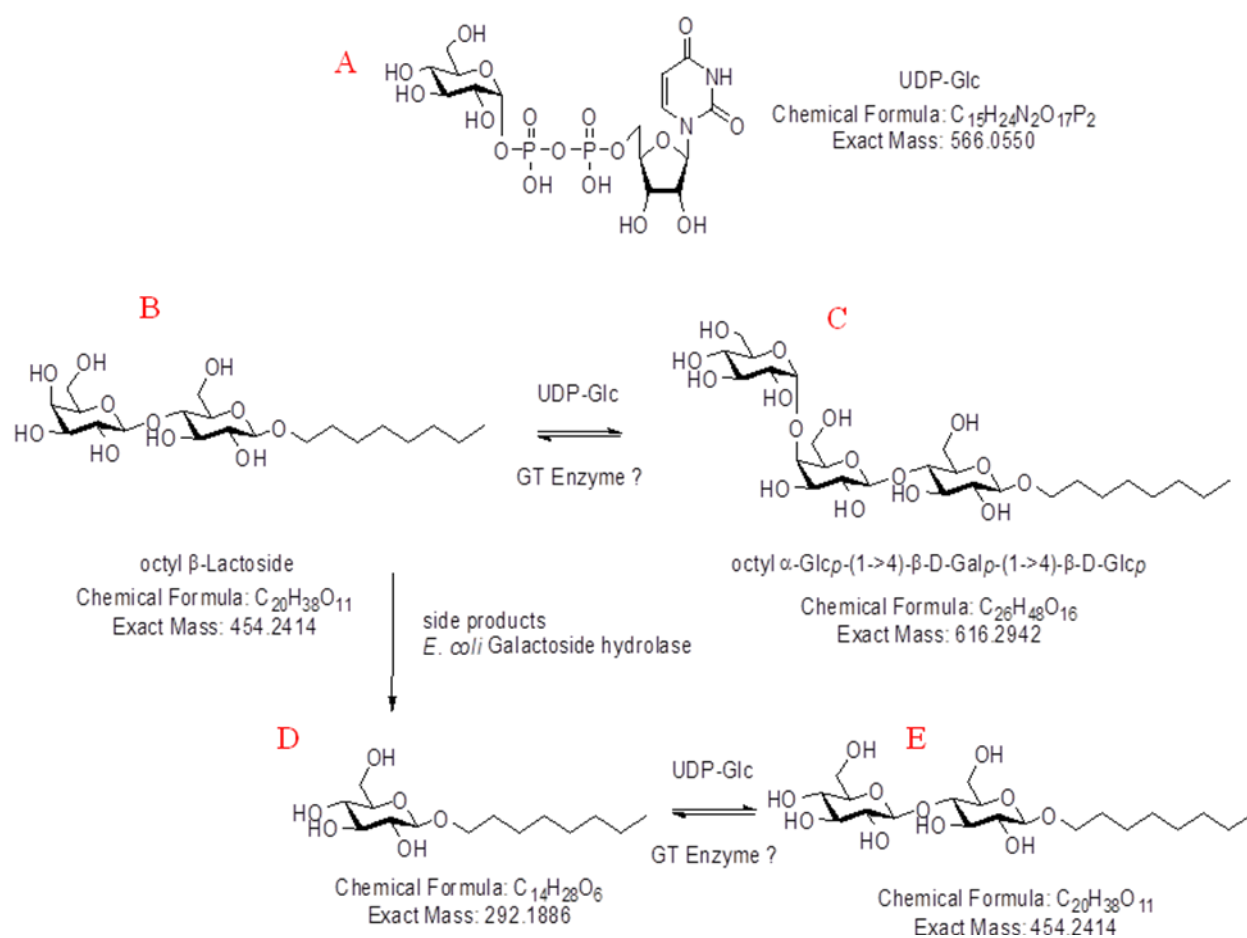


**Figure 7.26.** Schematic representation of activity assay in ED-1 reaction mixture with the crude GTF proteins from *E. coli* cell lysates: A) donor, UDP-Glc; B) acceptor, octyl-

lactoside; C) trisaccharide as a result of the glycosyl transfer by GTFs; D) glucopyranoside, side product of the reaction formed from the lactoside by the *E. coli* galactoside hydrolase; E) potential disaccharide formed after the glycosyl transfer from UDP-Glc to the glucopyranoside by GTFs and their exact masses.

Nevertheless, this was not our final expected product in ED-1 reaction. Importantly, another new product (Figure 7.25, spot d) was obtained from the reaction mixture of gtf4 crude protein and the purified gtf4, respectively, which was absent in the other samples which suggested the formation of the trisaccharide after the glycosyl transfer to the disaccharide acceptor Octyl  $\beta$ -D-Lactoside by gtf4 (Figure 7.25). This new product was observed as a very clear spot in the crude gtf4 reaction mixture in comparison to the weak spot in the purified gtf4 reaction mixture which had lower  $R_f$  value than disaccharide as expected. Importantly the intensity of the spot for Octyl  $\beta$ -D-Lactoside reduced in the purified gtf4 sample compared to the no enzyme control sample which suggested the consumption of this product in order to form the trisaccharide unit by gtf4. We also ran the UDP-  $\alpha$ -D-Glucose (Figure 7.25, spot a) and Octyl  $\beta$ -D-Lactoside together and each molecule individually but none of them showed production of the new spot which suggest that it can be potentially the trisaccharide molecule in the EPS repeating unit of *L. johnsonii* FI9785.

In order to confirm the presence of the potential products on TLC plates, all reaction mixtures were subjected to LC-MS analysis. Firstly, the exact masses of the donor UDP- $\alpha$ -D-Glucose, acceptor molecule Octyl  $\beta$ -D-Lactoside and the expected trisaccharide and the potential side product glucopyranoside were calculated from their chemical formulae which were 566.055, 454.2414, 616.2942 and 292.1886, respectively and these products were detected for all ED-1 reactions in the mass spectrometer in negative electrospray mode. The acceptor Octyl  $\beta$ -D-Lactoside was easily observed in the MS spectra of the no enzyme control sample in which more than one peak was generated with different retention times at this mass that may represent different isomers of Octyl  $\beta$ -D-Lactoside (Figure 7.27A3). We also detected the exact masses of the potential products in ED-1 reaction mixture (Figure 7.26) in the MS spectra of no enzyme control sample (Figure 7.27A). Although there were several peaks at the exact mass of the potential trisaccharide in the MS spectra of no enzyme control sample which were not appreciable but a reasonable peak with a retention time of 7 min that was in detection limit also generated (Figure 7.27A2). This peak might have originated from the impurities in the reaction buffer that might have the same exact mass with the final trisaccharide molecule in ED-1 reaction mixture. Similarly the exact mass of the glucopyranoside was also detected with two reasonable peaks at retention times 7.27 and 7.35

min, respectively, but these peaks were more likely represented side products that were formed after the ionisation of Octyl  $\beta$ -D-Lactoside (Figure 7.27A1).

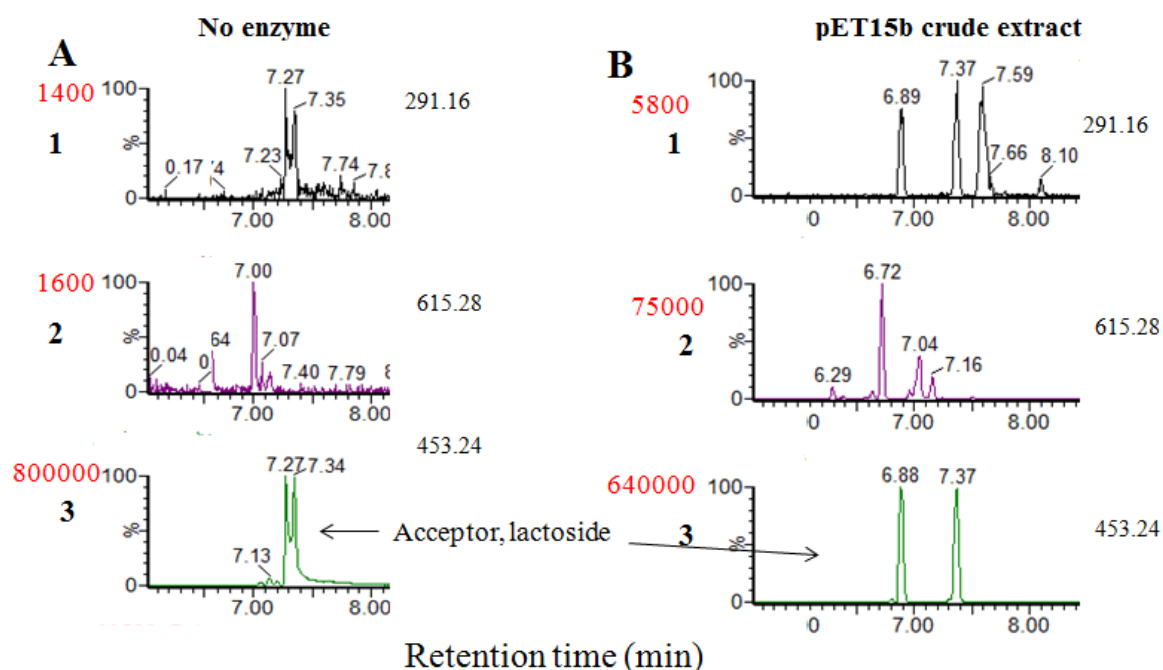


**Figure 7.27.** Negative electrospray ionisation LC-MS chromatogram of reaction mixture ED-1 with A) no enzyme as a control showing several insignificant peaks and a reasonable peak for glucopyranoside at exact mass of 291.16 (1) and trisaccharide at exact mass of 615.28 (2), respectively and showing the presence of lactoside at exact mass of 453.24 (3); B) crude pET15b extract generated some peaks for the glucopyranoside at exact mass of 291.16 (1) and trisaccharide at exact mass of 615.28 (2) and confirmed the presence of lactoside (3). Numbers in red at the left corner of each panel represents the intensity.

The similarity of the retention times and the appearance of the peaks detected in the exact masses of both glucopyranoside and Octyl  $\beta$ -D-Lactoside support this hypothesis. Nevertheless the detection of the exact masses of the potential products of ED-1 reaction was unexpected in the no enzyme control sample. It should also be noted that the intensities of the peaks at the exact masses of both potential trisaccharide and the glucopyranoside was significantly low. Secondly we detected the exact masses of these three products in the MS spectra of pET15b control sample (Figure 7.27B). The acceptor lactoside generated two clear peaks with retention times of around 6.88 and 7.37 min, respectively. Similar to the spectra of the no enzyme control sample two peaks at the same retention times with the isomers of lactoside generated in the exact mass of the glucopyranoside in pET15b control sample but there were additional peaks with different retention times suggesting the formation of glucopyranoside from acceptor lactoside by the action of *E. coli* galactoside hydrolases or suggesting the presence of some products with same exact mass of glucopyranoside in the *E.*

*coli* cell extracts (Figure 7.27B1). Additionally, several peaks were also detected at the exact mass of the potential trisaccharide molecule in the ionic spectra of pET15b control sample due to the extra resolution of the MS which probably originates from the cell extract of *E. coli* cells and the reaction buffer or different forms of the trisaccharide which is a very weak potential with respect to the spots on TLC plates (Figure 7.27B2).

These three products were also detected in the MS spectra of ED-1 reaction mixtures of crude GTF extracts and the purified gtf4. Figure 7.28 shows the negative electrospray ionisation LC-MS chromatogram of reaction mixture ED-1 incubated with the crude extracts of gtf5 (A) and gtf3 (B), respectively. The acceptor Octyl  $\beta$ -D-Lactoside generated two peaks with similar retention times in both samples which was identical to the spectra of pET15b control sample (Figure 28A3&B3).

As noted previously (see 7.25) several spots generated on the TLC plates of ED-1 reaction mixtures of crude GTF extracts which were absent in the vector only sample suggested the formation of potential disaccharide molecules in ED-1 reaction mixture but no difference was detected at the exact mass of 453.24 in the spectra of vector only and gtf5 and gtf3 crude extracts (Figure 28). Similarly there was no difference between the spectra of crude gtf5 and gtf3 ED-1 reaction mixtures and vector only sample in terms of the peaks generated for the potential trisaccharide and the glucopyranoside (Figure 7.28A&B). Additionally, no difference was detected in the spectra of ED-1 reaction mixtures of crude gtf2 and gtf1 in comparison to the spectra of vector only sample (data not shown).

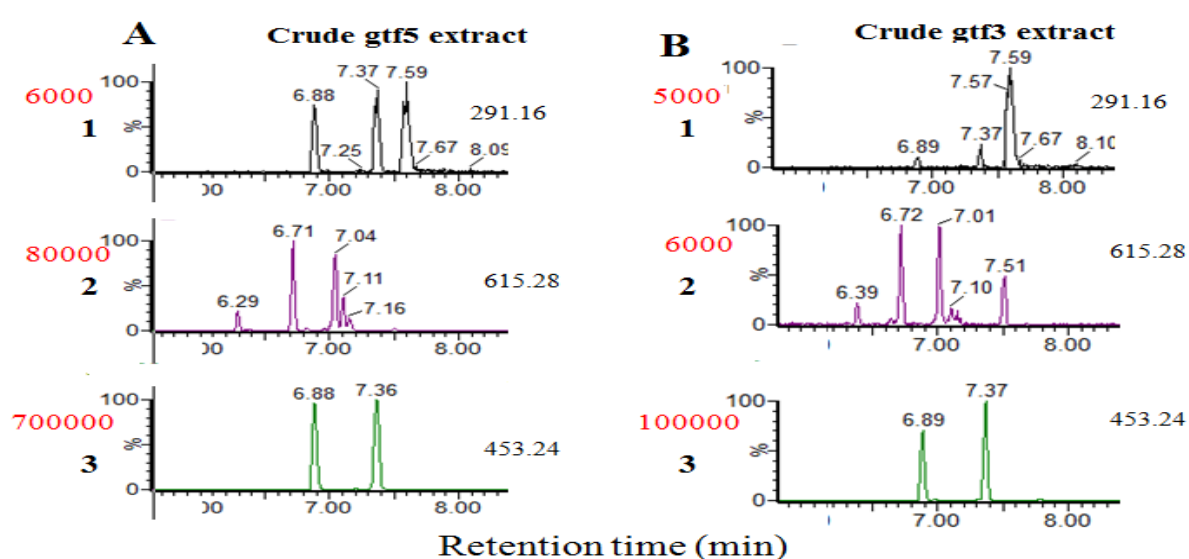


**Figure 7.28.** Negative electrospray ionisation LC-MS chromatogram of reaction mixture ED-1 containing A) crude protein of gtf5 from *E. coli* lysate generated some peaks for the

glucopyranoside at exact mass of 291.16 (1) and trisaccharide at exact mass of 615.28 (2) and confirmed the presence of lactoside (3), respectively; B) containing crude protein of gtf3 from *E. coli* lysate generated some peaks for the glucopyranoside at exact mass of 291.16 (1) and trisaccharide at exact mass of 615.28 (2) and confirmed the presence of lactoside (3), respectively. Numbers in red at the left corner of each panel represents the intensity.

It should be noted that although there were some potential spots on the TLC plates of the samples from the crude extracts, there was no difference in the MS spectra of samples either containing pET15b or crude extracts. These results show that the GTF assay was inconclusive for ED-1 reaction for crude proteins of gtf5, gtf3, gtf2 and gtf1 indicating that the conditions examined there was no clear evidence of glycosyltransferase activity in these crude extracts.

Incubation of the ED-1 reaction mixture with the crude protein of gtf4 as well as the partially purified protein gtf4 resulted in a new spot on TLC plate which was not present in other samples as shown previously (Figure 7.25). These samples were also subjected to LC-MS analysis (Figure 7.29).

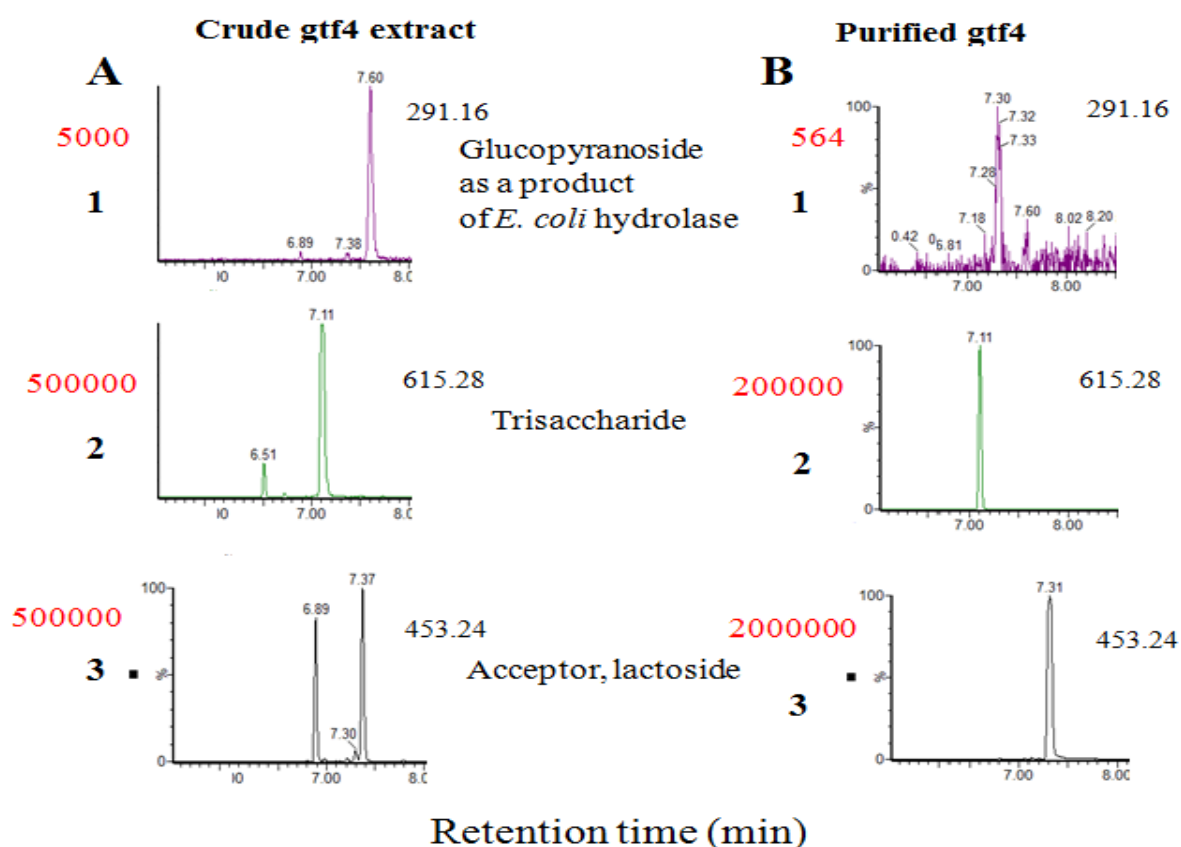


**Figure 7.29.** Negative electrospray ionisation LC-MS chromatogram of reaction mixture ED-1 containing A) crude protein of gtf4 from *E. coli* lysate showing glucopyranoside at exact mass of 291.16 (1), the expected trisaccharide at exact mass of 615.28 with two peaks (2) and the acceptor molecule at exact mass of 453.24 (3); B) purified gtf4 protein showing the lack of glucopyranoside at exact mass of 291.16 (1), a clear single peak for finally trisaccharide

molecule at exact mass of 615.28 (2) and the acceptor molecule at exact mass of 453.24 (3). Numbers in red at the left corner of each panel represents the intensity.

The acceptor lactoside was observed with two peaks in the crude gtf4 ED-1 reaction mixture as was the same with the other reaction mixtures including the pET15b control with the same retention time interval which was 6.89 and 7.37 min, respectively (Figure 7.29A3). In contrast, only one peak was generated for the acceptor lactoside in the spectra of the purified gtf4 reaction mixture in which the absence of the second peak might be due to the consumption of the lactoside as an acceptor in the formation of the trisaccharide (Figure 7.29B3). But this was not that clear as two different peaks were generated for lactoside in the crude gtf4 ED-1 reaction mixture where the exact mass of the trisaccharide was also detected (Figure 7.29A3). The exact mass of the expected trisaccharide molecule was detected with two peaks which were appeared with different retention times (6.51, 7.11) compared to the control samples in the spectra of gtf4 crude extract (Figure 7.29A2). The peak at 6.51 min retention time disappeared in the spectra of gtf4 purified protein for the trisaccharide molecule but a strong clear peak at 7.11 min generated similar to the crude gtf4 sample (Figure 7.29B2). Interestingly, several peaks were detected at exact mass of 291.16 for the glucopyranoside in the spectra of crude gtf4 sample which was absent in the spectra of purified gtf4 sample supporting the prediction of the formation of this monosaccharide by the potential function of the *E. coli* galactoside hydrolase in the crude extracts (Figure 7.29). This result also supports the proposed enzymatic activities summarized in Figure 7.26. Overall, both spectra of crude and purified gtf4 reaction mixtures generated clear peaks at exact mass of 615.28 which corresponds to trisaccharide (octyl  $\alpha$ -Glc $p$ -(1 $\rightarrow$ 4)- $\beta$ -Gal $p$ (1 $\rightarrow$ 4)- $\beta$ -Glc $p$ -(1 $\rightarrow$ 6) molecule (Figure 7.29A2&B2). This result was also in agreement with the TLC data where a new spot before the disaccharide was formed in gtf4 crude protein and gtf4 purified protein samples (Figure 7.25). In fact this spot was isolated from the TLC plate and subjected to LC-MS analysis but the chromatogram was blank suggested that the isolation process was not successful (data not shown).

We can clearly speculate that the new spot was showing the formation of the trisaccharide on the TLC plate. As a summary, these results may indicate that gtf4 is a potential glycosyltransferase which can use Octyl  $\beta$ -D-Lactoside as an acceptor substrate for the addition of the glucose residue from the donor substrate UDP- $\alpha$ -D-Glucose by forming an  $\alpha$ -1,4 bond. But future characterisation is definitely required in order to confirm the function of this enzyme as an  $\alpha$ (1,4)-GlcT. Although gtf4 is the 5<sup>th</sup> glycosyltransferase gene in the *eps*

cluster of *L. johnsonii* FI9785 (Figure 1.12), *gtf4* as a possible glycosyltransferase enzyme was potentially able to transfer a glycosyl residue to the last two sugar residues in the EPS-2 repeating unit structure of *L. johnsonii* FI9785 (Figure 3.6).

The second assay reaction examined was ED-2 where UDP- $\alpha$ -D-Glucose (Mass; 566.055) and Octyl  $\beta$ -D-glucopyranoside (Mass; 292.1886) were the donor and the acceptor molecules, respectively, in order to form the following disaccharide in the repeating unit of EPS-2:  $\alpha$ -Glc $p$ -(1 $\rightarrow$ 3)- $\beta$ -Glc $p$  (Mass; 454.2414). All five crude GTFs plus the purified *gtf4* protein, the negative control as well as *L. johnsonii* FI9785 cell extract as a positive control together with the donor and the acceptor molecules were incubated at 37°C for different time points and 5  $\mu$ l of each reaction mixtures were subjected to TLC analysis (Figure 7.30A).

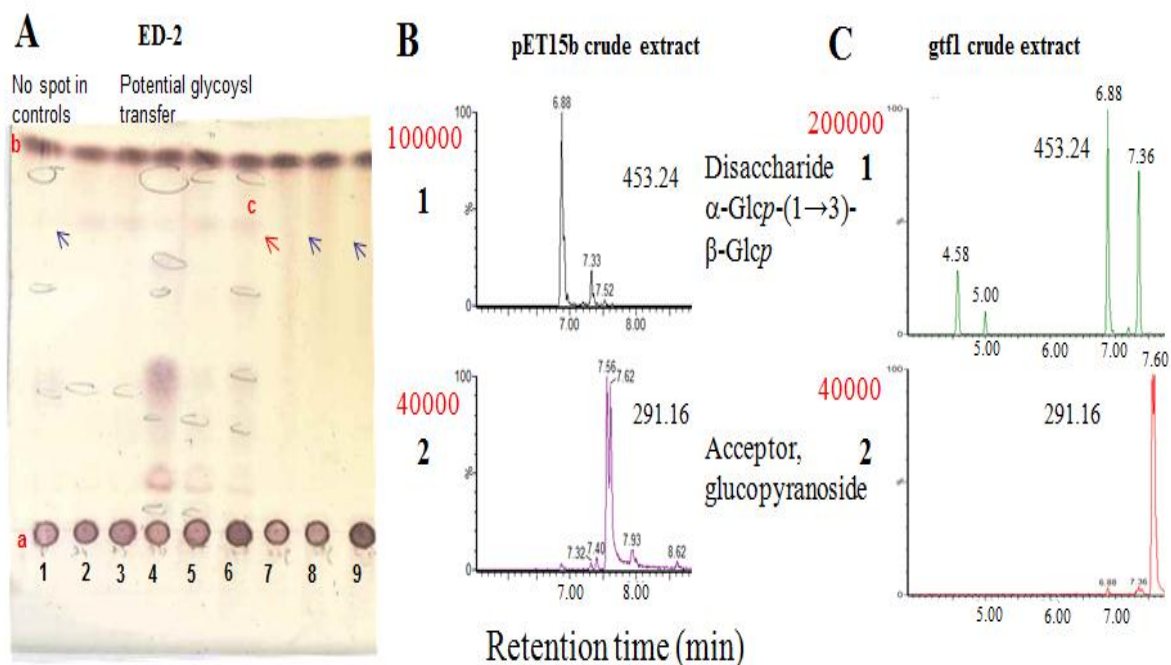


**Figure 7.30.** A) TLC analysis of ED-2 reactions with putative GTFs. Lane 1; reaction mixture with no enzyme showing the spots for UDP-Glc (spot a) and Octyl  $\beta$ -D-glucopyranoside (spot b), lane 2-6: ED-2 reaction mixtures with crude cell extracts of *gtf5*, *gtf4*, *gtf3*, *gtf2* and *gtf1*, respectively; spots before the acceptor molecule (spot c) may show the potential glycosyl transfer reactions which were not observed in the negative control sample harbouring pET15b, lane 7: ED-2 reaction mixture with crude cell extract of pET15b, lane 8: ED-2 reaction mixture with lysate of *L. johnsonii* FI9785, lane 9: ED-2 reaction mixture with purified *gtf3*. Activity assays were performed at 37°C for 20 h. B) Negative electrospray ionisation LC-MS chromatogram of reaction mixture ED-2 assayed with crude extract harbouring pET15b which shows 1) several peaks at the exact mass of the potential disaccharide molecule 2) a strong peak at the exact mass of the acceptor glucopyranoside. C) Negative electrospray ionisation LC-MS chromatogram of reaction mixture ED-2 assayed with *gtf1* crude cell extract which shows 1) several peaks at the exact mass of the potential

disaccharide molecule 2) a strong peak at the exact mass of the acceptor glucopyranoside. Numbers in red at the left corner of each panel represents the intensity.

Incubation of the crude GTFs with the donor and the acceptor molecule in ED-2 reaction resulted in some new spots (spot c) before the acceptor substrate on TLC plates (Figure 7.30A). But this spot was missing in the no enzyme control sample and more importantly in the crude extract of pET15b control sample which suggested that these new spots may be a result of glycosyl transfer from the donor molecule to the acceptor molecule by the function of GTF proteins (Figure 7.30A). Similarly the additional spot was not observed for the cell extract of *L. johnsonii* and purified gtf4 protein. An unpredicted strong spot in the reaction mixture of crude gtf3 appeared on the TLC plate which was potentially originated from the *E. coli* cell lysate harbouring pET15bgtf3 as this spot was detected in all TLC plates of crude gtf3 extract (data not shown).

To further investigate and confirm the potential products in the ED-2 reaction mixtures, all samples were subjected to LC-MS analysis. Although there was no new spot in the pET15b control sample on TLC plate, three peaks, which were in the exact mass of the disaccharide product, were generated in the LC-MS analysis of this sample (Figure 7.30B1). The expected disaccharide was also detected in the crude gtf1 ED-2 reaction mixture but not with three peaks with four peaks compared to the pET15b sample. The additional peak can be the result of the glycosyl transfer reaction in ED-2 reaction mixture as a function of the gtf1 as a glycosyltransferase (Figure 7.30C1). Furthermore the disaccharide product was also detected with more than three peaks with different retention times in the crude extracts of all GTF proteins (data not shown). Although there was no new spot for pET15b on the TLC plate where new spots were formed for crude extracts and there were clear differences between the LC-MS chromatograms of control and crude extract samples, the overall result with the crude cell extracts was inconclusive as the disaccharide molecule was also observed in the pET15b control sample with similar peaks. There is a potential that all these GTFs might transfer a glycosyl residue from the donor substrate UDP- $\alpha$ -D-Glucose to the acceptor Octyl  $\beta$ -D-glucopyranoside but it requires further characterisation with the purified enzymes.

The third reaction was ED-3 where UDP- $\alpha$ -D Galactose (Mass; 566.055) and Octyl  $\beta$ -D-glucopyranoside (Mass; 292.1886) were the donor and the acceptor molecules, respectively, in order to form the following disaccharide in the repeating unit of EPS-2:  $\beta$ -Galp(1 $\rightarrow$ 4)- $\beta$ -Glc<sub>p</sub>. The fourth reaction was ED-4 where UDP- $\alpha$ -D-Glucose (Mass; 566.055) and Octyl  $\alpha$ -D-glucopyranoside (Mass; 292.1886) were the donor and the acceptor molecules,

respectively, in order to form the following disaccharides in the repeating unit of EPS-1:  $\alpha$ -Glc $p$ -(1 $\rightarrow$ 2)- $\alpha$ -Glc $p$  or  $\alpha$ -Glc $p$ -(1 $\rightarrow$ 6)- $\alpha$ -Glc $p$ . The TLC analysis and the LC-MS analysis were conducted as described above with the crude extracts in both reactions. The results were similar to the results of ED-2 reaction; new spots appeared in crude GTF protein samples but not the pET15b control sample on TLC plates but the peaks related to the disaccharide molecules were generated in both pET15b control samples and the crude GTF samples in LC-MS analysis (data not shown). Overall the results for ED-3 and ED-4 were inconclusive. The purification of the GTFs was essential for the activity test due to the background effect of the *E. coli* lysates. However this was not pursued further due to the time limitations.

## 7.4 DISCUSSION

*L. johnsonii* FI9785 produces two novel EPS which are the homopolymeric EPS-1 (glucan) and the heteropolymeric EPS-2 (hexasaccharide with four glucose and two galactose residues) and the putative priming GTF, epsE, which is the first GTF in the *eps* cluster is crucial for the biosynthesis of EPS-2. Additionally the *eps* cluster which harbours six putative *gtf* genes is somehow responsible for the biosynthesis of both EPS as we showed previously (see Chapter 5). The proposed biosynthesis mechanism of the EPS repeating unit structure is the sequential addition of the each sugar monomer to the growing sugar chain by the responsible GTF [8]. In fact, this theory corresponds to the fact that the *eps* cluster of *L. johnsonii* FI9785 contains six GTFs and the repeating unit of the EPS-2 is composed of six sugar residues and the deletion of the priming GTF resulted in the loss of this hexasaccharide. In order to understand the function of each GTFs in the biosynthesis of EPS, deletion mutants were constructed by targeted mutagenesis in each GTF of *L. johnsonii* FI9785, individually. The attempts to create deletion mutants only succeeded in the second and the fourth GTFs despite repeated trials. Deletion of these two GTFs resulted in no alteration neither in the EPS repeating unit structure nor in the EPS production levels in comparison to the wild type strain and did not change the overall pathway. The lack of these GTFs might have been compensated by the functions of other GTFs which resulted in no alteration in EPS metabolism. This might be achieved by a bispecific feature of the GTFs which is the ability to transfer two different substrates to the growing EPS chain. In fact, it was previously proposed that some glycosyltransferases may have bifunctional roles which give them the ability to add different monomers to the acceptor substrates [245]. Moreover, several other bacterial glycosyltransferases which play a role in the cell wall biosynthesis of bacteria were

also shown to have bifunctional roles [329, 330]. Previously, it was reported that a glycosyltransferase encoded in the *eps* cluster of *S. thermophilus* Sfi6 might catalyse both GalNAc and Gal transfer reactions under different host conditions [339]. More recently, it was shown that a glycosyltransferase (Wcrl) encoded in the *cps* locus of *Streptococcus pneumoniae* serotype 11D has a bifunctional role; it can transfer  $\alpha$ -Glucose or  $\alpha$ -GlcNAC, or both of them to the growing CPS chain [340]. Additionally, it was also demonstrated that a single amino acid change in a pneumococcal glycosyltransferase resulted in the capability of transferring both galactose and glucose by this glycosyltransferase to the CPS chain [341]. The pneumococcal capsule is one of virulence factor for the pathogenicity of *S. pneumoniae* and so far nearly one hundred capsular serotypes were reported for this pathogen and this bacterium can alter the composition of its capsule and generates different serotypes to escape from vaccine control via mechanisms related to glycosyltransferases mentioned above [97, 342].

The EPS-2 structure of *L. johnsonii* FI9785 consists of both Galactopyranose (Galp) and Galactofuranose (Galf) residues in its repeating unit structure. The biosynthetic precursor of Galf in the EPS pathway is believed to be UDP-Galf which is converted from UDP-Galp by a specific UDP-galactopyranose mutase described as Glf [338]. In the final step, a transferase which has a high specificity to the galactofuranose adds this nucleotide sugar to the EPS repeating unit [334]. The activity assays with the putative Glf protein of *L. johnsonii* FI9785 were inconclusive and no conversion of UDP-Galp to UDP-Galf with the purified Glf protein or the crude extract was observed. However, the Glf protein of *L. johnsonii* FI9785 shows 62% amino acid identity with the biochemically characterised Glf protein from *E. coli* K12 [334]. Furthermore, the *eps* cluster harbours a putative galactofuranosyltransferase (*FI9785\_1174*) which is predicted to transfer UDP-Galf to the EPS chain by forming a  $\beta$ -1,6 bond [33]. In fact the Galactofuranose residue is linked with a  $\beta$ -1,6 bond in the EPS-2 structure. Taking all this together, most probably the *glf* gene can encode the UDP-galactopyranose mutase of *L. johnsonii* FI9785 but most likely the assay conditions used to observe the conversion with the purified or crude Glf protein were not optimal. Previously, it was reported that the conversion rate of Galp to Galf by Glf of *E. coli* K12 was around 6-9% under *in vitro* conditions and the authors proposed that the enzyme contains a flavin cofactor that was the reason for the yellow color of the purified protein, which can be important for the enzymatic activity. Later on, the mutase from *K. pneumoniae* was shown to require coenzymes NADH or NADPH for its enzymatic activity and the yellow color was also

mentioned for this mutase [338]. Following this study, the first crystal structure of UDP-galactopyranose mutase from *E. coli* was reported and shown that for the mutase activity the flavin cofactor must be in a reduced state [335]. Although the color of the crude or purified Glf protein was yellow (data not shown), the Glf protein might have lost the flavin cofactor during the expression and purification process or the Glf might have not integrated with the coenzymes and the cofactor which can be the reason for the inconclusive activity assays. Nevertheless, the function of the Glf protein of *L. johnsonii* FI9785 seems to be promising and the fact that even the positive control, mutase from *K. pneumoniae*, did show no activity; further optimisation of the assay condition may give the results.

The structure of EPS-1 and EPS-2 gives some clue about the catalytic function of the glycosyltransferases expressed by *L. johnsonii* FI9785. The homopolymeric EPS-1 is composed of glucose units with 1-6 and 1-2  $\alpha$  glycosidic bonds which shows that the novel GTF enzyme is a processive retaining enzyme that adds the glucose units to the growing chain. The identified *eps* gene cluster harbours six putative glycosyltransferases, some of them are retaining enzymes as EPS-2 contains  $\alpha$  glycosidic bond and in contrast some of them are inverting enzymes due to the presence of the  $\beta$  glycosidic bonds in the EPS-2 structure. The putative glycosyltransferases from *L. johnsonii* were cloned, then heterologously expressed and activity assays were performed using synthetically available donor and acceptor molecules mimicking the natural conditions for the biosynthesis of EPS repeating units. The GTF activity assays which were performed with the crude extracts were inconclusive except ED-1, in which a potential GTF activity was observed, due to the potential background GTF activity of *E. coli* BL21 (DE3) cells although previously *E. coli* BL21 crude extracts were used in GTF activity assays and no background GTF activity was reported [89]. Another limitation in the GTF activity assays was the lack of some synthetic donor and acceptor molecules such as UDP-Galf. In fact we would overcome this problem and mimic the absolute conditions in EPS biosynthesis with a cloning strategy that includes the subcloning of GTFs in a step by step process with an order in groups like *gtf1*, *gtf1-gtf2*, *gtf1-gtf2-gtf3* and then using the reaction products from previous reactions as an acceptor with the new GTF constructs as previously reported [89, 343]. Nevertheless, by using the heterologous expression of single GTFs, potential glycosyl transfer reactions were shown and importantly we proposed that *gtf4* is a potential  $\alpha(1,4)$ -GlcT. So far, several glycosyltransferases from LAB have been biochemically characterised using different acceptor molecules to form different glycosidic linkages [86, 89, 135, 343, 344]. However, to

the best of our knowledge this is the first report describing a potential  $\alpha(1,4)$ -GlcT transferring glucose from the donor UDP-Glucose to the Octyl  $\beta$ -D-Lactoside acceptor molecule by forming an  $\alpha$ -1,4-glycosidic bond from LAB and its heterologous expression. Although *gtf4* is the fifth GTF in the *eps* cluster of *L. johnsonii*, potentially it did not transfer a sugar monomer to complete the pentasaccharide structure in the EPS-2 repeating unit. Similarly, the priming GTF is the putative undecaprenyl-phosphate galactosephosphotransferase but the first sugar in the EPS repeating unit of EPS-2 is potentially glucose. Furthermore, the EPS-2 consists of Galf residue which is the third sugar residue in the EPS-2 repeating unit although only the last putative glycosyltransferase, *gtf5*, shows homology to genes encoding galactofuranosyltransferases [33]. It can be speculated that the repeating unit structure may not represent the order of the putative glycosyltransferases encoded in the *eps* clusters. Actually, it was demonstrated that although the order of four genes encoded in the *eps* cluster of *S. thermophilus* Sfi6 was *epsE*, *epsF*, *epsG* and *epsI* but the *in vitro* enzyme activities of the four glycosyltransferases showed that the catalytic order was *epsE*, *epsG*, *epsI* and *epsF* in the tetrasaccharide repeating unit biosynthesis which suggests that the order of the glycosyltransferases in the *eps* cluster might not always show their biochemical order [93]. But, previously it was also shown that the order of the glycosyltransferases encoded in the *eps* cluster of *L. helveticus* was also the order of the enzyme reactions for the biosynthesis of the EPS repeating unit and was also in agreement with the fact that each GTFs add the sugar monomer to the growing EPS chain sequentially to form the final structure [89]. Notably, the EPS production can be more complex than the sequential addition of each sugar monomer to the growing EPS chain depending on the strain and specific conditions. For instance, recently four different capsular polysaccharide clusters were identified in one *L. plantarum* strain in which second and fourth clusters harboured all functional genes for the capsular polysaccharide biosynthesis while the remaining two clusters lacked the genes for the chain length determination region and the priming glycosyltransferases although they contained several glycosyltransferase encoding genes. Deletion of the first cluster resulted in alteration in EPS composition but deletion of the other three clusters did not change the final EPS structure, although an important decrease in the final EPS production levels was observed [46].

In summary, this chapter described the unchanged EPS structure of *L. johnsonii* FI9785 after the deletion of the two putative glycosyltransferase encoding genes. More importantly, a potential  $\alpha(1,4)$ -GlcT was shown to be functional for the first time in LAB. Enzyme assays of

other glycosyltransferases and the Glf mutase was promising but not conclusive and future work is required for their characterisation. Overall, these observations will help the understanding of the biosynthesis mechanism of EPS and so their functional roles on probiotic related properties.

# Chapter 8

---

## Conclusions and Future Directions

## 8.1 CONCLUSIONS AND FUTURE DIRECTIONS

In the work presented in this thesis, we have studied the biosynthesis mechanism of EPS accumulated at the cell surface of a probiotic bacterium, *Lactobacillus johnsonii* FI9785. The structure analysis, genetics and biochemical characteristics of EPS production as well as its role in physiological and physicochemical properties of *L. johnsonii* FI9785 have been addressed. In addition we have also characterised the role of EPS in the *in vivo* passage and persistence properties of *L. johnsonii* FI9785.

*L. johnsonii* FI9785 switched its rough colony morphology to a smooth form after a spontaneous mutation in the *epsC* gene which is a putative protein kinase that is a member of the phosphoregulatory system together with *epsB* and *epsD* proposed to be involved in determining the chain length of the final EPS. Interestingly, this mutant again altered its phenotype to a rough colony morphology after complementation with the wild type *epsC* gene as previously reported [33]. In this study, we found that the EPS production in the smooth mutant increased in comparison to the wild type but interestingly the EPS production in the complemented smooth mutant which regained a rough colony morphology was also increased. These results suggest that the colony morphology can be related to the EPS production but not only the quantity but also the quality of the EPS accumulation regarding the final EPS chain length is important for the colony morphology. AFM can be the method of choice in order to compare the final chain length of EPS on live cells of these two mutants which may provide additional information about the relationship between EPS accumulation and surface morphology. A number of studies have shown the importance of the protein tyrosine kinases and the phosphoregulatory mechanism in polymerisation and export of the final EPS repeating units where several enzymes have also been identified for phosphorylation targets such as enzymes in the chain length determination region of the *eps* clusters [96, 117, 119] and also the priming glycosyltransferase [120, 345]. Furthermore, it was also reported that dephosphorylation of the protein tyrosine kinases are essential for the regulation of EPS biosynthesis [96, 117]. Although it was shown that inactivation of the phosphotyrosine-protein phosphatase (*epsD*) required for the dephosphorylation of protein tyrosine kinase caused higher CPS attachment to the cell wall in *S. pneumoniae* [346] and deletion of phosphotyrosine-protein phosphatase in *Myxococcus xanthus* resulted in higher EPS production than the wild type [347]. Also several studies reported that deletion of genes from the phosphoregulatory region resulted in reduction or complete abolishment of EPS biosynthesis in different strains [94, 96] suggesting the complexity of the phosphoregulatory

mechanism in EPS biosynthesis. However, there is no report related to the phosphoregulatory mechanism of the EPS production in the genus *Lactobacillus* and comparison of the proteins encoded in the *eps* clusters of the wild type and the *epsC* mutant in terms of phosphorylation patterns would advance our knowledge to underline the role of the phosphoregulatory mechanism of EPS production and could contribute to the increased EPS production strategies. Similarly, deletion of the gene or genes contributing to the phosphoregulatory mechanism of EPS production in *L. johnsonii* would represent major advances in our understanding of this process in LAB.

In Chapter 3, the structure of the EPS produced by *L. johnsonii* FI9785 was analysed and we found that *L. johnsonii* FI9785 is able to produce two types of EPS: homopolymer EPS-1 which is a branched dextran ( $\alpha$ -glucan) with the unusual feature that every backbone residue is substituted with a 2-linked glucose unit and heteropolymer EPS-2 which was shown to have a hexasaccharide repeating unit composed of two galactose and four glucose residues with different types of linkages between each sugar residue. Furthermore EPS-1 and EPS-2 were shown to be partially acetylated. There are several potential hypothetical acetyltransferases related to the biosynthesis of the cell wall of *L. johnsonii* FI9785 [195] which can also be related to the acetylation of the EPS-1 and EPS-2 but future identification is required in order to confirm this. In the context of the gut environment acetylation may provide protection of the EPS from many types of hydrolases produced by gut bacteria. Previously several LAB were shown to produce two different EPS [61, 221, 243] but this is the first time as a comprehensive report showing the structure of two different EPS produced by a LAB. Also it was shown that *L. johnsonii* NCC 533 produced a high molecular weight homopolymer inulin from sucrose [348]. It has been reported that the primary structure of the EPS from a number *L. rhamnosus* strains did not alter under different conditions including carbon source [47] but our preliminary data show that *L. johnsonii* FI9785 is able to produce a third EPS when grown with sucrose as a carbon source under anaerobic conditions. Identification of the role of different carbon sources and environmental conditions on the final EPS structure and EPS production levels of *L. johnsonii* FI9785 will be part of future projects.

The deletion of the putative priming glycosyltransferase gene, *epsE*, resulted in the loss of EPS-2 production but complementation of this gene in the  $\Delta epsE$  mutant restored the EPS-2 production suggesting that *epsE* is probably an undecaprenyl-phosphate galactosephosphotransferase although it has not been shown biochemically. Furthermore

using BLAST analysis, *epsE* was the only putative glycosyltransferase that shows conserved domains related to the priming step in the synthesis of the EPS repeating unit. This observation was in agreement with the recent study which showed the loss of the galactose rich EPS in *L. rhamnosus* GG after deletion of the putative priming glycosyltransferase, while the glucose rich one was still present on cell surface [61]. Nevertheless biochemical characterisation of *epsE* will represent a major advance in identification of the EPS production in *L. johnsonii* FI9785. The alterations in the EPS structures and accumulation levels in *L. johnsonii* FI9785 and its *eps* mutants (Table 1.4) were detected with several techniques including AFM, TEM, FTIR and FCM. We detected and localised the galactose of EPS-2 on live wild type cells and confirmed the removal of EPS-2 from the cell surface of the  $\Delta epsE$  mutant by AFM using a functionalised tip for the galactose residues. In a previous study the cell surface hydrophobicity of lactobacilli was investigated using AFM on live cells [349] and also it was shown that AFM can be applied to the EPS molecules to understand their conformational characteristics [226]. These applications can also be applied to the *L. johnsonii* cells as well as purified EPS molecules which will improve our knowledge of the role of EPS on surface morphology and adhesion properties. In this thesis a good example of the immunodetection of the cell surface alterations on live bacteria was demonstrated by FCM that has recently become an important tool to detect the antibody responses against live bacteria [350]. In this work the capsular EPS layer of *L. johnsonii* was shown to cover the cell surface epitopes on cell surface. In summary, the work presented in Chapter 3 has revealed simultaneous synthesis of two novel polysaccharide structures by *L. johnsonii* FI9785.

The cell wall architecture plays a crucial role in the physicochemical and functional characteristics of lactobacilli cells such as biofilm formation as it interacts with the bacterial environment including its host and determines the *in vivo* communication and adaptation properties [162]. To date the role of the EPS in biofilm formation was mainly focused on pathogenic bacteria in order to develop strategies to eliminate them. Recent studies also showed the role of EPS on biofilm formation of lactobacilli [63, 141, 142, 157]. Previously it was reported that loss of the homopolymeric EPS production in *L. reuteri* 100-21 did not alter the *in vivo* biofilm formation properties [142]. Our observations revealed that an increase in EPS levels had a slightly negative or no effect on biofilm formation while removal of EPS-2 in the  $\Delta epsE$  mutant had little effect compared to the wild type for *in vitro* biofilm formation properties probably due to the fact that cell surface of lactobacilli is highly a dynamic entity

and several molecules on cell surface contributes the biofilm formation properties [162, 256]. Nevertheless a lot of new techniques have emerged for biofilm formation assessments which can be applied to *L. johnsonii* EPS mutants as well as the acapsular mutants together with *in vivo* studies which would improve our knowledge about the role of EPS on biofilm formation of lactobacilli.

The surface properties of lactobacilli determine the interactions with the bacterial environment including the gut ecosystem. Previously it was reported that the physicochemical properties of bacteria, as we assessed by zeta potential measurements and cell surface hydrophobicity can determine the bacterial adhesion to epithelial cells [262]. Our observations were also in agreement with this hypothesis in which increased zeta potential and hydrophobicity after the reduction and alterations in the EPS layer of *L. johnsonii* resulted in higher adhesion to human epithelial cells *in vitro* and vice versa. Similarly, we confirmed the crucial role of the EPS on cell surface characteristics of lactobacilli together with the correlation between hydrophobicity and adhesion properties. But we should also note that in a previous study where several different *Lactobacillus* strains were tested for their adhesion properties to intestinal mucus and no correlation was observed between cell surface hydrophobicity and adhesion ability [351]. The relationship between hydrophobicity and adhesion properties can be strain specific or related to the tissue environment. We can extend our experiments to test the adhesion of *L. johnsonii* strains, which have been proven to have different hydrophobicity, to intestinal mucus as it covers the epithelial cells in the intestine to investigate the role of hydrophobicity in different tissue conditions. Similarly these adhesion experiments can also be applied to the chicken gut explants which would demonstrate the role of EPS related to the probiotic function of *L. johnsonii* and show the interactions with the cell surface in different environments.

Our findings also indicated that EPS plays an important role in aggregation of *L. johnsonii*, which could also be important in the adhesion and colonisation of probiotic strains [189, 190]. The increased aggregation properties as a non-specific factor for the adhesiveness can also be the reason for the increased adhesion to epithelial cells. The reduction of the EPS layer probably resulted in uncovering of aggregation promoting proteins on the cell surface of *L. johnsonii*, which were also shown to be mediators of autoaggregation in lactobacilli previously [63, 189, 192, 193, 269]. In fact the study of aggregation properties of lactobacilli is generally focussed on coaggregation with pathogens which might protect the epithelium from the pathogen adherence [352] and cell surface proteins were also shown to play a role in

this process [267]. So, the interactions of *L. johnsonii* wild type and mutant cells with pathogens such as *C. jejuni* in terms of coaggregation may contribute to the current knowledge about the role of EPS, and also characterisation of the cell surface proteins of *L. johnsonii* with regards to the aggregation properties is certainly required for future applications. In fact the proteolytic enzyme digestions in lactobacilli cells clearly showed the importance of cell surface proteins in cell surface interactions detected by antibody based techniques but future characterisation is crucial. Also this study demonstrated the FCM application as the method of choice for detection of bacterial cell surface changes alterations due to its sensitivity in determining the antibody-antigen saturation. As a summary, the work presented in chapter 4 has demonstrated the role of EPS accumulated at the cell surface of *L. johnsonii* FI9785 on biofilm formation, cell surface characteristics and aggregation and adhesion properties.

In Chapter 5, the essential role of the *eps* gene cluster not only in heteropolymeric EPS-2 production but also for homopolymeric EPS-1 production has been shown. Similarly the crucial role of the *epsA* gene as a putative transcriptional regulator in both EPS-1 and EPS-2 biosynthesis has been demonstrated for the first time for lactobacilli and complementation of this gene confirmed its essential role in EPS biosynthesis of *L. johnsonii* FI9785. Previously it was reported that the deletion of the entire *eps* cluster of *L. johnsonii* NCC 533 resulted in the complete loss of the EPS biosynthesis which is in agreement with our observations here although the structure of the EPS from NCC 533 strain has not yet been determined [62]. We also showed that the biosynthesis of EPS-1 was also dependant on the function of this *eps* cluster which can be either due to the role of a bifunctional glycosyltransferase encoded in this cluster or a novel gene from the genome of *L. johnsonii* FI9785 may be involved in EPS-1 production in conjunction with a gene/s in the *eps* cluster. A single gene described as *gtf* or *ftf* is responsible for the biosynthesis of the homopolymeric EPS in *Lactobacillus* strains [1, 63, 99, 103-105]. But there was no correlation between the identified *gtf* gene products with the gene products both from the *eps* cluster and in the *L. johnsonii* FI9785 genome. Furthermore the EPS-1 structure was also novel among EPS from LAB. Taken together these results suggest that a novel gene either in the *eps* cluster or in the genome of *L. johnsonii* FI9785 can be responsible for the biosynthesis of this homopolymer. Another possibility is two genes may be required for the biosynthesis of this branched dextran: one for chain and one for branch. We developed several strategies in order to demonstrate the role of the putative glycosyltransferases encoded in *eps* cluster which were discussed in Chapter 7 but

they were not successful to show a bifunctional glycosyltransferase. The GTF proteins are composed of a general structure consisting of an N-terminal signal sequence, a variable region, a catalytic domain and a glucan binding domain [48]. Due to the availability of the genome sequence of *L. johnsonii* FI9785, bioinformatics analysis can be conducted in order to find some candidate proteins that might be responsible for the homopolymer EPS-1 production and then cloning and deletion of these genes can be performed. Similarly a proteomics approach such as two-dimensional gel analysis of acapsular mutants and EPS-1 only producer  $\Delta epsE$  mutant may identify a potential candidate protein. Future studies are also required in order to understand the mechanism of the transcriptional regulation and identification of the promoters for the *eps* cluster of *L. johnsonii*. This cluster is probably transcribed as a single polycistronic mRNA as previously reported for the *L. lactis* strain [87] which has a similar genetic organisation with the *eps* cluster of *L. johnsonii* but a recent report showed that two genes in the *eps* cluster of *B. breve* were transcribed monocistronically and rest of the cluster was transcribed polycistronically [66]. It was also reported that the transcriptional of the substantial number of genes which are in the same orientation in the *eps* clusters of four *L. rhamnosus* strains occurred as a single mRNA but the putative transcriptional regulator was suggested to be transcribed separately and shown to have its own promoter [85]. Similarly, not only the genetic conditions of the transcriptional regulation of the EPS production require further investigations but also the effect of environmental conditions such as availability of carbon and non-carbon nutrients, stress and acid, bile salts conditions desire further characterisation as *L. johnsonii* is a member of a complex gut ecosystem. EPS production is a carbon intensive process which requires and competes for available carbon sources as well as sugar nucleotides which are also the major components in cell wall biosynthesis [134]. We observed that over-expression of the putative transcriptional regulator, *epsA*, resulted in the production of double amounts of EPS without any disruption in the cell growth of *L. johnsonii* FI9785. More studies on the EPS biosynthesis and its relationship with the central carbohydrate metabolism of lactobacilli cells can be performed in order to modify and improve the EPS production and over-expression of certain genes either in *eps* clusters or genes functioning in the sugar nucleotide or central carbon metabolism can be a clue for these purposes as we demonstrated for *epsA*.

In chapter 5 we also showed and confirmed that the EPS layer of *L. johnsonii* covers the cell surface antigens detected by anti-wild type polyclonal antibodies. In fact this was also in agreement with the role of the EPS layer of *B. breve* in which the EPS layer showed an

immune silencing effect [66]. The complete loss of the EPS production also resulted in a large increase in the adhesion to human epithelial cells *in vitro* which is probably due to uncovering of the surface adhesins as previously reported [62]. We also confirmed the role of the EPS layer on autoaggregation properties of *L. johnsonii* in which acapsular mutants showed a huge increase in aggregation probably due to the uncovering of aggregation promoting proteins whereas increased EPS production in the  $\Delta epsA::pepsA$  mutant resulted in a strong non-aggregating phenotype. Importantly this strain showed similar adhesion properties as wild type which suggested that autoaggregation is not the only factor determining the adhesion properties. Future studies on characterisation of the aggregation promoting proteins or surface proteins related to adhesion on the cell surface of *L. johnsonii* as well as their role in the antigenic properties of the cell surface will improve the current knowledge for the role of cell surface in probiotic action. For instance the genome of *L. johnsonii* FI9785 encodes putative mucus binding protein genes which can be a good example for future characterisation studies. In summary, the work presented in Chapter 5 has revealed that the EPS production of *L. johnsonii* is dependent on the identified *eps* cluster including the *epsA* gene; furthermore the impact of the EPS layer on adhesion and antigenic properties has been confirmed.

In chapter 6, the physiological role of the EPS accumulated to the cell surface of *L. johnsonii* was determined under *in vitro* conditions and we found that the EPS layer of *L. johnsonii* is a protective shield against different antibiotics and nisin. The contribution of the EPS and its chemical composition on the physiochemical characteristics of cell surface can be a factor for this protection as previously reported [139, 300]. To understand the role of the EPS layer under antibiotic treated conditions in complex gut ecosystem, an *in vivo* or an *in vitro* batch culture model test can be performed which can also be extended for the antimicrobial nisin. Similarly our observations revealed that this layer protects cells against bile salts, acid and temperature changes as well as under *in vitro* digestion conditions. Previously it was reported that *Bifidobacterium animalis* increased its EPS production under bile salts environment probably in order to stimulate its survival [305]. Analysis of the EPS production of *L. johnsonii* under harsh conditions as well as the investigation of the gene expression profiles under these conditions can be performed in order to understand the survival strategy of *L. johnsonii* related to the EPS layer. Although the EPS layer was found to be protective *in vitro*, there was no difference in the passage through the GIT and persistence profiles of wild type and the acapsular mutant in a mouse model. This can be related with the increased

adhesiveness of *L. johnsonii* after the loss of the EPS layer as previously reported [62] but the number of colonies recovered from the colon and caecum samples for wild type and acapsular mutant was similar suggesting that adhesiveness is not the only factor determining the survival of *L. johnsonii* strains during the GIT passage. There were some problems in the colonisation experiments in mice model due to the different *Lactobacillus* strains that were already colonised in mice GI tract. In order to eliminate this problem the resistance of *L. johnsonii* can be determined in different antibiotic combinations or germ free or *Lactobacillus* free mice models can be used for future characterisation of the functions of the EPS layer under *in vivo* conditions such *Lactobacillus* free mice models are available [142]. In fact, it is important to perform such colonisation and persistence experiments as well as pathogen exclusion tests in chicken model with wild type and *eps* mutant strains in order to understand the biological role of the EPS layer related to the probiotic properties of *L. johnsonii*. Similarly in this study several different mutants with different EPS characteristics have been generated which can provide a good model to investigate the immune-modulation properties of EPS under *in vivo* and *in vitro* conditions.

Purified EPS have also been reported for their immuno-modulatory properties [151] and identification of the role of purified EPS-1 and EPS-1-EPS-2 mixture in cytokine production is currently in progress at IFR. Finally there was not a huge alteration in the mice gut microbiota after treatments with wild type and acapsular mutant probably due to the shortness of the experimental period. But interestingly the treatments with *L. johnsonii* cells only induced an increase in the proportion of *Lactobacillales* in the acapsular mutant group while the proportion of this order did not alter in the wild type treated group. In contrast the proportion of *Erysipelotrichales* showed a huge increase only in the wild type treatment group. Previously this order was associated with the SCFA production from polysaccharides [315] and we suggested that the increase in *Erysipelotrichales* observed in the present study may have resulted from a selection toward *Erysipelotrichales* by the EPS when used as the substrate. A recent report revealed that both EPS and the EPS producer *P. parvulus* 2.6 altered the gut microbiota in a mice model but in a different manner [308]. Similarly, the purified EPS treatments may alter the gut microbiota due to the potential prebiotic effect of EPS of *L. johnsonii*, which requires further characterisation. Also, the microbiota analysis after the treatment with the wild type and the acapsular mutant in a chicken model may improve our knowledge about the biological function of the EPS layer. Overall, the work presented in Chapter 6 has revealed the physiological role of the EPS layer of *L. johnsonii*.

Furthermore the role of EPS layer under *in vivo* passage and persistence conditions as well as in gut microbiota alterations has been discussed.

The study presented in Chapter 7 showed that the deletion of the two putative glycosyltransferase encoding genes from the *eps* cluster resulted in no alteration in the final EPS structures or EPS production levels of *L. johnsonii* FI9785, potentially due to the compensation of their activity by the other glycosyltransferases encoded in this cluster which might have bifunctional roles as reported previously for other glycosyltransferases [339, 340]. Nevertheless identification of the role of the central region of the *eps* cluster containing the glycosyltransferases required for the repeating unit biosynthesis is crucial in order to understand and modify the EPS metabolism of *L. johnsonii* FI9785. We can clearly confirm that the biosynthesis of heteropolymer EPS-2 is dependent on the function of the *eps* gene cluster of *L. johnsonii* and we can propose the biosynthesis mechanism and the role of proteins encoded in different regions of the *eps* cluster for the production of EPS-2 as illustrated in Figure 8.1. However future work is definitely required in order to identify the exact mechanism of EPS production in *L. johnsonii* FI9785. Single, double or triple deletion mutants of the putative glycosyltransferase genes can be generated in order to determine the function of these genes in EPS biosynthesis. In this chapter the cloning and expression of four of these glycosyltransferases and the Glf mutase were performed. *In vitro* enzyme assays with the Glf mutase and these glycosyltransferases were conducted with different donor and acceptor molecules associated with the EPS-1 and EPS-2 structures in order to characterise these putative enzymes biochemically. Although the Glf mutase was expressed and purified successfully, the enzyme assays were not able to show the conversion of the UDP-galactopyranose to UDP-galactofuranose possibly due to the requirement of this enzyme for the flavin cofactor and coenzymes as reported previously [335, 338]. The enzymatic reaction or the expression conditions can be developed and then the activity of this Glf mutase can be shown as a future project. In addition the *glf* gene can be deleted from the *eps* cluster of *L. johnsonii* FI9785 in order to show its function in the EPS repeating unit biosynthesis. Similarly biochemical characterisation assays of glycosyltransferases were inconclusive possibly due to the potential enzymes expressed by *E. coli* BL21 (DE3) cells. In order to eliminate this problem the constructs can be expressed in *E. coli* DH5 $\alpha$  cells in which no background activity was detected [87] and also future work to optimise the expression and purification conditions could allow us to obtain larger amounts of purified enzymes for biochemical characterisation assays.

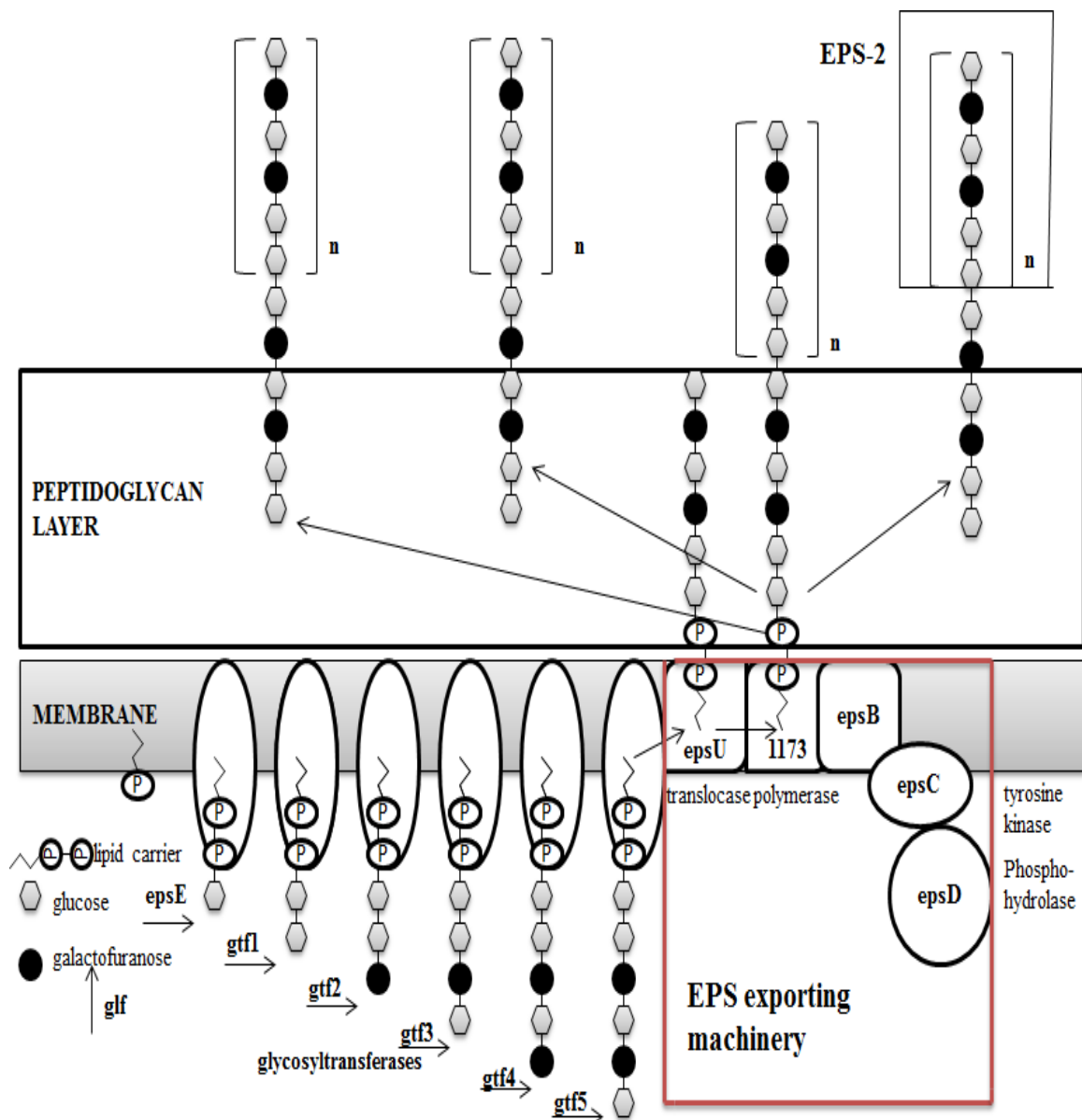


**Figure 8.1.** The schematic illustration of the gene functions in putative steps of EPS-2 biosynthesis in *L. johnsonii* FI9785. (Adapted from Lebeer et al., [61]).

The *gtf* genes could be expressed sequentially and using the previous reaction product as an acceptor substrate in the next reaction step. Nevertheless in this study we were able to express and obtain purified *gtf4* protein which is the fifth putative glycosyltransferase of the *eps* cluster and the initial biochemical characterisation of this enzyme revealed that this enzyme can be a potential  $\alpha(1,4)$ -GlcT which can use Octyl  $\beta$ -D-Lactoside as an acceptor substrate for the addition of the glucose residue from the donor substrate UDP- $\alpha$ -D-Glucose by forming an  $\alpha$ -1,4 bond. To the best of our knowledge this is the first study that shows a potential  $\alpha(1,4)$ -GlcT responsible in the biosynthesis of the EPS repeating unit structure of a

LAB but future work is definitely required for the confirmation of the activity of this potential glycosyltransferase.

In conclusion, the results presented in this thesis have revealed two novel EPS structures forming the capsular layer of *L. johnsonii* FI9785 whose synthesis is dependent on the identified *eps* gene cluster. The role of the capsular EPS layer in the physiological and physicochemical properties of *L. johnsonii* FI9785 has been determined under *in vitro* and *in vivo* conditions. These findings also contribute to the understanding of the role of capsular EPS layer in probiotic related functions.

## Appendix 1

### Antibiotics and their concentrations for plasmid selection

Antibiotic	Preparation and stock concentration	Final con. for <i>L. johnsonii</i>	Final con. for <i>E. coli</i>
Erythromycin (Ery)	Dissolved in ethanol	10 µg/ml	400 µg/ml
Chloramphenicol (Cat)	Dissolved in ethanol	7.5 µg /ml	15 µg /ml
Ampicillin (Amp)	Dissolved in UP H <sub>2</sub> O, filter-sterilized	7.5 µg/ml	100 ug/ml

## Appendix 2

### Primers used in this study

Primer Name	Sequence 5'-3'
pGhost R	TACTACTGACAGCTTCCAAGG
pGhost 1	AGTCACGACGTTGTAAAACGACG
5epsA_KpnF	AAAGGTACCAAATTAATAACAAGAG
epsA_R1	CGGTAAGTTAACTTTCATATCTCG
5epsB_XhoF	GACTCGAGAATAGGAAAAAGTGG
epsB_HindIIIR	GCAAAAGCTTGTGACTTTTCTG
CAT_XHOF	AACTCGAGCACCCATTAGTTC
CATR SPLICE1170	AGTACTGTCCTTTACTAACGGGGCAGGT
1170_ncR	TATTAAGCTTTCATTTCCTGC
1170F SPLICECAT	ACCTGCCCCGTTAGTAAAGGACAGTACT
1184_F	GGGCTTGCTCCTTAAATTG
espB_R1	GTTCTTAAAAGTTTGAGCAACTGC
CATP_R1	TTTAGGAGGCTTACTTGTCTGC

CAT_F1	ATTCAGGAATTGTCAGATAGGC
1170_ncR2	AAGACGTAGTGCTTAGATGCTTC
Cat1170epsAF	CGACGTAAAAAGTTTTGGCG
CATnc_R	AACGGGGCAGGTTAGTGAC
5epsA_NcoI	ATACCATGGATCATAAGAATAGTG
epsANcoI_R	TTCCATGGTTTCCTATTCTCC
p181	GCGAAGATAACAGTGA CTCTA
pForVec	ACAGCAATGTTACAAGTTGAAAT
epsAMidF	CCAGACTATTCACCAGCTAAG
5epsE_KpnF	ACCGGTACCAATGGAAGTAGAAG
epsERspliceCat	CGTTTGTTGAACTAATTCTCTAATATGCAC
CatFspliceepsE	GTGCATATTAGAGAATTAGTTCAACAAACG
1177 F spliceCat	CCGTTAGTTGAAGAGGTGAAATGAATGAA
CatR splice 1177	TTCATTCATTTACCTCTTCAACTAACGG
1177_HindR	TTCCAAGCTTTTATTCTCGCTACT
epsE_Fclone	GCTACCACAGTTATGGAATGTG
1177_Rclone	TATCAATGAAATCATCCACATC
5 1178_KpnF	GATGGTACCGATGGGATTTTAGTA
1178RspliceCat	TAATGGGTGCTTTAGTATTAATTTTCATTC
CatFsplice1178	GAATGAAAATTAATACTAAAGCACCCA TTA
1176F spliceCat	CCC GTT AGT TGA AGAGGAGAAGTTTTAATG
Cat R splice 1176	CAT TAA AAC TTC TCC TCT TCA ACT AAC GGG
1176_HindR	GATAAGCTTCCATTTCTTTATTG
5 1177_KpnF	TTTGGTACCAATAGTAAGGATGC
1177RspliceCat	TAATGGGTGCTTTAGTCTCCATTAATTATC
CatFsplice1177	GATAATTAATGGGAGACTAAAGCACCCATTA

1175Fsplicecat	CCCGTTAGTTGAAGAGTAATGAGGAGAAAT
Cat Rsplice1175	ATTTCTCCTCATTACTCTTCAACTAACGGG
1175HindR	CATAAGCTTTGACAAAAGCCCATT
1177_Fclone	TTCAAGAGGCACTTAATAATAGA
5 1176_KpnF	TTGAGGTACCTGTTTCATCAATATCTA
1176RspliceCat	TAATGGGTGCTTTAGCTCCTCATTACTTCT
CatFsplice1176	AGAAGTAATGAGGAGCTAAAGCACCCATTA
1174FspliceCat	CCCGTTAGTTGAAGAGAGAAAGTAAAGAAT
CatRsplice1174	ATTCTTTACTTTCTCTCTTCAACTAACGGG
1174HindR	AACAAGCTTCCAATTACTTTTATA
5_1175KpnF	TTACGGTACCAGTTGGCATGATGAT
1175RspliceCat	TAATGGGTGCTTTAGTTTCATTCTTTACTTTC
CatFsplice1175	GAAAGTAAAGAATGAAACTA AAG CAC CCA TTA
1173FspliceCat	CCCGTTAGTTGAAGAGGAAATAAACTAATG
CatRsplice1173	CATTAGTTTATTTCTCTTCAACTAACGGG
1173HindR	TTCTAAGCTTTATACTGTCTATCTTGAC
1178_NdeF	GAAAATCATATGGATAAAAGAATTAAAGT
1178_BamR	TGGATCCGG GAA CTA TAA TAT TAA TTT TC
1176_NdeF	GAAGTTCATATGGGATTAATAATGG
1176_BamR	TGGATCCTCATTACTTCTTAATAATTC
T7P2	TGAGCGGATAACAATTCCC
T7T	GCTAGTTATTGCTCAGCGG

### Appendix 3

#### **Buffers and their compositions used in this study**

##### **1 M TRIS buffer (pH 7, 7.5, 8)**

<b>Ingredients</b>	<b>Quantity (g/l)</b>
TRIZMA-Base (Sigma) MW 121.1	121.11
Milli Q water	Make up to 1 litre
Use 1 M HCl to adjust the pH	

##### **1 M MgCl<sub>2</sub>**

<b>Ingredients</b>	<b>Quantity (g/l)</b>
MgCl <sub>2</sub> (Sigma) MW 95.21	95.21
Milli Q water	Make up to 1 litre

##### **TE buffer (10 mM Tris HCl, 1 mM EDTA, pH 8)**

<b>Ingredients</b>	<b>Quantity (ml)</b>
1 M Tris pH 8	5 ml
0.5 M EDTA pH 8	1 ml
Milli Q water	494 ml

### 0.5 M EDTA pH 8

Ingredients	Quantity (g/l)
EDTA (Sigma) MW 292.24	146.12
Milli Q water	Make up to 1 litre

### STE Buffer

Ingredients
10 mM Tris pH 8
1 mM EDTA pH 8
100 mM NaCl
Milli Q water

### 0.1 M, 1 M NaCl

Ingredients	Quantity (g/l)
NaCl (Sigma) MW 58.44	5.844 for 0.1 M, 58.44 for 1 M
Milli Q water	Make up to 1 litre

### 0.1 M KCl

Ingredients	Quantity (g/l)
KCl (Sigma) MW 74.55	7.455
Milli Q water	Make up to 1 litre

### 0.1 M CaCl<sub>2</sub>

Ingredients	Quantity (g/l)
CaCl <sub>2</sub> (Sigma) MW 110.98	11.098
Milli Q water	Make up to 1 litre

### 10 mM K<sub>2</sub>HPO<sub>4</sub>

Ingredients	Quantity (g/l)
K <sub>2</sub> HPO <sub>4</sub> (Sigma) MW 174.18	11.098
Milli Q water	Make up to 1 litre

### TBS buffer

Ingredients
10 mM Tris pH 7.5
150 mM NaCl
Milli Q water

### TBS-Tween/Triton buffer

Ingredients
20 mM Tris pH 7.5
500 mM NaCl
0.05% (v/v) Tween 20 (Sigma)
0.2% (v/v) Triton X-100 (Sigma)
Milli Q water

**20 × NUPAGE Transfer buffer**

---

**Ingredients**

---

Bicine 10.2 g

Bis-Tris 13.1 g

EDTA 0.75 g

Milli Q water (125 ml)

---

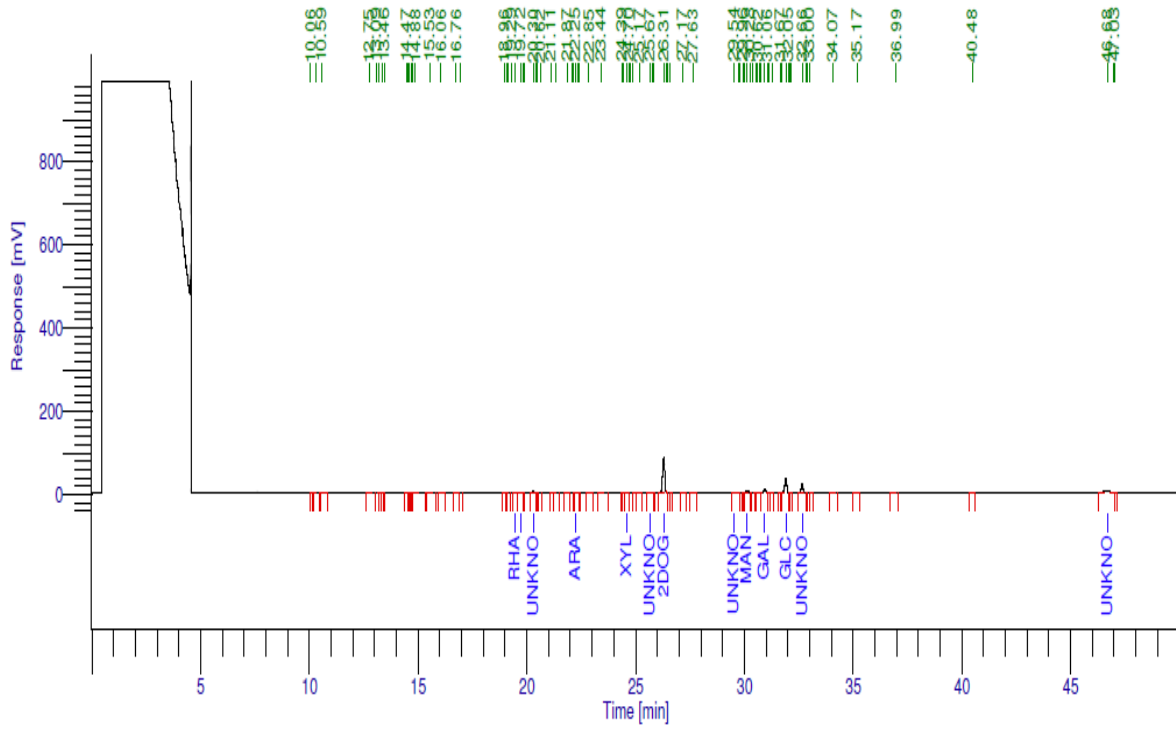
**1 × NUPAGE Transfer buffer**

<b>Ingredients</b>	<b>Reduced Samples</b>	<b>Non-Reduced Samples</b>
20 × NUPAGE buffer	50 ml	50 ml
NUPAGE antioxidant	1 ml	-
Methanol	100 ml	100 ml
Milli Q water	849 ml	850 ml

---

## Appendix 4

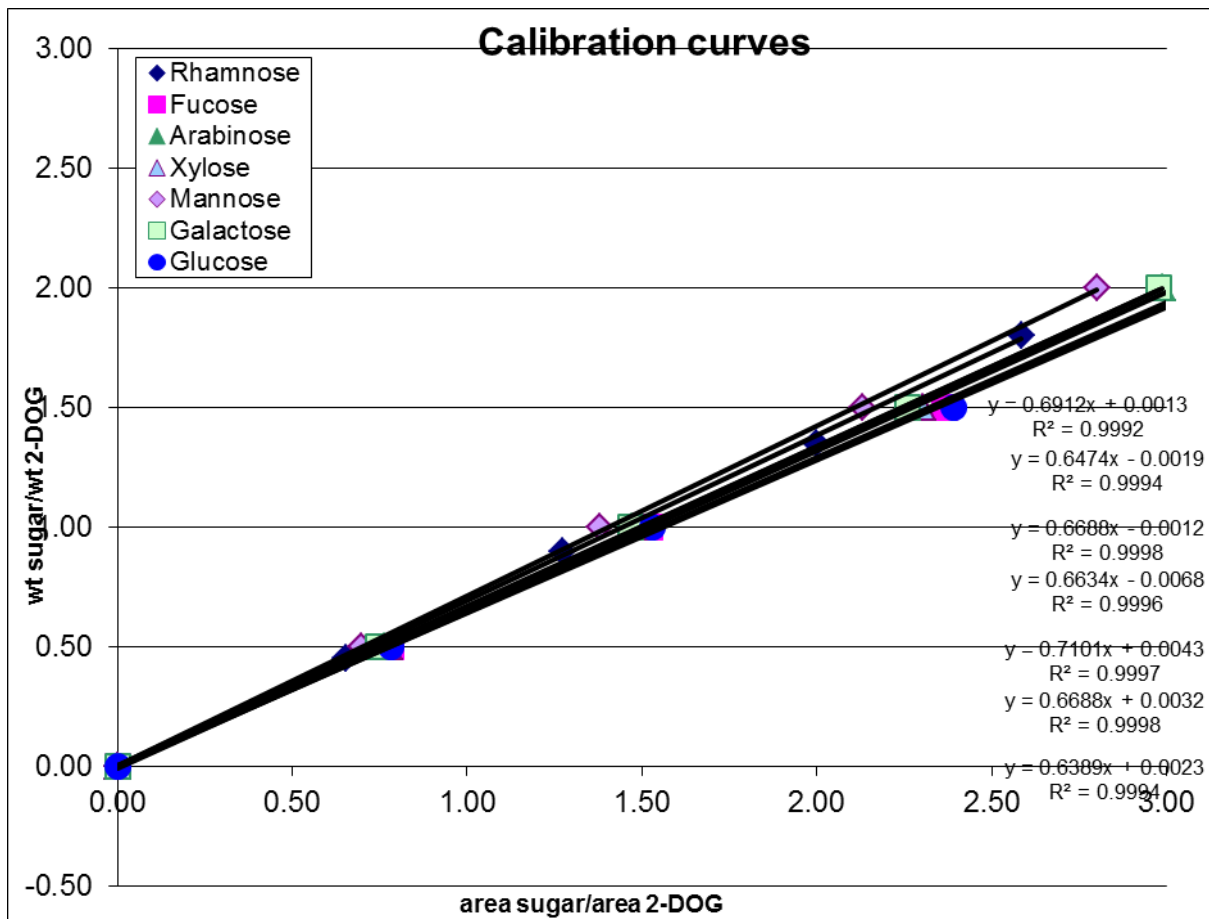
### An example of GC Chromatogram



Peak #	Component Name	Time [min]	Area [uV*sec]	Area [%]
24	Fuc	19.722	2777.62	0.24
27	Unknown A	20.301	17277.07	1.50
37	Ara	22.251	2852.74	0.25
44	Xyl	24.598	12074.97	1.05
50	Unknown B	25.669	10290.23	0.89
54	2DOG	26.308	574473.83	49.76
60	Unknown C	29.537	3332.96	0.29
65	Man	30.129	40879.01	3.54
73	Gal	30.932	53267.73	4.61
81	Glc	31.906	213975.19	18.53
85	Unknown D	32.664	127863.19	11.08
94	Unknown E	46.684	95428.11	8.27
			<b>1154492.65</b>	<b>100.00</b>

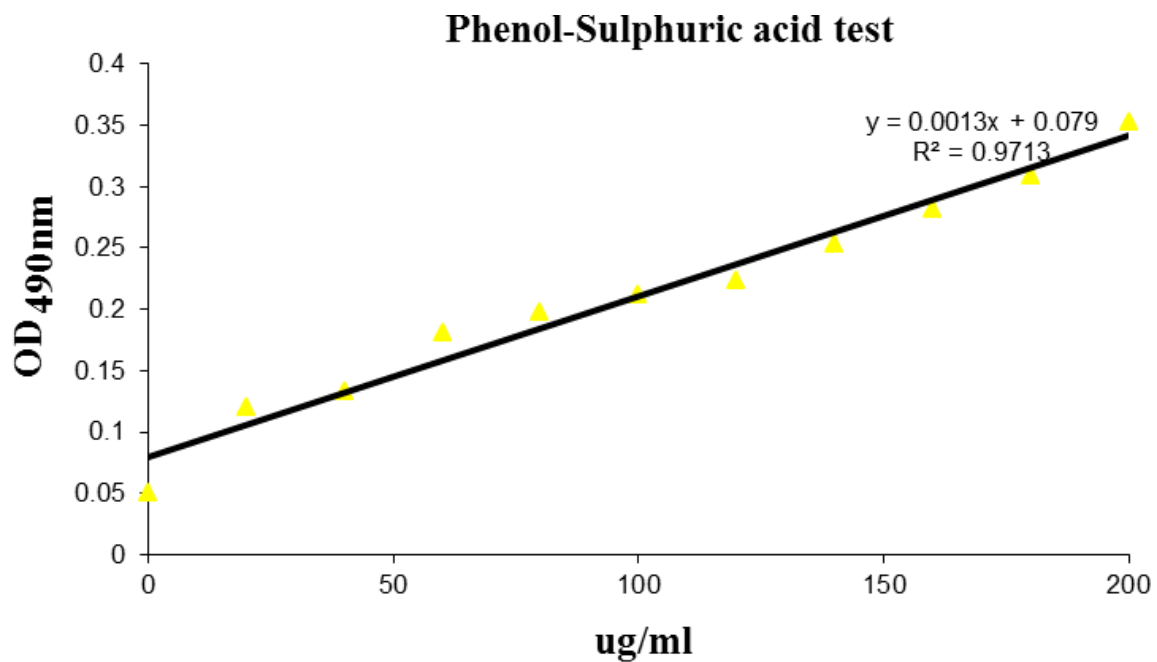
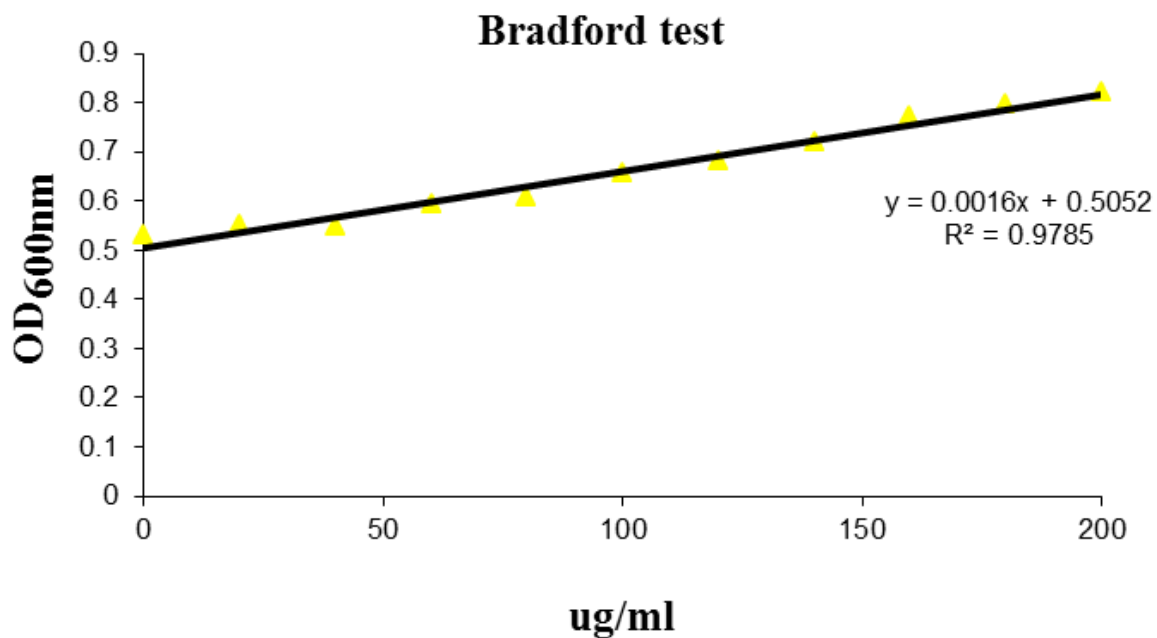
## Appendix 5

The calibration curve of each standard to calculate the concentration of each monosaccharide in the EPS samples. From the regression lines for each standard (for galactose  $y = 0.6688x + 0.0032$ ) the concentration of each monosaccharide is calculated.



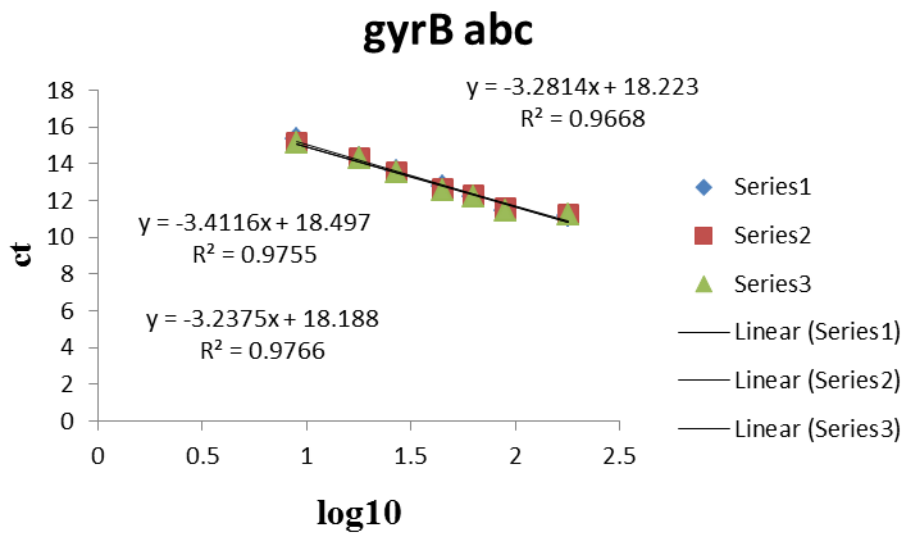
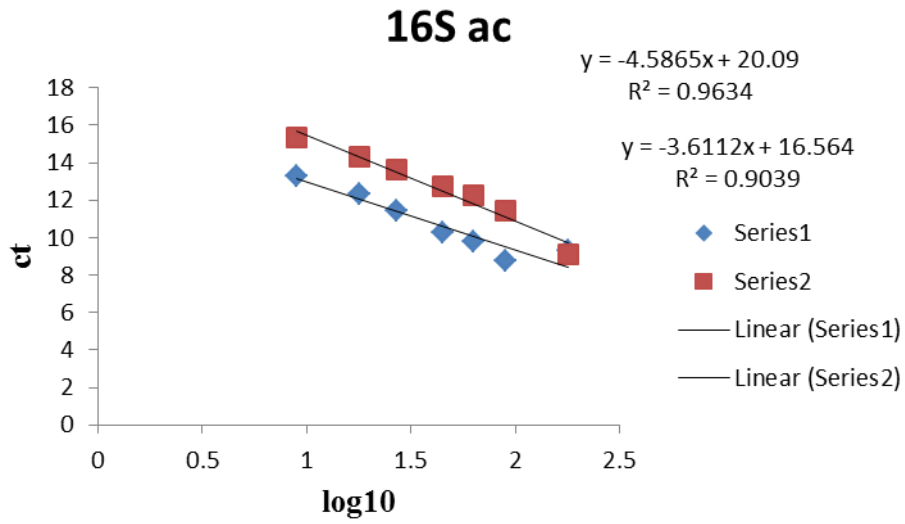
## Appendix 6

Examples of calibration curves used for protein and sugar concentration analysis, respectively.



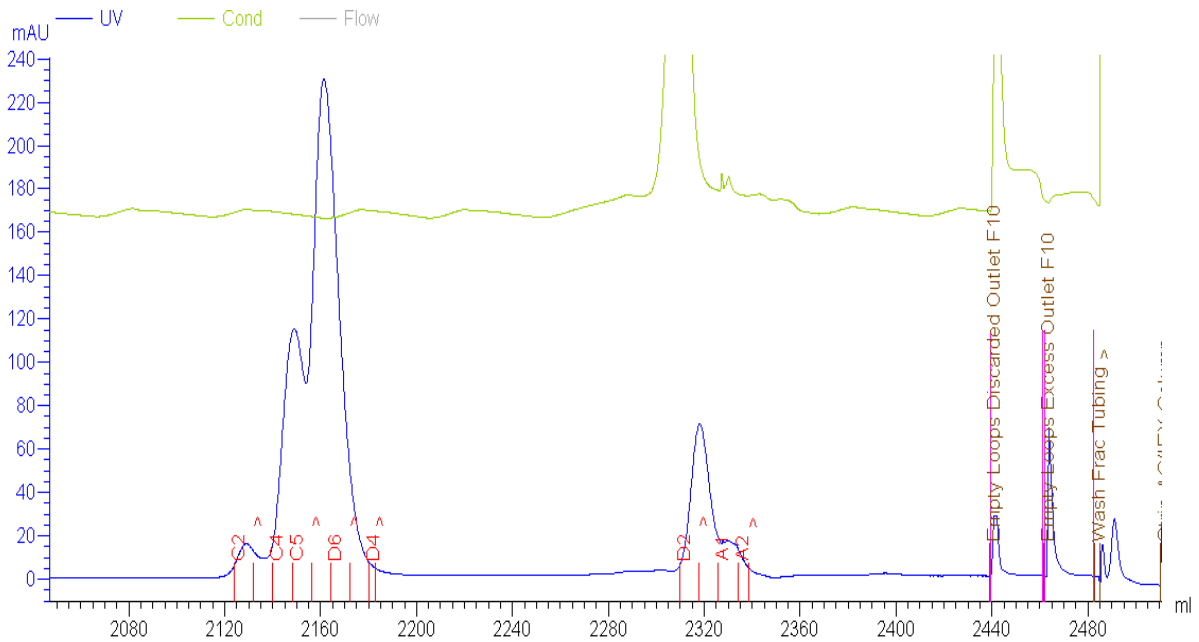
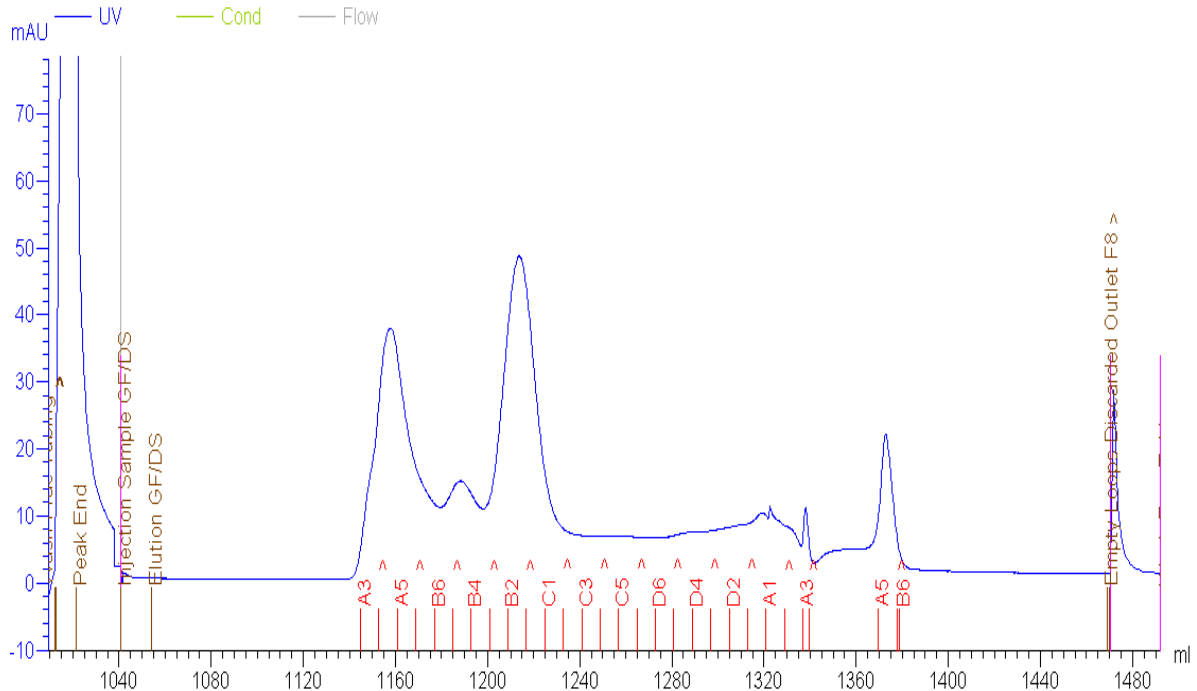
## Appendix 7

Examples of calibration curves used for testing the specificity of the primers for the *16S* rRNA and *gyrB* genes for the qPCR analysis.



## Appendix 8

Examples of FPLC chromatograms showing the collection of the proteins to the related wells for gtf2 and Glf, respectively (Cond, Conductivity).



## REFERENCES

1. Badel, S., T. Bernardi, and P. Michaud, *New perspectives for Lactobacilli exopolysaccharides*. *Biotechnol Adv*, 2011. **29**(1): p. 54-66.
2. Angelis, S., et al., *Co-Culture of Microalgae, Cyanobacteria, and Macromycetes for Exopolysaccharides Production: Process Preliminary Optimization and Partial Characterization*. *Applied Biochemistry and Biotechnology*, 2012. **167**(5): p. 1092-1106.
3. *Synthesis, Production, and Biotechnological Applications of Exopolysaccharides and Polyhydroxyalkanoates by Archaea*. *Archaea*, 2011. **2011**.
4. Montoya, S., O.J. Sanchez, and L. Levin, *Polysaccharide production by submerged and solid-state cultures from several medicinal higher Basidiomycetes*. *Int J Med Mushrooms*, 2013. **15**(1): p. 71-9.
5. Poli, A., et al., *Production and chemical characterization of an exopolysaccharide synthesized by psychrophilic yeast strain *Sporobolomyces salmonicolor* AL1 isolated from Livingston Island, Antarctica*. *Folia Microbiologica*, 2010. **55**(6): p. 576-581.
6. SUTHERLAND, I.W., *Biotechnology of microbial exopolysaccharides*. 1990, CAMBRIDGE: CAMBRIDGE UNIVERSITY PRESS.
7. Öner, E.T., *Microbial Production of Extracellular Polysaccharides from Biomass, in Pretreatment Techniques for Biofuels and Biorefineries*, Z. Fang, Editor. 2013, Springer Berlin Heidelberg. p. 35-56.
8. Broadbent, J.R., et al., *Biochemistry, genetics, and applications of exopolysaccharide production in *Streptococcus thermophilus*: a review*. *J Dairy Sci*, 2003. **86**(2): p. 407-23.
9. Kumar, A.S., K. Mody, and B. Jha, *Bacterial exopolysaccharides--a perception*. *J Basic Microbiol*, 2007. **47**(2): p. 103-17.
10. De Vuyst, L. and B. Degeest, *Heteropolysaccharides from lactic acid bacteria*. *FEMS Microbiol Rev*, 1999. **23**(2): p. 153-77.
11. Darzins, A., et al., *Clustering of mutations affecting alginate biosynthesis in mucoid *Pseudomonas aeruginosa**. *J Bacteriol*, 1985. **164**(2): p. 516-24.
12. Celik, G.Y., B. Aslim, and Y. Beyatli, *Characterization and production of the exopolysaccharide (EPS) from *Pseudomonas aeruginosa* G1 and *Pseudomonas putida* G12 strains*. *Carbohydrate Polymers*, 2008. **73**(1): p. 178-182.
13. Yasutake, Y., et al., *Structural characterization of the *Acetobacter xylinum* endo-beta-1,4-glucanase CMCax required for cellulose biosynthesis*. *Proteins*, 2006. **64**(4): p. 1069-77.
14. Wang, X., et al., *Modeling for gellan gum production by *Sphingomonas paucimobilis* ATCC 31461 in a simplified medium*. *Appl Environ Microbiol*, 2006. **72**(5): p. 3367-74.
15. Sarwat, F., et al., *Production & characterization of a unique dextran from an indigenous *Leuconostoc mesenteroides* CMG713*. *Int J Biol Sci*, 2008. **4**(6): p. 379-86.
16. Matsushita, M., *Curdlan, a (1----3)-beta-D-glucan from *Alcaligenes faecalis* var. *myxogenes* IFO13140, activates the alternative complement pathway by heat treatment*. *Immunol Lett*, 1990. **26**(1): p. 95-7.
17. Palaniraj, A. and V. Jayaraman, *Production, recovery and applications of xanthan gum by *Xanthomonas campestris**. *Journal of Food Engineering*, 2011. **106**(1): p. 1-12.
18. Han, Y.W. and M.A. Clarke, *Production and characterization of microbial levan*. *Journal of Agricultural and Food Chemistry*, 1990. **38**(2): p. 393-396.
19. Kanmani, P., et al., *Production and purification of a novel exopolysaccharide from lactic acid bacterium *Streptococcus phocae* PI80 and its functional characteristics activity in vitro*. *Bioresour Technol*, 2011. **102**(7): p. 4827-33.

20. Lebeer, S., J. Vanderleyden, and S.C. De Keersmaecker, *Genes and molecules of lactobacilli supporting probiotic action*. Microbiol Mol Biol Rev, 2008. **72**(4): p. 728-64, Table of Contents.
21. Gauri, S.S., et al., *Enhanced production and partial characterization of an extracellular polysaccharide from newly isolated Azotobacter sp. SSB81*. Bioresour Technol, 2009. **100**(18): p. 4240-3.
22. Wang, Y., et al., *Physicochemical properties of exopolysaccharide produced by Lactobacillus kefiranofaciens ZW3 isolated from Tibet kefir*. Int J Biol Macromol, 2008. **43**(3): p. 283-8.
23. Liu, C., et al., *Isolation, structural characterization and immunological activity of an exopolysaccharide produced by Bacillus licheniformis 8-37-0-1*. Bioresour Technol, 2010. **101**(14): p. 5528-33.
24. Pan, D. and X. Mei, *Antioxidant activity of an exopolysaccharide purified from Lactococcus lactis subsp. lactis 12*. Carbohydrate Polymers, 2010. **80**(3): p. 908-914.
25. Tannock, G.W., *A special fondness for lactobacilli*. Appl Environ Microbiol, 2004. **70**(6): p. 3189-94.
26. Garai-Ibabe, G., et al., *Naturally occurring 2-substituted (1,3)-beta-D-glucan producing Lactobacillus suebicus and Pediococcus parvulus strains with potential utility in the production of functional foods*. Bioresour Technol, 2010. **101**(23): p. 9254-63.
27. Duboc, P. and B. Mollet, *Applications of exopolysaccharides in the dairy industry*. International dairy journal / published in association with the International Dairy Federation, 2001. **11**(9): p. 759-768.
28. Nakajima, H., Y. Suzuki, and T. Hirota, *Cholesterol Lowering Activity of Ropy Fermented Milk*. Journal of Food Science, 1992. **57**(6): p. 1327-1329.
29. Hosono, A., et al., *Characterization of a water-soluble polysaccharide fraction with immunopotentiating activity from Bifidobacterium adolescentis M101-4*. Biosci Biotechnol Biochem, 1997. **61**(2): p. 312-6.
30. Chabot, S., et al., *Exopolysaccharides from Lactobacillus rhamnosus RW-9595M stimulate TNF*. Lait, 2001. **81**(6): p. 683-697.
31. Kitazawa, H., et al., *Phosphate group requirement for mitogenic activation of lymphocytes by an extracellular phosphopolysaccharide from Lactobacillus delbrueckii ssp. bulgaricus*. Int J Food Microbiol, 1998. **40**(3): p. 169-75.
32. La Ragione, R.M., et al., *In vivo characterization of Lactobacillus johnsonii F19785 for use as a defined competitive exclusion agent against bacterial pathogens in poultry*. Lett Appl Microbiol, 2004. **38**(3): p. 197-205.
33. Horn, N., et al., *Spontaneous Mutation Reveals Influence of Exopolysaccharide on Lactobacillus johnsonii Surface Characteristics*. PLoS One, 2013. **8**(3): p. e59957.
34. Claesson, M.J., D. van Sinderen, and P.W. O'Toole, *The genus Lactobacillus--a genomic basis for understanding its diversity*. FEMS Microbiol Lett, 2007. **269**(1): p. 22-8.
35. Walter, J., *Ecological role of lactobacilli in the gastrointestinal tract: implications for fundamental and biomedical research*. Appl Environ Microbiol, 2008. **74**(16): p. 4985-96.
36. Tlaskalova-Hogenova, H., et al., *The role of gut microbiota (commensal bacteria) and the mucosal barrier in the pathogenesis of inflammatory and autoimmune diseases and cancer: contribution of germ-free and gnotobiotic animal models of human diseases*. Cell Mol Immunol, 2011. **8**(2): p. 110-20.
37. Berg, R.D., *The indigenous gastrointestinal microflora*. Trends Microbiol, 1996. **4**(11): p. 430-5.
38. Dethlefsen, L., et al., *The pervasive effects of an antibiotic on the human gut microbiota, as revealed by deep 16S rRNA sequencing*. PLoS Biol, 2008. **6**(11): p. e280.
39. Falagas, M., G.I. Betsi, and S. Athanasiou, *Probiotics for the treatment of women with bacterial vaginosis*. Clin Microbiol Infect, 2007. **13**(7): p. 657-64.

40. Suau, A., et al., *Direct analysis of genes encoding 16S rRNA from complex communities reveals many novel molecular species within the human gut*. Appl Environ Microbiol, 1999. **65**(11): p. 4799-807.
41. Aleksandr Barinov, A.B., Philippe Langella, Emmanuelle Maguin and Maarten Van De Guchte, *Genomics of Genus Lactobacillus*, in *Lactic Acid Bacteria and Bifidobacteria Current Progress in Advanced Research*, K.S.a.A. Yokota, Editor. 2011, Caister Academic Press Norfolk, UK. p. 3-33.
42. Guan, L.L., et al., *Detection and identification of Lactobacillus species in crops of broilers of different ages by using PCR-denaturing gradient gel electrophoresis and amplified ribosomal DNA restriction analysis*. Appl Environ Microbiol, 2003. **69**(11): p. 6750-7.
43. Knarreborg, A., et al., *Effects of dietary fat source and subtherapeutic levels of antibiotic on the bacterial community in the ileum of broiler chickens at various ages*. Appl Environ Microbiol, 2002. **68**(12): p. 5918-24.
44. Fuller, R., *Ecological Studies on the Lactobacillus Flora Associated with the Crop Epithelium of the Fowl*. Journal of Applied Bacteriology, 1973. **36**(1): p. 131-139.
45. Fuller, R., *Nature of the determinant responsible for the adhesion of lactobacilli to chicken crop epithelial cells*. J Gen Microbiol, 1975. **87**(2): p. 245-50.
46. Remus, D.M., et al., *Impact of 4 Lactobacillus plantarum capsular polysaccharide clusters on surface glycan composition and host cell signaling*. Microb Cell Fact, 2012. **11**: p. 149.
47. Van Calsteren, M.R., et al., *Structure determination of the exopolysaccharide produced by Lactobacillus rhamnosus strains RW-9595M and R*. Biochem J, 2002. **363**(Pt 1): p. 7-17.
48. Monsan, P., et al., *Homopolysaccharides from lactic acid bacteria*. International Dairy Journal, 2001. **11**(9): p. 675-685.
49. Dueñas-Chasco, M.T., et al., *Structural analysis of the exopolysaccharides produced by Lactobacillus spp. G-77*. Carbohydrate Research, 1998. **307**(1-2): p. 125-133.
50. Yamamoto, Y., et al., *Structural study on an exocellular polysaccharide produced by Lactobacillus helveticus TY1-2*. Carbohydrate Research, 1994. **261**(1): p. 67-78.
51. Lemoine, J., et al., *Structural characterization of the exocellular polysaccharides produced by Streptococcus thermophilus SFi39 and SFi12*. Appl Environ Microbiol, 1997. **63**(9): p. 3512-8.
52. Robijn, G.W., et al., *Structural characterization of the exopolysaccharide produced by Lactobacillus acidophilus LMG9433*. Carbohydrate Research, 1996. **288**(0): p. 203-218.
53. van Casteren, W.H.M., et al., *Structural characterisation and enzymic modification of the exopolysaccharide produced by Lactococcus lactis subsp. cremoris B891*. Carbohydrate Research, 2000. **327**(4): p. 411-422.
54. Faber, E.J., J.P. Kamerling, and J.F.G. Vliegenthart, *Structure of the extracellular polysaccharide produced by Lactobacillus delbrueckii subsp. bulgaricus 291*. Carbohydrate Research, 2001. **331**(2): p. 183-194.
55. Landersjo, C., et al., *Structural studies of the exopolysaccharide produced by Lactobacillus rhamnosus strain GG (ATCC 53103)*. Biomacromolecules, 2002. **3**(4): p. 880-4.
56. Gorska-Fraczek, S., et al., *The structure and immunoreactivity of exopolysaccharide isolated from Lactobacillus johnsonii strain 151*. Carbohydr Res, 2013.
57. Gorska-Fraczek, S., et al., *Structural studies of the exopolysaccharide consisting of a nonasaccharide repeating unit isolated from Lactobacillus rhamnosus KL37B*. Carbohydr Res, 2011. **346**(18): p. 2926-32.
58. Garcia, E., et al., *Current trends in capsular polysaccharide biosynthesis of Streptococcus pneumoniae*. Res Microbiol, 2000. **151**(6): p. 429-35.
59. Gorska, S., et al., *Structural and immunochemical studies of neutral exopolysaccharide produced by Lactobacillus johnsonii 142*. Carbohydr Res, 2010. **345**(1): p. 108-14.
60. Yasuda, E., M. Serata, and T. Sako, *Suppressive effect on activation of macrophages by Lactobacillus casei strain Shirota genes determining the synthesis of cell wall-associated polysaccharides*. Appl Environ Microbiol, 2008. **74**(15): p. 4746-55.

61. Lebeer, S., et al., *Identification of a Gene Cluster for the Biosynthesis of a Long, Galactose-Rich Exopolysaccharide in Lactobacillus rhamnosus GG and Functional Analysis of the Priming Glycosyltransferase*. Appl Environ Microbiol, 2009. **75**(11): p. 3554-63.
62. Denou, E., et al., *Identification of genes associated with the long-gut-persistence phenotype of the probiotic Lactobacillus johnsonii strain NCC533 using a combination of genomics and transcriptome analysis*. J Bacteriol, 2008. **190**(9): p. 3161-8.
63. Walter, J., et al., *Glucosyltransferase A (GtfA) and inulosucrase (Inu) of Lactobacillus reuteri TMW1.106 contribute to cell aggregation, in vitro biofilm formation, and colonization of the mouse gastrointestinal tract*. Microbiology, 2008. **154**(Pt 1): p. 72-80.
64. Tzianabos, A.O., *Polysaccharide immunomodulators as therapeutic agents: structural aspects and biologic function*. Clin Microbiol Rev, 2000. **13**(4): p. 523-33.
65. Hidalgo-Cantabrana, C., et al., *Immune Modulation Capability of Exopolysaccharides Synthesised by Lactic Acid Bacteria and Bifidobacteria*. Probiotics and Antimicrobial Proteins, 2012. **4**(4): p. 227-237.
66. Fanning, S., et al., *Bifidobacterial surface-exopolysaccharide facilitates commensal-host interaction through immune modulation and pathogen protection*. Proc Natl Acad Sci U S A, 2012. **109**(6): p. 2108-13.
67. Lebeer, S., et al., *Exopolysaccharides of Lactobacillus rhamnosus GG form a protective shield against innate immune factors in the intestine*. Microb Biotechnol, 2011. **4**(3): p. 368-74.
68. Silhavy, T.J., D. Kahne, and S. Walker, *The bacterial cell envelope*. Cold Spring Harb Perspect Biol, 2010. **2**(5): p. a000414.
69. Lebeer, S., J. Vanderleyden, and S.C. De Keersmaecker, *Host interactions of probiotic bacterial surface molecules: comparison with commensals and pathogens*. Nat Rev Microbiol, 2010. **8**(3): p. 171-84.
70. Kleerebezem, M., et al., *The extracellular biology of the lactobacilli*. FEMS Microbiol Rev, 2010. **34**(2): p. 199-230.
71. Delcour, J., et al., *The biosynthesis and functionality of the cell-wall of lactic acid bacteria*. Antonie Van Leeuwenhoek, 1999. **76**(1-4): p. 159-84.
72. Neuhaus, F.C. and J. Baddiley, *A continuum of anionic charge: structures and functions of D-alanyl-teichoic acids in gram-positive bacteria*. Microbiol Mol Biol Rev, 2003. **67**(4): p. 686-723.
73. Buck, B.L., et al., *Functional analysis of putative adhesion factors in Lactobacillus acidophilus NCFM*. Appl Environ Microbiol, 2005. **71**(12): p. 8344-51.
74. Smit, E., et al., *Structural and functional analysis of the S-layer protein crystallisation domain of Lactobacillus acidophilus ATCC 4356: evidence for protein-protein interaction of two subdomains*. J Mol Biol, 2002. **324**(5): p. 953-64.
75. Granato, D., et al., *Cell surface-associated elongation factor Tu mediates the attachment of Lactobacillus johnsonii NCC533 (La1) to human intestinal cells and mucins*. Infect Immun, 2004. **72**(4): p. 2160-9.
76. Bergonzelli, G.E., et al., *GroEL of Lactobacillus johnsonii La1 (NCC 533) is cell surface associated: potential role in interactions with the host and the gastric pathogen Helicobacter pylori*. Infect Immun, 2006. **74**(1): p. 425-34.
77. Jolly, L. and F. Stinglele, *Molecular organization and functionality of exopolysaccharide gene clusters in lactic acid bacteria*. International Dairy Journal, 2001. **11**(9): p. 733-745.
78. Laws, A., Y. Gu, and V. Marshall, *Biosynthesis, characterisation, and design of bacterial exopolysaccharides from lactic acid bacteria*. Biotechnology Advances, 2001. **19**(8): p. 597-625.
79. Kojic, M., et al., *Analysis of exopolysaccharide production by Lactobacillus casei CG11, isolated from cheese*. Appl Environ Microbiol, 1992. **58**(12): p. 4086-8.

80. Dupont, I., D. Roy, and G. Lapointe, *Comparison of exopolysaccharide production by strains of Lactobacillus rhamnosus and Lactobacillus paracasei grown in chemically defined medium and milk*. Journal of Industrial Microbiology and Biotechnology, 2000. **24**(4): p. 251-255.
81. Welman, A.D. and I.S. Maddox, *Exopolysaccharides from lactic acid bacteria: perspectives and challenges*. Trends in biotechnology, 2003. **21**(6): p. 269-274.
82. Kleerebezem, M., et al., *Exopolysaccharides produced by Lactococcus lactis: from genetic engineering to improved rheological properties?* Antonie Van Leeuwenhoek, 1999. **76**(1-4): p. 357-65.
83. Grobben, G.J., et al., *Influence of fructose and glucose on the production of exopolysaccharides and the activities of enzymes involved in the sugar metabolism and the synthesis of sugar nucleotides in Lactobacillus delbrueckii subsp. bulgaricus NCFB 2772*. Applied Microbiology and Biotechnology, 1996. **46**(3): p. 279-284.
84. de Vos, W.M. and E.E. Vaughan, *Genetics of lactose utilization in lactic acid bacteria*. FEMS Microbiol Rev, 1994. **15**(2-3): p. 217-37.
85. Peant, B., et al., *Comparative analysis of the exopolysaccharide biosynthesis gene clusters from four strains of Lactobacillus rhamnosus*. Microbiology, 2005. **151**(Pt 6): p. 1839-51.
86. Stingele, F., J.R. Neeser, and B. Mollet, *Identification and characterization of the eps (Exopolysaccharide) gene cluster from Streptococcus thermophilus Sfi6*. J Bacteriol, 1996. **178**(6): p. 1680-90.
87. van Kranenburg, R., et al., *Molecular characterization of the plasmid-encoded eps gene cluster essential for exopolysaccharide biosynthesis in Lactococcus lactis*. Mol Microbiol, 1997. **24**(2): p. 387-97.
88. Nierop Groot, M.N. and M. Kleerebezem, *Mutational analysis of the Lactococcus lactis NIZO B40 exopolysaccharide (EPS) gene cluster: EPS biosynthesis correlates with unphosphorylated EpsB*. J Appl Microbiol, 2007. **103**(6): p. 2645-56.
89. Jolly, L., et al., *Lactobacillus helveticus glycosyltransferases: from genes to carbohydrate synthesis*. Glycobiology, 2002. **12**(5): p. 319-27.
90. Saxena, I.M., et al., *Multidomain architecture of beta-glycosyl transferases: implications for mechanism of action*. J Bacteriol, 1995. **177**(6): p. 1419-24.
91. María Laura Werning, S.N., Montserrat Nácher, Pilar Fernández de Palencia, Rosa Aznar and Paloma López *Biosynthesis, Purification and Biotechnological Use of Exopolysaccharides Produced by Lactic Acid Bacteria*. 2012( Food Additive).
92. Lairson, L.L., et al., *Glycosyltransferases: structures, functions, and mechanisms*. Annu Rev Biochem, 2008. **77**: p. 521-55.
93. Stingele, F., J.W. Newell, and J.R. Neeser, *Unraveling the function of glycosyltransferases in Streptococcus thermophilus Sfi6*. J Bacteriol, 1999. **181**(20): p. 6354-60.
94. Cieslewicz, M.J., et al., *Functional analysis in type Ia group B Streptococcus of a cluster of genes involved in extracellular polysaccharide production by diverse species of streptococci*. J Biol Chem, 2001. **276**(1): p. 139-46.
95. Morona, J.K., et al., *Mutational analysis of the carboxy-terminal (YGX)<sub>4</sub> repeat domain of CpsD, an autophosphorylating tyrosine kinase required for capsule biosynthesis in Streptococcus pneumoniae*. J Bacteriol, 2003. **185**(10): p. 3009-19.
96. Morona, J.K., et al., *Tyrosine phosphorylation of CpsD negatively regulates capsular polysaccharide biosynthesis in streptococcus pneumoniae*. Mol Microbiol, 2000. **35**(6): p. 1431-42.
97. Yother, J., *Capsules of Streptococcus pneumoniae and other bacteria: paradigms for polysaccharide biosynthesis and regulation*. Annu Rev Microbiol, 2011. **65**: p. 563-81.
98. Rahn, A., et al., *A novel outer membrane protein, Wzi, is involved in surface assembly of the Escherichia coli K30 group 1 capsule*. J Bacteriol, 2003. **185**(19): p. 5882-90.

99. Kralj, S., et al., *Glucan synthesis in the genus Lactobacillus: isolation and characterization of glucansucrase genes, enzymes and glucan products from six different strains*. Microbiology, 2004. **150**(Pt 11): p. 3681-90.
100. Donot, F., et al., *Microbial exopolysaccharides: Main examples of synthesis, excretion, genetics and extraction*. Carbohydrate Polymers, 2012. **87**(2): p. 951-962.
101. van Hijum, S.A., et al., *Structure-function relationships of glucansucrase and fructansucrase enzymes from lactic acid bacteria*. Microbiol Mol Biol Rev, 2006. **70**(1): p. 157-76.
102. Keenleyside, W.J. and C. Whitfield, *A novel pathway for O-polysaccharide biosynthesis in Salmonella enterica serovar Borreze*. J Biol Chem, 1996. **271**(45): p. 28581-92.
103. van Hijum, S.A., et al., *Characterization of a novel fructosyltransferase from Lactobacillus reuteri that synthesizes high-molecular-weight inulin and inulin oligosaccharides*. Appl Environ Microbiol, 2002. **68**(9): p. 4390-8.
104. Cote, G.L., et al., *The production of glucans via glucansucrases from Lactobacillus satsumensis isolated from a fermented beverage starter culture*. Appl Microbiol Biotechnol, 2012.
105. Kralj, S., et al., *Molecular characterization of a novel glucosyltransferase from Lactobacillus reuteri strain 121 synthesizing a unique, highly branched glucan with alpha-(1-->4) and alpha-(1-->6) glucosidic bonds*. Appl Environ Microbiol, 2002. **68**(9): p. 4283-91.
106. Korakli, M. and R.F. Vogel, *Structure/function relationship of homopolysaccharide producing glykansucrases and therapeutic potential of their synthesised glycans*. Appl Microbiol Biotechnol, 2006. **71**(6): p. 790-803.
107. Van der Meulen, R., et al., *Screening of lactic acid bacteria isolates from dairy and cereal products for exopolysaccharide production and genes involved*. Int J Food Microbiol, 2007. **118**(3): p. 250-8.
108. van Leeuwen, S.S., et al., *Structural analysis of bioengineered alpha-D-glucan produced by a triple mutant of the Glucansucrase GTF180 enzyme from Lactobacillus reuteri strain 180: generation of (alpha1-->4) linkages in a native (1-->3)(1-->6)-alpha-D-glucan*. Biomacromolecules, 2008. **9**(8): p. 2251-8.
109. Schwab, C. and M.G. Ganzle, *Effect of membrane lateral pressure on the expression of fructosyltransferases in Lactobacillus reuteri*. Syst Appl Microbiol, 2006. **29**(2): p. 89-99.
110. Monchois, V., M. Arguello-Morales, and R.R. Russell, *Isolation of an active catalytic core of Streptococcus downei MFe28 GTF-I glucosyltransferase*. J Bacteriol, 1999. **181**(7): p. 2290-2.
111. Kralj, S., et al., *Biochemical and molecular characterization of Lactobacillus reuteri 121 reuteransucrase*. Microbiology, 2004. **150**(Pt 7): p. 2099-112.
112. Germond, J.E., et al., *Heterologous expression and characterization of the exopolysaccharide from Streptococcus thermophilus Sfi39*. Eur J Biochem, 2001. **268**(19): p. 5149-56.
113. Almiron-Roig, E., et al., *The complete cps gene cluster from Streptococcus thermophilus NCFB 2393 involved in the biosynthesis of a new exopolysaccharide*. Microbiology, 2000. **146** ( Pt 11): p. 2793-802.
114. Lamothe, G.T., et al., *Genetic and biochemical characterization of exopolysaccharide biosynthesis by Lactobacillus delbrueckii subsp. bulgaricus*. Arch Microbiol, 2002. **178**(3): p. 218-28.
115. Bender, M.H., R.T. Cartee, and J. Yother, *Positive correlation between tyrosine phosphorylation of CpsD and capsular polysaccharide production in Streptococcus pneumoniae*. J Bacteriol, 2003. **185**(20): p. 6057-66.
116. Vincent, C., et al., *Cells of Escherichia coli contain a protein-tyrosine kinase, Wzc, and a phosphotyrosine-protein phosphatase, Wzb*. J Bacteriol, 1999. **181**(11): p. 3472-7.
117. Morona, J.K., et al., *Streptococcus pneumoniae capsule biosynthesis protein CpsB is a novel manganese-dependent phosphotyrosine-protein phosphatase*. J Bacteriol, 2002. **184**(2): p. 577-83.

118. Cozzone, A.J., et al., *Protein phosphorylation on tyrosine in bacteria*. Arch Microbiol, 2004. **181**(3): p. 171-81.
119. Bender, M.H. and J. Yother, *CpsB is a modulator of capsule-associated tyrosine kinase activity in Streptococcus pneumoniae*. J Biol Chem, 2001. **276**(51): p. 47966-74.
120. Minic, Z., et al., *Control of EpsE, the phosphoglycosyltransferase initiating exopolysaccharide synthesis in Streptococcus thermophilus, by EpsD tyrosine kinase*. J Bacteriol, 2007. **189**(4): p. 1351-7.
121. Bentley, S.D., et al., *Genetic analysis of the capsular biosynthetic locus from all 90 pneumococcal serotypes*. PLoS Genet, 2006. **2**(3): p. e31.
122. Dabour, N. and G. LaPointe, *Identification and molecular characterization of the chromosomal exopolysaccharide biosynthesis gene cluster from Lactococcus lactis subsp. cremoris SMQ-461*. Appl Environ Microbiol, 2005. **71**(11): p. 7414-25.
123. Boels, I.C., et al., *Increased exopolysaccharide production in Lactococcus lactis due to increased levels of expression of the NIZO B40 eps gene cluster*. Appl Environ Microbiol, 2003. **69**(8): p. 5029-31.
124. Cerning, J., et al., *Carbon Source Requirements for Exopolysaccharide Production by Lactobacillus casei CG11 and Partial Structure Analysis of the Polymer*. Appl Environ Microbiol, 1994. **60**(11): p. 3914-9.
125. Boels, I.C., et al., *Functional analysis of the Lactococcus lactis galU and galE genes and their impact on sugar nucleotide and exopolysaccharide biosynthesis*. Appl Environ Microbiol, 2001. **67**(7): p. 3033-40.
126. Levander, F., M. Svensson, and P. Radstrom, *Enhanced exopolysaccharide production by metabolic engineering of Streptococcus thermophilus*. Appl Environ Microbiol, 2002. **68**(2): p. 784-90.
127. Looijesteijn, P.J., et al., *Regulation of exopolysaccharide production by Lactococcus lactis subsp. cremoris By the sugar source*. Appl Environ Microbiol, 1999. **65**(11): p. 5003-8.
128. Svensson, M., et al., *Metabolically improved exopolysaccharide production by Streptococcus thermophilus and its influence on the rheological properties of fermented milk*. Appl Environ Microbiol, 2005. **71**(10): p. 6398-400.
129. Audy, J., et al., *Sugar source modulates exopolysaccharide biosynthesis in Bifidobacterium longum subsp. longum CRC 002*. Microbiology, 2010. **156**(Pt 3): p. 653-64.
130. Aslim, B., et al., *Exopolysaccharide production by Lactobacillus delbrueckii subsp. bulgaricus and Streptococcus thermophilus strains under different growth conditions*. World Journal of Microbiology and Biotechnology, 2005. **21**(5): p. 673-677.
131. Cerning, J., et al., *Exocellular polysaccharide production by Streptococcus thermophilus*. Biotechnology Letters, 1988. **10**(4): p. 255-260.
132. Cerning, J., et al., *Isolation and Characterization of Exopolysaccharides from Slime-Forming Mesophilic Lactic Acid Bacteria*. J Dairy Sci, 1992. **75**(3): p. 692-699.
133. Pham, P.L., et al., *Production of exopolysaccharide by Lactobacillus rhamnosus R and analysis of its enzymatic degradation during prolonged fermentation*. Appl Environ Microbiol, 2000. **66**(6): p. 2302-10.
134. Ramos, A., et al., *Relationship between glycolysis and exopolysaccharide biosynthesis in Lactococcus lactis*. Appl Environ Microbiol, 2001. **67**(1): p. 33-41.
135. van Kranenburg, R., et al., *Functional analysis of glycosyltransferase genes from Lactococcus lactis and other gram-positive cocci: complementation, expression, and diversity*. J Bacteriol, 1999. **181**(20): p. 6347-53.
136. {Cerning, B., K. and G. LaPointe, *Use of antisense RNA to modulate glycosyltransferase gene expression and exopolysaccharide molecular mass in Lactobacillus rhamnosus*. Journal of Microbiological Methods, 2006. **65**(2): p. 216-225.
137. Breedveld, M., K. Bonting, and L. Dijkhuizen, *Mutational analysis of exopolysaccharide biosynthesis by Lactobacillus sakei 0-1*. FEMS Microbiol Lett, 1998. **169**(2): p. 241-9.

138. Degeest, B., B. Janssens, and L. De Vuyst, *Exopolysaccharide (EPS) biosynthesis by Lactobacillus sakei O-1: production kinetics, enzyme activities and EPS yields*. J Appl Microbiol, 2001. **91**(3): p. 470-7.
139. Looijesteijn, P.J., et al., *Physiological function of exopolysaccharides produced by Lactococcus lactis*. International Journal of Food Microbiology, 2001. **64**(1-2): p. 71-80.
140. Ruas-Madiedo, P., J. Hugenholtz, and P. Zoon, *An overview of the functionality of exopolysaccharides produced by lactic acid bacteria*. International Dairy Journal, 2002. **12**(2-3): p. 163-171.
141. Lebeer, S., et al., *Impact of environmental and genetic factors on biofilm formation by the probiotic strain Lactobacillus rhamnosus GG*. Appl Environ Microbiol, 2007. **73**(21): p. 6768-75.
142. Sims, I.M., et al., *Structure and functions of exopolysaccharide produced by gut commensal Lactobacillus reuteri 100-23*. ISME J, 2011. **5**(7): p. 1115-24.
143. Roberfroid, M., *Prebiotics: the concept revisited*. J Nutr, 2007. **137**(3 Suppl 2): p. 830S-7S.
144. Korakli, M., M.G. Ganzle, and R.F. Vogel, *Metabolism by bifidobacteria and lactic acid bacteria of polysaccharides from wheat and rye, and exopolysaccharides produced by Lactobacillus sanfranciscensis*. J Appl Microbiol, 2002. **92**(5): p. 958-65.
145. Cerning, J., *Exocellular polysaccharides produced by lactic acid bacteria*. FEMS Microbiol Rev, 1990. **7**(1-2): p. 113-30.
146. Bleau, C., et al., *Intermediate chains of exopolysaccharides from Lactobacillus rhamnosus RW-9595M increase IL-10 production by macrophages*. J Appl Microbiol, 2010. **108**(2): p. 666-75.
147. Nikolic, M., et al., *Characterisation of the exopolysaccharide (EPS)-producing Lactobacillus paraplantarum BGCG11 and its non-EPS producing derivative strains as potential probiotics*. Int J Food Microbiol, 2012. **158**(2): p. 155-62.
148. Vinderola, G., et al., *Effects of the oral administration of the exopolysaccharide produced by Lactobacillus kefiranofaciens on the gut mucosal immunity*. Cytokine, 2006. **36**(5-6): p. 254-260.
149. Kitazawa, H., et al., *Induction of IFN-gamma and IL-1 alpha production in macrophages stimulated with phosphopolysaccharide produced by Lactococcus lactis ssp. cremoris*. Int J Food Microbiol, 1996. **31**(1-3): p. 99-106.
150. Nishimura-Uemura, J., et al., *Functional alteration of murine macrophages stimulated with extracellular polysaccharides from Lactobacillus delbrueckii ssp. bulgaricus OLL1073R-1*. Food Microbiology, 2003. **20**(3): p. 267-273.
151. Liu, C.F., et al., *Immunomodulatory and antioxidant potential of Lactobacillus exopolysaccharides*. J Sci Food Agric, 2011. **91**(12): p. 2284-91.
152. Sato, T., et al., *Dextran from Leuconostoc mesenteroides augments immunostimulatory effects by the introduction of phosphate groups*. J Food Prot, 2004. **67**(8): p. 1719-24.
153. Xu, R., N. Shang, and P. Li, *In vitro and in vivo antioxidant activity of exopolysaccharide fractions from Bifidobacterium animalis RH*. Anaerobe, 2011. **17**(5): p. 226-31.
154. Vu, B., et al., *Bacterial Extracellular Polysaccharides Involved in Biofilm Formation*. Molecules, 2009. **14**(7): p. 2535-2554.
155. Mayer, C., et al., *The role of intermolecular interactions: studies on model systems for bacterial biofilms*. Int J Biol Macromol, 1999. **26**(1): p. 3-16.
156. Branda, S.S., et al., *Biofilms: the matrix revisited*. Trends Microbiol, 2005. **13**(1): p. 20-6.
157. Jones, S.E. and J. Versalovic, *Probiotic Lactobacillus reuteri biofilms produce antimicrobial and anti-inflammatory factors*. BMC Microbiol, 2009. **9**: p. 35.
158. Rickard, A.H., et al., *Bacterial coaggregation: an integral process in the development of multi-species biofilms*. Trends Microbiol, 2003. **11**(2): p. 94-100.
159. Ochoa-Reparaz, J., et al., *A polysaccharide from the human commensal Bacteroides fragilis protects against CNS demyelinating disease*. Mucosal Immunol, 2010. **3**(5): p. 487-95.

160. Mazmanian, S.K., J.L. Round, and D.L. Kasper, *A microbial symbiosis factor prevents intestinal inflammatory disease*. *Nature*, 2008. **453**(7195): p. 620-5.
161. Mao, Y.K., et al., *Bacteroides fragilis polysaccharide A is necessary and sufficient for acute activation of intestinal sensory neurons*. *Nat Commun*, 2013. **4**: p. 1465.
162. Sengupta, R., et al., *The Role of Cell Surface Architecture of Lactobacilli in Host-Microbe Interactions in the Gastrointestinal Tract*. *Mediators of Inflammation*, 2013. **2013**: p. 16.
163. Mackenzie, D.A., et al., *Strain-specific diversity of mucus-binding proteins in the adhesion and aggregation properties of Lactobacillus reuteri*. *Microbiology*, 2010. **156**(Pt 11): p. 3368-78.
164. Roos, S. and H. Jonsson, *A high-molecular-mass cell-surface protein from Lactobacillus reuteri 1063 adheres to mucus components*. *Microbiology*, 2002. **148**(Pt 2): p. 433-42.
165. Sun, Z., et al., *Characterization of a S-layer protein from Lactobacillus crispatus K313 and the domains responsible for binding to cell wall and adherence to collagen*. *Applied Microbiology and Biotechnology*, 2013. **97**(5): p. 1941-1952.
166. Chen, X., et al., *The S-layer proteins of Lactobacillus crispatus strain ZJ001 is responsible for competitive exclusion against Escherichia coli O157:H7 and Salmonella typhimurium*. *International Journal of Food Microbiology*, 2007. **115**(3): p. 307-312.
167. Khang, Y.H., et al., *Recombinant S-layer proteins of Lactobacillus brevis mediating antibody adhesion to calf intestine alleviated neonatal diarrhea syndrome*. *J Microbiol Biotechnol*, 2009. **19**(5): p. 511-9.
168. Åvall-Jääskeläinen, S. and A. Palva, *Lactobacillus surface layers and their applications*. *FEMS Microbiol Rev*, 2005. **29**(3): p. 511-529.
169. Malik, S., et al., *The Highly Autoaggregative and Adhesive Phenotype of the Vaginal Lactobacillus plantarum Strain CMPG5300 Is Sortase Dependent*. *Appl Environ Microbiol*, 2013. **79**(15): p. 4576-85.
170. Granato, D., et al., *Cell Surface-Associated Elongation Factor Tu Mediates the Attachment of Lactobacillus johnsonii NCC533 (La1) to Human Intestinal Cells and Mucins*. *Infection and Immunity*, 2004. **72**(4): p. 2160-2169.
171. Hsueh, H.Y., et al., *Increase of the adhesion ability and display of a rumen fungal xylanase on the cell surface of Lactobacillus casei by using a listerial cell-wall-anchoring protein*. *J Sci Food Agric*, 2013.
172. Adlerberth, I., et al., *A mannose-specific adherence mechanism in Lactobacillus plantarum conferring binding to the human colonic cell line HT-29*. *Appl Environ Microbiol*, 1996. **62**(7): p. 2244-51.
173. Gross, G., et al., *Biodiversity of mannose-specific adhesion in Lactobacillus plantarum revisited: strain-specific domain composition of the mannose-adhesin*. *Benef Microbes*, 2010. **1**(1): p. 61-6.
174. Neeser, J.R., et al., *Lactobacillus johnsonii La1 shares carbohydrate-binding specificities with several enteropathogenic bacteria*. *Glycobiology*, 2000. **10**(11): p. 1193-9.
175. Schar-Zammaretti, P. and J. Ubbink, *The cell wall of lactic acid bacteria: surface constituents and macromolecular conformations*. *Biophys J*, 2003. **85**(6): p. 4076-92.
176. Deepika, G., et al., *Effect of growth time on the surface and adhesion properties of Lactobacillus rhamnosus GG*. *J Appl Microbiol*, 2009. **107**(4): p. 1230-40.
177. Saito, T., et al., *Adherence of oral streptococci to an immobilized antimicrobial agent*. *Arch Oral Biol*, 1997. **42**(8): p. 539-45.
178. Lebeer, S., et al., *Functional analysis of Lactobacillus rhamnosus GG pili in relation to adhesion and immunomodulatory interactions with intestinal epithelial cells*. *Appl Environ Microbiol*, 2012. **78**(1): p. 185-93.
179. Kankainen, M., et al., *Comparative genomic analysis of Lactobacillus rhamnosus GG reveals pili containing a human- mucus binding protein*. *Proc Natl Acad Sci U S A*, 2009. **106**(40): p. 17193-8.

180. Granato, D., et al., *Cell surface-associated lipoteichoic acid acts as an adhesion factor for attachment of Lactobacillus johnsonii La1 to human enterocyte-like Caco-2 cells*. Appl Environ Microbiol, 1999. **65**(3): p. 1071-7.
181. Ruas-Madiedo, P., et al., *Exopolysaccharides produced by probiotic strains modify the adhesion of probiotics and enteropathogens to human intestinal mucus*. J Food Prot, 2006. **69**(8): p. 2011-5.
182. Magee, A.D. and J. Yother, *Requirement for capsule in colonization by Streptococcus pneumoniae*. Infect Immun, 2001. **69**(6): p. 3755-61.
183. Morona, J.K., et al., *The effect that mutations in the conserved capsular polysaccharide biosynthesis genes cpsA, cpsB, and cpsD have on virulence of Streptococcus pneumoniae*. J Infect Dis, 2004. **189**(10): p. 1905-13.
184. Marttinen, A.M., et al., *Effects of Lactobacillus reuteri PTA 5289 and L. paracasei DSMZ16671 on the Adhesion and Biofilm Formation of Streptococcus mutans*. Curr Microbiol, 2013.
185. Jalasvuori, H., A. Haukioja, and J. Tenovuo, *Probiotic Lactobacillus reuteri strains ATCC PTA 5289 and ATCC 55730 differ in their cariogenic properties in vitro*. Arch Oral Biol, 2012. **57**(12): p. 1633-8.
186. Wang, S.Y., et al., *Investigation of microorganisms involved in biosynthesis of the kefir grain*. Food Microbiol, 2012. **32**(2): p. 274-85.
187. Macfarlane, S. and J.F. Dillon, *Microbial biofilms in the human gastrointestinal tract*. J Appl Microbiol, 2007. **102**(5): p. 1187-96.
188. Gañzle, M.G.S., C., *Exopolysaccharide production by intestinal lactobacilli*. , in *In Probiotics and Prebiotics: Scientific Aspects*, G.W. Tannock, Editor. 2005, Wymondham: Horizon Scientific Press. p. 83–96.
189. Kos, B., et al., *Adhesion and aggregation ability of probiotic strain Lactobacillus acidophilus M92*. J Appl Microbiol, 2003. **94**(6): p. 981-7.
190. Kojic, M., et al., *Cloning and expression of a novel lactococcal aggregation factor from Lactococcus lactis subsp. lactis BGKP1*. BMC Microbiol, 2011. **11**: p. 265.
191. Roos, S., S. Lindgren, and H. Jonsson, *Autoaggregation of Lactobacillus reuteri is mediated by a putative DEAD-box helicase*. Mol Microbiol, 1999. **32**(2): p. 427-36.
192. Goh, Y.J. and T.R. Klaenhammer, *Functional roles of aggregation-promoting-like factor in stress tolerance and adherence of Lactobacillus acidophilus NCFM*. Appl Environ Microbiol, 2010. **76**(15): p. 5005-12.
193. Voltan, S., et al., *Aggregating phenotype in Lactobacillus crispatus determines intestinal colonization and TLR2 and TLR4 modulation in murine colonic mucosa*. Clin Vaccine Immunol, 2007. **14**(9): p. 1138-48.
194. Abdallah Ismail, N., et al., *Frequency of Firmicutes and Bacteroidetes in gut microbiota in obese and normal weight Egyptian children and adults*. Arch Med Sci, 2011. **7**(3): p. 501-7.
195. Wegmann, U., et al., *Complete genome sequence of Lactobacillus johnsonii FI9785, a competitive exclusion agent against pathogens in poultry*. J Bacteriol, 2009. **191**(22): p. 7142-3.
196. Pridmore, R.D., et al., *The genome sequence of the probiotic intestinal bacterium Lactobacillus johnsonii NCC 533*. Proceedings of the National Academy of Sciences of the United States of America, 2004. **101**(8): p. 2512-2517.
197. Haller, D., et al., *Activation of human NK cells by staphylococci and lactobacilli requires cell contact-dependent costimulation by autologous monocytes*. Clin Diagn Lab Immunol, 2002. **9**(3): p. 649-57.
198. Haller, D., et al., *Non-pathogenic bacteria elicit a differential cytokine response by intestinal epithelial cell/leucocyte co-cultures*. Gut, 2000. **47**(1): p. 79-87.

199. Ibnou-Zekri, N., et al., *Divergent patterns of colonization and immune response elicited from two intestinal Lactobacillus strains that display similar properties in vitro*. Infect Immun, 2003. **71**(1): p. 428-36.
200. Bernet, M.F., et al., *Lactobacillus acidophilus LA 1 binds to cultured human intestinal cell lines and inhibits cell attachment and cell invasion by enterovirulent bacteria*. Gut, 1994. **35**(4): p. 483-489.
201. Valladares, R., et al., *Lactobacillus johnsonii inhibits indoleamine 2,3-dioxygenase and alters tryptophan metabolite levels in BioBreeding rats*. FASEB J, 2013. **27**(4): p. 1711-20.
202. Hsieh, P.S., et al., *Eradication of Helicobacter pylori infection by the probiotic strains Lactobacillus johnsonii MH-68 and L. salivarius ssp. salicinius AP-32*. Helicobacter, 2012. **17**(6): p. 466-77.
203. Sgouras, D.N., et al., *Lactobacillus johnsonii La1 attenuates Helicobacter pylori-associated gastritis and reduces levels of proinflammatory chemokines in C57BL/6 mice*. Clin Diagn Lab Immunol, 2005. **12**(12): p. 1378-86.
204. Zhang, Y.C., et al., *Screening of probiotic lactobacilli for inhibition of Shigella sonnei and the macromolecules involved in inhibition*. Anaerobe, 2012. **18**(5): p. 498-503.
205. Abee, T., T.R. Klaenhammer, and L. Letellier, *Kinetic studies of the action of lactacin F, a bacteriocin produced by Lactobacillus johnsonii that forms poration complexes in the cytoplasmic membrane*. Appl Environ Microbiol, 1994. **60**(3): p. 1006-1013.
206. Audisio, M.C. and M.R. Benitez-Ahrendts, *Lactobacillus johnsonii CRL1647, isolated from Apis mellifera L. bee-gut, exhibited a beneficial effect on honeybee colonies*. Benef Microbes, 2011. **2**(1): p. 29-34.
207. Kingma, S.D., et al., *Lactobacillus johnsonii N6.2 stimulates the innate immune response through Toll-like receptor 9 in Caco-2 cells and increases intestinal crypt Paneth cell number in biobreeding diabetes-prone rats*. J Nutr, 2011. **141**(6): p. 1023-8.
208. Fayol-Messaoudi, D., et al., *pH-, Lactic acid-, and non-lactic acid-dependent activities of probiotic Lactobacilli against Salmonella enterica Serovar Typhimurium*. Appl Environ Microbiol, 2005. **71**(10): p. 6008-13.
209. Pridmore, R.D., et al., *Hydrogen peroxide production by Lactobacillus johnsonii NCC 533 and its role in anti-Salmonella activity*. FEMS Microbiol Lett, 2008. **283**(2): p. 210-5.
210. Araya, M., L. Morelli, G. Reid, M.E. Sanders, and C. Stanton, *Guidelines for the Evaluation of Probiotics in Food*, in Report of a Joint FAO/WHO Working Group on Drafting Guidelines for the Evaluation of Probiotics in Food 2002, FAO/WHO.
211. Alp, G. and B. Aslim, *Relationship between the resistance to bile salts and low pH with exopolysaccharide (EPS) production of Bifidobacterium spp. isolated from infants feces and breast milk*. Anaerobe, 2010. **16**(2): p. 101-5.
212. Ozturk, S., B. Aslim, and Z. Suludere, *Evaluation of chromium(VI) removal behaviour by two isolates of Synechocystis sp. in terms of exopolysaccharide (EPS) production and monomer composition*. Bioresour Technol, 2009. **100**(23): p. 5588-93.
213. Mozzi, F., et al., *Functionality of exopolysaccharides produced by lactic acid bacteria in an in vitro gastric system*. J Appl Microbiol, 2009. **107**(1): p. 56-64.
214. Horn, N., et al., *Characterisation of a novel plasmid p9785S from Lactobacillus johnsonii FI9785*. Plasmid, 2005. **54**(2): p. 176-183.
215. Sambrook J., F.E.F., Maniatis T., *Molecular cloning: a laboratory manual*. 2nd Edition ed ed. 1989: Cold Spring Harbor Laboratory Press.
216. Maguin, E., et al., *Efficient insertional mutagenesis in lactococci and other gram-positive bacteria*. J Bacteriol, 1996. **178**(3): p. 931-5.
217. Wegmann, U., et al., *Introduction of peptidase genes from Lactobacillus delbrueckii subsp. lactis into Lactococcus lactis and controlled expression*. Appl Environ Microbiol, 1999. **65**(11): p. 4729-33.

218. Ho, S.N., et al., *Site-directed mutagenesis by overlap extension using the polymerase chain reaction*. *Gene*, 1989. **77**(1): p. 51-9.
219. Bradford, M.M., *A rapid and sensitive method for the quantitation of microgram quantities of protein utilizing the principle of protein-dye binding*. *Anal Biochem*, 1976. **72**: p. 248-54.
220. Ruas-Madiedo, P. and C.G. de los Reyes-Gavilán, *Invited Review: Methods for the Screening, Isolation, and Characterization of Exopolysaccharides Produced by Lactic Acid Bacteria*. *Journal of Dairy Science*, 2005. **88**(3): p. 843-856.
221. Tallon, R., P. Bressollier, and M.C. Urdaci, *Isolation and characterization of two exopolysaccharides produced by Lactobacillus plantarum EP56*. *Res Microbiol*, 2003. **154**(10): p. 705-12.
222. DuBois, M., et al., *Colorimetric Method for Determination of Sugars and Related Substances*. *Analytical Chemistry*, 1956. **28**(3): p. 350-356.
223. Blakeney, A.B., et al., *A simple and rapid preparation of alditol acetates for monosaccharide analysis*. *Carbohydrate Research*, 1983. **113**(2): p. 291-299.
224. Faber, E.J., J.P. Kamerling, and J.F. Vliegthart, *Structure of the extracellular polysaccharide produced by Lactobacillus delbrueckii subsp. bulgaricus 291*. *Carbohydr Res*, 2001. **331**(2): p. 183-94.
225. Schaer-Zammaretti, P. and J. Ubbink, *Imaging of lactic acid bacteria with AFM--elasticity and adhesion maps and their relationship to biological and structural data*. *Ultramicroscopy*, 2003. **97**(1-4): p. 199-208.
226. Ahmed, Z., et al., *Characterization of new exopolysaccharides produced by coculturing of L. kefiranofaciens with yoghurt strains*. *Int J Biol Macromol*, 2013.
227. Sajna, K.V., et al., *Studies on structural and physical characteristics of a novel exopolysaccharide from Pseudozyma sp. NII 08165*. *Int J Biol Macromol*, 2013. **59C**: p. 84-89.
228. Qin, F., et al., *Higher order structures of a bioactive, water-soluble (1-->3)-beta-D-glucan derived from Saccharomyces cerevisiae*. *Carbohydr Polym*, 2013. **92**(2): p. 1026-32.
229. Deutsch, S.M., et al., *Contribution of surface beta-glucan polysaccharide to physicochemical and immunomodulatory properties of Propionibacterium freudenreichii*. *Appl Environ Microbiol*, 2012. **78**(6): p. 1765-75.
230. Dertli, E., et al., *Structure and Biosynthesis of Two Exopolysaccharides Produced by Lactobacillus johnsonii F19785*. *J Biol Chem*, 2013. **288**(44): p. 31938-51.
231. Hutter, J.L., and Bechhoefer, J. , *Calibration of atomic force microscope tips*. *Rev. Sci. Instrum.* , 1993. **64**: p. 1868-1873.
232. Gunning, A.P., et al., *Mapping specific adhesive interactions on living human intestinal epithelial cells with atomic force microscopy*. *FASEB J*, 2008. **22**(7): p. 2331-9.
233. Kratky, O. and G. Porod, *Röntgenuntersuchung gelöster Fadenmoleküle*. *Recueil des Travaux Chimiques des Pays-Bas*, 1949. **68**(12): p. 1106-1122.
234. Flory, P., *Statistical Mechanics of Chain Molecules*. 1998, Munchen: Hanser.
235. Yuan, S.J., et al., *Identification of key constituents and structure of the extracellular polymeric substances excreted by Bacillus megaterium TF10 for their flocculation capacity*. *Environ Sci Technol*, 2011. **45**(3): p. 1152-7.
236. Yin, R., et al., *Photo-crosslinked glucose-sensitive hydrogels based on methacrylate modified dextran--concanavalin A and PEG dimethacrylate*. *Carbohydrate Polymers*, 2010. **82**(2): p. 412-418.
237. Ismail, B. and K.M. Nampoothiri, *Production, purification and structural characterization of an exopolysaccharide produced by a probiotic Lactobacillus plantarum MTCC 9510*. *Arch Microbiol*, 2010. **192**(12): p. 1049-57.
238. Braissant, O., et al., *Characteristics and turnover of exopolymeric substances in a hypersaline microbial mat*. *FEMS Microbiol Ecol*, 2009. **67**(2): p. 293-307.
239. Morris, V.J., Kirby, A. R., and Gunning, A. P., *Atomic Force Microscopy for Biologists*. 2nd ed. 2009, London: Imperial College Press.

240. Zhou, T., et al., *Structure of the ArsA ATPase: the catalytic subunit of a heavy metal resistance pump*. EMBO J, 2000. **19**(17): p. 4838-45.
241. Casper-Lindley, C. and F.H. Yildiz, *VpsT is a transcriptional regulator required for expression of vps biosynthesis genes and the development of rugose colonial morphology in Vibrio cholerae O1 El Tor*. J Bacteriol, 2004. **186**(5): p. 1574-8.
242. Alp, G., et al., *The role of hemagglutination and effect of exopolysaccharide production on bifidobacteria adhesion to Caco-2 cells in vitro*. Microbiol Immunol, 2010. **54**(11): p. 658-65.
243. Paulo, E.M., et al., *Production, extraction and characterization of exopolysaccharides produced by the native Leuconostoc pseudomesenteroides R2 strain*. An Acad Bras Cienc, 2012. **84**(2): p. 495-508.
244. Notararigo, S., et al., *Comparative analysis of production and purification of homo- and hetero-polysaccharides produced by lactic acid bacteria*. Carbohydr Polym, 2013. **93**(1): p. 57-64.
245. Luzhetskyy, A. and A. Bechthold, *Features and applications of bacterial glycosyltransferases: current state and prospects*. Appl Microbiol Biotechnol, 2008. **80**(6): p. 945-52.
246. Francius, G., et al., *Detection, localization, and conformational analysis of single polysaccharide molecules on live bacteria*. ACS Nano, 2008. **2**(9): p. 1921-9.
247. Iwamori, M., et al., *Distribution of receptor glycolipids for Lactobacilli in murine digestive tract and production of antibodies cross-reactive with them by immunization of rabbits with Lactobacilli*. J Biochem, 2009. **146**(2): p. 185-91.
248. Tuomola, E.M., A.C. Ouwehand, and S.J. Salminen, *The effect of probiotic bacteria on the adhesion of pathogens to human intestinal mucus*. FEMS Immunol Med Microbiol, 1999. **26**(2): p. 137-42.
249. Mafu, A.A., et al., *Characterization of physicochemical forces involved in adhesion of Listeria monocytogenes to surfaces*. Appl Environ Microbiol, 1991. **57**(7): p. 1969-73.
250. Reuter, M., et al., *Biofilm formation by Campylobacter jejuni is increased under aerobic conditions*. Appl Environ Microbiol, 2010. **76**(7): p. 2122-8.
251. Nielsen, L., X. Li, and L.J. Halverson, *Cell-cell and cell-surface interactions mediated by cellulose and a novel exopolysaccharide contribute to Pseudomonas putida biofilm formation and fitness under water-limiting conditions*. Environ Microbiol, 2011. **13**(5): p. 1342-56.
252. Killiny, N., et al., *The exopolysaccharide of Xylella fastidiosa is essential for biofilm formation, plant virulence, and vector transmission*. Mol Plant Microbe Interact, 2013. **26**(9): p. 1044-53.
253. Irie, Y., et al., *Self-produced exopolysaccharide is a signal that stimulates biofilm formation in Pseudomonas aeruginosa*. Proc Natl Acad Sci U S A, 2012. **109**(50): p. 20632-6.
254. Sturme, M.H., et al., *An agr-like two-component regulatory system in Lactobacillus plantarum is involved in production of a novel cyclic peptide and regulation of adherence*. J Bacteriol, 2005. **187**(15): p. 5224-35.
255. Chai, Y., et al., *Galactose metabolism plays a crucial role in biofilm formation by Bacillus subtilis*. MBio, 2012. **3**(4): p. e00184-12.
256. Sutherland, I., *Biofilm exopolysaccharides: a strong and sticky framework*. Microbiology, 2001. **147**(Pt 1): p. 3-9.
257. Vuong, C., et al., *A crucial role for exopolysaccharide modification in bacterial biofilm formation, immune evasion, and virulence*. J Biol Chem, 2004. **279**(52): p. 54881-6.
258. Ambalam, P., et al., *Bile stimulates cell surface hydrophobicity, Congo red binding and biofilm formation of Lactobacillus strains*. FEMS Microbiol Lett, 2012. **333**(1): p. 10-9.
259. Pratt, L.A. and R. Kolter, *Genetic analysis of Escherichia coli biofilm formation: roles of flagella, motility, chemotaxis and type I pili*. Mol Microbiol, 1998. **30**(2): p. 285-93.
260. Reisner, A., et al., *In vitro biofilm formation of commensal and pathogenic Escherichia coli strains: impact of environmental and genetic factors*. J Bacteriol, 2006. **188**(10): p. 3572-81.

261. Imbert, M. and R. Blondeau, *On the iron requirement of lactobacilli grown in chemically defined medium*. *Curr Microbiol*, 1998. **37**(1): p. 64-6.
262. Canzi, E., et al., *Conditions affecting cell surface properties of human intestinal bifidobacteria*. *Antonie Van Leeuwenhoek*, 2005. **88**(3-4): p. 207-19.
263. Schar-Zammaretti, P., et al., *Influence of fermentation medium composition on physicochemical surface properties of *Lactobacillus acidophilus**. *Appl Environ Microbiol*, 2005. **71**(12): p. 8165-73.
264. Kaushik, J.K., et al., *Functional and probiotic attributes of an indigenous isolate of *Lactobacillus plantarum**. *PLoS One*, 2009. **4**(12): p. e8099.
265. Schillinger, U., C. Guigas, and W. Heinrich Holzapfel, *In vitro adherence and other properties of lactobacilli used in probiotic yoghurt-like products*. *International Dairy Journal*, 2005. **15**(12): p. 1289-1297.
266. van der Mei, H.C., et al., *Cell surface hydrophobicity is conveyed by S-layer proteins—a study in recombinant lactobacilli*. *Colloids and Surfaces B: Biointerfaces*, 2003. **28**(2–3): p. 127-134.
267. Schachtsiek, M., W.P. Hammes, and C. Hertel, *Characterization of *Lactobacillus coryniformis* DSM 20001T surface protein Cpf mediating coaggregation with and aggregation among pathogens*. *Appl Environ Microbiol*, 2004. **70**(12): p. 7078-85.
268. Gonzalez-Rodriguez, I., et al., *Role of extracellular transaldolase from *Bifidobacterium bifidum* in mucin adhesion and aggregation*. *Appl Environ Microbiol*, 2012. **78**(11): p. 3992-8.
269. Ventura, M., et al., *Identification and characterization of novel surface proteins in *Lactobacillus johnsonii* and *Lactobacillus gasserii**. *Appl Environ Microbiol*, 2002. **68**(12): p. 6172-81.
270. Lee, H., et al., *Functional properties of *Lactobacillus* strains isolated from kimchi*. *Int J Food Microbiol*, 2011. **145**(1): p. 155-61.
271. Vizoso Pinto, M.G., et al., *Adhesive and chemokine stimulatory properties of potentially probiotic *Lactobacillus* strains*. *J Food Prot*, 2007. **70**(1): p. 125-34.
272. Del Re, B., et al., *Adhesion, autoaggregation and hydrophobicity of 13 strains of *Bifidobacterium longum**. *Lett Appl Microbiol*, 2000. **31**(6): p. 438-42.
273. Muller, J.A., et al., *Modification of the technical properties of *Lactobacillus johnsonii* NCC 533 by supplementing the growth medium with unsaturated fatty acids*. *Appl Environ Microbiol*, 2011. **77**(19): p. 6889-98.
274. Becker, A., et al., *Regulation of succinoglycan and galactoglucan biosynthesis in *Sinorhizobium meliloti**. *J Mol Microbiol Biotechnol*, 2002. **4**(3): p. 187-90.
275. Janczarek, M., *Environmental signals and regulatory pathways that influence exopolysaccharide production in rhizobia*. *Int J Mol Sci*, 2011. **12**(11): p. 7898-933.
276. Nielsen, S.S., *Phenol-Sulfuric Acid Method for Total Carbohydrates*, in *Food Analysis Laboratory Manual*. 2010, Springer US. p. 47-53.
277. Coyne, M.J., et al., *Mpi recombinase globally modulates the surface architecture of a human commensal bacterium*. *Proc Natl Acad Sci U S A*, 2003. **100**(18): p. 10446-51.
278. Hathaway, L.J., et al., *Capsule type of *Streptococcus pneumoniae* determines growth phenotype*. *PLoS Pathog*, 2012. **8**(3): p. e1002574.
279. Wu, M.H., et al., *Exopolysaccharide activities from probiotic bifidobacterium: Immunomodulatory effects (on J774A.1 macrophages) and antimicrobial properties*. *Int J Food Microbiol*, 2010. **144**(1): p. 104-10.
280. Karlyshev, A.V., et al., *The *Campylobacter jejuni* general glycosylation system is important for attachment to human epithelial cells and in the colonization of chicks*. *Microbiology*, 2004. **150**(Pt 6): p. 1957-64.
281. Boke Hatice, A.B., Alp Gulcin, *The role of resistance to bile salts and acid tolerance of exopolysaccharides (EPSS) produced by yogurt starter bacteria*. *Archives of Biological Sciences*, 2010 **62**(2): p. 323-328.

282. Dunne, C., et al., *In vitro selection criteria for probiotic bacteria of human origin: correlation with in vivo findings*. Am J Clin Nutr, 2001. **73**(2 Suppl): p. 386S-392S.
283. Holzapfel, W.H., et al., *Overview of gut flora and probiotics*. Int J Food Microbiol, 1998. **41**(2): p. 85-101.
284. Hardy, H., et al., *Probiotics, prebiotics and immunomodulation of gut mucosal defences: homeostasis and immunopathology*. Nutrients, 2013. **5**(6): p. 1869-912.
285. Toole, P.W. and J.C. Cooney, *Probiotic Bacteria Influence the Composition and Function of the Intestinal Microbiota*. Interdisciplinary Perspectives on Infectious Diseases, 2008. **2008**.
286. Nueno-Palop, C. and A. Narbad, *Probiotic assessment of Enterococcus faecalis CP58 isolated from human gut*. Int J Food Microbiol, 2011. **145**(2-3): p. 390-4.
287. Wang, Q., et al., *Naive Bayesian classifier for rapid assignment of rRNA sequences into the new bacterial taxonomy*. Appl Environ Microbiol, 2007. **73**(16): p. 5261-7.
288. Wang, Y. and P.Y. Qian, *Conservative fragments in bacterial 16S rRNA genes and primer design for 16S ribosomal DNA amplicons in metagenomic studies*. PLoS One, 2009. **4**(10): p. e7401.
289. Caporaso, J.G., et al., *QIIME allows analysis of high-throughput community sequencing data*. Nat Methods, 2010. **7**(5): p. 335-6.
290. Edgar, R.C., *Search and clustering orders of magnitude faster than BLAST*. Bioinformatics, 2010. **26**(19): p. 2460-1.
291. DeSantis, T.Z., et al., *Greengenes, a chimera-checked 16S rRNA gene database and workbench compatible with ARB*. Appl Environ Microbiol, 2006. **72**(7): p. 5069-72.
292. Caporaso, J.G., et al., *PyNAST: a flexible tool for aligning sequences to a template alignment*. Bioinformatics, 2010. **26**(2): p. 266-7.
293. Price, M.N., P.S. Dehal, and A.P. Arkin, *FastTree 2--approximately maximum-likelihood trees for large alignments*. PLoS One, 2010. **5**(3): p. e9490.
294. Nikaido, H. and M. Vaara, *Molecular basis of bacterial outer membrane permeability*. Microbiol Rev, 1985. **49**(1): p. 1-32.
295. Liu, C., et al., *Antibiotic resistance of probiotic strains of lactic acid bacteria isolated from marketed foods and drugs*. Biomed Environ Sci, 2009. **22**(5): p. 401-12.
296. Tenover, F.C., *Mechanisms of antimicrobial resistance in bacteria*. Am J Infect Control, 2006. **34**(5 Suppl 1): p. S3-10; discussion S64-73.
297. Fayaz, A.M., et al., *Biogenic synthesis of silver nanoparticles and their synergistic effect with antibiotics: a study against gram-positive and gram-negative bacteria*. Nanomedicine: Nanotechnology, Biology and Medicine, 2010. **6**(1): p. 103-109.
298. Folkes, E.F.G.a.J.P., *The assimilation of amino-acids by bacteria. 14. Nucleic acid and protein synthesis in Staphylococcus aureus*. Biochem. J. , 1953 **53**: p. 483-0.
299. webpage, D. *DrugBank: Showing Furazolidone (DB00614)*. 2008-12-19.
300. Jeon, B., et al., *Roles of lipooligosaccharide and capsular polysaccharide in antimicrobial resistance and natural transformation of Campylobacter jejuni*. J Antimicrob Chemother, 2009. **63**(3): p. 462-8.
301. van Kraaij, C., et al., *Pore formation by nisin involves translocation of its C-terminal part across the membrane*. Biochemistry, 1998. **37**(46): p. 16033-40.
302. Tuomola, E., et al., *Quality assurance criteria for probiotic bacteria*. Am J Clin Nutr, 2001. **73**(2 Suppl): p. 393S-398S.
303. Sanders, M.E., *Probiotics: definition, sources, selection, and uses*. Clin Infect Dis, 2008. **46 Suppl 2**: p. S58-61; discussion S144-51.
304. Begley, M., C.G. Gahan, and C. Hill, *The interaction between bacteria and bile*. FEMS Microbiol Rev, 2005. **29**(4): p. 625-51.
305. Ruas-Madiedo, P., et al., *Bile affects the synthesis of exopolysaccharides by Bifidobacterium animalis*. Appl Environ Microbiol, 2009. **75**(4): p. 1204-7.

306. Bezkorovainy, A., *Probiotics: determinants of survival and growth in the gut*. Am J Clin Nutr, 2001. **73**(2 Suppl): p. 399S-405S.
307. Steer, T., et al., *Perspectives on the role of the human gut microbiota and its modulation by pro- and prebiotics*. Nutr Res Rev, 2000. **13**(2): p. 229-54.
308. Lindstrom, C., et al., *Oral Administration of Live Exopolysaccharide-Producing *Pediococcus parvulus*, but Not Purified Exopolysaccharide, Suppressed Enterobacteriaceae without Affecting Bacterial Diversity in Ceca of Mice*. Appl Environ Microbiol, 2013. **79**(16): p. 5030-7.
309. Valladares, R., et al., *Lactobacillus johnsonii N6.2 mitigates the development of type 1 diabetes in BB-DP rats*. PLoS One, 2010. **5**(5): p. e10507.
310. Salazar, N., et al., *Exopolysaccharides produced by *Bifidobacterium longum* IPLA E44 and *Bifidobacterium animalis* subsp. *lactis* IPLA R1 modify the composition and metabolic activity of human faecal microbiota in pH-controlled batch cultures*. Int J Food Microbiol, 2009. **135**(3): p. 260-7.
311. Bello, F.D., et al., *In vitro study of prebiotic properties of levan-type exopolysaccharides from Lactobacilli and non-digestible carbohydrates using denaturing gradient gel electrophoresis*. Syst Appl Microbiol, 2001. **24**(2): p. 232-7.
312. Salazar, N., et al., *Exopolysaccharides produced by intestinal *Bifidobacterium* strains act as fermentable substrates for human intestinal bacteria*. Appl Environ Microbiol, 2008. **74**(15): p. 4737-45.
313. Cinquin, C., et al., *Comparative effects of exopolysaccharides from lactic acid bacteria and fructo-oligosaccharides on infant gut microbiota tested in an in vitro colonic model with immobilized cells*. FEMS Microbiol Ecol, 2006. **57**(2): p. 226-38.
314. Mårtensson, O., et al., *Fermented, ropy, oat-based products reduce cholesterol levels and stimulate the bifidobacteria flora in humans*. Nutrition Research, 2005. **25**(5): p. 429-442.
315. Zhang, H., et al., *Human gut microbiota in obesity and after gastric bypass*. Proc Natl Acad Sci U S A, 2009. **106**(7): p. 2365-70.
316. Chen, W., et al., *Human intestinal lumen and mucosa-associated microbiota in patients with colorectal cancer*. PLoS One, 2012. **7**(6): p. e39743.
317. Ruijsenaars, H.J., F. Stingele, and S. Hartmans, *Biodegradability of Food-Associated Extracellular Polysaccharides*. Current Microbiology, 2000. **40**(3): p. 194-199.
318. Tsuda, H. and T. Miyamoto, *Production of Exopolysaccharide by *Lactobacillus plantarum* and the Prebiotic Activity of the Exopolysaccharide*. Food Science and Technology Research, 2010. **16**(1): p. 87-92.
319. Synytsya, A., et al., *Glucans from fruit bodies of cultivated mushrooms *Pleurotus ostreatus* and *Pleurotus eryngii*: Structure and potential prebiotic activity*. Carbohydrate Polymers, 2009. **76**(4): p. 548-556.
320. Bello, F.D., et al., *In vitro study of Prebiotic Properties of Levan-type Exopolysaccharides from Lactobacilli and Non-digestible Carbohydrates Using Denaturing Gradient Gel Electrophoresis*. Systematic and Applied Microbiology, 2001. **24**(2): p. 232-237.
321. Hughes, S.A., et al., *In vitro fermentation of oat and barley derived  $\beta$ -glucans by human faecal microbiota*. FEMS Microbiology Ecology, 2008. **64**(3): p. 482-493.
322. Sanz, M.L., G.R. Gibson, and R.A. Rastall, *Influence of Disaccharide Structure on Prebiotic Selectivity in Vitro*. Journal of Agricultural and Food Chemistry, 2005. **53**(13): p. 5192-5199.
323. Weijers, C.A., M.C. Franssen, and G.M. Visser, *Glycosyltransferase-catalyzed synthesis of bioactive oligosaccharides*. Biotechnol Adv, 2008. **26**(5): p. 436-56.
324. Wagner, G.K. and T. Pesnot, *Glycosyltransferases and their assays*. Chembiochem, 2010. **11**(14): p. 1939-49.
325. Roychoudhury, R. and N.L. Pohl, *New structures, chemical functions, and inhibitors for glycosyltransferases*. Curr Opin Chem Biol, 2010. **14**(2): p. 168-73.
326. Breton, C., et al., *Structures and mechanisms of glycosyltransferases*. Glycobiology, 2006. **16**(2): p. 29R-37R.

327. Palcic, M.M., *Glycosyltransferases as biocatalysts*. Curr Opin Chem Biol, 2011. **15**(2): p. 226-33.
328. Kolkman, M.A., et al., *Capsular polysaccharide synthesis in Streptococcus pneumoniae serotype 14: molecular analysis of the complete cps locus and identification of genes encoding glycosyltransferases required for the biosynthesis of the tetrasaccharide subunit*. Mol Microbiol, 1997. **26**(1): p. 197-208.
329. Zawadzka-Skomial, J., et al., *Characterization of the bifunctional glycosyltransferase/acyltransferase penicillin-binding protein 4 of Listeria monocytogenes*. J Bacteriol, 2006. **188**(5): p. 1875-81.
330. Terrak, M., et al., *The catalytic, glycosyl transferase and acyl transferase modules of the cell wall peptidoglycan-polymerizing penicillin-binding protein 1b of Escherichia coli*. Mol Microbiol, 1999. **34**(2): p. 350-64.
331. Heiss, C., et al., *Unusual galactofuranose modification of a capsule polysaccharide in the pathogenic yeast Cryptococcus neoformans*. J Biol Chem, 2013. **288**(16): p. 10994-1003.
332. Sarvas, M. and H. Nikaido, *Biosynthesis of T1 antigen in Salmonella: origin of D-galactofuranose and D-ribofuranose residues*. J Bacteriol, 1971. **105**(3): p. 1063-72.
333. Stevenson, G., et al., *Structure of the O antigen of Escherichia coli K-12 and the sequence of its rfb gene cluster*. J Bacteriol, 1994. **176**(13): p. 4144-56.
334. Nassau, P.M., et al., *Galactofuranose biosynthesis in Escherichia coli K-12: identification and cloning of UDP-galactopyranose mutase*. J Bacteriol, 1996. **178**(4): p. 1047-52.
335. Sanders, D.A., et al., *UDP-galactopyranose mutase has a novel structure and mechanism*. Nat Struct Biol, 2001. **8**(10): p. 858-63.
336. Wing, C., et al., *Expression and initial characterization of WbbI, a putative D-Galf:alpha-D-Glc beta-1,6-galactofuranosyltransferase from Escherichia coli K-12*. Org Biomol Chem, 2006. **4**(21): p. 3945-50.
337. Mayer, M.J., A. Narbad, and M.J. Gasson, *Molecular characterization of a Clostridium difficile bacteriophage and its cloned biologically active endolysin*. J Bacteriol, 2008. **190**(20): p. 6734-40.
338. Koplín, R., J.R. Brisson, and C. Whitfield, *UDP-galactofuranose precursor required for formation of the lipopolysaccharide O antigen of Klebsiella pneumoniae serotype O1 is synthesized by the product of the rfbDKPO1 gene*. J Biol Chem, 1997. **272**(7): p. 4121-8.
339. Stingle, F., et al., *Introduction of the exopolysaccharide gene cluster from Streptococcus thermophilus Sfi6 into Lactococcus lactis MG1363: production and characterization of an altered polysaccharide*. Mol Microbiol, 1999. **32**(6): p. 1287-95.
340. Oliver, M.B., et al., *Streptococcus pneumoniae Serotype 11D Has a Bispecific Glycosyltransferase and Expresses Two Different Capsular Polysaccharide Repeating Units*. J Biol Chem, 2013. **288**(30): p. 21945-54.
341. Oliver, M.B., et al., *Discovery of Streptococcus pneumoniae serotype 6 variants with glycosyltransferases synthesizing two differing repeating units*. J Biol Chem, 2013.
342. Sheppard, C.L., et al., *Streptococcus pneumoniae isolates expressing a capsule with epitopes of both serotypes 6A and 6B*. Clin Vaccine Immunol, 2010. **17**(11): p. 1820-2.
343. van Kranenburg, R., et al., *Exopolysaccharide biosynthesis in Lactococcus lactis NIZO B40: functional analysis of the glycosyltransferase genes involved in synthesis of the polysaccharide backbone*. J Bacteriol, 1999. **181**(1): p. 338-40.
344. Van Geel-Schutten, G.H., et al., *Biochemical and structural characterization of the glucan and fructan exopolysaccharides synthesized by the lactobacillus reuteri wild-type strain and by mutant strains*. Appl Environ Microbiol, 1999. **65**(7): p. 3008-14.
345. Lin, M.H., et al., *Phosphoproteomics of Klebsiella pneumoniae NTUH-K2044 reveals a tight link between tyrosine phosphorylation and virulence*. Mol Cell Proteomics, 2009. **8**(12): p. 2613-23.

346. Morona, J.K., R. Morona, and J.C. Paton, *Attachment of capsular polysaccharide to the cell wall of Streptococcus pneumoniae type 2 is required for invasive disease*. Proc Natl Acad Sci U S A, 2006. **103**(22): p. 8505-10.
347. Mori, Y., et al., *PhpA, a tyrosine phosphatase of Myxococcus xanthus, is involved in the production of exopolysaccharide*. Microbiology, 2012. **158**(Pt 10): p. 2546-55.
348. Anwar, M.A., et al., *The probiotic Lactobacillus johnsonii NCC 533 produces high-molecular-mass inulin from sucrose by using an inulosucrase enzyme*. Appl Environ Microbiol, 2008. **74**(11): p. 3426-33.
349. Vadillo-Rodríguez, V., et al., *Role of lactobacillus cell surface hydrophobicity as probed by AFM in adhesion to surfaces at low and high ionic strength*. Colloids and Surfaces B: Biointerfaces, 2005. **41**(1): p. 33-41.
350. Haas, A., et al., *Systemic antibody responses to gut commensal bacteria during chronic HIV-1 infection*. Gut, 2011. **60**(11): p. 1506-19.
351. Ouwehand, A.C., et al., *Adhesion of probiotic micro-organisms to intestinal mucus*. International Dairy Journal, 1999. **9**(9): p. 623-630.
352. Boris, S., et al., *Adherence of human vaginal lactobacilli to vaginal epithelial cells and interaction with uropathogens*. Infect Immun, 1998. **66**(5): p. 1985-9.